GENETIC MAPPING AND PHENOTYPIC CHARACTERIZATION OF WHEAT FOR YIELD, YIELD COMPONENTS AND AGRONOMIC TRAITS

A Dissertation

by

SILVANO ASSANGA OCHEYA

Submitted to the Office of Graduate and Professional Studies of
Texas A&M University
in partial fulfillment of the requirements for the degree of

DOCTOR OF PHILOSOPHY

Chair of Committee,	Shuyu Liu
Co-Chair of Committee,	Amir M.H. Ibrahim
Committee Members,	Jackie C. Rudd
	William Rooney
	Qingwu Xue
Head of Department,	David D. Baltensperger

August 2016

Major Subject: Plant Breeding

ABSTRACT

Defining genetic architecture of complex traits is a fundamental step towards marker-assisted selection. The objective of this study was to use a saturated genetic map derived from 90K single nucleotide polymorphic (SNP) array to map quantitative trait loci (QTL) associated with grain yield (GY), yield components, agronomic and end-use quality traits. A population of 217 recombinant inbred lines (RIL), parents and checks were phenotyped across six dryland and two well-watered environments in the United States. In a separate study, the RIL were evaluated for resistance to wheat streak mosaic virus (WSMV) disease. The objective of this study was to map *Wsm2*, a gene that confers resistance to WSMV disease.

GY QTL were detected on chromosome 2B, 5A, and 5B with significant QTL-by-environment interactions (QEI) observed for the QTL on 2B and 5A. Three QTL for GY were mapped on 2B with additive effect ranging from 0.23-0.38, 0.13-0.46 and 0.06-0.19 t ha^{-1}, respectively. The maximum coefficient of determination (R^2) corresponding to the three QTL on 2B was 31.2%, 46.7% and 27.2%, respectively. Chromosome 5A and 5B had a single QTL each for GY with maximal additive effect of 0.25 t ha^{-1} and 0.27 t ha^{-1}, respectively. Yield components were mapped on different chromosomes with some QTL showing QEI. Chromosome 2B was a hotspot for many QTL associated with multiple traits. Multi-trait QTL analysis revealed significant QTL-by-trait interactions (QTI) for all QTL detected. The additive effect for GY QTL detected using multi-trait model was 0.19 t ha^{-1} and 0.33 t ha^{-1} for the QTL detected on chromosome 5A.1 and 5B,

respectively. The genetic connectivity among QTL and traits revealed that GY and biomass were enhanced by QTL detected on 2B, 5A and 5B.

End-use quality analysis revealed QTL for 10 rheological parameters co-located on chromosome 1A. The co-location was supported by results from the multi-trait QTL mapping. Chromosome 1D.1 had QTL for midline right time and midline peak integral located within 12 cM whereas midline time_X value and midline time_X width were located within 13.6 cM. The QTL for kernel hardness index (HDI) were detected on chromosome 1A, 2B and 2D. The additive effect for HDI QTL was 1.8 and 2.1 for the QTL on 1A and 2D, respectively, whereas the QTL on 2B had an additive effect range of 1.5-2.5. The corresponding R^2 was 13.4%, 7.8-23.2%, and 14.9% for the QTL on 1A, 2B and 2D, respectively. Flour protein content QTL were detected on chromosome 3B and 5B with an R^2 range of 4.2-11.5% and 4.5-11.8%, respectively. NCBI search of markers linked to end-use quality revealed that the SNP M11264 was linked to gliadin/avenin-like mRNA.

Genetic mapping for *Wsm2* revealed that the gene is located on chromosome 3BS. Nine SNP flanking the gene were detected within 2.0 cM. The markers linked to *Wsm2* will be important in development of resistant varieties and protection of yield in wheat.

DEDICATION

To my lovely wife

Anne Gesare Timu

And

My beautiful daughters, Aimee Chichi Assanga and Joy Kwamboka Assanga.

They are the joy of my life!

ACKNOWLEDGEMENTS

It has been a journey up to this point and, certainly, the achievements I have made would not have been possible without the concerted effort from a number of persons. I would like to thank my committee chairs, Dr. Shuyu Liu and Dr. Amir M.H Ibrahim for their exemplary guidance and commitment during the course of my study. I also thank my committee members, Dr. Jackie Rudd, Dr. William Rooney, and Dr. Qingwu Xue for their guidance and relentless support throughout the course of my doctoral program.

I owe my gratitude to Maria Fuentealba (Pilar) for the incredible amount of support she offered during my research study. It is impossible to imagine the accomplishment I made without the help from her and no amount of gratitude is commensurate with her work. Her performance was always above and beyond expectation. Specifically, I thank Pilar for her help in DNA extraction, phenotyping and logistical support for seed shipment to cooperators. I also thank Cody Shachter, Jay Martin, Serina Nelson, Ashley Holmes and the whole team at the wheat genetics lab for their help in this study.

My sincere gratitude goes to Monsanto Beachell-Borlaug International Scholars program for the financial support of my doctorate studies. I thank USAID Fellowship of the United States government's Feed the Future Initiative administered through Borlaug Leadership Enhancement in Agriculture Program (BLEAP) at the University of California Davis, for their support in leadership and training at the International Maize and Improvement Center (CIMMYT). In this regard, I am also grateful to Dr. Bhavani Sridhar for his training at the CIMMYT, Njoro. I am thankful for financial support from the

Borlaug International Scholars program at Texas A&M University and the Texas Wheat Producers Board.

I am indebted to Dr. Edward Runge, the chair of the MBBIS judging committee for his continued support and encouragement throughout my study. The leadership training I received at Tero International courtesy of MBBIS program had a positive impact in my life and improved my role as a change agent in the society. I have become a better leader since then.

I am grateful to Dr. Tom Jondiko for his guidance and his warm welcome to College Station and taking immense amount of time to walk me through the entire registration rigor, orientation and for helping me to complete the State and Federal paperwork. His help facilitated all the logistics and my smooth transition to the graduate school at TAMU. I also thank Dr. Lubinda Walubita for his support and guidance during my stay in College Station.

I am indebted to my colleagues and the entire wheat breeding and genetics lab team who made my research study achievable. I thank Smith Dhakal and Dr. Bharath Reddy for their support in field phenotyping, Dr. Geraldine Opena and Bryan Simoneaux for logistical support and Sharris Vader for end-use quality analysis. I would like to thank Geraldo Carvalho Jr from Sorghum breeding and genetics lab for immense and fruitful discussions on genetics, mixed models and statistical analysis.

I am grateful to Dr. Shiaoman Chao and her team at the USDA-ARS Genotyping lab in Fargo, ND for their help in genotyping. I also thank Dr. Dirk Hays, Professor Molecular and Environmental Plant Sciences and Dr. Charlie Johnson, associate director

at the Texas A&M Centre for Bioinformatics and Genomic System Engineering for the provision of genotyping computer software for processing genotyping data.

I am also thankful to Dr. Scott Haley at Colorado State University, Dr. Guorong Zhang at Kansas State University, and Dr. Jianli Chen at University of Idaho for their help in phenotyping at their respective location. I thank Jason Baker, Kirk Jessup, and Dr. Ravindra Devkota for developing the population in the present study and for their support in phenotypic evaluation in Texas, USA.

I am grateful to the administrative staff at the Department of Soil and Crop Sciences and Texas A&M AgriLife Research particularly the Department Head Dr. David Baltensperger, and program manager Carol Rhodes for their support and facilitation of my doctoral research program. Thanks also go to my friends and colleagues and the department faculty and staff for making my time at Texas A&M University a great experience.

Thanks to my mother for her encouragement and to my wife, Anne Gesare and my daughters, Aimee C. Assanga and Joy K. Assanga for their patience and love. Finally, I thank the Almighty God for everything in my life and I firmly believe nothing is impossible before Him.

NOMENCLATURE

ANOVA	Analysis of variance
BLAST	Basic Local Alignment Search Tool
BLUE	Best Linear Unbiased Estimate
BLUP	Best Linear Unbiased Predictor
CAPE	Combined Analysis of Pleiotropy and Epistasis
CIM	Composite Interval Mapping
CTAB	Cetyltrimethylammonium Bromide
DNA	Deoxyribonucleic Acid
DPI	Days Post-inoculation
GEI	Genotype-by-Environment Interaction
GLM	General Linear Model
HMW-GS	High Molecular Weight Glutenins Sub-units
HVA	High Value Allele
KASP	Kompetitive Allele Specific PCR
LMM	Linear Mixed Model
LOD	Log of Odds
MAS	Marker-Assisted Selection
ML	Maximum Likelihood
PCR	Polymerase Chain Reaction
QEI	QTL-by-Environment Interaction

QTI	QTL-by-Trait Interaction
QTL	Quantitative Trait Loci
REML	Residual Maximum Likelihood
RIL	Recombinant Inbred Lines
RWA	Russian Wheat Aphid
SIC	Schwarz Information Criterion
SIM	Simple Interval Mapping
SKCS	Single Kernel Characterization System
SNP	Single Nucleotide Polymorphism
SSR	Simple Sequence Repeat
VCOV	Variance-Covariance
WSMV	Wheat Streak Mosaic Virus

TABLE OF CONTENTS

Page

LIST OF FIGURES

Page

LIST OF TABLES

CHAPTER I

INTRODUCTION AND LITERATURE REVIEW

Wheat (*Triticum aestivum* L.) plays a fundamental global nutritional role supplying significant amount of calories and proteins. It is the most widely planted crop in terms of acreage and can be processed into a broad spectrum of products spanning different cultural backgrounds. Globally, wheat contributes approximately 20% of daily calories and 15% proteins (Ray et al., 2013). These percentages underscore the importance of investing in wheat research to improve yield per unit area while conserving resources. The ramifications of suboptimal wheat production *vis a vis* the demand can lead to a humanitarian crisis particularly in those regions where wheat is the stable food. Currently, the annual genetic gain in wheat is barely 1.0% and in some regions yield plateau has been reported, a trend that is worrisome based on the projected global wheat demand. A spectrum of factors acting individually or interactively, both biotic and abiotic contributes to the low rate of increase and these include drought, heat, diseases, and poor soil fertility. Studies have shown that an annual increase in yield of about 2.4% annually is required in order to reach the demand threshold required to suffice the global population in the next few decades (Hawkesford et al., 2013).

Drought stress is one of the major global constraints driving the decline in wheat productivity and this is complicated by turbulent climatic conditions experienced in different parts of the World (Dixon et al., 2009). Most wheat production zones experience prolonged and more intense drought stress. In Texas, drought stress is common and since

2000-2015, the State has experienced drought annually with variation occurring in intensity and coverage (US drought monitor, http://droughtmonitor.unl.edu). Even though drought stress can be alleviated through irrigation systems, pressure on available water resources, which include competing needs from urbanization, renders this option unsustainable. In Texas High Plains (THP) for instance, the main source of water for irrigation is the Ogallala aquifer. The water level in the aquifer has shown a declining trend that is higher than recharge rate (Postel, 2012). The dwindling water levels have necessitated administrative cap limiting the amount of water that can be pumped for irrigation (Postel, 2012). An alternative option beside irrigation that can increase wheat production is the expansion of the total area under wheat cultivation. However, this option is also unsustainable owing to growth of urbanization and industrialization and concerns over terrestrial and aquatic ecosystem (Tilman et al., 2002). The unsustainability of increasing yield through irrigation and expansion of wheat area implies that the demand required in less than four decades to come can only be met sustainably by improving the genetic yield potential of wheat. This requires careful mating schemes backed up with both phenotypic and molecular data to accumulate alleles with substantial breeding values for yield and other desirable traits.

The climatic turbulence has also contributed to an increase in biotic stresses. Exotic pathogens and related diseases and insect pests have been reported in regions where they weren't before and this is primarily attributed to the conducive conditions provided by climate change (Hawkesford et al., 2013). Among the biotic stresses, wheat streak mosaic virus (WSMV) which causes WSMV disease is of primary concern in the Southern Great

Plains and other parts of the World. The economic impact of WSMV is significant with yield losses as high as 76.3% and biomass reduction as high as 46.4% reported in the literature (Velandia et al., 2010). Additionally, WSMV has negative impact on water use efficiency (WUE) and in their study, Velandia et al. (2010) reported a reduction in WUE as high as 74.4% in THP. This is a major concern particularly in the THP where the main source of irrigation water is limited (Price et al., 2010). Thus, for wheat production, every drop of water must be used optimally to produce grain yield and/or forage. The development of drought resilient wheat varieties is an essential objective for Texas A&M AgriLife Research wheat program.

The small grains breeding and genetics program of Texas AgriLife Research has a meticulous program on building resilience to biotic and abiotic stress. Success stories include the development and release of TAM 111 in 2003 (Lazar et al., 2004) and the recent release of 'TAM 112' (Rudd et al., 2014; PI 643143), 'TAM 113' (Rudd et al., 2014); and newly developed 'TAM 114' and 'TAM 204' (Kay, 2014). For more than a decade, TAM 111 has maintained superiority in performance and is among the top preferred wheat variety by Texas producers as well as producers in other areas of the Great Plains, including Kansas, Nebraska, and Colorado (www.nass.usda.gov). Despite its superiority, limited information on the genetic basis underlying yield, yield components, agronomic and end-use quality is available. The physiological and transcriptome analyses have revealed clues on the role of abscisic acid (ABA), stomatal conductance and upregulation of transcriptome associated with photosynthesis, phytohormone metabolism and carbohydrate metabolism (Reddy et al., 2014). Information on genetic loci modulating

yield, yield components, agronomic and end-use quality is unknown and this information is essential for marker-assisted selection (MAS) strategy. MAS requires tagged diagnostic markers flanking, within 1 to 2 cM, the gene of interest, and preferably codominant, abundant and amenable to both to multiplexing and uniplexing (Semagn et al., 2014). Diagnostic markers are primarily detected via genetic mapping, QTL analysis and marker validation studies.

QTL studies provide prime information on the action, interaction, number and effect of QTL/genes controlling quantitative traits. The primary traits targeted in genetic mapping in wheat include yield, quality traits and yield components under abiotic stress (drought, heat, and salinity), and biotic stress (disease and insect pest resistance). The International Maize and Wheat Improvement Center (CIMMYT) has developed a RIL population specifically derived for drought studies from the cross Seri M82/Babax, two parents with contrasting yield performance under drought stress conditions. This population has been widely used for QTL mapping and therefore it provides a reliable comparative basis for genetic studies across environments (Olivares-Villegas et al., 2007). McIntyre et al. (2010) used 587 markers (74 SSR, 264 DArT, 249 AFLP) and 198 RIL derived from Seri M82/Babax and reported putative QTL for grain yield on chromosome 6D, 7A and unassigned linkage group. The yield QTL were co-located with QTL for flowering, grain weight and water-soluble carbohydrates, hectoliter weight, harvest index, grain metre^{-2}, and reduced grain screenings (McIntyre et al., 2010). In a similar study but using 167 RIL derived from Seri M82/Babax and same genetic map developed by McIntyre et al. (2010), Pinto et al. (2010) reported a major yield QTL on chromosome 4A

explaining 27% of the phenotypic variation. Lopes et al. (2013) used the Seri M82/Babax RIL population for genetic mapping and QTL analysis and detected grain yield QTL on chromosome 4A, 4B, 5A, 6B and 7B with all the QTL for grain yield exhibiting significant interaction with the environment. In addition, they detected three QTL for grain weight on chromosome 5B, 6B and 6D and 7D with the QTL on 7D accounting for 39% of the total variation; and four consistent QTL for grain metre^{-2} on chromosome 1A, 4A, 4B and 6D.

In a separate QTL study using a DH population derived from the cross Spark x Rialto, Simmonds et al. (2014) reported significant QTL for grain yield, grain weight and green canopy duration on chromosome 6A. They validated their QTL results using near isogenic lines (NIL) where the introgression of the high value allele from Rialto resulted in 5.5 and 5.1% increase in grain yield and grain weight, respectively. In addition, they mapped *TaGW2,* a gene modulating grain width and grain weight within the interval of mapped QTLs. The *TaGW2* is orthologous to the rice *OsGW2* gene which codes for E3 Ubiquitin ligase that negatively regulates grain width and weight in rice. However, the function of the *TaGW2* is not clear with one study indicating it as a negative regulator of grain size and width (Yang et al., 2012) while another study reported it as a positive regulator (Bednarek et al., 2012).

Recently, CIMMYT also developed and characterized an association-mapping panel abbreviated as WAMI- wheat association mapping initiative. This panel was specifically designed for a narrow range in plant height and days to heading to minimize the confounding effects of the two traits on estimation of QTL for yield and other quantitative traits (Lopes et al., 2015). Due to the diversity of the WAMI population,

marker-trait association results obtained using this population provides a good standard for comparison with other QTL studies. Sukumaran et al. (2015) genotyped 287 lines from the WAMI using the 90K infinium SNP array and conducted marker-trait association studies under temperate irrigated environments. They reported four SNP significantly associated with yield on 3B, 5A, 5B and 6A. The locus on 5A and 6A were also associated with grain metre^{-2} and explained 5% and 6% of the variation, respectively. Loci linked to maturity were mapped on 2B, 3B, 4B, 4D and 6A whereas plant height was significantly associated with loci on 1A and 6A. Loci significantly associated with biomass were mapped on 3D and 6A; harvest index on 1D, 1B and 3B; canopy temperature at grain filling on 2D, 4D and 6A; and chlorophyll index on 3B and 6A (Sukumaran et al., 2015). Using a dataset pooled across environments, Lopes et al. 2015 conducted association-mapping studies using WAMI population and the 9K SNP array and reported significant association for grain yield on 2D, 3A and 3B. The SNP associated with grain yield on 3B were consistent across drought, heat, and combined heat and drought stress environments. Days to heading was associated with *Vrn-1* gene and SNP on chromosome 5A whereas plant height was associated with *Rht-B1, Rht-D1* and several markers on chromosome 6A but only under drought and irrigated environments (Lopes et al., 2015). Considering the results of Lopes et al. (2015), Pinto et al. (2010), Lopes et al. (2013), McIntyre et al. (2010) and Sukumaran et al. (2015), chromosome 3B seems to play a significant role in modulating grain yield under stress and irrigated environments. Bonneau et al. (2013) reported similar findings where QTL for grain yield, grain weight and early vigor were detected on the short arm chromosome 3B. In their study, they modelled interaction terms

and observed significant QTL by environment interaction as well as pleiotropic effects across 21 environments used in their study (Bonneau et al., 2013).

Classical breeding methods have led to substantial improvement in wheat yield over the last 5 decades particularly through introduction of dwarfing genes (*Rht*) which were the hallmark of Green Revolution (Hedden, 2003). However, genetic improvement using classical approach particularly for complex traits such as yield has significant time liability primarily due to low-moderate heritability expressed by these traits (McIntyre et al., 2010; Walsh, 2001). It is possible to offset in part the time liability through integration of molecular assets in the selection program e.g. application of indirect selection based on diagnostic markers linked to quantitative traits. The integration of molecular markers has shown promising results with some cultivars developed through marker-assisted selection (MAS) already available in the market (Eathington et al., 2007). This however, requires genetic tagging of important traits through meticulous process of genotype-phenotype statistical association to identify diagnostic markers for specific traits. Advances in nano-technology have enabled genotyping millions of SNP in a single run through development of micro beads where genetic probes are annealed. This has been backed with advances in artificial intelligence through computing as well as improvement in algorithm development for processing large genomic and phenomic data.

Most QTL studies to date used sparse genetic map for linkage mapping and QTL analysis. Application of large number of markers evenly distributed across the genome increases the odds of detecting a QTL in linkage disequilibrium with at least one marker. In wheat, the 90K SNP array is the largest SNP chip publicly available for genotyping

(Wang et al., 2014). Limited genetic studies have developed saturated genetic maps to determine the location of QTLs associated with different traits. Furthermore, few studies have reported the magnitude of both QTL-by-QTL interaction and QTL-by-environment. This dissertation focuses on yield, yield components, end-use quality as well as well as *Wsm2*, presented in chapter II, III and IV. Chapter II covers characterization and genetic mapping for grain yield, yield components and agronomic traits based on a linear mixed model (LMM) for multi-environment and multi-trait QTL analysis. Chapter III focuses on *Wsm2*, a gene that confers resistance to WSMV disease. The *Wsm2* has been incorporated in a number of commercial wheat varieties in the US through traditional breeding techniques. However, WSMV is transmitted primarily by wheat curl mites (*Aceria tosichella* K.) which are primarily disseminated by wind (Navia et al., 2013). The wind depended locomotion makes field phenotyping for WSMV difficult owing to non-uniformity of infection in the field trials. This makes it difficult to distinguish resistant wheat lines from the disease escapes; hence, diagnostic markers will be a valuable genetic tool for development of WSMV resistant wheat lines. In addition, early-planted wheat targeted for grazing are more vulnerable to WSMV due to a high population of wheat curl mite that usually occurs in the early season. The diagnostic markers are potential genetic tools for rapid integration of WSMV resistance into early season wheat varieties to protect the forage as well as grain yield of dual-purpose wheat. Finally, chapter IV looks at the genetic mapping for end-use quality with a primary focus on kernel characteristics and rheological parameters of the dough.

CHAPTER II

MAPPING QTL FOR GRAIN YIELD, YIELD COMPONENTS AND AGRONOMIC TRAITS

INTRODUCTION

The cardinal role of plant breeding and genetics is the development of cultivars with enhanced genetic fitness coupled with high yield, superior quality and tolerance to biotic and abiotic stresses. Over time, this was achieved through selection schemes that relied almost entirely on phenotypic selection encompassing testing and selection of diverse germplasm under relevant test conditions that mimic farmer's environments. In the recent few decades, complementary integration of molecular markers and other contemporary techniques in crop improvement has shown promising results with some potential application reported in both public and private commercial breeding programs (Collard et al., 2008; Eathington et al., 2007). One of the initial phases in marker-assisted selection (MAS) involves genetic tagging of economically and agronomically important traits to identify molecular signatures linked to genomic blocks modulating phenotypic traits. Organismal phenotype or other molecular endophenotypes such as transcripts can be used for statistical association with the molecular variants (Mackay et al., 2009). The dissection of genetic architecture of quantitative traits provides prime information on the chromosomal location, action, interaction, number and effect of QTL/genes controlling quantitative traits. The approach used in QTL mapping integrates nucleotide polymorphism and phenotypic response in a statistical model to infer presence-absence of a genomic region modulating a trait. This implies that improvement in dissection of the

genetic basis of a quantitative trait and accurate tagging of single nucleotide polymorphism (SNP) linked to QTL can be achieved through several ways including improvement in statistical modeling, accurate field plot technique and experimental design, accurate data recording, and improvement in genotyping accuracy. Significant improvement has been achieved in the latter and presently SNP are routinely used to fingerprint individuals for mapping and other genetic applications. The preference for SNPs is primarily due to their ubiquitous nature, low assay cost per data point, co-dominance inheritance pattern, relatively low genotyping errors, locus specificity, and amenability to both multiplexing and uniplexing (Schlotterer, 2004; Semagn et al., 2014). Commercial high throughput genotyping platforms are available for genotyping 100s to 1000s of individuals using SNPs leading to the construction of dense and ultra-dense genetic maps (Semagn et al., 2014). Improvement in nanotechnology and computing capability has contributed to the development of arrays with SNPs ranging from 1000s to millions enabling better genome coverage and development of dense and ultra-dense genetic maps. In addition, high throughput uniplexing platform are also available such as Kompetitive Allele Specific PCR (KASP) (www.lgcgroup.com , accessed 15 November 2015), which among other applications provides an option to convert diagnostic markers from multiplex to uniplex platform for marker validation and marker-assisted selection (MAS).

In wheat, the 90K SNP array (Illumina Inc., San Diego, CA, USA) is publicly available for genetic studies but to date only a few genetic studies have been published using this array (Avni et al., 2014; Liu et al., 2016; Sukumaran et al., 2015). Previously,

the wheat 9K SNP chip was used in wheat genetic studies (Akhunov et al., 2009; Cavanagh et al., 2013). Comparison of the assay design files for 9k and 90k showed that 7000 SNPs from 9k SNP chip were included on 90k SNP array (http://129.130.90.211/snp/ , accessed 16 February 2016). Recently, a public axiom SNP array for wheat and its relatives consisting of 820K SNPs and related information is publicly available (Wilkinson et al., 2012). The arrays could play a fundamental role in genetic application for improvement of wheat yield to meet the rising demand. Improvement in experimental design coupled with statistical modeling is fundamental in detection of the loci underlying the genetic basis of a trait. Applications of linear mixed models (LMM) have been shown to be more powerful because of their flexibility to include variance-covariance structure that account for heterogeneity in genetic variances and environmental correlation (Malosetti et al., 2013; Smith et al., 2005). In addition, LMM within the frame work of QTL analysis can account for both QTL-by-trait interactions (QTI) and QTL-by-environment interactions (QEI) including interaction with environmental co-variables such as temperature, light duration and moisture levels (Boer et al., 2007; Malosetti et al., 2013; Pastina et al., 2012).

Many genetic studies in wheat have reported QTL using different types of population and molecular markers (Bonneau et al., 2013; Lopes et al., 2015; Lopes et al., 2013; McIntyre et al., 2010; Pinto et al., 2010; Simmonds et al., 2014; Zanke et al., 2015). However, most of the studies relied on sparse genetic maps to tag QTL for different traits under different environmental conditions. In addition, the application of inflexible statistical model used in most studies limits the ability to model variance-covariance structure to account for genetic heterogeneity and correlation among environments (Boer

et al., 2007; Malosetti et al., 2013; Van Eeuwijk et al., 2010). In contrast to previous QTL studies, we used a dense linkage map constructed using 90K SNP array and implemented LMM using residual maximum likelihood (REML) in GenStat software (Malosetti et al., 2013; VSN International, 2015). The objectives were to map QTL for grain yield, yield components and agronomic traits within the framework of single trait multi-environment and multi-trait analysis model. Additionally, the QTL identified in multi-trait and single-trait QTL analysis were used to determine genetic connectivity among QTL and between QTL and traits based on combined analysis of pleiotropy and epistasis algorithm (Tyler et al., 2013).

MATERIALS AND METHODS

Experimental population and trial evaluation

A bi-parental mapping population with individuals expectedly containing about 50% of the genome from each parent was derived from an elite-by-elite cross between CO960293-2, (Haley et al., 2002) and TAM 111, (Lazar et al., 2004). The maternal parent, CO960293-2, was developed by Colorado Agricultural Experiment Station and co-released by Colorado and Kansas Agricultural Experiment Stations primarily for resistance to wheat streak mosaic virus (WSMV) and Russian Wheat Aphid (Haley et al., 2002). The paternal parent, TAM 111, was developed and released by Texas A&M AgriLife Research (Lazar et al., 2004). It has excellent performance under drought stress and possesses good quality characteristics for bread making. A trial comprising of 217 F7 recombinant inbred lines (RIL) plus three checks (four checks in 2012/13) was planted in eight environments from 2012 to 2014 (Location-by-year combination was considered as

an environment). The locations used in this study were Texas AgriLife Research stations in Bushland (35° 06' N, 102° 27' W), Chillicothe (34° 07' N, 99° 18' W) and Etter (35° 59' N, 101° 59' W) in TX; Kansas State University Agricultural Research Center, Hays (38°51' N, 99°20' W), KS; University of Idaho Aberdeen Research and Extension Center, Aberdeen (42° 57' N, 112° 49' W), ID; and Colorado State University Agricultural Experiment Station, Walsh (37° 25' N, 102° 18' W), CO. The trials in Etter, TX and Hays, KS were planted both in 2012/13 and 2013/14 cropping seasons. The trials in Idaho and Walsh were under well-watered conditions whereas the remaining trials were under dryland conditions. The plot size was 50 square feet (4.645 m^2), and the seeding rate was approximately 108 kg ha^{-1}. For each plot, six rows were planted with inter-row spacing of 10 inch in Hays whereas in other locations seven rows were planted with a spacing of 7 inch between rows. All trials were planted in an alpha-lattice design (0, 1) with an incomplete block size of five plots (13 plots in 2012/13) and 44 incomplete blocks per replication (17 incomplete blocks in 2012/13). Standard agronomic practices were carried out for each environment.

Trait measurements and statistical analysis

Grain yield (GY) was recorded in all the environments but due to logistical reasons the yield components, plant height (PH) and days to heading (DTH) were recorded in a subset of environments. Yield components were recorded in all the environments except Idaho 2013 (ID13), Walsh 2014 (WA14) and Hays 2014 (HY14). PH was recorded in all the environments except WA14 and Etter 2013 (ET13) whereas DTH was recorded in ET13, Hays 2013 (HY13), ID13 and Bushland 2014 (BS14). The trait measurements were

recorded as follows: DTH was recorded as the number of days from January 1st to when 50% of the spikes had emerged from the boot; PH was measured at physiological maturity in centimeters from representative plants as the distance from the base of the stem to the tip of the spike excluding awns; percentage of green leaf area (GLA) was visually rated at three weeks post-heading on a scale of 0.0 to 100% where 0.0% = all the leaves senesced and 100% = all leaves green. Similarly, the greenness of the flag leaf (GFL) was rated three weeks post-heading where 0.0% = whole flag leaf senesced and 100% = whole flag leaf green. A week before harvesting, half meter row samples from uniformly filled and representative inner row was harvested from each plot and used for determination of biomass and yield components. The samples were oven dried at 140°F (60°C) for three days and the weight of each sample recorded. The total number of stems (TS) and the number of heads were determined for each sample. The spikes metre^{-2} (SPM), mean single head weight (MSHW), kernels spike^{-1} (KPS), and thousand kernel weight (TKW) were calculated from the plot sample. The SPM was computed by dividing the number of heads by the sample plot area and expressed in metre^{-2}. The TKW in grams (g) was determined by counting and weighing 1000 kernels for each plot. MSHW (g) was calculated by dividing the total dry head weight per plot by the number of heads. All trials were harvested using a combine harvester and the grain yield (GY) plot^{-1} was recorded. The harvest index (HI) was calculated as grain weight per sample divided by total weight of biomass plus grain. To compute GY per hectare, the yield plot (in kg) from the combine and its respective grain weight (converted from g to kg) from the biomass sample were summed and used to convert GY per plot to metric tons per hectare using the formula:

[(plot weight (kg)/1,000 kg ton^{-1}) × (10,000 m^2 ha^{-1}/plot area (m^2)]. Test weight (TW) was measured using Seedburo TW equipment (www.seedburo.com, Des Plaines, IL, USA).

Individual environment data was subjected to analysis of variance (ANOVA) to determine the significance of genotypic component in each environment. The statistical model used for individual environment analysis was as follows:

$$Y_{ik} = \mu + R_k + G_i + \varepsilon_{ik}$$

Where $\mathbf{Y_{ik}}$ is the observed phenotypic value of the $\boldsymbol{i^{th}}$ genotype in $\boldsymbol{k^{th}}$ replicate, μ is the overall mean, $\mathbf{R_k}$ is the replication effect, $\mathbf{G_i}$ is the genetic effect of i^{th} genotype and $\boldsymbol{\varepsilon_{ik}}$ is the residual. Combined ANOVA was done within the framework of a linear mixed model where environment and genotype-by-environment interaction (GEI) were considered random. The total phenotypic variance was decomposed into environments, genotypes, replication nested within environment, and GEI based on the following statistical model:

$$Y_{ijk} = \mu + R(E) + G_i + E_j + (GEI)_{ij} + \varepsilon_{ijk}$$

Where $\mathbf{Y_{ijk}}$ is the observed value of the $\mathbf{i^{th}}$ genotype in the $\mathbf{j^{th}}$ environment and $\mathbf{k^{th}}$ replicate, **R(E)** is rep nested within the environment, $\mathbf{E_j}$ is the effect of the environment, $\mathbf{(GEI)_{ij}}$ is genotype-by-environment interaction, $\boldsymbol{\varepsilon_{ijk}}$ is the residual. To compute variance components, all components were considered as random. Best linear unbiased prediction (BLUP) for each genotype were computed using restricted maximum likelihood (REML) adapted to META-R macro (Gregorio et al., 2015). For single trait multi-environment

QTL analysis, the appropriate variance-covariance (VCOV) structure was modeled in GenStat to account for heterogeneity of genetic variances and correlation among environments (Boer et al., 2007; Malosetti et al., 2013). A parsimonious model for VCOV was selected based on Schwarz information criterion (SIC). The genetic correlations (r_G) among traits were computed using the following formula:

$$r_G = \frac{Cov_{x,y}}{(\sigma_x^2\ \sigma_y^2)^{1/2}}$$

Where COVx,y is the covariance between trait one and trait two, is the variance of trait one and is the variance of trait two. The entry-mean heritability estimates were computed based on Fehr et al. (1987) using the formula:

$$\text{Individual environment } h^2 = \frac{\sigma_g^2}{\sigma_e^2/_r + \sigma_g^2}$$

$$\text{Combined environment } h^2 = \frac{\sigma_g^2}{\sigma_e^2/_{rt} + {}^{\sigma_{ge}^2}/_t + \sigma_g^2}$$

Where **r** is the number of replication, **t** is the number of environments, $\boldsymbol{\sigma^2_g}$ is genotype variance, $\boldsymbol{\sigma^2_{ge}}$ is the GEI variance, and $\boldsymbol{\sigma^2_e}$ is the residual variance.

DNA extraction and genotyping

Total genomic DNA was extracted from leaf samples of 152 RIL using CTAB method with minor modification as described by Liu et al. (2013). The RIL plus four sets of each parent were fingerprinted using 90K Illumina's Infinium iSelect array based on the manufacturer's protocol (www.illumina.com). The fluorescence signal was captured

by Illumina scanner and subsequently processed using GenomeStudio software (www.illumina.com). BeadChip were decoded and processed *in silico* using GenomeStudio GT Module software from Illumina (www.illumina.com). The cluster file was uploaded as a guide on the most plausible position of the genotype clusters. The initial processing of the data involved normalization to account for variation in the background noise and two color channels. A two-in-one GenCall data analysis software comprising of clustering algorithm and genotype calling algorithm was applied to discriminate between clusters and classify genotypes into pools. The results for each SNP was displayed in a Cartesian plane with normalized signal intensity on the y-axis and normalized theta values (deviation of the cluster from zero) on the x-axis. The x-axis reflects the genotype frequency for A and B locus with zero = AA genotype and 1.0 = BB genotype. The clusters were color coded with red color representing homozygous AA genotype, blue color for homozygous BB genotype and grey color for the heterozygotes (AB).

A series of quality control metrics were used to assess the reliability of genotype calls in GenomeStudio. The threshold value for signal intensity was set at 0.15 and any genotype below this value was designated as null (uncalled). The call frequency (proportion of all RIL at each loci that have call scores above 0.15) at each locus was used to assess the reliability at each of the called SNPs. Call rate (ratio of number of genotype with signal intensity > user defined value total genotypes) was used filter out SNPs with a rate lower than 97%. The average normalized theta for the heterozygote (mean AB), an indicator of heterozygote cluster separation from the homozygote was assessed and

curated manually to separate the clusters or zeroed in cases where the cluster separation was ambiguous. Manual curation to adjust clusters with skewed cluster separation was done by examining the clusters in a Cartesian plot. The GenTrain score, a score for each SNP averaged across all the samples was used to evaluate the integrity of each SNP assay and a cutoff of 0.5 was used to eliminate low quality SNP. Although the constraint for signal intensity was set at 0.15, loci with low average normalized intensity and those with undefined clusters were excluded prior to downstream statistical analysis. The data set comprising of 8819 high quality and polymorphic SNPs was exported for downstream statistical analysis including linkage mapping and QTL analysis (Liu et al., 2016).

Linkage mapping and QTL analysis

The data output from GenomeStudio software was used for linkage mapping using JoinMap version 4.0 software (Van Ooijen, 2006). Prior to linkage analysis, SNPs with a similarity loci score of 1.0 were omitted to eliminate genetic redundancy and improve computation efficiency. In addition, all SNPs with significant segregation distortion based on Chi square test ($P < 0.05$) were also omitted. Several controls under calculation options were set to optimize the linkage map and SNP order. Grouping of loci into linkage groups was done based on Independence LOD parameter with increasing stringency from 2.0 to 30.0 and the incremental step of 1.0. Kosambi mapping function was used to convert recombination frequency into centiMorgans. Pairwise recombination frequency was calculated based on a maximum likelihood (ML) algorithm with the default settings in JoinMap version 4.0 (Van Ooijen, 2006). To construct the genetic map, a multipoint maximum likelihood approach adapted to JoinMap was used. A linkage map of 5200 SNPs

covering 30 linkage groups together with loci file were exported for QTL analysis. Linkage groups were assigned to chromosomes based on loci information in the 9K and 40K genetic maps (Cavanagh et al., 2013; Wang et al., 2014).

Multi-environment and multi-trait QTL analysis was implemented in GenStat based on a linear mixed model (LMM) framework as outlined by several authors (Boer et al., 2007; Malosetti et al., 2013; Van Eeuwijk et al., 2010). Under the LMM framework, multi-environment QTL mapping was implemented in a stepwise process commencing with simple interval mapping (SIM) followed by two or more successive rounds of composite interval mapping (CIM) using QTL identified in SIM to control the genetic background (Bernardo, 2013; Jansen and Stam, 1994; Zeng, 1994). QTL identified using LMM were used for combined analysis of pleiotropy and epistasis using CAPE package in R (R Core Team, 2015; Tyler et al., 2013; Tyler et al., 2014). A detailed description of CAPE algorithm and its application is outlined in the literature (Carter et al., 2012; Tyler et al., 2013; Tyler et al., 2014).

RESULTS

Analysis of variance, heritability and phenotypic performance

Combined ANOVA across environments revealed high significant genotypic differences for all traits (Table 1). The component due to GEI was significant for all traits except for biomass weight (BW) and for all the traits, a high proportion of variation was explained by the environment source of variation (Table 1). The high environmental variation is not uncommon given the great environmental variations our study had. For all traits, the genotypic component of variation was higher than GEI component. The entry-

mean heritability ranged from moderate (0.4 to 0.6) to high (>0.6) except for BW which showed heritability of 0.3. GY, harvest index (HI), grains meter^{-2} (GM) and tiller number (TS) exhibited moderate heritability while the remaining traits showed high heritability. The coefficient of determination (R^2) was high for all the traits with the least R^2 of 0.77 observed for TW (Table 1).

Table 1 Mean square for pooled analysis of variance, heritability and mean performance across drought and well-watered environments

		Env	Rep(Env)	Entry	GEI	Residual	R^2	h^2	Mean
Trait	df / units	1-6	1-7	219-222	1-1309	220-1510	-	-	-
GY	t ha^{-1}	**1640.62**	**14.32**	**1.17**	**0.66**	0.52	0.93	0.4	3.6
TW	Ib bu^{-1}	**670.61**	**23.15**	**19.01**	**4.27**	3.35	0.77	0.9	58.3
DTH	days	**24874.55**	**29.23**	**12.57**	**2.95**	2.38	0.97	0.8	141.9
PH	cm	**84078.85**	**2157.35**	**111.67**	**40.38**	32.4	0.92	0.6	63.2
HI	#	**1.83**	**0.05**	**0.01**	0.002	0.002	0.83	0.5	0.3
GM	#	**1510.37**	10.28	1.06	0.49	0.47	0.93	0.5	3596.0
BW	g m^{-2}	**766672.40**	**5614.59**	**407.09**	319.78	344.13	0.90	0.3	116.4
SPM	#	**9714769.80**	**47606.72**	**16359.35**	**4316.75**	2870.31	0.94	0.7	376.4
KPS	#	**6936.18**	**286.35**	**50.32**	**13.79**	9.22	0.84	0.7	27.8
MSHW	g	**14.25**	**0.17**	**0.04**	**0.01**	0.01	0.91	0.8	0.7
TKW	g	**14041.07**	**77.25**	**40.56**	**6.03**	2.24	0.97	0.9	26.2
TS	#	**477356.05**	**2778.40**	**667.01**	**237.8**	240.06	0.89	0.6	96.4
GLA	%	**153621.74**	**1132.91**	**645.98**	**225.05**	60.55	0.93	0.7	19.5
GFL	%	**97798.56**	**1767.10**	**1108.49**	**205.07**	135.45	0.87	0.8	50.0

Env, environments; Rep (Env), replication nested within environments; Gen, genotype; GEI, genotype-by-environment interaction; GY, grain yield; TW, test weight; DTH, days to heading; PH, plant height; HI, harvest index; GM, grains m^{-2}; BW, biomass weight. SPM, spike metre^{-2}; KPS, kernels spike^{-1}; MSHW, mean single head weight; TKW, thousand kernel weight; TS, tiller number; GLA, green leaf area; GFL, greenness of flag leaf

R^2, coefficient of determination.

Bold values are significant at $P < 0.01$, underlined value is significant at $P < 0.05$

The average GY pooled across environments was 3.6 t ha^{-1} with a corresponding TW of 58.3 lb bu^{-1}. On average, the population had 142 DTH and the mean PH was 63.2 cm. The average number of SPM was 376 with a corresponding GM of 3,596. A single spike had an average of 28 kernels and weighed 0.7 grams on average. The average TKW was 26.2 grams (Table 1).

Fig. 1 shows the grain yield performance of genotypes in individual environments. We observed high phenotypic plasticity in performance both within and across environments (Fig. 1). The highest range in phenotypic performance was observed in well-watered experiments compared to drought experiments. Dryland experiments showed differences in phenotypic plasticity with the trial in Chillicothe (CH14) showing the least range in performance. This low range in CH14 (0.5-2.0 t ha^{-1}) was primarily due to a severe drought stress leading to a narrow window for the grain filling stage. Nonetheless, we still detected significant genetic differences among the genotypes and the entry-mean heritability was 0.65 (data not shown). Although some genotypes showed relatively better genetic fitness under both drought and well-watered environments, environment-specific good performers were also observed. On average, GY under drought condition ranged from 0.5 t ha^{-1} in CH14 to 3.9 t ha^{-1} in HY13. ET13 and ET14 in Texas and HY13 in Kansas had a similar average yield, but interquartile range differed with HY14 showing a wider range. The trials in ID13 and WA14 were under well-watered environment and had average yield of 6.5 and 5.7 t ha^{-1}, respectively.

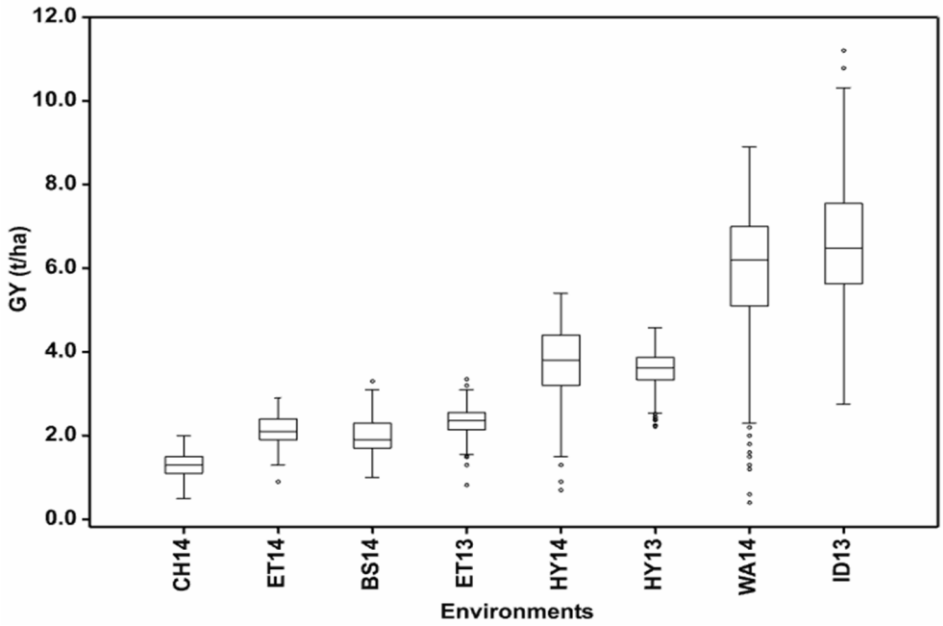

Figure 1. Individual environment boxplot for grain yield.
The mid line in the box represent the median, the lower and upper horizontal lines of the box represent 25 and 75 percentile respectively. The lower whisker represents the 25th percentile minus 1.5 x inter-quartile range (IQR) and the upper whisker is the 75th percentile plus 1.5 x IQR. BS14, Bushland 2014; CH14, Chillicothe 2014; ET13, Etter 2013; ET14, Etter 2014; HY13, Hays 2013; HY14, Hays 2014; ID13; Idaho 2013; WA14, Walsh 2014.

Genetic correlation between grain yield and other traits

The magnitude and direction of genetic correlation (r_G) between GY and other traits varied across environments (Table 2). Among the other traits, BW and SPM showed high and significant genetic correlation with GY in all dry-land trials where the trait was recorded. GM was highly correlated with GY in three environments but was not correlated with GY in CH14 (Table 2). TW showed consistent positive correlation with GY although the correlation was weak (< 0.3) in all dry-land trials. DTH showed mixed correlation response with GY. Positive but low correlation between GY and DTH were observed in

BS14 and a negative correlation in HY13 and ET13. A similar mixed response was observed for GLA whereas GFL revealed significant negative correlation in ET14. PH showed a moderate correlation with GY in two environments and a weak correlation in the remaining two environments. There was no correlation between tiller number (TS) and GY except in ET14 where it showed a negative and significant correlation. TKW revealed positive correlation in HY13 and CH14 although the correlation in HY13 was low. In ET13, the correlation between GY and TKW was negative. PH showed positive correlation in HY13 and CH14 and non-significant correlation in BS14 and ET14. The number of kernels spike^{-1} (KPS) revealed positive correlation in three environments but a negative correlation in ET14 and non-significant correlation in CH14 (Table 2).

Table 2 Genetic correlation between grain yield, yield components and agronomic traits and other traits for individual environments

	HY13	BS14	CH14	ET14	ET13
	Grain yield				
DTH	**-0.37**	0.14	-	-	**-0.30**
TW	**0.24**	**0.21**	**0.26**	0.13	0.03
PH	**0.35**	-0.09	**0.34**	0.04	-
HI	**0.59**	**0.80**	**0.55**	-	**-0.24**
GM	**0.94**	**0.56**	0.01	-	**0.66**
BW	**1.00**	**0.56**	**0.86**	-	**0.89**
SPM	**0.44**	**0.71**	**0.73**	**0.65**	**0.72**
KPS	**0.19**	**0.21**	0.14	**-0.53**	**0.22**
MSHW	**0.41**	**0.20**	**0.62**	-0.12	**-0.21**
TKW	**0.18**	0.02	**0.49**	**0.39**	**-0.61**
TS	-0.10	0.04	-0.08	**-0.40**	-
GLA	-	0.15	**-0.49**	-	-
GFL	-	0.07	**-0.62**	-	-

HY13, Hays 2013; BS14, Bushland 2014; CH14, Chillicothe 2014; ET14, Etter 2014; ET13, Etter 2013; DTH, days to heading; TW, test weight; PH, plant height; HI, harvest index; GM, grains metre^{-2}; BW, biomass weight, SPM, spikes metre^{-2}, KPS, kernels spike^{-1}; MSHW, mean single head weight; TKW, thousand kernel weight; TS, tiller number; GLA, green leaf area; GFL, greenness of the flag leaf

Across environments and traits, GY showed significant genetic correlation ($P < 0.01$) with DTH, HI, GM, BW, SPM, GLA, and GFL (Table 3). The negative correlation observed for GY with both GLA and GFL suggest that delayed senescence may not necessarily lead to increased GY. Although both GLA and GFL showed a negative and significant correlation with GY based on the data averaged across environments, the GLA showed positive correlation with GY in BS14 and a negative correlation in CH14 (Table A2). The significant genetic correlation between GY and HI, GM, BW and SPM suggest that improvement in GY is achievable through indirect selection on these traits. Relative to GY, the highest significant correlation was observed with GM (Table 3). BW, SPM and HI showed positive and significant correlation with GY although the correlation was low (<0.3).

Statistically, TW showed no correlation with GY across environments, which corroborates a report from North Dakota State University (NDSU Agriculture News, www.ag.ndsu.edu/news/newsreleases/2012/aug-20-2012/grain-yield-not-related-to-test-weight). In individual environment however, there was mixed results with two environments showing non-significant correlation and three environments showing positive correlation. However, the correlation was less than 0.3 (Table A2). TW is a volumetric measurement indicating the number of units of weight that fills a specified volume and this is used as a proxy for wheat bulk density.

Mohtasham et al. (2012) reported a significant correlation coefficient between GY and TW under drought but through path coefficient analysis, they found out that the direct effect due to TW was negligible (-0.004). Even though TW showed no correlation with

GY in the present study, it had significant correlation with HI, GM, SPM, TKW, SKW and BW (Table 3), suggesting that it may indirectly affect GY through these traits. Across environments, PH showed significant correlation with all traits except GY and DTH. The magnitude of the correlation ranged from low to moderate with BW, MSHW and TKW showing positive correlation whereas HI, GM, SPM, KPS, TS, GLA and GFL showing negative correlation.

Table 3 Genetic correlation among traits for the data averaged across environments

Traits	GY	TW	DTH	PH	HI	GM	BW	SPM	KPS	MSH	TK	TS	GLA
TW	0.04												
DTH	**-0.29**	-0.30											
PH	0.09	0.01	**0.46**										
HI	**0.24**	**0.44**	**-0.90**	**-0.26**									
GM	**0.43**	**0.35**	**-0.35**	**-0.42**	**0.37**								
BW	**0.18**	**0.62**	**0.63**	**0.21**	**-0.25**	**0.56**							
SPM	**0.32**	0.13	0.15	**-0.35**	-0.11	**0.64**	**0.52**						
KPS	0.02	-0.09	0.06	**-0.48**	**0.24**	**0.43**	**-0.38**	**-0.45**					
MSH	0.03	0.12	-0.07	0.16	**0.34**	**-0.33**	**-0.23**	**-0.81**	**0.57**				
TKW	0.05	**0.21**	-0.13	**0.57**	0.14	**-0.80**	0.07	**-0.54**	**-0.29**	**0.61**			
TS	0.04	**0.22**	0.16	**-0.44**	**-0.29**	**0.53**	**0.30**	**0.80**	**-0.75**	**-0.96**	**-0.47**		
GLA	**-0.38**	0.10	**0.99**	**-0.27**	**-0.77**	-0.10	**0.35**	**-0.28**	**-0.23**	**-0.33**	**-0.33**	0.01	
GFL	**-0.19**	0.24	**0.85**	**-0.27**	**-0.61**	-0.17	**0.43**	-0.02	**-0.47**	**-0.34**	-0.07	0.09	**0.99**

GY, grain yield; TW, test weight; DTH, days to heading; PH, plant height; HI, harvest index; GM, grains metre^{-2}, BW, biomass weight, SPM, spikes metre^{-2}, KPS, kernel spike^{-1}, MSHW, mean single head weigh; TKW, thousand kernel weight; TS, tiller number; GLA, green leaf area; GFL, greenness of the flag leaf.
Bold values are significant at $P < 0.01$, underlined values are significant at $P < 0.05$

In HY13, BS14 and CH14, PH had either positive or positive and significant correlation with BW, MSHW and TKW whereas in ET14, the correlation was positive and significant for TKW but negative and weak for MSHW (Table A2). PH showed negative and significant correlation with SPM in BS14 and CH14 whereas in other environments there was no correlation. In addition, PH had negative correlation with both HI and TS in all environments where they were recorded with the latter showing significant correlation in all the individual environments (Table A2).

Analysis of data averaged across environments revealed positive and significant genetic correlation between HI and GM, KPS and MSHW whereas negative and significant correlation were observed between HI and BW, TS, GLA and GFL (Table 3). MSHW showed consistent positive and significant correlation with HI whereas TS, GLA and GFL revealed consistent negative and significant correlation in all individual environments where the traits were recorded (Table A2)**.** Besides the correlations described above for GM, it showed positive and significant correlation with BW, SPM, KPS and TS for the data averaged across environments (Table 3). In addition, the correlation between GM and MSHW, TKW and GFL was significant but negative (Table 3). The negative correlation observed for MSHW and TKW suggests a compensatory effect whereby increasing kernel weight and spike weight may compromise the number of kernels per spike based on source-sink relationship. In individual environment, SPM and KPS were positively and significantly correlated with GM whereas BW showed mixed response with some environment exhibiting positive correlation and others negative

correlation. TS had consistent positive correlation although in HY13 the correlation was statistically indistinguishable from zero (Table A2)

Excluding correlation involving BW already discussed in the preceding section, it also showed a positive and significant correlation with SPM, TS, GLA and GFL, but an increased biomass might result in a decrease in KPS and MSHW as indicated by their negative correlations (Table 3). Among these traits, only SPM showed consistent positive and significant correlation with BW in individual environments (Table A2). Based on the data averaged across environments, SPM was positively and significantly correlated with TS although it showed negative and significant correlation with most traits including KPS, MSHW, TKW and GLA (Table 3). These results corroborated the individual environment analysis except for GLA which showed significant but contrasting correlations and TKW which had positive correlation in CH14 and negative correlation in ET13, HY13 and BS14 (Table A2). KPS was positively correlated with MSHW but negatively correlated with TKW, TS, GLA and GFL both in individual and across environment except for GLA in CH14 which showed non-significant correlation (Table 3, Table A2). MSHW showed a strong positive correlation with TKW but a negative correlation with TS, GLA and GFL in individual (Table A2) and across environments (Table 3).

Quantitative trait loci for grain yield, yield components and agronomic traits

The results of QTL analysis for GY and yield components based on single trait multi-environment model are shown in Fig. 2. A genome-wide scan revealed significant GY QTL on chromosome 2B, 5A.1 and 5B. A switch in color from one environment to the next (red to blue and vice versa) for a specific QTL indicates the presence of crossover

QEI. For a QTL with same color code across environment, a variation in the color intensity from one environment to the next indicates presence of non-crossover QEI (Boer et al., 2007; Malosetti et al., 2013). In this context, the first QTL detected on chromosome 2B and 5A.1 showed significant crossover QEI (Fig 2). In contrast, the QTL on 5B and the third QTL mapped on chromosome 2B showed non-crossover QEI. Chromosome 3B, 6B and 7A.1 showed relatively high peak, but they did not meet the statistical threshold for significant QTL in the present study. A major QTL for GY was detected on chromosome 2B with a –log (P) value of 17.3 (Table 4). The GY QTL on chromosome 5B was detected under drought and well-watered conditions suggesting that it is environment non-specific. This is consistent with the observation that it had non-significant crossover QEI. The proportion of phenotypic variance accounted for by the GY QTL ranged from 11.3-46.7% for the first QTL on 2B, 1.9-27.2% for the second QTL on 2B and 6.8-31.2 for the third QTL on 2B (Table 4). The QTL on 5A.1 and 5B explained 2.5-5.0% and 2.2-11.8% of the phenotypic variance respectively (Table 4).

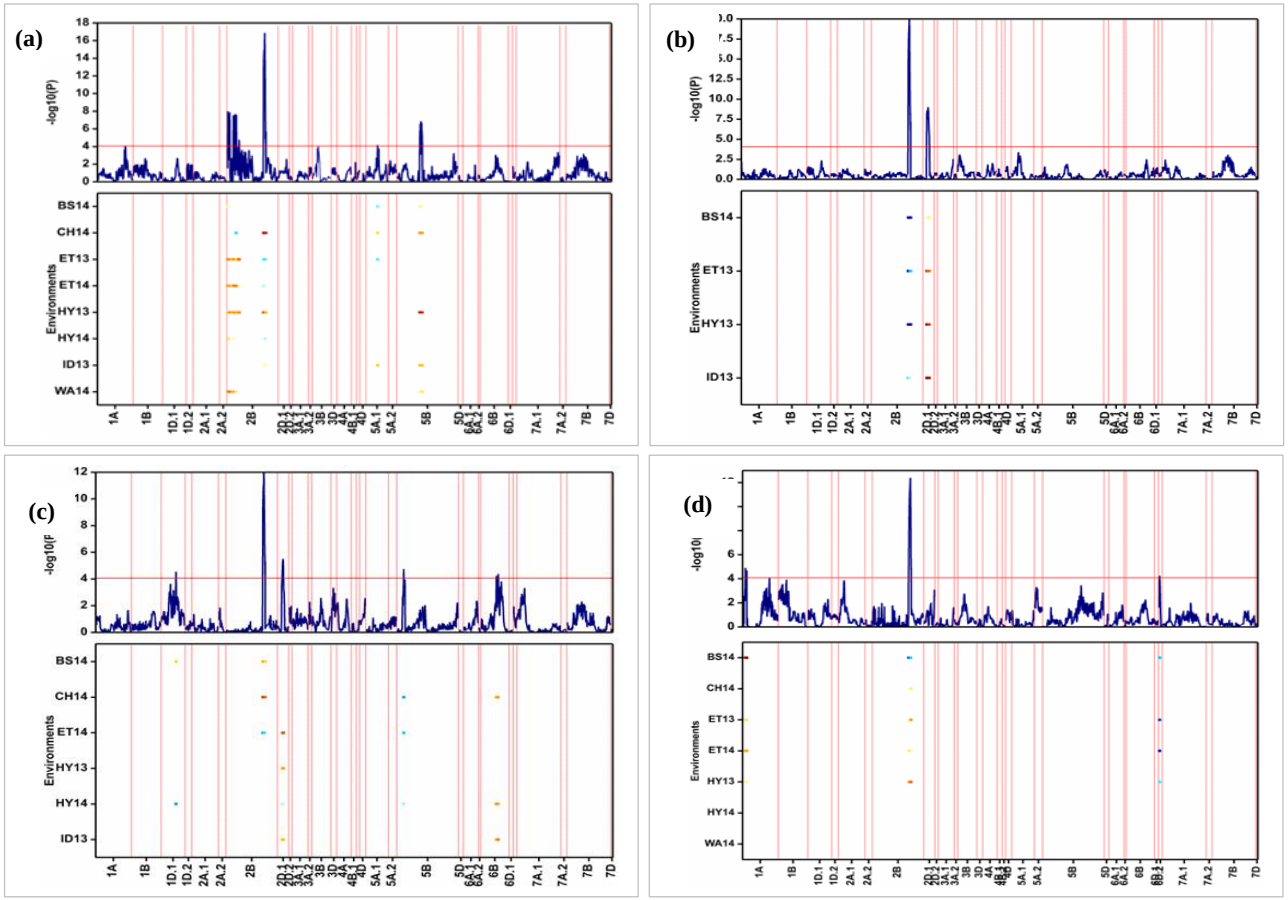

Figure 2. Genome-wide QTL scan for grain yield and agronomic traits across multiple environments.
The upper graph is the QTL profile plot with the y-axis representing the log of likelihood, -log (P), for declaring significant QTL. The red horizontal line represents the threshold corrected for the number of independent tests using Li and Ji (1997). The lower plot is the genome-wide heat map of significant QTL across environments. The y-axis is the environments and the x-axis represents the linkage groups. Two vertical dotted lines or a dotted and continuous line delineate a linkage group. The light blue to blue color indicates the high value allele (HVA) originates from CO960293-2 and the yellow-red color indicates the HVA originates from TAM 111. (a) Grain yield (GY) (b) Days to heading (DTH) (c) Plant height (PH) (d) Test weight (TW)

Table 4 QTL detected using single trait multi-environment QTL mapping model

QTL name	Chr.	Peak SNP‡	Pos.	CI_LL	CI_UL	Min. A	Max. A	Min. R^2	Max. R^2	-log10(P)	Trait†
Qtw.tamu.1A	1A	M11395	31.7	15.3	48.1	0.35	0.35	9.2	9.2	6.1	TW
Qspm.tamu.1A	1A	M56355	231.0	219.0	243.0	13.10	21.80	5.5	11.6	4.8	SPM
Qmshw.tamu.1A	1A	M63891	269.0	260.1	277.9	0.03	0.03	5.5	14.8	9.5	MSHW
Qtkw.tamu.1A	1A	M72042	292.8	251.9	333.7	0.29	0.53	2.4	5.5	4.7	TKW
Qph.tamu.1D.1	1D.1	M60470	156.7	125.9	187.5	0.64	1.57	4.6	6.2	4.0	PH
Qkps.tamu.2A.1	2A.1	M64705	58.1	40.5	75.7	0.86	0.86	5.5	8.7	7.3	KPS
Qgy.tamu.2B	2B	M27744	5.6	1.8	9.4	0.23	0.38	6.8	31.2	7.8	GY
Qgy.tamu.2B	2B	M2943	129.3	126.8	131.8	0.13	0.46	11.3	46.7	7.2	GY
Qtkw.tamu.2B	2B	M30115	403.8	399.7	408.0	0.54	1.26	8.7	28.9	25.8	TKW
Qgy.tamu.2B	2B	M3178	406.1	401.7	410.5	0.06	0.19	1.9	27.2	17.3	GY
Qdth.tamu.2B	2B	M3178	406.1	402.6	409.6	0.33	0.91	2.3	33.9	21.3	DTH
Qspm.tamu.2B	2B	M72380	406.2	380.9	431.5	9.32	16.88	5.2	7.0	9.0	SPM
Qph.tamu.2B	2B	M16370	406.3	389.8	422.8	0.70	1.41	5.5	9.2	11.1	PH
Qtw.tamu.2B	2B	C7P408	408.1	400.2	416.1	0.21	0.71	3.0	16.2	22.1	TW
Qdth.tamu.2D.1	2D.1	M41046	50.4	45.3	55.5	0.25	1.05	2.3	23.9	9.0	DTH
Qph.tamu.2D.1	2D.1	M17212	55.0	43.7	66.3	1.18	2.55	8.8	12.2	5.7	PH
Qgy.tamu.5A.1	5A.1	M35863	122.4	67.3	177.5	0.04	0.25	2.5	5.0	4.3	GY
Qtkw.tamu.5A.2	5A.2	M11474	11.0	0.0	25.2	0.48	0.89	4.2	10.2	5.7	TKW
Qph.tamu.5B	5B	M23725	70.1	38.0	102.2	0.77	1.11	4.2	6.1	4.1	PH
Qgy.tamu.5B	5B	M3083	257.3	245.5	269.1	0.05	0.27	2.2	11.8	6.3	GY
Qkps.tamu.5B	5B	M79424	538.2	523.5	553.0	0.82	1.01	7.8	9.9	5.6	KPS
Qtkw.tamu.6A.1	6A.1	M13129	128.5	117.7	139.3	0.51	0.92	5.2	12.6	8.1	TKW
Qph.tamu.6B	6B	M62061	184.2	165.7	202.7	0.77	2.50	5.2	8.5	4.1	PH
Qtw.tamu.6D.2	6D.2	M20798	6.4	0.0	29.3	0.28	0.28	1.8	6.0	4.1	TW
Qkps.tamu.7A.1	7A.1	M6693	415.6	399.4	431.8	0.47	1.11	2.1	5.6	6.2	KPS
Qtkw.tamu.7B	7B	M46562	16.8	0.0	46.2	0.46	0.46	2.7	6.4	4.1	TKW

Chr., chromosome; Pos, position of the peak SNP; CI_LL, lower limit of QTL confidence interval; CI_UL, upper limit of QTL confidence interval; Min., minimum; Max., maximum; A, additive effect; R^2, proportion of phenotypic variance explained by QTL

†GY, grain yield; DTH, days to heading; PH, plant height; TW, test weight; TKW, thousand kernel weight; MSHW, mean single head weight; SPM, spike metre^{-2}; KPS, kernel spike^{-1}

‡All SNP markers on the array are abbreviated using letter M and their respective index number whereas pseudo-markers are abbreviated using the linkage group and their position on the linkage group e.g C7P408 refers to a pseudo-marker on linkage group 7 (chromosome 2B) at position 408 cM.

Individual environment mapping revealed GY QTL on chromosome 7B in BS14; 2B and 3B in CH14; 3B in ET13; 2B and 5B in HY13; and 5B in WA14. The QTL on chromosome 5B in HY13, and the QTL detected on chromosome 2B in CH14 and HY13 were also detected in a single trait multi-environment QTL mapping (Table 5).

DTH QTL were detected on chromosome 2B and 2D.1 (Fig. 2B). The map positions for DTH QTL were consistent both in individual and across environments (Table 5). The DTH QTL on 2B consistently showed HVA from the maternal parent whereas the QTL on 2D.1 showed HVA from the paternal parent. No significant crossover QEI was observed for these two QTL suggesting that they are environment non-specific. In addition, the single trait multi-environment model detected these QTL in all the environments where data was recorded suggesting that these QTL were constitutive at least for the environment used in this study (Table 4).

In a single trait multi-environment mapping model, PH QTL were detected on chromosome 1D.1, 2B, 2D.1, 5B and 6B although none of the QTL was detected in all the environments (Fig. 2c). The QTL on 1D.1, 2B, and 2D.1 showed significant QEI and similar to most of the traits, the largest peak was observed on chromosome 2B. Single environment QTL analysis revealed PH QTL on chromosome 2B in CH14, 7A.1 in ET14 and 2D.2 in HY13 (Table 5). The QTL on 2B and 2D.2 were also detected in a multi-environment QTL analysis (Table 4).

Table 5 Individual environment quantitative trait loci

Env†	QTL name	Chr.	Peak	Pos.	CI_LL	CI_UL	A‡	R^2	Trait	-log10(P)
BS14	*Qtw.tamu.1A*	1A	M73184	32.2	20.9	43.5	-0.40	12.2	TW	6.1
ET13	*Qmshw.tamu.1A*	1A	M54227	186.2	172.0	200.4	-0.03	10.2	MSHW	3.5
ET14	*Qtw.tamu.1A*	1A	M40942	210.4	198.3	222.5	-0.42	11.5	TW	5.3
CH14	*Qkps.tamu.1A*	1A	M2320	239.0	222.3	255.7	-0.88	9.1	KPS	4.1
ET13	*Qspm.tamu.1A*	1A	M78483	266.8	256.1	277.5	22.85	12.7	SPM	5.5
HY13	*Qmshw.tamu.1A*	1A	M51724	269.0	261.2	276.8	-0.03	16.4	MSHW	3.0
BS14	*Qspm.tamu.1A*	1A	M51724	269.0	253.1	284.9	15.42	9.4	SPM	4.2
HY13	*Qtw.tamu.1A*	1A	M28622	298.4	284.3	312.5	-0.67	10.3	TW	5.2
HY13	*Qtw.tamu.1B*	1B	M58050	40.5	28.3	52.7	-0.71	11.4	TW	6.1
ET13	*Qtw.tamu.1B*	1B	M79445	84.1	67.9	100.3	-0.45	9.3	TW	4.1
HY14	*Qgy.tamu.1D.1*	1D.1	M60470	156.7	144.0	169.4	0.29	11.1	GY	4.9
HY13	*Qkps.tamu.2A.1*	2A.1	M7015	55.3	40.7	69.9	-1.02	10.0	KPS	4.0
ET13	*Qkps.tamu.2A.1*	2A.1	M20877	61.4	51.0	71.7	-1.32	13.0	KPS	5.0
BS14	*Qts.tamu.2A.2*	2A.2	M27612	49.9	42.0	57.8	4.56	16.3	TS	4.7
HY13	*Qgy.tamu.2B*	2B	M21618	399.4	379.8	419.0	-0.11	8.2	GY	4.0
CH14	*Qmshw.tamu.2B*	2B	M21618	399.4	392.2	406.6	-0.03	17.7	MSHW	6.5
ET14	*Qtkw.tamu.2B*	2B	M21618	403.8	391.8	415.8	-0.95	11.6	TKW	5.5
HY13	*Qtkw.tamu.2B*	2B	M21618	403.8	390.0	417.6	-0.73	10.4	TKW	5.9
BS14	*Qgla.tamu.2B*	2B	M21618	403.8	401.1	406.5	12.47	43.8	GLA	21.9
ET13	*Qdth.tamu.2B*	2B	M8143	404.3	394.2	414.4	0.46	13.4	DTH	5.7
BS14	*Qgfl.tamu.2B*	2B	M8143	404.3	401.6	407.0	11.17	43.9	GFL	21.0
CH14	*Qgy.tamu.2B*	2B	M3178	406.1	401.2	411.0	-0.11	24.9	GY	11.5
BS14	*Qdth.tamu.2B*	2B	M3178	406.1	402.3	409.9	0.91	31.5	DTH	13.7
HY13	*Qdth.tamu.2B*	2B	M3178	406.1	402.6	409.6	0.76	33.9	DTH	16.2
CH14	*Qtkw.tamu.2B*	2B	M3178	406.1	402.4	409.8	-1.33	32.5	TKW	14.3
HY13	*Qtw.tamu.2B*	2B	M3178	406.1	388.8	423.4	-0.63	8.9	TW	5.1
CH14	*Qgfl.tamu.2B*	2B	M3178	406.1	404.3	407.9	14.84	63.9	GFL	32.0

Env., environment; Chr., chromosome; Pos, position of the peak SNP; CI_LL, lower limit of QTL confidence interval; CI_UL, upper limit of QTL confidence interval; A, additive effect; R^2, proportion of phenotypic variance explained by QTL; HVA, high value allele; MT, maternal parent; PP, paternal parent.

GY, grain yield; DTH, days to heading; HI, harvest index; KPS, kernels spike^{-1}; MSHW, mean single head weight; SPM, spike metre^{-2}; TKW, thousand kernel weight; TS, tiller number; TW, test weight; GFL, greenness of the flag leaf; GLA, green leaf area.

†BS14, Bushland 2014; CH14, Chillicothe,2014; ET13, Etter 2013; HY13, Hays 2013; HY14, Hays 2014; ID13, Idaho 2013; WA, Walsh 2014; ET14, Etter 2014.

‡Negative additive effect indicate high value allele (HVA) from TAM 111, positive values correspond to HVA from CO960293-2**.**

Table 5 Continued

Env†	QTL name	Chr.	Peak SNP	Pos.	CI_LL	CI_UL	A‡	R^2	Trait	-log10(P)
CH14	*Qgla.tamu.2B*	2B	M3178	406.1	401.3	410.9	4.38	25.5	GLA	10.9
BS14	*Qtw.tamu.2B*	2B	M43273	406.2	388.0	424.4	0.33	8.6	TW	3.8
CH14	*Qph.tamu.2B*	2B	M53589	413.6	400.7	426.5	-1.03	10.9	PH	4.8
ET14	*Qspm.tamu.2B*	2B	M34527	429.4	419.0	439.8	19.56	13.0	SPM	4.1
HY13	*Qdth.tamu.2D.1*	2D.1	M41046	50.4	40.5	60.3	-0.48	13.5	DTH	6.1
ID13	*Qdth.tamu.2D.1*	2D.1	M41046	50.4	45.3	55.4	-1.06	24.2	DTH	8.0
ET14	*Qtw.tamu.2D.1*	2D.1	M16362	68.7	62.4	75.0	0.55	19.8	TW	7.3
CH14	*Qtw.tamu.2D.1*	2D.1	M16362	72.7	56.7	88.7	0.46	9.4	TW	4.1
HY13	*Qtw.tamu.2D.1*	2D.1	M80047	74.9	66.0	83.8	0.81	14.8	TW	7.6
HY13	*Qph.tamu.2D.2*	2D.2	M63568	22.4	7.3	23.9	-1.22	9.8	PH	4.1
HY13	*Qtkw.tamu.3A.1*	3A.1	M27980	27.2	0.0	66.4	-0.53	5.6	TKW	3.5
ET13	*Qgy.tamu.3B*	3B	M79678	37.6	27.0	48.2	0.09	12.8	GY	5.5
BS14	*Qgla.tamu.3B*	3B	M80866	65.1	49.2	81.0	5.78	9.4	GLA	5.9
CH14	*Qgy.tamu.3B*	3B	M34153	70.7	54.9	86.5	0.07	9.4	GY	5.1
HY13	*Qgy.tamu.5B*	5B	M3083	257.3	246.7	267.9	-0.13	12.8	GY	6.1
WA14	*Qgy.tamu.5B*	5B	M35160	377.2	359.6	394.8	-0.23	8.7	GY	3.9
BS14	*Qkps.tamu.5B*	5B	M44296	511.4	495.9	526.9	-0.91	9.6	KPS	4.2
ET13	*Qtkw.tamu.6A.1*	6A.1	M13129	128.5	119.8	137.2	0.71	15.0	TKW	6.3
ET14	*Qtkw.tamu.6A.1*	6A.1	M13129	128.5	118.2	138.8	1.01	13.1	TKW	6.0
CH14	*Qtkw.tamu.6A.1*	6A.1	M21913	129.9	99.6	155.1	0.59	6.3	TKW	3.8
HY13	*Qhi.tamu.6D.2*	6D.2	M4286	13.8	0.6	27.0	0.02	10.8	HI	4.5
ET14	*Qph.tamu.7A.1*	7A.1	M36479	49.6	41.0	58.2	-2.12	15.3	PH	6.2
HY13	*Qtkw.tamu.7A.1*	7A.1	M35275	417.5	395.8	439.2	0.62	7.6	TKW	4.6
BS14	*Qtkw.tamu.7B*	7B	M66570	16.9	0.1	33.7	0.79	9.0	TKW	4.0
BS14	*Qgy.tamu.7B*	7B	M5325	145.0	128.7	161.3	0.11	9.2	GY	4.2

The QTL linked to TW were detected on chromosome 1A, 2B, and 6D.2 based on a single trait multi-environment mapping model (Fig. 2D, Table 4). In individual environment analysis, TW QTL were detected on chromosome 1A and 2B in BS14, chromosome 1A and 2D.1 in ET14, chromosome 2D.1 in both ET13 and CH14 (Table 5). The QTL on chromosome 1A in BS14 and chromosome 2B in BS14 and HY13 showed consistent position with single trait multi-environment QTL analysis results (Table 5).

Multi-environment QTL analysis for TKW revealed significant QTL on five different chromosomes *viz.* 1A, 2B, 5A.2, 6A.1 and 7B (Fig. 3a). All QTL except for the QTL on chromosome 2B had no significant crossover QEI suggesting environment non-specificity for these QTL. The QTL on chromosome 5A.2, 6A.1 and 7B had HVA from

the maternal parent whereas the QTL on 1A showed HVA from paternal parent. The TKW QTL on chromosome 2B and 6A.1 were detected in all the five environments where the trait was recorded (Fig. 3a). Although the QTL on chromosome 2B showed significant QEI as indicated by a color change in the heat map, four of the five environments showed paternal consistency for HVA. In comparison with single environment QTL analysis, the QTL for TKW on chromosome 2B was detected in CH14, ET13 and HY13 whereas the QTL on chromosome 7B was detected only in BS14 (Table 5). The TKW QTL on chromosome 6A.1 was detected in CH14, ET13 and ET14 (Table 5).

A constitutive QTL for MSHW was mapped on chromosome 1A in a multi-environment model and regardless of the environment, the HVA originated from the paternal parent (Fig. 3b). For this trait several peaks were observed on chromosome 2B, 3B, 6A.1, 6B and 7A.1 but they did not meet the threshold to be declared significant QTL. Thus, other regions in the genome could be linked to MSHW (Fig.3b). In the single-environment QTL analysis model, QTL for MSHW was mapped on chromosome 1A in ET13 and HY13 with the QTL position in HY13 consistent with the QTL position in a multi-environment model (Table 5). In BS14, MSHW QTL was detected on chromosome 2B (Table 5). A constitutive QTL for KPS was mapped on chromosome 2A.1 with HVA from the paternal parent (Fig. 3d). Other QTL for KPS were detected on chromosome 5B and 7A.1 although none of these QTL was expressed constitutively. In individual environment QTL analysis, KPS QTL was detected on chromosome 5B in BS14, chromosome 1A in CH14, and chromosome 2A.1 in ET13 and HY13 (Table 5). In all the environments except ET14, the HVA was consistently from the paternal parent (Table 5).

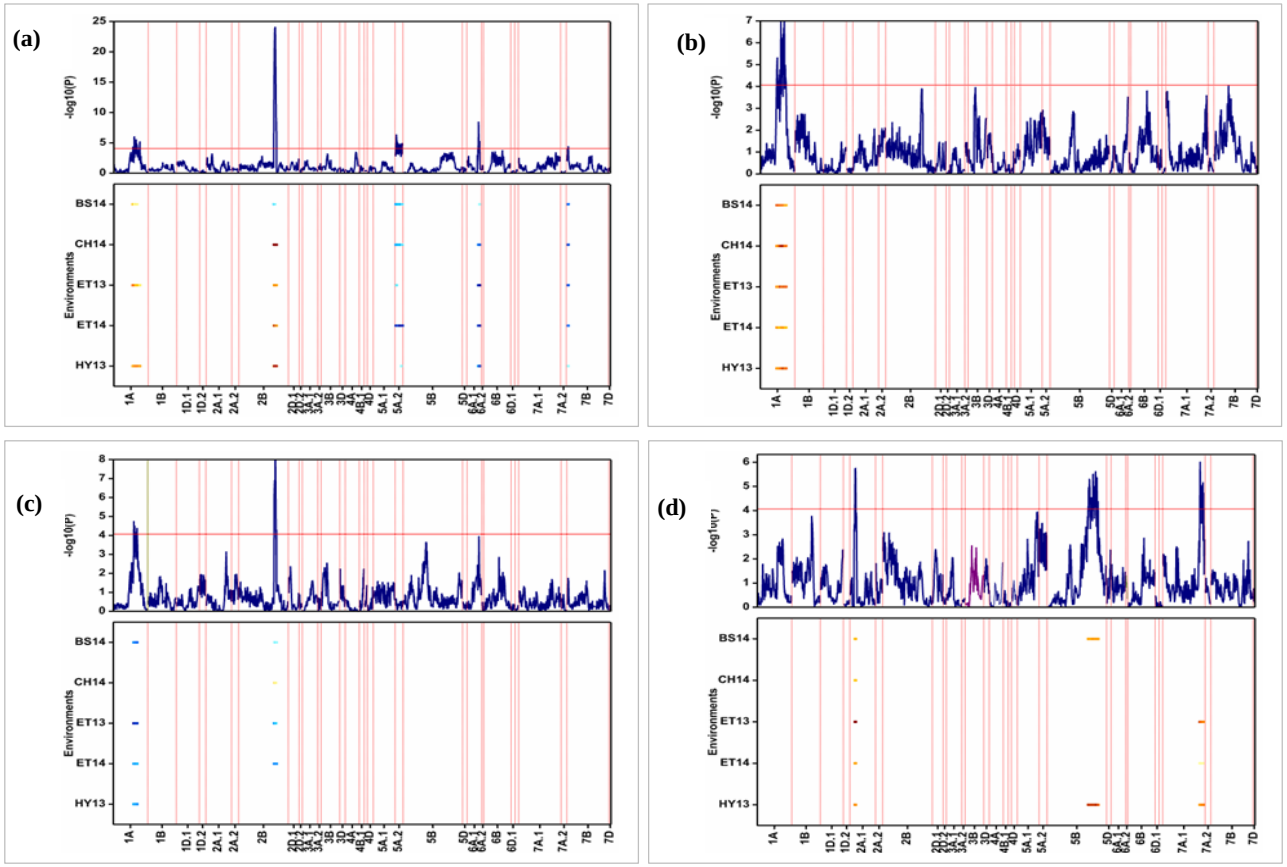

Figure 3. Single trait genome-wide QTL scan for yield components across the multiple environments.
The upper graph is the QTL profile plot with the y-axis representing the log of likelihood, -log (P), for declaring significance of QTL. The red horizontal represents the threshold corrected for the number of independent tests using Li and Ji (1997). The lower plot is the genome-wide heat map of significant QTL across environments. The y-axis is the environments and the x-axis represents the linkage groups. Two vertical dotted lines or a dotted and continuous line delineate a linkage group. The light blue to blue color indicates the high value allele (HVA) originates from CO960293-2 and the yellow-red color indicates the HVA originates from TAM 111. (a) Thousand kernel weight (TKW) (b) Mean single head weight (MSHW) (c) Spike metre^{-2} (SPM) (d) Kernels spike^{-1} (KPS) (e) Greenness of the flag leaf (GFL)
BS14, Bushland 2014; CH14, Chillicothe 2014; ET13, Etter 2013; ET14, Etter 2014; HY13, Hays 2013; HY14, Hays 2014

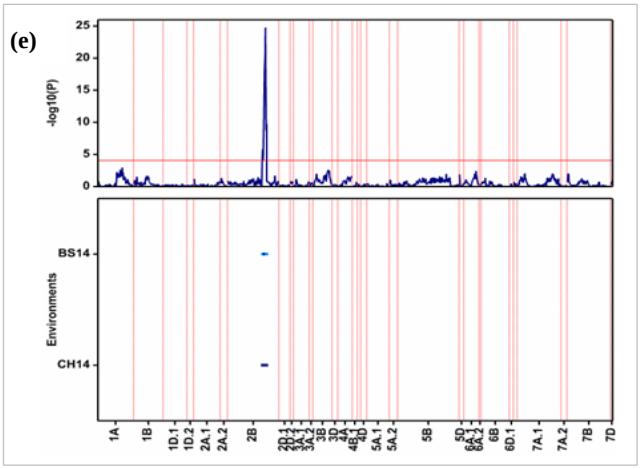

Figure 3 Continued

The SPM QTL were detected on chromosome 1A and 2B in BS14, ET13 based on individual environment mapping algorithm (Table 5) and single trait multi-environment QTL mapping (Table 4, Fig 3c). The GFL QTL was detected on chromosome 2B both in individual (Table 5) and in combined environment analysis (Table 4, Fig. 3f).

In a multi-environment QTL analysis model, QTL for GY, DTH, PH, TW, TKW, and SPM were co-located on chromosome 2B whereas DTH and PH were co-located on chromosome 2D.1 (Table 4). In the individual environment QTL analysis, BS14 showed co-location of QTL for GFL, DTH and TW on chromosome 2B and in the same position as the single trait multi-environment co-location (Table 5). In addition, QTL for PH and GY were co-located on chromosome 7B. In CH14, the QTL for GY, TKW, GFL, and PH were co-located on chromosome 2B and in the same position as the co-location observed in BS14. The co-location of QTL for TKW and KPS on chromosome 2B was observed in ET14 whereas the co-location of QTL for GY, HI, TKW, DTH and TW was observed in

HY13. The co-location of QTL for different traits could partly explain the genetic correlation observed in this study.

Additive effect and proportion of phenotypic variance explained by the QTL

The QTL additive effect varied across chromosomes and environments (Fig. 4). The highest additive effect for GY was observed on chromosome 2B where a maximum value of 0.46 t ha^{-1} was recorded with HVA originating from the paternal parent (Table 4, Fig. 4a). The first GY QTL on chromosome 2B had a maximum additive effect of 0.38 t ha^{-1} with HVA originating from the maternal parent (CO960293-2) (Fig. 4a). The third QTL on 2B and the QTL mapped on chromosome 5A.1 and 5B showed an oscillation in QTL additive effect ranging from 0.06 to 0.27 t ha^{-1} (Fig. 4a). The HVA for the QTL on 5B was consistent across all the environments indicating a negligible role of QEI on the additive effect for this QTL. However, for QTL on 2B and 5A.1 the HVA switched among environments, hence the QEI was important for these QTL (Fig. 4a).

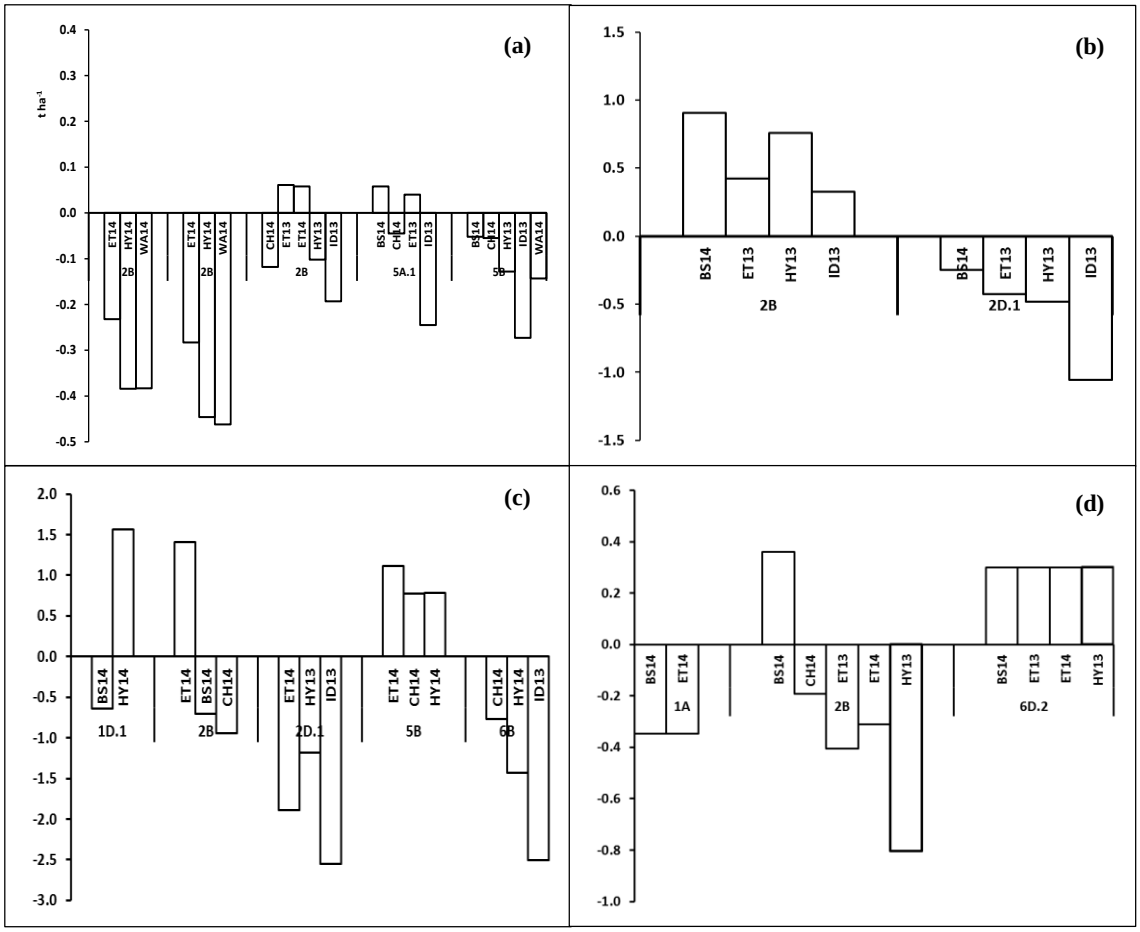

Figure 4. Multi-environment QTL additive effect for grain yield and yield components. The y-axis represents the additive effect and the x-axis is the environment and chromosome where QTL with significant effect were mapped. Positive values indicate high value (HVA) from CO960293-2 whereas negative values indicate HVA from TAM 111. Each QTL is represented by a cluster of bar graph. (a) Grain yield (GY) (b) Days to heading (DTH) (c) Plant height (PH) (d) Test weight (TW) (e) Thousand kernel weight (TKW) (f) Mean single head weight (MSHW) (g) Spike metre^{-2} (SPM) (h) Kernel spike^{-1}(KPS) (i) Greenness of the flag leaf (GFL).
BS14, Bushland 2014; CH14, Chillicothe 2014; ET13, Etter 2013; ET14, Etter 2014; HY13, Hays 2013; HY14, Hays 2014; ID13; Idaho 2013; WA14, Walsh 2014.

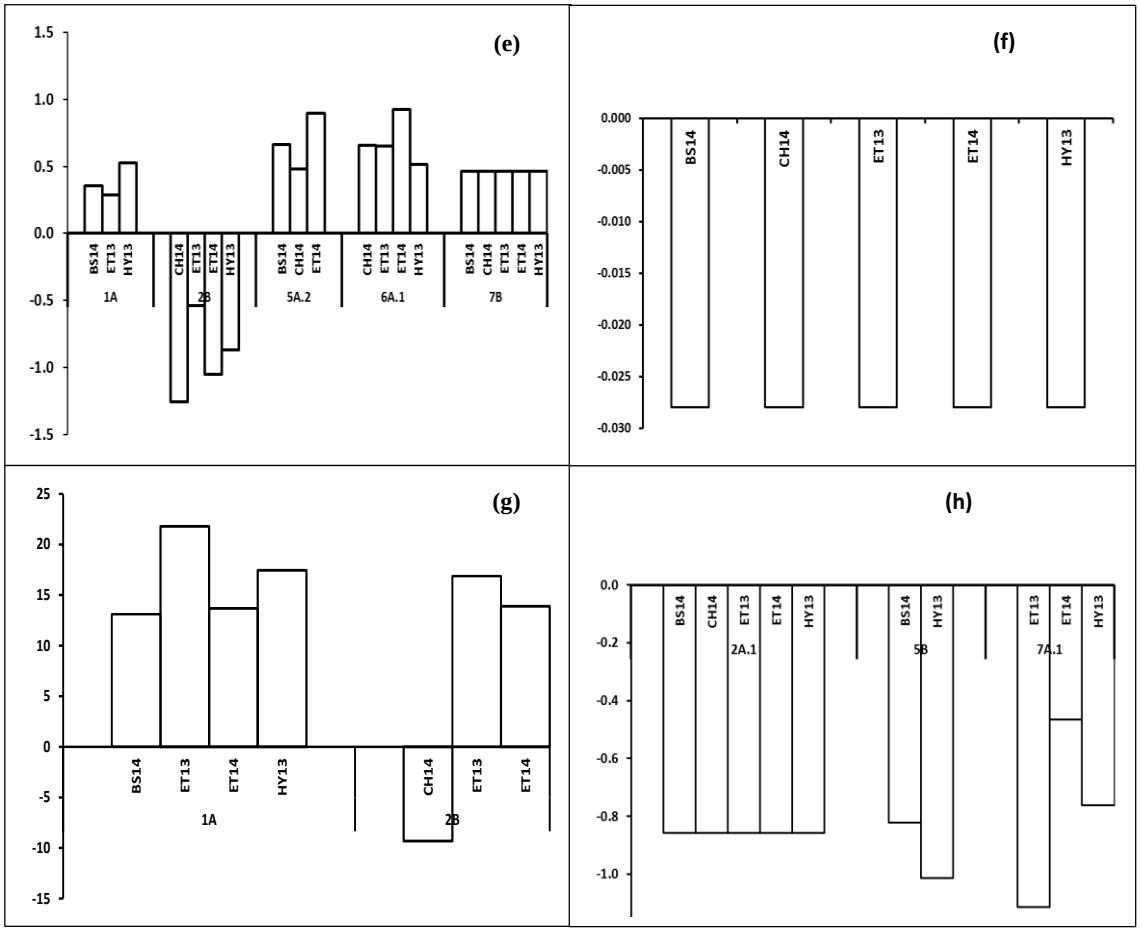

Figure 4 Continued

The switch from negative to positive and vice versa is due to significant crossover QEI. The multiple QTL observed for GY in the present study underscores the complex genetic architecture underlying this trait and the need for multi-environment testing to dissect the underlying basis of modulation. Although none of the QTL was identified in all the environments used in this study, most of the QTL for GY were mapped under both

drought and well-watered environments. This suggests some similarity in mechanisms regulating GY under contrasting moisture conditions.

The additive effect for the TKW QTL on chromosome 1A ranged from an absolute value of 0.29 to 0.53 grams (Table 4). Among the three environments where the TKW QTL were detected on chromosome 1A, ET13 and HY13 had significant additive effect with an R^2 ranging from 2.4 to 5.5% (Table 4). The additive effect for TKW QTL on chromosome 2B was significant in all the environments except BS14 and it ranged from 0.54 to 1.26 grams. The corresponding R^2 ranged from 8.7 to 28.9%. The TKW QTL mapped on 5A.2 had an additive effect range of 0.14-0.89 grams although only three of the five environments had statistically distinguishable values for the genetic effects. The corresponding R^2 explained by the QTL for TKW on 5A.2 ranged from 4.2 to 10.2% (Table 4). The additive effect for TKW QTL on 6A.1 ranged from 0.13 to 0.92 grams. All the environments except BS14 showed significant additive effect (Fig. 4e) and the R^2 ranged from 5.2 to 12.6% (Table 4). The QTL on 7B was constitutive with respect to the environments where the trait was recorded. This QTL showed the same magnitude of additive effect in all environments (Fig. 4e) and the R^2 ranged from 2.7 to 6.4% (Table 4). The HVA for TKW was consistent for most QTL except for the QTL on 2B which showed a change in the source of HVA depending on the environment (Fig. 3a, Fig. 4e). Despite the switch in the source of HVA, the results in this study suggest that TKW did not show significant QEI because the additive effect of the QTL on 2B was not statistically significant in BS14.

Days to heading (DTH) showed significant additive effect ranging from 0.33-0.91 days on chromosome 2B and 0.25 to 1.05 days on chromosome 2D.1. The R^2 for the DTH QTL on 2B ranged from 2.3 to 33.9% whereas the QTL on 2D.1 had an R^2 range of 2.3 to 23.9% (Table 4). The HVA for the DTH QTL on chromosome 2B and 2D.1 was contributed by the maternal and paternal parent respectively (Fig 4b)

The additive effect of QTL for PH on chromosome 1D.1, 2B, 2D.1, 5B and 6B ranged from 0.64 to 1.57 cm, 0.70 to 1.41 cm, 1.18 to 2.55 cm, 0.77 to 1.11 cm and 0.77 to 2.50 cm, respectively. The highest R^2 was observed on chromosome 2D.1 while the remaining QTL had an R^2 less than 10% with a range of 4.2 to 9.2% (Table 4). The QTL on chromosome 2D.1, 5B and 6B showed consistency in terms of HVA whereas the QTL on chromosome1D.1 and 2B showed an oscillation in the source of HVA depending on the environment (Fig 4c). The highest R^2 was observed on chromosome 2D.1 which ranged from 8.8 to 12.2%. The rest of the QTL on chromosome 1D.1, 2B, 5B and 6B had an R^2 less than 10% (Table 4).

Three QTL for TW had a significant additive effect (Fig 4d). The TW QTL on chromosome 1A and the first QTL on chromosome 6D.2 showed consistent effects across all the environments suggesting that the expression of these QTL was independent of the environmental conditions in this study. The QTL on chromosome 2B showed variable additive effect across environments with a range of 0.2 to 0.70 Ib/bu. We observed variable R^2 for all the three QTL, albeit the QTL on chromosome 1A and the first QTL on chromosome 6D.2 having a constant additive effect across environments. The range in R^2 for the QTL on chromosome 1A was 2.7 to 9.2% whereas the QTL on chromosome 2B

and 6D.2 had a range of 3.0 to 16.2% and 1.8 to 6.0%, respectively (Table 4). The HVA for TW QTL were consistent across environments except for the QTL on chromosome 2B (Fig 4d).

The sole and constitutive QTL for MSHW detected in this study showed a significant additive effect of 0.03 grams with a variable R^2 ranging from 5.5 to 14.8%. In addition, the HVA was consistent in all environments (Fig. 5f). The SPM had two QTL with significant additive effect on chromosome 1A and 2B. The range in additive effect for the two QTL was ≈13 to 22 spikes and ≈ 9.0 to 17 spikes, respectively. The two QTL explained a maximum proportion of phenotypic variance of 11.6% and 7.0%, respectively. The HVA for the QTL on 1A was from the maternal parent in all the environments whereas the QTL on chromosome 2B showed a switch between the parents depending on the environment (Fig 4g)

QTL with significant additive effect for KPS were mapped on chromosome 2A.1, 5B and 7A.1. The QTL detected on chromosome 1A showed a constant additive effect in all the environments but had a variable R^2 ranging from 5.5 to 8.7% (Table 4, Fig 4h). The QTL on chromosome 5B and 7A.1 showed variability both in additive effect and the R^2. The additive effect for the QTL on chromosome 5B ranged from 0.82 to 1.11 kernels with a corresponding R^2 range of 7.8 to 9.9% whereas the additive effect for the QTL on 7A.1 ranged from 0.47 to 1.11 kernels with an R^2 range of 2.1 to 5.6% (Table 4, Fig.4h)

Table 6 Multi- trait QTL detected using data pooled across environments.

QTL name	Chr	Peak SNP†	Pos	CI_LL	CI_UL	A‡	R^2	-log10(P)	Trait
Qkps.tamu.2A	2A	M64705	58.1	49.5	66.7	-0.39	15.2	5.8	KPS
Qmshw.tamu.2A	2A	M64705	58.1	49.5	66.7	-0.17	2.7	5.8	MSHW
Qts.tamu.2A	2A	M64705	58.1	49.5	66.7	0.23	5.2	5.8	TS
Qtw.tamu.2A	2A	M64705	58.1	49.5	66.7	0.20	4.2	5.8	TW
Qdth.tamu.2B	2B	M3178	406.1	404.2	408.0	0.48	22.6	48.2	DTH
Qgfl.tamu.2B	2B	M3178	406.1	404.2	408.0	0.79	61.7	48.2	GFL
Qgla.tamu.2B	2B	M3178	406.1	404.2	408.0	0.67	44.3	48.2	GLA
Qhi.tamu.2B	2B	M3178	406.1	404.2	408.0	-0.51	25.9	48.2	HI
Qmshw.tamu.2B	2B	M3178	406.1	404.2	408.0	-0.33	11.0	48.2	MSHW
Qtkw.tamu.2B	2B	M3178	406.1	404.2	408.0	-0.36	13.1	48.2	TKW
Qts.tamu.2B	2B	M3178	406.1	404.2	408.0	0.24	5.8	48.2	TS
Qtw.tamu.2B	2B	M3178	406.1	404.2	408.0	-0.16	2.5	48.2	TW
Qdth.tamu.2D.1	2D.1	C8P52	51.7	45.7	57.7	-0.45	20.6	8.0	DTH
Qgla.tamu.2D.1	2D.1	C8P52	51.7	45.7	57.7	-0.22	4.7	8.0	GLA
Qph.tamu.2D.1	2D.1	C8P52	51.7	45.7	57.7	-0.38	14.6	8.0	PH
Qts.tamu.2D.1	2D.1	C8P52	51.7	45.7	57.7	0.14	2.0	8.0	TS
Qtw.tamu.2D.1	2D.1	C8P52	51.7	45.7	57.7	0.29	8.2	8.0	TW
Qgm.tamu.5A.1	5A.1	C18P118	118.4	96.9	139.9	0.14	2.0	3.4	GM
Qgy.tamu.5A.1	5A.1	C18P118	118.4	96.9	139.9	-0.19	3.6	3.4	GY

Chr, chromosome; Pos, position of peak SNP; CI_LL, lower limit of QTL confidence interval; CI_UL, upper limit of QTL confidence interval; A, additive effect; R^2, percentage of phenotypic variance explained by the QTL.

†KPS, kernel spike^{-1}; MSHW, mean single head weight; SPM, TS, tiller number; TW, test weight; DTH, days to heading; GFL, greenness of the flag leaf; GLA, green leaf area; HI, harvest index; TKW, thousand kernel weight; PH, plant height; GM, grain metre^{-2}; GY, grain yield; SPM, spikes metre^{-2}; BW, biomass weight.

†All SNP markers on the array are abbreviated using letter M and their respective index number whereas pseudo-markers are abbreviated using the linkage group and their position on the linkage group e.g C8P52 refers to a pseudo-marker on linkage group 8 (chromosome 2D) at position 55 cM.

‡Negative additive effect indicate high value allele (HVA) from TAM 111, positive values correspond to HVA from CO960293-2

Table 6 Continued

QTL name	Chr	Peak SNP†	Pos	CI_LL	CI_UL	A‡	R2	-log10(P)	Trait
Qmshw.tamu.5A.1	5A.1	C18P118	118.4	96.9	139.9	-0.22	4.7	3.4	MSHW
Qspm.tamu.5A.1	5A.1	C18P118	118.4	96.9	139.9	0.15	2.2	3.4	SPM
Qtkw.tamu.5A.1	5A.1	C18P118	118.4	96.9	139.9	-0.24	5.9	3.4	TKW
Qts.tamu.5A.1	5A.1	C18P118	118.4	96.9	139.9	0.28	7.7	3.4	TS
Qdth.tamu.5B	5B	M45680	267.2	254.6	279.8	0.16	2.5	3.3	DTH
Qgfl.tamu.5B	5B	M45680	267.2	254.6	279.8	0.16	2.4	3.3	GFL
Qgla.tamu.5B	5B	M45680	267.2	254.6	279.8	0.16	2.7	3.3	GLA
Qgy.tamu.5B	5B	M45680	267.2	254.6	279.8	-0.33	11.2	3.3	GY
Qhi.tamu.5B	5B	M45680	267.2	254.6	279.8	-0.20	3.8	3.3	HI
Qspm.tamu.5B	5B	M45680	267.2	254.6	279.8	-0.15	2.3	3.3	SPM
Qhi.tamu.6A.1	6A.1	C22P146	145.6	135.5	155.1	0.31	9.6	6.3	HI
Qmshw.tamu.6A.1	6A.1	C22P146	145.6	135.5	155.1	0.30	8.9	6.3	MSHW
Qph.tamu.6A.1	6A.1	C22P146	145.6	135.5	155.1	0.22	5.0	6.3	PH
Qtkw.tamu.6A.1	6A.1	C22P146	145.6	135.5	155.1	0.37	13.3	6.3	TKW
Qts.tamu.6A.1	6A.1	C22P146	145.6	135.5	155.1	-0.26	6.9	6.3	TS
Qtw.tamu.6A.1	6A.1	C22P146	145.6	135.5	155.1	0.26	6.9	6.3	TW
Qbw.tamu.6B	6B	C24P188	187.7	163.1	212.4	0.13	2.0	5.1	BW
Qgm.tamu.6B	6B	C24P188	187.7	163.1	212.4	0.21	4.3	5.1	GM
Qmshw.tamu.6B	6B	C24P188	187.7	163.1	212.4	-0.17	2.8	5.1	MSHW
Qph.tamu.6B	6B	C24P188	187.7	163.1	212.4	-0.27	7.1	5.1	PH
Qspm.tamu.6B	6B	C24P188	187.7	163.1	212.4	0.26	6.9	5.1	SPM
Qtkw.tamu.6B	6B	C24P188	187.7	163.1	212.4	-0.14	1.8	5.1	TKW
Qts.tamu.6B	6B	C24P188	187.7	163.1	212.4	0.22	5.0	5.1	TS
Qtw.tamu.6B	6B	C24P188	187.7	163.1	212.4	0.21	4.6	5.1	TW

QTL linked to multiple traits based on multi-trait QTL scanning

Genome-wide multi-trait QTL scan for data averaged across seven environments revealed significant QTL on chromosome 2A.1, 2B, 2D.1, 5A.1, 5B, 6A.1, and 6B (Table 6, Fig. 5).For each QTL mapped, a change in direction of HVA (a switch in color from red to blue and vice versa) indicates presence of significant crossover QTI (Boer et al., 2007; Malosetti et al., 2013). Thus, all QTL detected using multi-trait mapping model revealed significant QTI (Fig. 5). The QTL on 2A.1 had a significant additive effect on KPS, MSHW, TS and TW. This QTL showed both crossover and non-crossover QTI as indicated by contrasting source of HVA and the variation in the intensity of the color respectively (Table 6). A similar explanation holds true for all other QTL mapped in the

heat map. Chromosome 2B was a hotspot for QTL associated with multiple traits suggesting that these genomic regions are essential (Fig. 5).

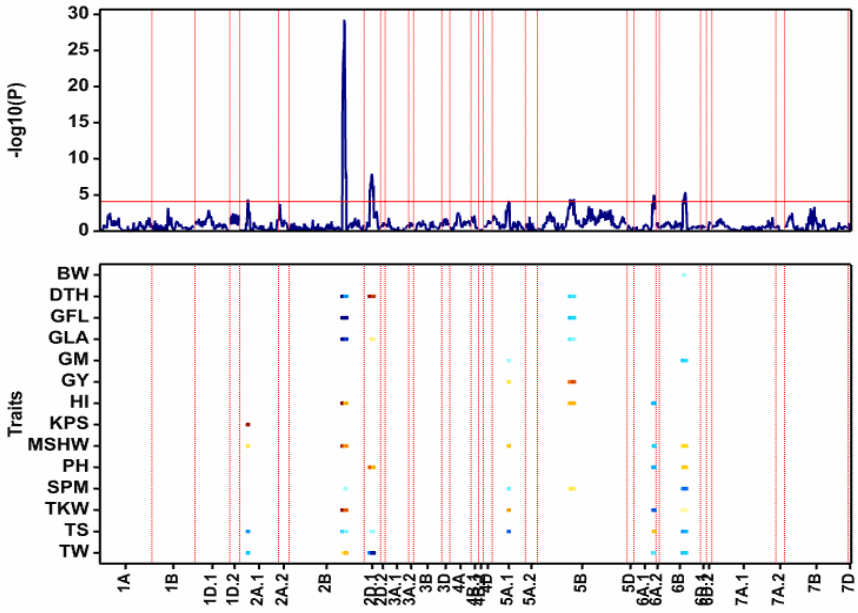

Figure 5. Genome-wide scan for multi-trait QTL for yield and yield components using data averaged across environment.

The upper graph is the QTL profile plot with the y-axis representing the log of likelihood, -log (P), for declaring significance of QTL. The red horizontal line represents the threshold corrected for the number of independent tests using Li and Ji (1997). The lower profile is the genome-wide heat map of significant QTL across environments. The y-axis is the traits and the x-axis represents the chromosomes. The light blue to blue color indicates the favorable allele originates from CO960293-2 and the yellow-red color indicates the favorable allele originates from TAM 111.BW, biomass weight; DTH, days to heading; GFL, greenness of the flag leaf; GLA, greenness of the leaf area; GM, grans metre^{-2}; GY, grain yield; HI, harvest index; KPS, kernels spike^{-1}; MSHW, mean single head weight; PH, plant height; SPM, spike metre^{-2}; TKW, thousand kernel weight; TS, tiller number; TW, test weight.

The QTL detected on chromosome 2B had a major peak and had a significant additive effect on all the traits except BW, GM, GY, KPS and PH (Fig. 5). The multi-trait QTL linked to GY were detected on chromosome 5A.1 and 5B with both QTL showing HVA from the paternal parent (TAM 111) (Fig. 5). BW QTL was mapped on chromosome

6B although the QTL accounted for very low percentage of phenotypic variation (Table 6). The QTL for PH were detected on chromosome 2D.1, 6A.1 and 6B and the chromosomal locations of QTL for PH on 2D.1 and 6B agreed with single trait multi-environment model (Figure 2c and Fig 5). All QTL for PH except the QTL on chromosome 6A.1 had HVA from paternal parent. DTH QTL were detected on 2B, 2D.1 and 5B whereas GLA and GFL QTL were both mapped on chromosome 2B and 5B although GLA had an additional QTL on 2D.1. The QTL for GM were detected on chromosome 5A.1 and 6B. HI QTL were mapped on 2B, 5B and 6A.1. KPS QTL was detected on chromosome 2A.1 with HVA from the paternal parent. In a single trait multi-environment model, we detected the QTL for KPS on chromosome 2A.1, 5B and 7A.1. MSHW showed five QTL on chromosomes 2A.1, 2B, 5A.1, 6A.1 and 6B. All the QTL for MSHW except QTL mapped on chromosome 6A.1 had HVA from the paternal parent. TKW QTL were mapped on chromosome 2B, 5A.1, 6A.1 and 6B (Fig 5). The QTL for TKW detected on 2B and 6A.1 were also detected in a single trait multi-environment model (Fig 3a). The QTL linked to SPM were detected on chromosome 5A.1, 5B and 6B with all the QTL except on 5B exhibiting HVA from the maternal parent. The QTL for TW were mapped on chromosome 2A.1, 2B, 2D.1, 6A.1 and 6B whereas the QTL for TS were detected on chromosome 2A.1, 2B, 2D.1, 5A.1, 6A.1 and 6B (Fig. 5).

The magnitude of additive effect for GY QTL under a multi-trait model was 0.19 t ha^{-1} for the QTL detected on chromosome 5A.1 and 0.33 t ha^{-1} for the QTL on chromosome 5B (Table 6) . For each multi-trait QTL detected, the additive effect and R^2 varied depending on the trait. The QTL on chromosome 2A.1 showed the highest additive

effect for KPS and lowest additive effect for TW. The highest proportion of phenotypic variance accounted by the multi-trait QTL on chromosome 2A.1 was observed on KPS. Comparatively, the multi-trait QTL detected on 2B was linked to the highest number of traits. The phenotypic variance accounted by the multi-trait QTL on 2B was highest for GFL (61.7%) followed by GLA (44.3%), HI (25.9%) and DTH (22.6%). The remaining traits had less than 14.0% of the phenotypic variance explained by this QTL (Table 6). For the multi-trait QTL detected on chromosome 2D.1, the additive effect ranged from 0.14 for TS to 0.45 for DTH. The DTH had the highest proportion of phenotypic variance (20.6%) accounted by the multi-trait QTL on chromosome 2D.1 (Table 6). The additive effect for the multi-trait QTL detected on chromosome 5A.1 ranged from 0.14 to 0.28 and for all the traits the proportion of variance accounted by this QTL was less than 10% (Table 6). The QTL detected on 5B had the highest additive effect on GY with a corresponding R^2 of 11%. Although this QTL had a significant additive effect on DTH, GFL, GLA, HI and SPM, the proportion of phenotypic variance accounted was low (Table 6). The range of additive effect for the multi-trait QTL detected on chromosome 6A.1 was 0.22 for PH to 0.37 TKW. The corresponding range of the proportion of phenotypic variance was 5.5% to 13.3%. The multi-trait QTL on chromosome 6B showed the highest additive effect for PH with a corresponding proportion of phenotypic variance of 7.1% (Table 6)

Combined analysis of pleiotropy and epistasis

Combined analysis of pleiotropy and epistasis is presented in Fig. 6. The black concentric rings represent linkage groups. Light grey concentric rings represents traits

with the innermost concentric ring representing GY followed sequentially by DTH, PH, BW, GM, TKW, MSHW, KPS, SPM and TW. A network of interaction patterns among QTL are represented by color-coded arrow line depending on whether the interaction is favorable or unfavorable (Fig. 6). The segment of the linkage group involved in the interaction is presented as a grey dot inside the black bar. The dots on the light grey concentric ring represents the main effect calculated based on a subset of SNP (SNP with significant effect in the previous section).

The GY QTL mapped on chromosome 2B, 5A.2 and 5B, consistent with the previous results from GenStat analyses. The interaction patterns were depicted using arrowed lines. The purple lines indicate favorable interaction whereas green lines indicate unfavorable interactions. QTL on chromosome 2B showed favorable interaction with QTL on chromosome 6B. The QTL on chromosome 1D and 7B showed favorable interaction with a QTL on chromosome 1B which in turn had favorable interaction with QTL on chromosome 2B. Similarly, a QTL on chromosome 7A had a favorable interaction with a QTL on chromosome 2B and a QTL on chromosome 2D.1 showed favorable interaction with a QTL on chromosome 6A.1 which in turn showed a favorable interaction with a QTL on chromosome 2B. We observed favorable interaction between genomic regions on chromosome 5A.1 and 5A.2 but the directionality was not resolvable based on the present data (Fig. 6a). Possibly, an increase in the number of phenotypic data points would aid in resolving the directionality of the genetic interaction

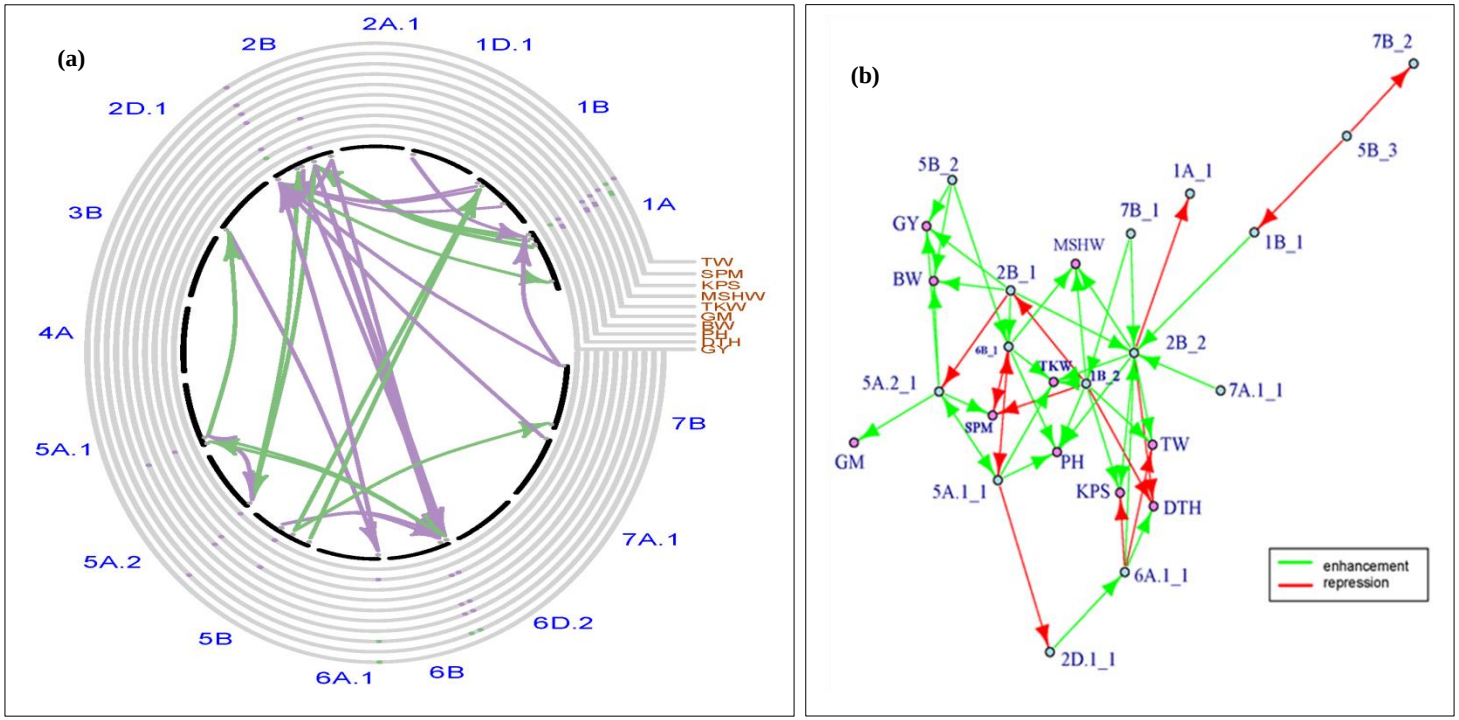

Figure 6. Results for QTL interactions and pleiotropic patterns based on a subset of markers linked to significant QTL
(a) Sub-network of QTL interactions involving different linkage groups. Green arrows represent favorable interactions between QTL on different linkage groups whereas purple represent unfavorable interaction QTL on different linkage groups (b) Genetic connectivity showing significant interactions among QTL and between QTL and traits. QTL and traits are represented as nodes and the arrows are the interactions. GY, grain yield; DTH, days to heading; PH, plant height; BW, biomass weight; GM, grains metre^{-2}; TKW, thousand kernel weight; MSHW, mean single head weight; KPS, kernels spike^{-1}; SPM, spikes metre^{-2}; TW, test weight.

Unfavorable patterns of interaction were also observed. The QTL detected on chromosome 2B had unfavorable interaction with the QTL on chromosome 5A.2 and 1A. The QTL detected on chromosome 1A revealed unfavorable interaction with some QTL on 2B (Fig. 6a) whereas the QTL detected on chromosome 5B revealed unfavorable interaction with a QTL on chromosome 7B and a QTL on chromosome 5A.1 and 6B showed unfavorable interaction although the directionality could not be resolved. QTL on chromosome 5B showed unfavorable interaction with a QTL on 1B (Fig. 6a).

A view of genetic connectivity between QTL and traits indicated positive, negative and a combination of pleiotropic effect (Fig. 6b). The effects are color coded, with green representing enhancement and red representing a repressor effect. The loci on chromosome 2B_1, 5A.2._1 and 5B_2 both enhanced GY and had a positive pleiotropic effect on BW. The loci on 6B_1 had a positive effect on TKW and also showed a positive pleiotropic effect on PH. Similarly, the loci on chromosome 1B_2 showed positive pleiotropic effect on TW, KPS, PH and MSHW. However, this locus also showed negative pleiotropic effect with DTH and SPM. The locus on 6A.1_1 showed a positive effect on DTH but a negative effect on KPS and TW. The QTL on chromosome 5A.1_1 enhanced TKW but did not show any direct pleiotropic effect on any other trait.

Indirectly, the QTL on chromosome 1B_2 suppressed GY and BW through chromosome 2B whereas the QTL on chromosome 7B_1 enhanced TW through chromosome 2B_2 and 1B_2. The QTL on chromosome 7B_1 also enhanced PH, KPS through 1B_2. The QTL on chromosome 2B_1 enhanced TKW through chromosome 6B_1, and MSHW, TW, PH and TKW through chromosome 1B_2. The QTL on

chromosome 7A_1 indirectly suppressed MSHW, TW, TKW, KPS and PH through chromosome 1B_2. A higher order of interaction patterns were also observed, for example, the QTL on chromosome 5A.1_1 suppressed DTH through a negative effect on chromosome 2D.1_1 that enhances a QTL on chromosome 6A.1_1. Similarly, a QTL on chromosome 5B_3 had a suppressor effect on a QTL on chromosome 1B_1 which enhances MSHW, TW, TKW and PH. For some cases, the directionality of the effects was not resolvable based on the data of the present study. Examples include the QTL on chromosome 5A.1_1 vs. 5A.2_1 which showed enhancement and the QTL on chromosome 5A.1_1 vs. 6B_1 which showed a repression effect. The bi-directionality indicates that a QTL showed same effect in the presence another QTL elsewhere in the genome and vice versa hence more phenotypic data point can help resolve the directionality. QTL on 1A_1 and 7B_2 did not show any direct or indirect interaction pattern with traits based on the subset data in the present study (Fig. 6b).

DISCUSSION

Understanding the genetic basis of phenotypic traits is of prime interest in wheat improvement programs. In line with this, the integration of molecular assets in plant breeding has shifted the selection trajectory for genotypes with genetic merit in different environmental conditions. To apply these tools, studies on identification of diagnostic molecular variants to distinguish superior genotypes are of primary interest in a breeding program. One approach used for tagging diagnostic markers is based on statistical association between phenotype and genotype. This approach was used in the present study where we applied different statistical models to define the underlying genetic basis of

quantitative traits measured. Based on phenotypic data analysis, we observed significant genetic variability among the genotypes for all traits both in individual and combined environments. GEI was significant for most traits indicating that at least for some genotypes, the performance was contingent on the environment where they were evaluated. Accounting for this differential response particularly crossover GEI is an important aspect of wheat improvement programs and can help in the distinction of genotypes with broad vs. specific adaptation. Entry mean heritability ranged from moderate (0.4-0.6) to high (> 0.6) except for BW which had heritability of 0.3. The population used in the current study was a RIL and therefore the heritability herein represents an upper limit of narrow sense heritability (Hanson and Robinson, 1963). Based on Mendelian expectation for a segregating locus at F_7, there is minimal proportion of heterozygosity hence the dominance component of genetic variation is also expected to be low. Thus, a high proportion of additive genetic variance constitutes the numerator component in the heritability formula.

The genetic correlations between traits were variable ranging from negative values to positive value. This indicates the presence of linkage and/or pleiotropy in genomic regions modulating the quantitative traits. This was further supported by co-localization of QTL linked to yield, yield components and agronomic traits. Positive correlation among traits indicates a common biological process or a common genetic structure (Mackay et al., 2009). In addition, positive genetic correlation indicates possible linkage that exists in coupling phase or presence of protagonistic pleiotropic effects. On the other hand, the

negative genetic correlation indicates a possible repulsion linkage or presence of antagonistic pleiotropic effects (Mackay et al., 2009).

A single trait multi-environment QTL analysis revealed that most QTL had significant QEI, underscoring the need of multi-environment phenotyping to account for this variation. Similar observations were made by Boer et al. (2007) and Malosetti et al. (2013) although in the former study they incorporated environmental co-variables such as weather and geographic information to model QEI. GY was mapped on chromosomes 2B, 5A.1 and 5B based on a single-trait multi-environment model. However, the QTL on 5B was not detected in a multi-trait model suggesting that its effect was modified by other traits.

We observed significant crossover QEI for all traits except MSHW. In multi-environment QTL mapping model, all QTL for GY except the QTL on 5B showed crossover QEI. Thus, for most traits it is vital to account for these components for a better definition of the underlying genetic architecture of the traits. All QTL mapped within the frame work of a multi-trait model showed significant QTI suggesting the inter-relationship among traits. Although multi-trait analysis indicated QTI for all the QTL detected, the QTL on chromosome 2B and 5A showed position consistency both in the single trait and multi-trait model. The QTL on chromosome 2B and 5A were mapped at position 406.1 and 122.4 cM, respectively and had a significant effect on GY and many other traits (Table 6). The multi-trait model revealed more QTL than single-trait models suggesting a better fit of the model and the importance of accounting for interactions among traits. In addition, this suggests that epistatic interactions among different QTL can contribute to significant

variation. Empirical studies on epistasis have reported mixed results with some reporting significant contribution of epistasis in the modulation of quantitative traits while other studies have shown non-significant contribution (Carlborg and Haley, 2004). Thus, incorporation of epistasis models can provide insights on the traits and/or populations in which these interactions are important. In addition, accounting for significant pleiotropic effects can improve accuracy through minimization of bias in the estimates of QTL main effects.

Combined analysis of pleiotropic and epistasis showed various patterns of interactions and genetic connectivity among QTL and traits. The genetic connectivity network revealed various effects with some effects showing enhancement and others having repression effects. We observed positive, negative and a combination of positive and negative direct and indirect pleiotropic effects. For example, the loci influencing GY on 2B_2, 5A.2_1 and 5B_2 showed positive pleiotropic effect on BW. On the other hand, the loci on 1B_2 enhancing MSHW had antagonistic pleiotropic effect on SPM. Loci influencing other traits showed a similar pattern of pleiotropy. In addition, we observed high order positive and negative pleiotropic effects. The indirect and high order interaction patterns may suggest a possible *cis* and *trans* acting effect within pathways regulating phenotypic traits in wheat. These interactions may also suggest the presence of conditional pleiotropy where a locus depicts interactions only when a second variant located elsewhere in the genome is present, which has been reported in animal studies (Carter et al., 2012; Tyler et al., 2014). Thus, a detailed analysis to disentangle the underlying genetic connectivity among QTL and traits elucidated more insight on the underlying genetic

architecture of traits. The analysis for CAPE clearly indicates that the expression of phenotypic traits depends on the genotypes at multiple loci.

Together with information from QTL main effects, it might be possible to deduce a QTL network model involving only paths that have an overall enhancement effects. In addition, QTL that have repressor effect on an important traits being pursued can be selected out using markers that are in linkage disequilibrium (LD) with the QTL. In the current study, GY and BW were enhanced by the QTL on chromosome 2B, 5A and 5B. Thus, MAS could be implemented targeting the SNPs in LD with these three QTL. However, a QTL on chromosome 1B had a repressor effect on the QTL on chromosome 2B. The GY main effect for the QTL on chromosome 2B was greater than that on chromosome 1B and therefore selection against the QTL on chromosome 1B would be logical if the objective is to improve GY and BW. Although the QTL on 2B had a repressor effect on chromosome 5A, the main effect of chromosome 2B was higher than chromosome 5A and therefore selection based on SNPs in LD with the three QTL will likely lead to improvement in both traits. Even though the QTL on 2B represses a QTL on chromosome 5A that has a positive effect on GM, this QTL enhanced a QTL for TKW and MSHW on chromosome 6B. Thus, there seem to be a compensatory effect for this particular QTL and this underscores the importance of disentangling the genetic connectivity in order to view the complex relationship underlying the QTL detected. Yield components showed a diverse pattern of genetic connectivity including loci located on different linkage groups. GM and SPM were both enhanced by a QTL on chromosome 5A.2. However, SPM was repressed by the QTL on 6B and 1B. TKW was enhanced by

QTL on 2B, 5A and 6B. Unidirectional and bi-directional interactions suggest different levels of complexity with the latter suggesting higher order interaction patterns. Similar patterns were observed in a study of neurological disease using mice as a model (Tyler et al., 2014).

The complexity surrounding the yield and yield components in wheat requires meticulous analysis to disentangle their relationship. Focusing on single trait QTL analysis may not discern the complex nature of QTL and their relationships. Carlborg and Haley (2004) indicated that epistasis plays an important role in the genetics of complex traits and that results from epistasis provide more insights on the genetic basis of complex traits. The CAPE results in the present study were based on a subset of molecular markers that showed a significant main effect in single trait model QTL analysis. We could not include all the SNPs because the pair-wise permutation was computationally intractable. It will be interesting to investigate a model with all markers as algorithms that are computationally tractable become available. We anticipate that this will refine the network of interaction and may elucidate more on loci without significant main effect but with significant epistatic interactions. In addition, epistatic interactions with the genetic background are likely to play a role in the main effect and interactions observed in the present study. Simulation studies have alluded to the presence of significant interaction with the genetic backgrounds (Jannink, 2007), and therefore the validation of markers associated with QTL can provide a better understanding of this type of interactions. However, information generated in the present study may be useful for the wheat breeding and genetics and future genetic studies targeting yield improvement in wheat. The information will also

contribute to our understanding of the genetic basis of yield, yield components and agronomic traits in pursuit of wheat genotypes with yield advantage under stress and non-stress environments.

CHAPTER III

SATURATED GENETIC MAPPING OF WHEAT STREAK MOSAIC VIRUS RESISTANCE IN WHEAT

INTRODUCTION

The global nutritional importance of wheat underscores the need to examine the agronomically important traits at genome level to accelerate the understanding and the interplay of loci controlling the traits. Remarkable progress in genotyping technology and computational capability has enabled development of relatively low cost multiplex and uniplex assay that provides a platform to differentiate wheat genotypes with better genetic fitness under stress and non-stress environments. Single nucleotide polymorphic (SNP) markers have been used routinely to capture quantitative trait loci (QTL) regulating agronomically important traits under stress and non-stress environments. Among biotic stresses in wheat, wheat streak mosaic virus (WSMV) is a major threat for wheat productivity especially in the U.S. Great Plains and its impact on wheat yield accentuates the need to develop wheat varieties with enhanced host plant resistance. The WSMV is vectored by wheat curl mite (WCM) and the locomotive behavior of WCM correlates with the spread of WSMV as well other viral diseases transmitted by WCM. The migration of WCM occurs primarily through walking, aerial dispersal as well phoresy and their survival strategy involves movement to the leaf whorls where they evade desiccation, predation as well as dislodgement (Navia et al., 2013). The migratory strategies employed by WCM ensure its continuity in survival and spread of the WSMV. Towards the end of the wheat season, the WCM migrates to alternative host that provide a green bridge until the

beginning of the new crop when the WCM migrate to wheat plants and cause infection (Navia et al., 2013).

Systemic infection of WSMV occurs through the ability of the virus to replicate in the infected cell and subsequent translocation into other cells through plasmodesmata (Lucas, 2006; Tatineni et al., 2011). The genomic region regulating long distance transport of the virus in the host has been mapped at the N-terminal of a coat protein. This region was reported to be host and strain specific (Tatineni et al., 2011). Cell to cell trafficking of the virus through plasmodesmata is driven by interaction of host proteins and viral movement proteins whereas long distance movement involves both active transport through plasmodesmata and passive transport through the phloem (Tatineni et al., 2011; Waigmann et al., 2004). WSMV induced cytological and morphological changes includes presence of cylindrical inclusions in the cytoplasm, smaller chloroplast, double membrane-bound invaginations in the chloroplast and enlarged nuclei (Gao and Nassuth, 1992; Gao and Nassuth, 1994). The genetic, cytological, morphological and physiological changes due to the infection results in significant economic losses in susceptible wheat genotypes.

Economic analysis of losses due to WSMV disease has been reported by various authors (Byamukama et al., 2013; Velandia et al., 2010; Workneh et al., 2009). The losses occurs primarily due to morphological and physiological impacts, including stunted growth and poor tiller development, reduced root biomass, reduced shoot biomass, and chlorotic and necrotic symptoms on leaves which reduces the forage quality. The reduction in root biomass has been linked to reduced water use efficiency (WUE) and this

is critical especially for irrigated wheat growers given that water is one of the major factors limiting wheat productivity and with competing needs from urbanization and industrialization. Further, the reduction in forage quality and yield as well as grain yield constitutes a major component of revenue reduction both for dryland and irrigated wheat producers. The irrigated wheat producers incur additional cost of increased irrigation labor and irrigation energy which further reduces the marginal revenue (Velandia et al., 2010). In their study, Velandia et al. (2010) reported significant reduction in forage and grain yield across all water regimes in WSMV-inoculated plots. In Texas High Plains, economic analysis of the impact of WSMV showed that it significantly affects farmers' profits and the situation is exacerbated for irrigated wheat producers due to reduced WUE (Velandia et al., 2010). Water is also one of the greatest limiting factors to wheat productivity in this region given that the main source of water for irrigation is the Ogallala aquifer in which water levels have subsided and there are conservation efforts to protect the aquifer from drying off and these efforts include restriction on the amount of water for irrigation purpose (Velandia et al., 2010). In line with conservation efforts and to protect yield from the WSMV disease, there is a need to develop wheat lines possessing enhanced resistance to the virus and reduce the virus induced water use inefficiency and consequently improve yields.

One effective and sustainable strategy to combat WSMV menace is through the development of WSMV resistant varieties. Host plant resistance provides both environmental and socio-economic sustainability in dealing with the WSMV disease. Development of WSMV resistant varieties reduces the infection from volunteer crop

which act as biological bridge for survival of the wheat curl mite from one season to the next (Harvey et al., 2005). In their study, they reported that acquisition of the virus by the WCM from resistant cultivar was 4% while it was 86% in the susceptible cultivar s(Harvey et al., 2005). There is considerable amount of literature regarding WSMV resistant sources. The first resistance gene, *Wsm1*, was derived from intermediate wheat grass (*Thinopyrum intermedium*) through robertsonian translocation and has been used in breeding for resistance to WSMV in wheat (Graybosch et al., 2009; Triebe et al., 1991). The discovery of *Wsm1* set the stage for development of host plant genetic resistance providing cost effective approach to control the disease in the farmer's field. However, this source of resistance has an associated yield penalty due to linkage drag (Sharp et al., 2002). Later, researchers discovered another gene in a wheat germplasm line, CO960293-2 (Haley et al., 2002). The gene was named as *Wsm2* and has been widely used to develop resistant wheat varieties especially in the High Plains of North America. Commercial varieties possessing *Wsm2* include Oakley CL (Zhang et al., 2015), Clara CL (Martin et al., 2014), Snowmass (Haley et al., 2011), RonL (PI 648020; (Seifers et al., 2007). The *Wsm2* gene has a breeding merit in that it doesn't involve translocation and therefore does not render challenges of linkage drag (Seifers et al., 2013b). Fahim et al. (2012a) did not find yield disadvantage for those *Wsm2*-introgressed lines in the absence of WSMV.

Both *Wsm1* and *Wsm2* are temperature sensitive conferring resistance up to a certain threshold value beyond which the resistance will be lost. Threshold values reported in literature varies depending on the genetic backgrounds. *Wsm2* could hold its resistance at 18 ^{o}C while *Wsm1* at 20 ^{o}C (Seifers et al., 2013a). The WSMV resistance genes also

express different responses to different isolates of the virus. The *Wsm2*-bearing RonL cultivar expressed differential reaction when inoculated with PV57, Sidney81 and GH95 strains of WSMV at 20°C regime whereas the *Wsm1*-bearing cultivar KS96HW10-3 showed no symptoms at 7 days after inoculation (Seifers et al., 2013a). The temporal reaction of *Wsm2* was also reported by Seifers et al. (2013a). Despite the variability in response, the resistance conferred by *Wsm2* gene provides significant protection against yield loss in field trials (Lu et al., 2011; Price et al., 2013; Seifers et al., 2013a; Seifers et al., 2006). In Australia, the *Wsm2* conferred resistances to an Australian isolate in both glasshouse and field experiments suggesting a broad range of resistance in *Wsm2* (Fahim et al., 2012a; Fahim et al., 2012b).

Development of WSMV resistant varieties through field screening is challenging owing to non-uniformity of infection caused by locomotive behavior of the vector. Typically, a disease symptom gradient is observed in the field depending on the direction of the wind with the windward side showing less disease pressure compared to the leeward side. Conventionally, it is difficult to distinguish between resistant genotypes versus disease escapes due to the variability in disease pressure. Molecular markers therefore will be useful in rapid screening and selection of genotypes possessing *Wsm2* gene. Despite the advantage of the resistance conferred by the *Wsm2* gene, little is known on tightly linked markers that are associated with *Wsm2* gene. High throughput SNP genotyping provides an excellent opportunity to map QTLs and/or genes within a short genetic distance that exist in linkage disequilibrium with the target trait. The use of dense genetic maps increases the odds of detecting a marker or QTL in linkage disequilibrium with the

target trait. Previous work reported that *Wsm2* gene is a single dominant gene located on chromosome 3BS (Lu et al., 2012; Lu et al., 2011; Zhang et al., 2014). The first genetic mapping study based on 83 polymorphic simple sequence repeat (SSR) markers and an F_2 population reported the nearest flanking markers at 30.8 cM and 45.4 cM, a genetic distance not amenable for MAS (Lu et al., 2011). Subsequently, a consensus map using 48 SSR and sequence tagged sites (STS) markers narrowed the genetic distance of nearest flanking marker to 3.9 cM in one population and 5.2 cM in the second population (Lu et al., 2012). However, the flanking marker at 5.2 cM failed to amplify in some genetic background. The main objective of the present study is to fine map *Wsm2* using 90K Illumina Infinium SNP array and identify tightly linked SNP for MAS. This information will be valuable for wheat breeding programs in the context of broadening the spectrum of diagnostic markers for rapid development and deployment of WSMV resistant varieties.

MATERIAL AND METHODS

Population structure and phenotyping

A total of 214 RIL derived from CO960293-2/TAM 111 plus three resistant (CO960293-2, RonL, Snowmass) and four susceptible (T81, Karl 92, TAM 111, TAM 112) checks with various levels of WSMV resistance were evaluated for their WSMV resistance in growth chambers at the Kansas State University Agricultural Research Center in Hays, KS. The genotypes were planted in metal flats filled with Sungro® Metro-Mix. Each flat had 22 rows and each genotype was planted in one row with 12 seeds. To avoid any confounding effect of the resistance to WCM, inoculation was done mechanically with the virus isolate Sidney81 at two-leaf stage. The temperature in the

growth chamber was maintained at 18°C with a 12h light duration. The experiment was conducted repeatedly in the year 2013 and 2014. Ratings per plant basis were taken at 21 days post-inoculation (DPI) and 28 DPI, respectively. Each plant was rated with a scale of 1 to 5 (1 is resistant without symptom while 5 is the most susceptible). The average severity score was estimated for each row and it was used for downstream statistical analysis.

Statistical analyses

Replication henceforth referred to as rep, was considered over time hence the data from 2013 was considered as rep1 and 2014 as rep2. The data for disease severity both at 21 DPI and 28 DPI was subjected to analysis of variance (ANOVA) using PROC GLM of SAS based on the following model:

$$y_{ij} = \mu + \tau_i + \gamma_j + \varepsilon_{ij}$$

where y_{ij} is the response of treatment ***i*** within rep ***j***, $\boldsymbol{\mu}$ is the trial mean, $\boldsymbol{\tau_i}$ is the $\boldsymbol{i^{th}}$ treatment effect, $\boldsymbol{\gamma_j}$ is the $\boldsymbol{j^{th}}$ replicate effect, and $\boldsymbol{\varepsilon_{ij}}$ is the random error term. We assumed that all $\boldsymbol{\varepsilon_{ij}}$ are independent and the expected value of $\boldsymbol{\varepsilon_{ij}} = 0$ and variance of $\boldsymbol{\varepsilon_{ij}} = \boldsymbol{\sigma^2_\varepsilon}$. The constraints on the additive model were as follows: the $\sum_i \boldsymbol{\tau_i} = 0$ and the $\sum_k \boldsymbol{\gamma_j} = 0$. Thus the $y_{ij} \sim N(\mu + \tau_i + \gamma_j, \sigma^2_\varepsilon)$. The variance components were computed using restricted maximum likelihood (REML) procedure in SAS version 9.4 (SAS Institute Inc., 2015). Both reps and genotypes were considered random. Orthogonal contrasts were computed for RIL vs all checks, RIL vs resistant checks and RIL vs susceptible checks in SAS version 9.4 (SAS Institute Inc., 2015). To compute entry-mean

heritability, all the checks were excluded from the analysis and the calculation was done in SAS based on the formula:

$$h^2 = \sigma_g^2 \Big/ (\sigma_e^2/r + \sigma_{g)}^2$$

where σ^2_g is the genotype variance, σ_e^2 is the residual (error) variance and r is the number of rep (Fehr et al., 1987). The means for RIL were compared to the means of the resistant checks and susceptible checks using Dunnett procedure in SAS (SAS Institute Inc., 2015). A chi-square test based on segregation ratio of resistant and susceptible genotypes was conducted using SAS version 9.4 (SAS Institute Inc., 2015).

Localization of *Wsm2* onto genetic map

To localize *Wsm2* onto the genetic map constructed using 90K SNP array, the RIL were grouped into two groups, that is, resistant and susceptible group. All RIL with disease severity score ≤ 2.0 were considered resistant whereas RIL with disease severity score > 2.0 were considered susceptible (Lu et al., 2011) . In the present study, most RIL had scores of either ≤ 2.0 or ≥ 3.0. Prior to linkage analysis, chi-square test was conducted to test the Mendelian expectation for a single dominant gene segregating at F_7 with the null hypothesis that the two groups fits 1:1 ratio. A statistical test at $\alpha = 0.01$ failed to reject the null hypothesis further supporting a single dominant gene model for *Wsm2*. The resistant group was converted to 'A' genotype scores whereas the susceptible group were converted to 'B' genotype. The genetic map was re-constructed in JoinMap with same parameter settings as described in material and methods in Chapter II.

RESULTS

Wheat streak mosaic virus evaluation

The decomposition of total phenotypic variance through analysis of variance (ANOVA) for disease severity at 21 DPI and 28 DPI revealed high significant differences ($P < 0.01$) among the genotypes (RIL plus checks) used in this study (Table 7). The significant results indicated that the differences observed were not by chance but had an underlying genetic basis. The adjusted R^2 was 0.95 and 0.96 at 21 and 28 DPI, respectively hence the model used in this study fits the data. A large proportion of variance was accounted by genotype and less than 5% was accounted for by the residual and replication (Table 7). Thus, it is not surprising that the heritability estimates both at 21 and 28 DPI were high ($h^2 = 0.93$). The high heritability estimates suggest that the proportion of variability that is due to the genetics was substantial in the current population and therefore the disease severity scores provides reliable estimates of genetic fitness of individuals under WSMV disease pressure. However, the estimates need to be interpreted judiciously because heritability is an elastic parameter that fluctuates depending on the population under investigation, the environment as well as the method used in estimation (Falconer and Mackay, 1996). The environments in this study were fairly uniform, and the RIL are highly homozygous and homogenous hence explaining in part the high heritability observed in this study.

Table 7 Mean squares and variance components for wheat streak mosaic disease severity at 21 and 28 days post infection.

		Mean		Var. Components	
Source	df	21 DPI	28 DPI	21 DPI	28 DPI
Rep	1	**0.43**	**0.72**	0.20	0.24
Genotype	220	**1.74**	**2.52**	95.14	95.55
Residual	219	0.04	0.05	4.66	4.21
Res. RIL vs Res.	1	0.02	0.24	-	-
Sus. RIL vs Sus.	1	0.13	0.15	-	-

†Res, Resistant; Sus., Susceptible. Bold values are significant at $P < 0.01$

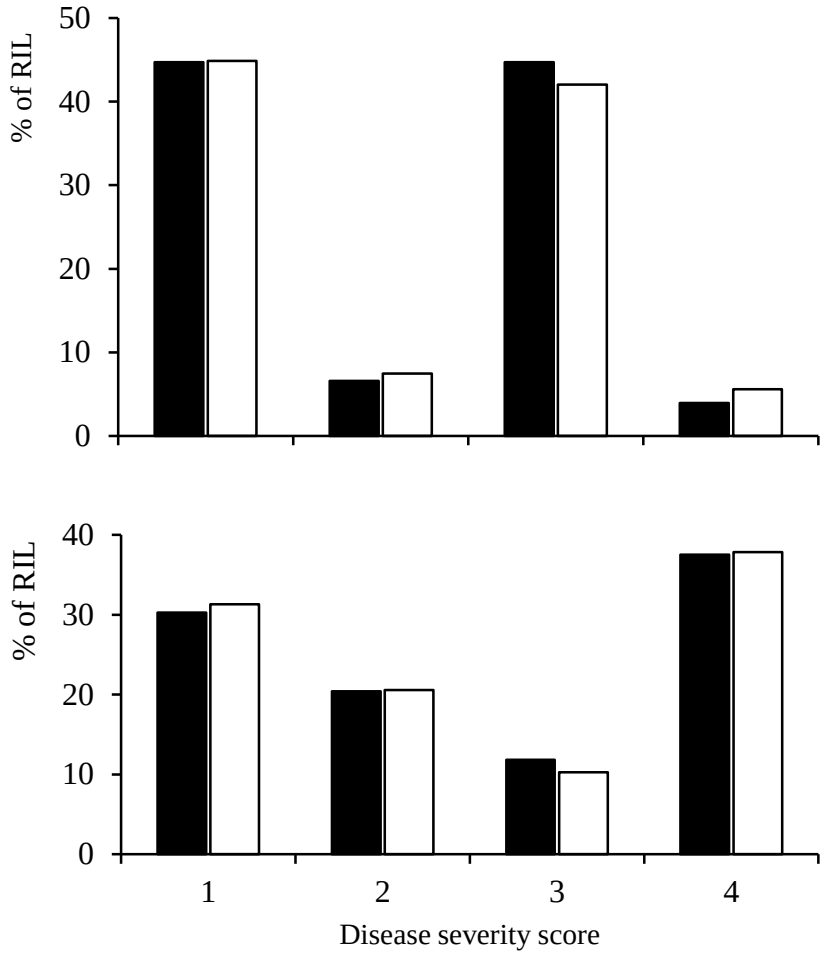

Figure 7. Percent distribution of RIL at 21 DPI (upper bar graph) and 28 DPI (lower bar graph).
Solid filled bars represent randomly selected set of 152 RIL and open bars represent the total population of 214 RIL. The y-axis is the percentage of RIL that were scored, the x-axis represents disease severity range. Disease score level 1 = RIL that were rated with a score of 1.0, level 2 = RIL with scores > 1.0 but ≤ 2.0, level 3 = RIL with scores > 2.0 but ≤ 3.0, and level 4 = RIL with scores > 3.0 but ≤ 4.0

Comparison of 214 RIL and the randomly selected genotyping subset of 152 RIL showed a similar distribution pattern for disease severity (Figure 7). Among the 214 RIL evaluated in this study, 112 (52.3%) were classified as resistant at 21 DPI based on the

criteria of a consistent score of ≤ 2 whereas 102 RIL (47.7%) were susceptible (Figure 7). A similar trend was observed at 28 DPI where 111 RIL (51.9%) were resistant and 103 RIL (48.1%) were classified as susceptible (Figure 7). For the randomly selected genotyping subset of 152 RIL, 78 (51.3%) were resistant and 74 (48.7%) were susceptible at 21 DPI (Figure 7). At 28 DPI, 77 RIL (50.7%) were resistant and 75 RIL (49.3%) were susceptible (Figure 7). Further, side by side visualization of the box plot for the population and its subset showed a more or less similar patterns both at 21 DPI and 28 DPI (Figure 8). The median disease score was slightly higher for the randomly selected subset compared to total RIL but the interquartile range was similar in both cases (Figure 8).

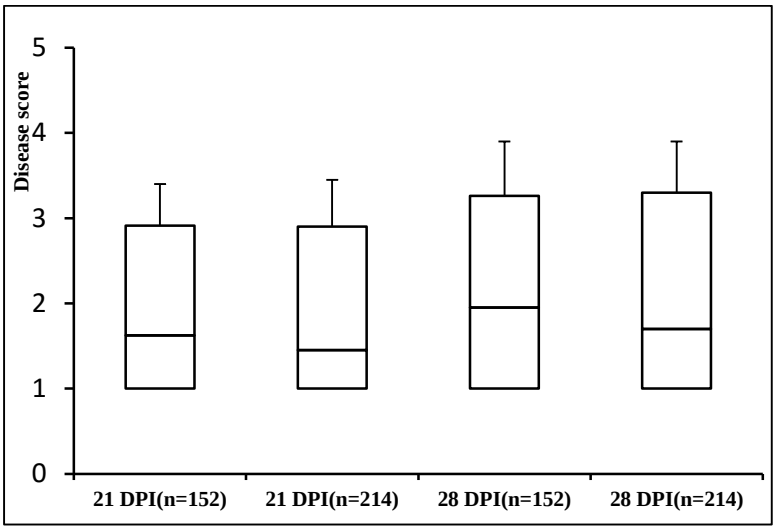

Figure 8. Boxplot for disease severity score at 21 DPI and 28 DPI for 214 RIL and randomly selected subset of 152 RIL.
The lower quartile is equal to 1.0 in both cases and the mid line in each box is the median score. The upper whisker represents the 75 percentile plus 1.5×IQR.

These results indicate negligible bias in the selection of the subset for genotyping and that they are representative of the initial population. The RIL showed consistent scores at 21 DPI and 28 DPI with a Pearson correlation of 0.98 ($P < 0.001$) between the two ratings. The disease severity scores at 21 DPI ranged from 1.0-3.5 (Table 8). The parental genotype TAM 111 and CO960293-2 had a disease severity score of 2.8 and 1.1, respectively at 21 DPI (Table 8). Thus, the disease severity range at 21 DPI showed transgressive segregation towards TAM 111. The susceptible checks, Karl 92 and T81 had a score of 3.1 and 3.2, respectively, whereas the resistant checks, RonL and Snowmass, had a score of 1.0 and 1.7, respectively (Table 8). At 28 DPI, the score range for RIL was 1.0 to 3.9 with the parental lines, TAM 111 and CO960293-2, scoring 3.2 and 1.2, respectively (Table 8). The RIL categorized as resistant had an average score of 1.1 both at 21 and 28 DPI with a range of 1.0-1.7 at 21 DPI and 1.0-2.0 at 28 DPI. The susceptible RIL had an average score of 2.9 and 3.3 at 21 and 28 DPI respectively and the score range was 2.0 to 3.5 and 2.3 to 3.9, respectively (Table 8). Comparison of disease scores between resistant RIL vs resistant checks was not significant. Similarly, single degree of freedom contrast between susceptible RIL vs susceptible checks was not significant (Table 1). Segregation among the 214 RIL conformed to a 1:1 ratio of resistant to susceptible genotypes at 21 DPI ($\chi^2 = 0.67$, $P = 0.41$) and 28 DPI ($\chi^2 = 0.08$, $P = 0.78$). Similar segregation ratios were observed for the randomly selected subset with chi-square of 0.11 ($P = 0.75$) at 21 DPI and 0.03 ($P = 0.87$) at 28 DPI. The non-significant chi-square confirmed that *Wsm2* is a single dominant gene, results that corroborate previous studies (Lu et al. 2011; Lu et al. 2012).

Table 8 Average disease severity ratings and range for the parents, RIL and checks

		21 DPI		28 DPI	
	Description	Mean ± SE	Range	Mean ± SE	Range
CT Population	214 RIL	1.9 ± 0.04	1.0-3.5	2.1 ± 0.05	1.0-3.9
CO960293	♀ Parent	1.1 ± 0.06	1.0-1.2	1.2 ± 0.07	1.0-1.6
TAM 111	♂ Parent	2.8 ± 0.06	2.5-3.0	3.2 ± 0.07	2.9-3.5
RonL	Res. check	1.0 ± 0.11	1.0-1.0	1.0 ± 0.11	1.0-1.0
Snowmass	Res. check	1.7 ± 0.11	1.0-2.7	1.8 ± 0.11	1.4-2.3
T81	Sus. check	3.2 ± 0.11	3.0-3.6	3.5 ± 0.05	3.3-3.7
TAM 112	Int. check	2.5 ± 0.11	2.0-2.7	2.9 ± 0.11	2.6-3.1
Karl92	Sus. check	3.1 ± 0.05	2.7-3.7	3.6 ± 0.06	3.3-4.0
Res. RIL	RIL with score ≤ 2.0	1.1 ± 0.02	1.0-1.7	1.1 ± 0.02	1.0-2.0
Sus. RIL	RIL with score >2.0	2.9 ± 0.02	2.0-3.5	3.3 ± 0.02	2.3-3.9

SE, standard error; Res., resistant; Sus., susceptible; Int., intermediate; RIL, recombinant inbred line

Genome-wide marker coverage

With exception of chromosome 1, the D subgenome had the lowest number of polymorphic SNPs (13.2%), whereas the B genome had the highest number of markers (51.7%) (Table 9). Overall, chromosome 5B had the highest relative percent of polymorphic SNPs (12.7%), whereas chromosome 4D had the lowest relative proportion (0.6%). Groups 2, 5 and 6 showed marked differences in the distribution of the markers across the A, B and D genome, whereas groups 1 and 4 showed minimal difference in the proportion of SNPs across the three subgenomes (Table 9). Group 3 showed high number of markers for the B subgenome but relatively similar number for the A and D subgenomes. At chromosome level, chromosome 7A and 7B had relatively similar proportion of polymorphic markers (7.9 vs 8.3%), whereas the 7D had approximately 1.0% (Table 9). Comparison of distribution of markers across the chromosomes relative to the genetic distance covered showed a similar pattern and the correlation between the

number of markers and the genetic distance per chromosome was high ($r = 0.97$, $P < 0.0001$).

Table 9 Distribution of markers and the genetic distance across the genome

Linkage group	No. of SNP	% SNP	Genetic distance (cM)	SNP cM^{-1}
1A	334	6.4	382.0	0.9
1B	359	6.9	309.6	1.2
1D.1	221	4.3	248.2	0.9
1D.2	117	2.3	63.0	1.9
2A.1	235	4.5	278.9	0.8
2A.2	59	1.1	68.9	0.9
2B	637	12.3	547.7	1.2
2D.1	60	1.2	112.4	0.5
2D.2	49	0.9	23.9	2.1
3A.1	96	1.8	164.5	0.6
3A.2	64	1.2	27.2	2.4
3B	139	2.7	198.6	0.7
3D	67	1.3	50.7	1.3
4A	58	1.1	147.9	0.4
4B.1	68	1.3	45.9	1.5
4B.2	27	0.5	24.3	1.1
4D	33	0.6	56.6	0.6
5A.1	154	3.0	235.6	0.7
5A.2	157	3.0	80.0	2.0
5B	660	12.7	655.7	1.0
5D	36	0.7	41.0	0.9
6A.1	85	1.6	155.1	0.5
6A.2	43	0.8	14.5	3.0
6B	296	5.7	295.4	1.0
6D.1	38	0.7	34.7	1.1
6D.2	26	0.5	29.3	0.9
7A.1	498	9.6	466.2	1.1
7A.2	44	0.8	54.5	0.8
7B	502	9.7	463.0	1.1
7D	37	0.7	17.4	2.1

Genetic map construction and mapping of *Wsm2*

A total of 30 linkage groups were generated covering all the 21 chromosomes of the wheat genome. The total genetic distance mapped was 5292.7 cM with chromosome 5B having the largest coverage of 655.7 cM and chromosome 7D having the lowest coverage of 17.4 cM (Table 9) based on genetic distance summation of fragments for each

chromosome. The average number of SNPs per cM varied across chromosomes and subgenomes (Table 9). Chromosome 6A.2 had the highest SNPs per cM whereas chromosome 4A had the lowest number of SNPs per cM suggesting low frequency of recombination. Chromosome 3B which harbors *Wsm2* gene had a total coverage of 198.6 cM with an average of 1.0 SNPs per cM. The *Wsm2* was mapped on chromosome 3BS (Figure 9). All the markers flanking *Wsm2* were on the short arm of chromosome 3B based on the inference from the consensus map by Wang et al. (2014). The mapping of *Wsm2* on chromosome 3BS is in agreement with the previous studies (Lu et al., 2012; Lu et al., 2011). However, the previously reported markers for this gene in two populations were 5.2 cM and 3.9 cM distal to *Wsm2* in CO960293-2/TAM 111 and CO960293-2/Yuma populations respectively with *Xbarc102* being the closest to *Wsm2* (2.4 cM) in the consensus map (Lu et al., 2012). In the current study, nine tightly linked flanking SNPs were mapped within 2.0 cM from the *Wsm2* gene (Figure 9). The nine flanking SNP from 72.5 cM to 74.5 cM were 'BS00088683_51', '*Excalibur_rep_c104532_80*', '*Excalibur_rep_c104498_168*', '*RAC875_c8885_74*', '*Kukri_rep_c101341_425*','*GENE-1856_1005*', '*Excalibur_c9206_836*', '*TA003677-1077*', and '*RAC875_c29353_979*'. This set of linked SNPs provides a potential selection tool for MAS of WSMV resistant genotypes in different genetic backgrounds.

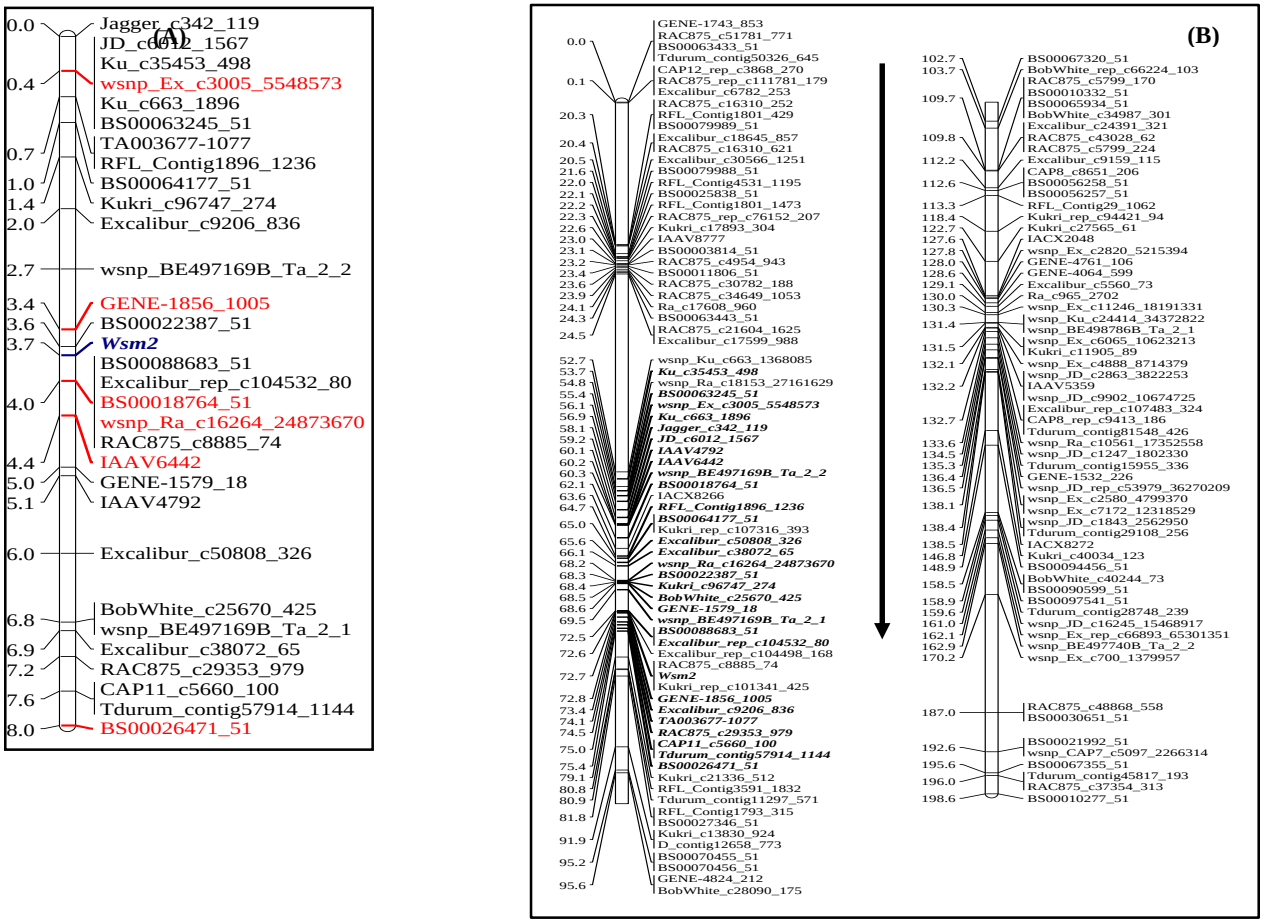

Figure 9. Genetic linkage map of SNPs flanking *Wsm2* gene on chromosome 3BS
(A) The map length represents a sub-fragment of chromosome 3B. The number to the left of the chromosome are the genetic distances of adjacent SNPs in centiMorgans. (B) Integrated genetic map of chromosome 3B constructed from the sub-fragments of 3B in the CT RIL population. Markers flanking *Wsm2* are bold and italic. The arrow points towards the direction of the centromere from the short arm orientation inferred from the 40K consensus map by Wang et al. (2014).

DISCUSSION

Generally, MAS is a powerful tool for breeding traits that are phenotypically expensive to screen and/or difficult to measure (Ribaut et al., 2002). For a trait like WSMV resistance, MAS is important because it is difficult to evaluate, which often requires controlled environment and artificial inoculation. The objectives of this study was to identify tightly linked flanking SNPs closer to *Wsm2* as potential selection tool to accelerate screening for genotypes with genetic merit under WSMV pressure. This is also a fundamental initial step in the process of map-based cloning of *Wsm2* gene. The objective was achieved using 8,819 SNPs from the 90K Infinium iSelect Wheat BeadChip to develop a high density genetic map in the CO960293-2/TAM 111 mapping population and subsequent detection of WSMV resistance gene on chromosome 3BS. The first genetic map based on 83 polymorphic SSR markers using an F_2 population derived from a cross between CO960293-2 and TAM 111 had the nearest flanking markers at 30.8 cM and 45.4 cM (Lu et al., 2011). Subsequently, a consensus genetic map constructed using 48 SSR or STS markers narrowed the genetic distance of nearest flanking marker. In the consensus genetic map, the SSR marker *Xbarc102* was 3.9 cM away from *Wsm2* in a population derived from CO960293-2/Yuma and *XSTS3B-55* was 5.2 cM away in a population derived from CO960293-2/TAM 111 (Lu et al., 2012). However, both flanking markers failed to amplify in some genetic backgrounds.

Usefulness of the markers in MAS is dependent on the level of polymorphism and genetic distance between the markers and the gene of interest. A single marker linked to target genes may not be sufficient to screen diverse polymorphism across different genetic

backgrounds. Therefore, a set of tightly linked flanking markers are the best predictor for *Wsm2* with higher accuracies. In this study, nine tightly linked flanking SNPs were mapped within 2 cM. Besides the SSR markers previously reported, the SNP in the present study provides a broad spectrum option for different genetic backgrounds. Thus, if a marker does not work in one genetic backgrounds, there are alternative markers that can be tested for MAS. The improvement in the genetic map reported herein could be partly due to the different marker and population type used in the linkage mapping. In general, F_2 generations have less recombination events compared to RIL populations, hence large linkage blocks could lead to declaring an association between a marker and a trait when in reality they are not in gametic phase linkage disequilibrium. Regardless, more effort is needed to validate these SNPs in diverse genetic backgrounds. This information will be vital in MAS.

Chromosome 3B is a hub for other important traits in wheat and it will be important to study the interaction of *Wsm2* with other genes to elucidate more on the mechanism of resistance to the WSMV and determine if there is an overlap of genes for different traits. The recent completion of draft sequence will be useful in providing more insight on genes located on chromosome 3B and identification of more markers linked to agronomically important traits as well as their interaction with *Wsm2*. More than 7,000 protein coding genes have been identified on chromosome 3B and were widely involved in cellular component, molecular function and biological processes including genes related with virus infection cycle (Choulet et al., 2014). The mechanism underlying *Wsm2* virus resistance was beyond the scope of the current study. However, the plant defense system

and the downstream products such as salicylic acid, jasmonic acid, nitride oxide, and reactive oxygen species play important roles in the establishment of local and systemic acquired viral resistance (Carr et al., 2010).

We observed that some RIL genotypes consistently showed no disease symptom whereas some showed consistent susceptibility both during first and second screening. The presence of minor symptoms on the donor parent suggests that the *Wsm2* gene alone does not provide absolute resistance but the levels of resistance are sufficient enough to suppress the viral effects. In a previous study, Seifers et al. (2013a) reported that no virus isolate was able to overcome the *Wsm2* resistance completely. However, we cannot rule out that the presence of the symptoms on the donor parent could be due to environmental conditions such as temperature, light and humidity that might have affected the expression of *Wsm2* gene. Based on phenotypic data, the presence of completely symptomless RIL suggests that the combination of major allele from the donor parent and minor alleles from TAM 111 could provide a better defense system against WSMV. We have mapped some QTL with minor effects on WSMV resistance in both TAM 111 and TAM 112 (S. Liu et al. unpublished data).

CHAPTER IV

QTL MAPPING FOR END-USE QUALITY IN WHEAT

INTRODUCTION

The trajectory of a wheat breeding program is dictated by the both agronomic and end-use quality needs which are intricately related to market requirements. The complete chain of wheat breeding involves many stakeholders with differential preference and in the pipeline there are breeders, producers, millers, bakers, retailers and consumers. From the producers to the consumers, the needs at each level may vary but most importantly the information that tweaks a breeding program flows in a bottom-up approach, from the consumer to the breeder. Wheat has broad-spectrum end products but these products are contingent upon the inherent quality characteristics of a given genotype. Thus, end-use quality analysis is one of the primary components of wheat breeding pipeline. The physical attributes of the kernels, the composition and profile of the protein fraction of the flour, and the rheological properties of the dough are used as indicators of end-use quality in wheat. The kernel hardness index (HDI) is used primarily as a criterion for textural classification of wheat with the classes ranging from extra soft (HDI $\leq$ 10) to extra hard (HDI > 90) wheat based on the AACC method 55-31.01 (AACC International, 2010).

The mixograph metrics which quantify the rheological parametric of the dough are recorded both at envelope and midline where the envelope represents the inner and outer trace of the mixogram. The variables are recorded at peak, one minute before peak, two minutes after the peak and at set time point which is normally set at eight minutes (Walker and Walker, 2004). The variables recorded include time, such as peak time, defined as

the number of minutes required to reach maximum dough consistency, integral values which reflect the amount of work input up to a certain point in time and is used as an indicator of dough strength. The integral value is computed as the area under the curve up to a certain point on the mixogram and is expressed as % TQ × min. The width of the trace is used as a proxy for dough tolerance to mixing and is expressed as a percentage of the full scale (100 mixograph units on the y-axis), whereas the curve height, also expressed as percentage of the full scale, is used to determine dough consistency. The ascending and descending slopes of the mixogram are computed at the left and right of peak, respectively, and are expressed as % min^{-1}. Smaller values for the slope indicate a stable curve whereas large values indicate a rapid rise and/or breakdown (Miles et al., 2013). The absolute sum of the left and right slope is used as an indicator of mixing stability or tolerance. Small values are desirable because they indicate a stable curve, whereas large values correspond to rapid rise and/or breakdown of the dough (Miles et al., 2013; Walker and Walker, 2004). The midline right slope corresponds to the resistance of the dough to breakdown. The midline parameters have been reported to be highly repeatable (Martinant et al., 1998) and the present study focuses on these parameters.

The standard laboratory protocol for end-use quality analysis involves single kernel characterization, flour yield determination, protein content analysis, and analysis for rheological properties. Some protocols such as mixograph analysis are time consuming; for instance, a 10 gram mixograph requires eight minutes per sample plus an additional time for sample preparation which is depended on the speed of the operator. Moreover, the amount of seed available during early generations is often insufficient for

extensive end-use quality analyses. These factors are the primary reason why quality analysis is often relegated towards advanced stages of the wheat breeding cycle when there is significant reduction in the number of lines to be analyzed and when the amount of seed is adequate. There are potential demerits of testing the lines at advanced stages. First, a potentially superior line, which could be used as a donor line for end-use quality improvement, might be selected out during the early generation phase. Second, the lines tested for end-use quality at advanced stage may not possess the quality attributes required for the target market, which might necessitate redefining the breeding plan. This might be costly and might reduce the genetic gain $cycle^{-1}$. Thus, use of molecular signatures as a proxy for end-use quality can be a valuable tool for wheat improvement programs.

Numerous studies focusing on quantitative trait loci (QTL) mapping for end-use quality have been reported. Arbelbide and Bernardo (2006) used a genetic map derived from 65 simple sequence repeat (SSR) and a linear mixed model approach to map QTL for kernel hardness and dough strength. They detected two QTL for kernel hardness on chromosome 1A and 5D and four QTL for dough strength on chromosome 1A, 1B, 1D and 5D. The QTL detected on 1A were in the neighborhood of the *Glu-A3* locus whereas the QTL on 5D was near *Ha* locus that modulates grain hardness in wheat (Arbelbide and Bernardo, 2006). Huang et al. (2006) reported QTL for mixing time and energy to peak on chromosome 1B, 1D and 3B. The peak height was mapped on 1B, 1D and 4D; flour protein content QTL were detected on 2D and 4D whereas the left slope was mapped on 1D and 4D (Huang et al., 2006). Sun et al. (2008) used a genetic map derived from 381 markers and reported 15 QTL for protein content spanning different chromosomes with

most of them clustered on 1D, 3B, and 6D. In their study, 20 QTL mostly clustered on chromosome 3D, 6B, and 7B were linked to starch related traits (Sun et al., 2008). Based on a population derived from soft × hard wheat and a genetic map of 263 SSR markers, Kerfal et al. (2010) detected QTL for mixing time on 1DL and 3BS; and mixing tolerance on 2AS and 7AS. The dough strength QTL were mapped on 1BS, 2AS, and 5DL (Kerfal et al., 2010). In a QTL mapping study for end-use quality in spring wheat using a genetic map of 534 markers, Tsilo et al. (2011) reported major QTL for endosperm texture on chromosome 1A, 5A, and 5D. They detected 34 dough-mixing strength and bread making properties QTL spanning nine chromosomes. They also detected midline peak width (MPW) QTL on 1A, 1B and 6D; midline peak integral (MPI) QTL on 1B, 1D, 6D and 7D; midline peak time (MPT) QTL on 1B, 1D, 2A, 6D and 7D; and midline peak value (MPV) QTL on 1A, 1B, 1D and 6D (Tsilo et al., 2011). Prashant et al. (2015) used a genetic map constructed using 202 SSR markers to map QTL for rheological properties of the dough and reported 144 QTL linked to dough rheology and 14 QTL linked to grain protein content, loaf volume, and specific volume. El-Feki et al. (2013) reported QTL for MPT on 1A, 1B, 6A, 6B, 7B, and 7D. The peak height QTL were detected on 1A, 1B, 1D, 2B, 4A and 7B whereas peak width QTL were mapped on 1A and 5D (El-Feki et al., 2013). Echeverry-Solarte et al. (2015) detected QTL for grain protein content on chromosome 1A, 1B, 2D, 3D, 6B and 7B. The midline peak energy QTL were mapped on 1B, 1D, 2D, 3D, 6B and 7D whereas MPT QTL were mapped on chromosome 1B, 1D, 2D, 3A, 5B and 6B (Echeverry-Solarte et al., 2015). Others studies on QTL mapping for end-use

quality include McCartney et al. (2006); Miwako et al. (2015); Patil et al. (2009) and Zhang et al. (2009).

The present study used a saturated genetic map derived from 90K Illumina iSelect array and RIL derived from an elite-by-elite winter wheat cross. The QTL analysis was implemented in GenStat based on the framework of linear mixed model (LMM) (Malosetti et al., 2013). The LMM uses the variance-covariance (VCOV) structure to account for the heterogeneity of genetic variance and covariance in the phenotypic data. Based on this framework, the objective of the present study was to determine the characteristics and map QTL linked to kernel and dough mixing parameters in RIL population derived from elite-by-elite hard red winter wheat.

MATERIALS AND METHODS

Germplasm

An elite-by-elite cross, CO960293-2/TAM 111, was used to generate a 214 RIL population. TAM 111 has excellent performance under drought stress and possesses good quality characteristics for bread making. It has glutenin to gliadin ratio of 0.79 and high molecular to low molecular glutenin weight ratio of 0.30 based on the analysis conducted at Texas A&M Cereal Quality Lab (Jondiko, 2014). The RIL plus parents and checks were phenotyped across eight environments and samples for end-use quality analysis were drawn from three randomly selected environments. The selected environments were Etter, TX (35° 59' N, 101° 59' W); Bushland, TX (35° 06' N, 102° 27' W) and Hays, KS (38°51' N, 99°20' W). From each genotype, 80 and 30 grams of clean seed samples were drawn

with the latter being used for single kernel characterization and the former for milling and rheological studies, both conducted at Texas A&M Cereal Quality Lab.

Single kernel characterization, tempering and milling

For each RIL, 30 gram sample were used for textural characterization using SCKS 4100 (Perten Instruments, Hagersten, Sweden) comprising of the main console interfaced with a Windows computer system (www.perten.com). Briefly, the sample was supplied to the machine through a knobbed hopper. From the sample, an automated singulator picked single kernel at time up to 300 kernels and each kernel was weighed and relayed into a toothed rotor and a progressively narrowing crescent (SKCS 4100 operation manual). The force exerted in crushing each kernel and the conductivity between the rotor and the crescent are recorded and used in computing the hardness index (0-100 scale) and kernel diameter (in millimeters), respectively. Percent moisture content of the kernel was also recorded on individual kernel basis. The analytical phase of the data was conducted in silico using SKCS 4100 software where the distribution, mean and standard deviation of each parameter were computed and printed to file electronically (SKCS 4100 operation manual).

A milling sample comprising of 80 grams of clean seed was weighed from each genotype. To optimize the milling yield, the samples were tempered to 14% moisture content. Computation of moisture adjustment was based on the moisture content obtained from the SKCS 4100 system. To achieve homogenous distribution of moisture, each sample was weighed in a 500 ml plastic flask, the appropriate amount of water was added and the flask were capped and loaded on a E6000 mid-range reciprocal shaker connected

to a timer (Eberbach Corporation, Ann Arbor, MI, USA; www.eberbachlabtools.com). The shaker was set to run for 60 minutes at a constant speed of 260 oscillation minute^{-1}. The samples were kept overnight at room temperature and were milled using the Brabender Quadramat Jr. Precision laboratory roller mill (Brabender Instruments, South Hackensack, NJ, USA) based on AACC Method 26-50 (AACC International, 2010).

NIR-based protein quantification and mixograph mixing properties

The flour protein content (FPC) was determined in real time using the third generation diode array near infra-red spectroscopy (NIR), model DA 7250 (Perten Instruments, Hagersten, Sweden). This is an automated stand-alone system that integrates speed, ease, high analytical accuracy and broad-spectrum application providing a range of variables including moisture, protein and fat content. In addition, the method is robust against vibration and temperature turbulence with the ambient operation temperature range of 5-40°C (www.perten.com). Prior to protein analysis, absorbance scale was validated using a polystyrene reference according to manufacturer protocol. After the calibration, the flour sample per RIL was loaded on to the magnetic tray and positioned in the beam array. The tray was automatically rotated at a constant speed during the FPC determination to ensure uniformity. The analysis was implemented using Simplicity plus software v2.86, a general user interface program. Besides FPC, the ash and moisture content were also recorded.

The rheological properties of the dough was determined using a 10-gram mixograph (National Manufacturing Co. Lincoln, NE) based on AACC method 54-40.02 (AACC International, 2010). The amount of distilled water added to the flour was

computed according to AACC method 54-40.02 (AACC International, 2010). The percent optimum water absorption (y) was calculated using the formula y = 1.5 x FPC + 43.6 where FPC is the flour protein content on 14% moisture basis. The mixograph system was interfaced with a computerized data acquisition and analysis system loaded with MixSmart software version 1.0.404 (Walker and Walker, 2004). The inbuilt algorithms of the software outputs parameters both at midline and envelope of the mixogram. The envelope is defined by the inner and outer trace of the Mixogram with the midline representing the average of the inner and outer trace. Measurements were computed at the peak, one minute before peak (left of the peak), two minutes after the peak (right of the peak) and at time_X which was 8 minutes in the present study. The variables recorded were time, height, width, slope and integral values (Table 1).

Statistical analyses

A general linear model (GLM) was implemented in SAS to partition the total variation into components due to genotype, replication and the residual. Replication, herein referred to as rep, was considered over space and therefore each environment was treated as a rep. The partitioning of total variation was based on the following model:

$$Y_{ik} = \mu + G_i + E_k + GE_{ik}$$

Where $\mathbf{Y_{ik}}$ is the observed phenotypic value of the $\mathbf{i^{th}}$ genotype in $\mathbf{k^{th}}$ environment, μ is the overall mean, $\mathbf{E_k}$ is the rep effect, $\mathbf{G_i}$ is the genetic effect of $\mathbf{i^{th}}$ genotype and $\mathbf{GE_{ik}}$ is the residual term corresponding to a *quasi* genotype-by-environment interaction (GEI).

In conventional analysis of variance across environments, the significance of GEI is tested against the residual term. The current study had spatial rep, and, therefore, the

analysis of variance (ANOVA) follows a statistical linear model of single environment analysis. In this context, the interaction of replication (environment in this case) with genotype was used as the error term to test the significance of genotypes. Although we cannot separate the GEI component from the error term in this study, we computed the magnitude of variance component due to each source of variation to determine the relative proportion of each component. The variance components were computed using PROC VARCOMP in SAS 9.4 (SAS Institute Inc., 2015). The entry-mean heritability estimates was calculated according to Fehr et al. (1987) using the formula:

$$h^2 = \frac{\sigma_g^2}{\sigma_e^2/r + \sigma_g^2}$$

Where r is the number of rep, σ^2_g is the genotype variance, and σ^2_e is the residual variance. PROC CORR in SAS was used to compute Pearson correlation coefficients (r_P) based on the following formula:

$$r_P = \frac{Cov_{x,y}}{(\sigma_x^2\ \sigma_y^2)^{1/2}}$$

QTL analysis was performed using GenStat software version 18 as outlined by Malosetti et al. (2013). The genetic map developed using 90K SNP array and RIL derived from CO960293-2 and TAM 111 was used for QTL analysis (described in chapter II). First, single-trait QTL analysis was performed for each environment and for the data averaged across environment. This was followed by single trait multi-environment QTL mapping based on a linear mixed model (LMM) framework as outlined by several authors (Boer et al., 2007; Malosetti et al., 2013; Van Eeuwijk et al., 2010). A parsimonious model

for the best VCOV structure for multi-environment QTL mapping was chosen based on Schwarz information criterion (SIC). Under the LMM framework, multi-environment QTL mapping was implemented in a stepwise process commencing with simple interval mapping (SIM) followed by two or more successive rounds of composite interval mapping (CIM) using QTL identified in SIM as cofactors to control the effect genetic background (Boer et al., 2007; Malosetti et al., 2013; Van Eeuwijk et al., 2010). Subsequently, a final CIM model selection that runs backward elimination was implemented to select significant QTL and compute main effect as well as interactions. Final QTL analysis involved multi-trait QTL analysis using data averaged across environments to detect genomic regions linked to multiple traits. For all the QTL analyses the genetic predictors were calculated at every 2 cM and the cofactor window for CIM was set at 30 cM. Pairwise additive-by-additive epistatic interactions among significant peak loci was calculated in SAS using Epistacy version 2.0, a modification of the original SAS code (Holland, 1998).

RESULTS

Analysis of variance and heritability

ANOVA revealed highly significant differences ($P < 0.001$) among genotypes for all the mixograph variables and physical kernel characteristics (Table 10). We defined heritability into low, moderate and high as ≤ 0.3, 0.4-0.6 and > 0.6, respectively (Table 10). The average single kernel weight (SKW) based on a 300 kernel sample was 28.7 mg with a high entry-mean heritability of 0.73. The flour protein content (FPC) was on average 13% and this trait showed moderate heritability whereas the water absorption

(WAB) was 61% on average with heritability of 0.41. The average midline left time (MLT) was 3.7 minutes and its corresponding average midline left value (MLV) was 49.9%. The average hardness index (HDI) was 68.6, generally expected since the population was derived for hard × hard wheat cross. The heritability for MLT was 0.82 whereas the heritability for MLV was 0.37. At the left of the peak, the midline left slope (MLS) and the midline left width (MLW) were 8.5% min^{-1} and 31.8%, respectively, and their corresponding heritability was 0.71 and 0.45, respectively. The average midline left integral (MLI) was 122.7% TQ × min and was highly heritable. At peak level, the midline peak time (MPT) that reflects average time to maximum dough consistency was 4.7 minutes and was highly heritable. The peak height, represented by the midline peak value (MPV) revealed moderate heritability and an average value of 54.6%. The average midline peak width (MPW) was 24.1% with a heritability of 0.32 whereas the midline peak integral (MPI) had an average of 175.7% TQ x min with a corresponding heritability of 0.75. The right of peak parameters had a moderate-high heritability with midline right value (MRV) exhibiting the lowest heritability of 0.35. The average midline right time (MRT) was 5.7 minutes with a corresponding average midline value (MRV) of 51.9%. The average slope at the right of peak (MRS) was -2.8% min^{-1} whereas the average midline right width (MRW) and midline right integral (MRI) were 16.0% and 244.5% TQ × min respectively. Heritability at the time_X also ranged from moderate-high values similar to what was observed at the midline right parameters. At this position which was 8 minutes, the average midline time_X value (MTXV), midline time_X width (MTXW) and midline time_X integral (MTXI) were 46.4%, 11.9% and 343.6% TQ × min, respectively.

Table 10 Analysis of variance, heritability and mean performance for end-use quality

Variable name	Abbr.	Units	σ^2_{Gen}	σ^2_{Env}	σ^2_{Res}	h^2	$\bar{x} \pm SE$
Midline left time	MLT	min	1.4	1.0	0.9	0.82	3.7 ± 0.06
Midline left value	MLV	%	7.3	13.7	38.1	0.37	49.9 ± 0.42
Midline left slope	MLS	% min^{-1}	16.3	16.3	20.1	0.71	8.5 ± 0.28
Midline left width	MLW	%	13.5	31.1	49.1	0.45	31.8 ± 1.07
Midline left integral	MLI	% TQ × min	1478.8	638.5	1191.9	0.79	122.7 ± 2.00
Midline peak time	MPT	min	1.4	1.0	0.9	0.82	4.7 ± 0.06
Midline peak value	MPV	%	12.0	34.3	38.4	0.48	54.6 ± 0.42
Midline peak width	MPW	%	5.0	5.3	30.8	0.33	24.1 ± 0.37
Midline peak integral	MPI	% TQ × min	1328.1	446.8	1319.0	0.75	175.7 ± 2.15
Midline right time	MRT	min	0.7	0.4	0.9	0.68	5.7 ± 0.06
Midline right value	MRV	%	3.3	2.3	18.7	0.35	51.9 ± 0.29
Midline right slope	MRS	% min^{-1}	0.9	1.5	2.1	0.58	-2.8 ± 0.10
Midline right width	MRW	%	7.9	6.2	17.4	0.58	16.0 ± 0.27
Midline right integral	MRI	% TQ × min	824.4	487.7	1978.9	0.56	244.5 ± 2.79
Midline time _X value	MTXV	%	3.4	1.5	27.4	0.27	46.4 ± 0.35
Midline time_X slope†	MTXS	% min^{-1}	0.4	2.5	60.0	0.02	-0.09 ± 0.06
Midline time _X width	MTXW	%	15.2	13.2	19.0	0.71	11.9 ± 0.27
Midline time _X integral	MTXI	% TQ × min	660.8	1061.2	1719.5	0.54	343.6 ± 2.78
Midline mixing stability or tolerance	MMST	%	25.4	32.5	29.2	0.72	38.8 ± 0.81
Hardness index	HDI	%	9.7	22.2	20.4	0.59	68.6 ± 0.29
Single kernel weight	SKW	mg	2.6	18.8	2.9	0.73	28.7 ± 0.11
Flour protein content	FPC	%	0.1	0.2	0.3	0.54	13.0 ± 0.04
Water absorption	WAB	%	0.2	7.0	1.0	0.41	61.0 ± 0.07
Kernel diameter†	KD	mm	0.2	2.5	0.4	0.62	2.5 ± 0.004

† Original value of variance components was multiplied by 10^2
σ^2_{Gen}, genotypic variance; σ^2_{Env}, variance due to environment; σ^2_{Env}, residual variance; h^2, entry-mean heritability, Abbrev., abbreviation
All the variables except MTXS were significant at $P < 0.001$.

The parents showed significant differences for MLS, MLI, MPI, MRT, and HDI (Table 11). The HDI ranged from 57.9 -78.1% which falls within the range of medium-hard to hard as described in AACC Method 55-31.01 (AACC International, 2010). The HDI is an essential measurement for breeders, producers, millers, bakers and is used primarily to determine the suitability of different wheat varieties for various end-use products. Hard wheat is mainly used for bread whereas soft wheat is used for cookies

(Morris and Rose, 1996). The HDI values in the present study were nearly within the limits of the parental lines, which ranged from 61.1-78.3% (Table 11). The FPC ranged from 11.7 to 14.6%, SKW ranged from 24.0 to 37.8 milligrams, and WAB ranged from 59.2 to 62.9%. At the left of the peak, MLV, MLS, MLW, and MLI ranged from 33.3 to 67.0%, 1.2 to 27.6% min^{-1}, 19.6 to 50.1%, and 34.8 to 245.0% TQ × min, respectively. The range for MPT, MPV, MPW and MPI were 2.0 to 7.7 mintes, 36.0 to 69.3%, 15.9 to 37.9%, and 85.2 to 295.3% TQ x min respectively (Table 11). The MRT, MRV, MRS, MRW and MRI ranged from 3.0 to 8.5 minutes, 45.1 to 66.6%, -7.2 to 0.1% min^{-1}, 7.0 to 27.9% and 137.3 to 369.2% TQ × min, respectively, whereas the MTXV, MTXS, MTXW and MTXI ranged from 36.3 to 59.2%, -1.9 to 0.1% TQ × min^{-1}, 4.4-31.0% and 213.0 to 466.4% TQ × min, respectively (Table 11).

Transgressive segregation towards both maternal (CO960293-2) and paternal (TAM 111) parent was observed for MLV, MLI, MRW, MTXI, MMST, KD, SKW, FPC and WAB. The MLS and MRV revealed transgressive segregation towards the paternal parent whereas MLT, MPT, MPV, MPI, MRT, MRS, MRI, MTXV, and MTXS showed transgressive segregation towards the maternal parent. The difference between the maternal and paternal parents were significant for MLT, MLS, MLI, MPT, MPI, MRT, MRV, MRS, MMST, and HDI. Even though the rest of the traits showed only numerical difference between the parents, statistical difference was observed for all the variables except MTXS (Table 10). Transgressive segregation suggests that a different set of genes are expressed between the parents and that complementarity between this set of genes can lead to an increased phenotype.

Table 11 End-use quality average performance of the parents, RIL and commercial checks

Trait†	P1	P2	TAM 112	Karl92	RIL mean	Min	Max	LSD	Max-Min	|P2-P1|	|Min-LP|	|Max-HP|
MLT	4.9	1.8	3.9	3.2	3.7	1.0	6.7	1.4	5.7	3.1	0.8	1.8
MLV	47.9	51.6	52.7	55.3	49.9	33.3	67.0	10.0	33.8	3.6	14.7	15.5
MLS	3.8	13.3	4.5	12.8	8.5	1.2	27.6	6.9	26.3	9.5	2.6	14.3
MLW	30.6	41.8	34.6	33.9	31.7	19.6	50.1	11.3	30.5	11.2	11.0	8.3
MLI	173.4	65.4	142.1	116.6	122.7	34.8	245.0	48.1	210.1	107.9	138.6	179.5
MPT	5.9	2.8	4.9	4.2	4.7	2.0	7.7	1.4	5.7	3.1	0.8	1.8
MPV	50.3	59.4	54.7	62.4	54.6	36.0	69.3	10.0	33.3	9.1	14.3	9.9
MPW	23.6	30.6	24.2	26.9	24.1	15.9	37.9	8.8	22.0	7.0	7.7	7.3
MPI	222.9	122.2	196.0	176.7	175.6	85.2	295.3	51.7	210.1	100.7	37.0	72.4
MRT	6.4	4.2	6.6	5.5	5.7	3.0	8.5	1.5	5.5	2.2	1.1	2.1
MRV	49.9	54.0	52.0	56.3	51.9	45.1	66.6	8.1	21.5	4.1	4.8	12.6
MRS	-2.1	-3.3	-2.2	-3.5	-2.8	-7.2	0.1	2.7	7.3	1.3	3.9	2.1
MRW	18.2	16.2	16.9	16.3	15.9	7.0	27.9	7.4	20.9	2.1	9.2	9.7
MRI	256.3	199.0	285.4	259.0	244.4	137.3	369.2	75.5	231.8	57.4	61.6	112.8
MTXV	46.6	45.3	49.1	49.9	46.3	36.3	59.2	8.4	23.0	1.3	9.0	12.7
MTXS	-0.1	0.2	-0.1	-0.3	-0.1	-1.9	0.1	1.4	2.0	0.4	1.8	0.1
MTXW	12.2	9.6	15.2	9.0	12.0	4.4	31.0	6.4	26.7	2.5	5.3	18.9
MTXI	325.6	385.9	356.4	388.2	343.2	213.0	466.4	66.7	253.5	60.2	112.7	80.6
MMST	34.0	47.6	31.4	42.4	38.8	12.6	70.8	19.2	58.2	13.6	21.4	23.2
HDI	78.3	61.1	68.6	55.0	68.7	57.9	78.1	7.0	20.2	17.2	3.3	0.2
KD	2.6	2.6	2.5	2.5	2.5	2.4	2.8	0.1	0.4	0.0	0.2	0.2
SKW	29.5	29.8	29.0	28.5	28.7	24.0	37.8	2.6	13.8	0.3	5.5	8.0
FPC	13.3	13.1	13.1	14.1	13.0	11.7	14.6	1.0	2.9	0.2	1.4	1.3
WAB	61.2	60.9	61.1	62.8	61.0	59.2	62.9	1.6	3.7	0.3	1.7	1.7

Min., minimum; Max., maximum, LP, Low parent, HP, High parent

†MLT, midline left time; MLV, midline left value; MLS, midline left slope; MLW, midline left width; MLI, midline left integral; MPT, midline peak time; MPV, midline peak value; MPW, midline peak width; MPI, midline peak integral; MRT, midline right time; MRV, midline right value; MRS, midline right slope; MRW, midline right width; MRI, midline right integral; MMST, midline mixing stability or tolerance; MTXV, midline time_X value; MTXS, midline time_X slope; MTXW, midline time_X width; MTXI, midline time_X integral; HDI, hardness index; KD, kernel diameter; SKW, single kernel weight; FPC, flour protein content; WAB, water absorption. Underlined values represent significant ($P < 0.05$) transgressive segregants.

Pearson correlation coefficients

The relationship between variables in the present study was determined using Pearson correlations (Table 12, Table A2). Similar to the classification used for heritability, we classified Pearson correlation into three categories. The correlation ≤ 0.3 was considered low except for zero correlation, 0.4-0.6 was considered as moderate and > 0.6 as high. In all the environments kernel characteristics had low correlation with rheological properties of the dough suggesting that this set of traits can be improved independently and those kernel characteristics are poor predictors of the dough properties. In both individual and combined environments, the FPC was positively and significantly correlated with MPW, MLV, MPV, MTXI and MTXV (Table 12, Table A2). Similar findings were observed by Bordes et al. (2008) except for MLV which was not significant in their study. The FPC showed positive and significant correlation with MLS, MRV, MMST but a negative and significant correlation with MRS in BS14, ET14 and for data averaged across environments (Table 12, Table A2). The FPC was highly correlated with water absorption (WAB) in both individual and across environments with a range in correlation of 0.67-0.97. The SKW revealed low or no correlation with the rest of the traits with significance observed for its correlation with HDI in ET14 and HY13, MRT and MRI across environment. The MLT showed a perfect correlation with MPT in all the environments and across the environments suggesting that improving MLT will improve MPT and vice versa. In addition, MLT had high positive correlation with MLI, MPI and MTXW both in individual and combined environments and had positive and significant correlation with MRT and MRI for the data combined across environments .

Table 12 Correlation matrix for kernel characteristics and rheological properties for data averaged across environments.

	MLT	MLV	MLS	MLW	MLI	MPT	MPV	MPW	MPI	MRT	MRV	MRS	MRW	MRI	MTXV	MTXW	MTXI	MMST	HDI	SKW	FPC
MLV	**-0.27**																				
MLS	**-0.79**	0.02																			
MLW	**-0.31**	**0.64**	**0.24**																		
MLI	**0.95**	-0.01	**-0.81**	-0.13																	
MPT	**0.99**	**-0.27**	**-0.79**	**-0.31**	**0.95**																
MPV	**-0.62**	**0.85**	**0.51**	**0.68**	**-0.41**	**-0.62**															
MPW	0.05	**0.39**	0.01	**0.69**	**0.20**	0.05	**0.36**														
MPI	**0.92**	0.09	**-0.79**	-0.06	**0.99**	**0.92**	**-0.32**	**0.25**													
MRT	**0.80**	**0.01**	**-0.73**	**-0.20**	**0.80**	**0.80**	**-0.36**	0.00	**0.80**												
MRV	0.03	**0.66**	-0.10	**0.59**	**0.20**	0.03	**0.51**	**0.61**	**0.27**	-0.01											
MRS	**0.60**	-0.10	**-0.66**	-0.14	**0.61**	**0.60**	**-0.41**	0.08	**0.59**	**0.68**	-0.06										
MRW	**0.48**	**0.24**	**-0.56**	**0.32**	**0.58**	**0.48**	-0.06	**0.57**	**0.60**	**0.45**	**0.56**	**0.60**									
MRI	**0.73**	**0.29**	**-0.71**	0.02	**0.82**	**0.73**	-0.10	**0.16**	**0.84**	**0.92**	**0.33**	**0.58**	**0.56**								
MTXV	**0.26**	**0.77**	**-0.31**	**0.55**	**0.50**	**0.26**	**0.52**	**0.60**	**0.58**	**0.39**	**0.71**	**0.26**	**0.59**	**0.61**							
MTXW	**0.83**	-0.04	**-0.60**	0.02	**0.87**	**0.83**	**-0.32**	**0.43**	**0.87**	**0.62**	**0.25**	**0.53**	**0.59**	**0.65**	**0.50**						
MTXI	**-0.67**	**0.85**	**0.40**	**0.68**	**-0.43**	**-0.67**	**0.93**	**0.38**	**-0.34**	**-0.41**	**0.57**	**-0.34**	0.04	**-0.14**	**0.49**	**-0.36**					
MMST	**-0.80**	0.04	**0.99**	**0.24**	**-0.82**	**-0.80**	**0.52**	-0.01	**-0.80**	**-0.77**	-0.07	**-0.77**	**-0.60**	**-0.72**	**-0.31**	**-0.62**	**0.41**				
HDI	0.13	0.10	-0.13	0.04	0.14	0.13	0.00	-0.02	0.15	0.12	0.14	0.12	0.12	0.14	0.16	0.10	0.00	-0.14			
SKW	0.06	0.07	-0.09	0.04	0.06	0.06	0.03	0.11	0.07	0.14	0.07	0.04	0.09	0.14	0.12	0.07	0.00	-0.08	-0.04		
FPC	**-0.26**	**0.36**	**0.29**	**0.34**	**-0.15**	**-0.26**	**0.44**	**0.25**	-0.10	**-0.18**	**0.29**	**-0.15**	0.01	-0.07	**0.26**	-0.10	**0.43**	**0.28**	**0.15**	0.00	
WAB	-0.11	**0.15**	**0.21**	0.12	-0.09	-0.11	**0.23**	0.11	-0.07	-0.09	**0.14**	**-0.14**	-0.06	-0.05	0.12	-0.05	0.16	**0.21**	**0.15**	0.10	**0.83**

MLT, midline left time; MLV, midline left value; MLS, midline left slope; MLW, midline left width; MLI, midline left integral; MPT, midline peak time; MPV, midline peak value; MPW, midline peak width; MPI, midline peak integral; MRT, midline right time; MRV, midline right value; MRS, midline right slope; MRW, midline right width; MRI, midline right integral; MTXV, midline time_X value; MTXS, midline time_X slope; MTXW, midline time_X width; MTXI, midline time_X integral; MMST, midline mixing stability or tolerance; HDI, hardness index; SKW, single kernel weight; FPC, flour protein content; WAB, water absorption.

Bold values are significant at $P < 0.01$, underlined values are significant at $P < 0.05$

Similar observation was made between MLT and MRT except for the correlation in HY13 which was moderate. MLV showed consistently high correlation with MPV, MTXV, MTXI and MRV except that for the latter, the correlation in HY13 was moderate. Significant correlation between MLV and other traits showed inconsistent results except for MLW that had consistently moderate correlation in all the environments (Table 12, Table A2). The MLS consistently showed negative and high correlation with MLI and MPT suggesting that divergent selection is plausible. MLS showed high and significant positive correlation with MMST. Although combined correlation across environments between MLS and MPI, MRT, and MRT were negative and high, the correlations in individual environments were inconsistent revealing variation in both the magnitude and the direction of the correlation (Table 12, Table A2). The correlation between MLS and MRS were negative and significant.

The MLW had high positive and significant correlation with MTXI in individual and across environments. Similar results were observed with MPW, MRV and MPV but the magnitude of the correlation varied from low to high. The MLI had consistently positive and high correlation with MPT, MPI, and MTXW and it also showed consistently negative and high correlation with MMST (Table 12, Table A2). The correlation between MLI and MRT and between MLI and MRI was moderate but consistent in all the environments. MPT had high and consistent correlation with MPI, MRT, MTXW and MMST. Either moderate or high correlation was observed between MPV and several variables that include MTXI, MRV, MTXV and MMST. Similar observations were made for the correlation between MPW and MRV as well as MTXV and MTXI

The correlation between MPW with both MRV and MTXW oscillated from low to high. High positive correlation was observed between MPI and MTXW (Table 12, Table A2). The correlation between MPI with MRT, MRI, and MTXV was also positive although it ranged from moderate to high. Similar findings were observed for the correlation between MPI and MMST although in this case the correlation was negative (Table 12, Table A2). MRT and MRI were highly correlated in individual and combined environment. The correlation between MRT and MMST was negative in all the environments and it ranged from moderate to high. MRS consistently showed positive and moderate correlation with both MRW and MRS. MRV showed a high positive correlation with MTXV whereas the correlation with MTXI was positive and ranged from moderate to high. The correlation between MRW and MMST was negative and the magnitude ranged from low to high in individual environments. The correlation of MRW with MTXV and MTXW was also moderate for the data averaged across environments. In individual environments, the correlations ranged from low to high for MTXV and low to moderate for MTXW (Table A2).

Although the correlation between MRI and MMST was consistently negative, there was variability in the magnitude from one environment to the next. Similar observations were made for the correlation between MRI with both MTXV and MTXW although in this case the correlation was positive. MTXV had an overall moderate positive correlation with both MTXW and MTXI but a negative correlation with MMST. The correlations between TMXW with both MTXI and MMST were negative in all the environments. The latter two variables were positively correlated (Table 12, Table A2).

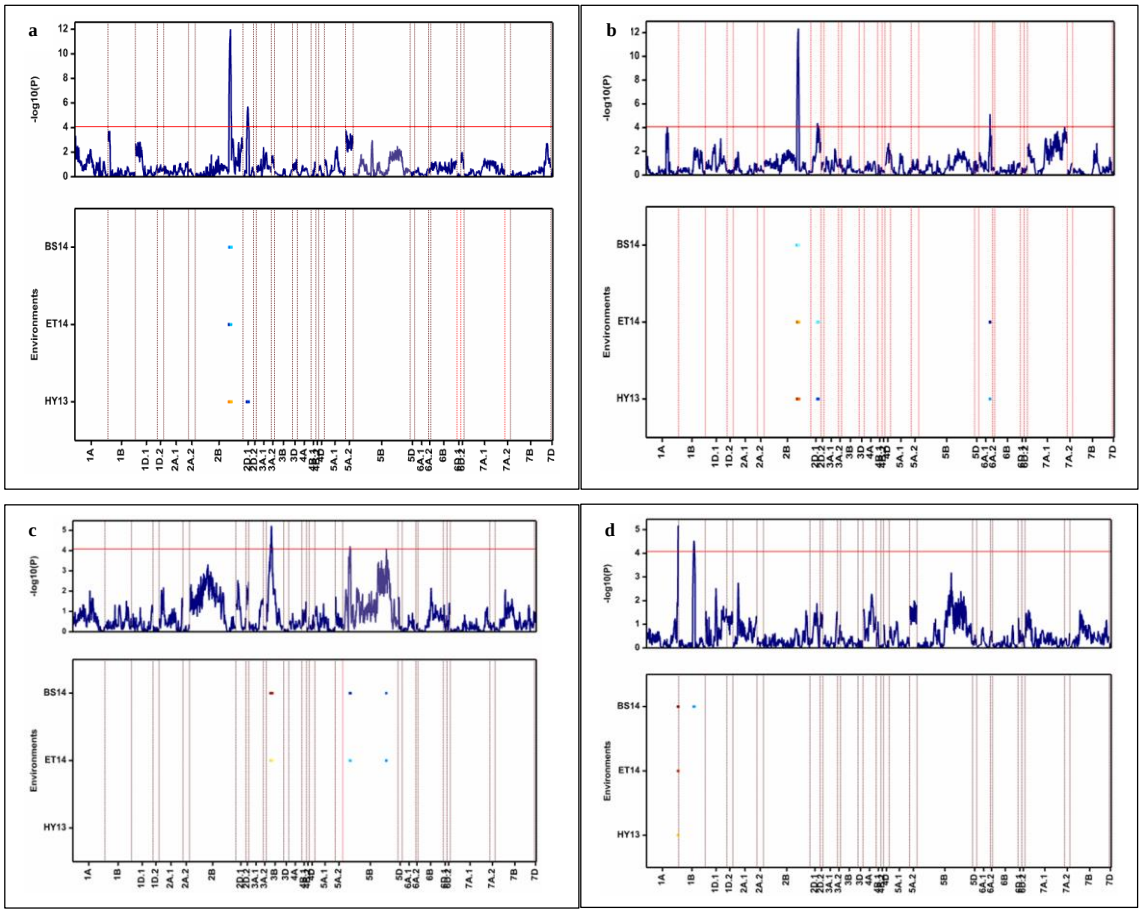

Figure 10. End-use QTL detected based on a single trait multi-environment QTL mapping model.

The upper graph is QTL profile plot with the y-axis = threshold for declaring significance of QTL. The red line represents the threshold corrected for the number of independent tests using Li and Ji (2005). The lower profile is the genome-wide heat map of significant QTL across traits. The y-axis is the traits and the x-axis represents the chromosomes. The light blue to blue color indicates the favorable allele originates from CO960293-2 and the red color indicates the favorable allele originates from TAM 111. (a) hardness index (HDI) (b) kernel diameter (KD) (c) flour protein content (FPC) (d) midline peak time (MPT) (e) midline peak integral (MPI) (f) midline left time (MLT) (g) midline time_X value (MTXV) (h) midline time_X width (MTXW) (i) midline left integral (MLI) (j) midline right integral (MRI) (k) midline right width (MRW) (l) midline peak width (MPW) (m) midline right value (MRI).

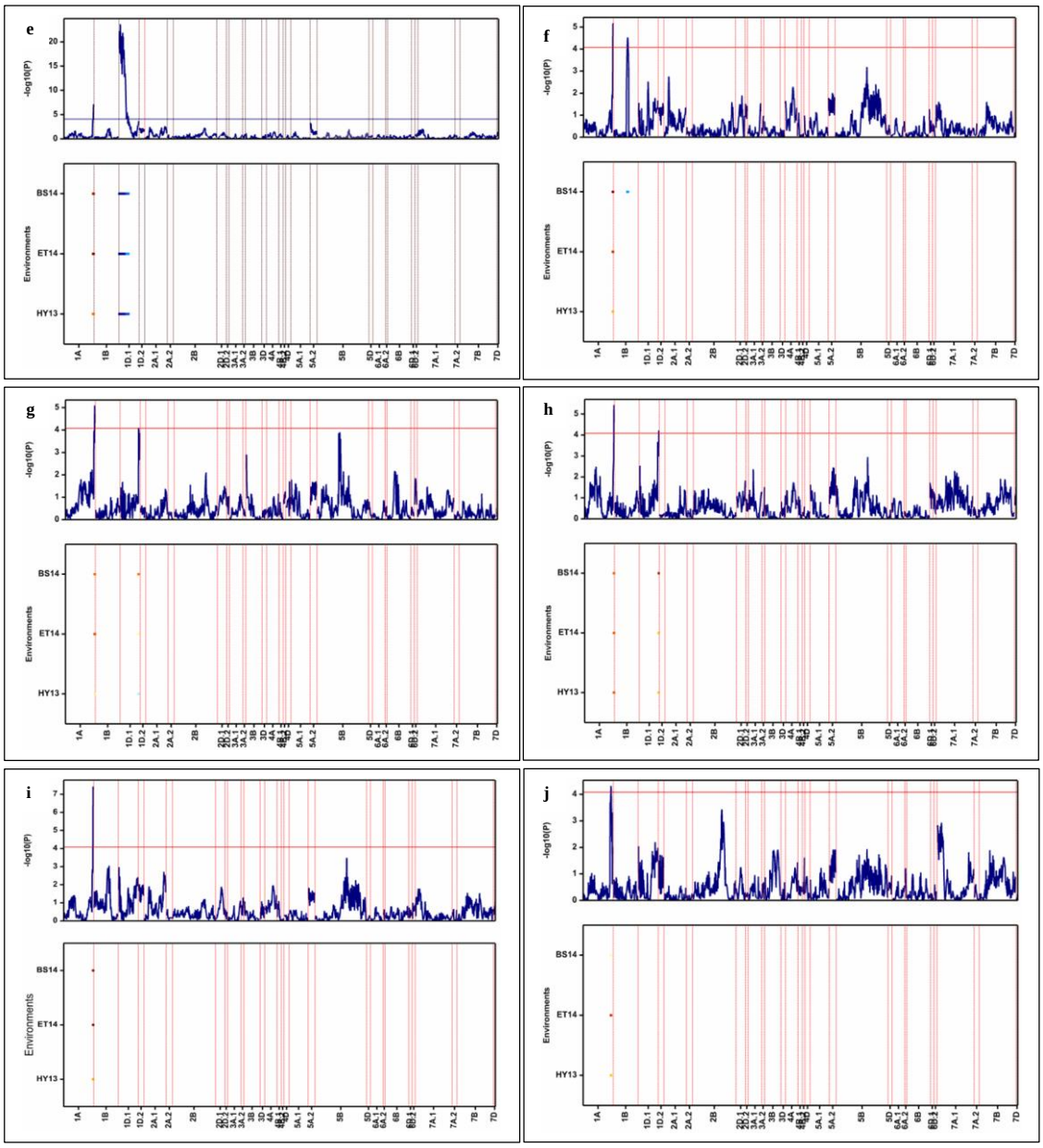

Figure 10 Continued

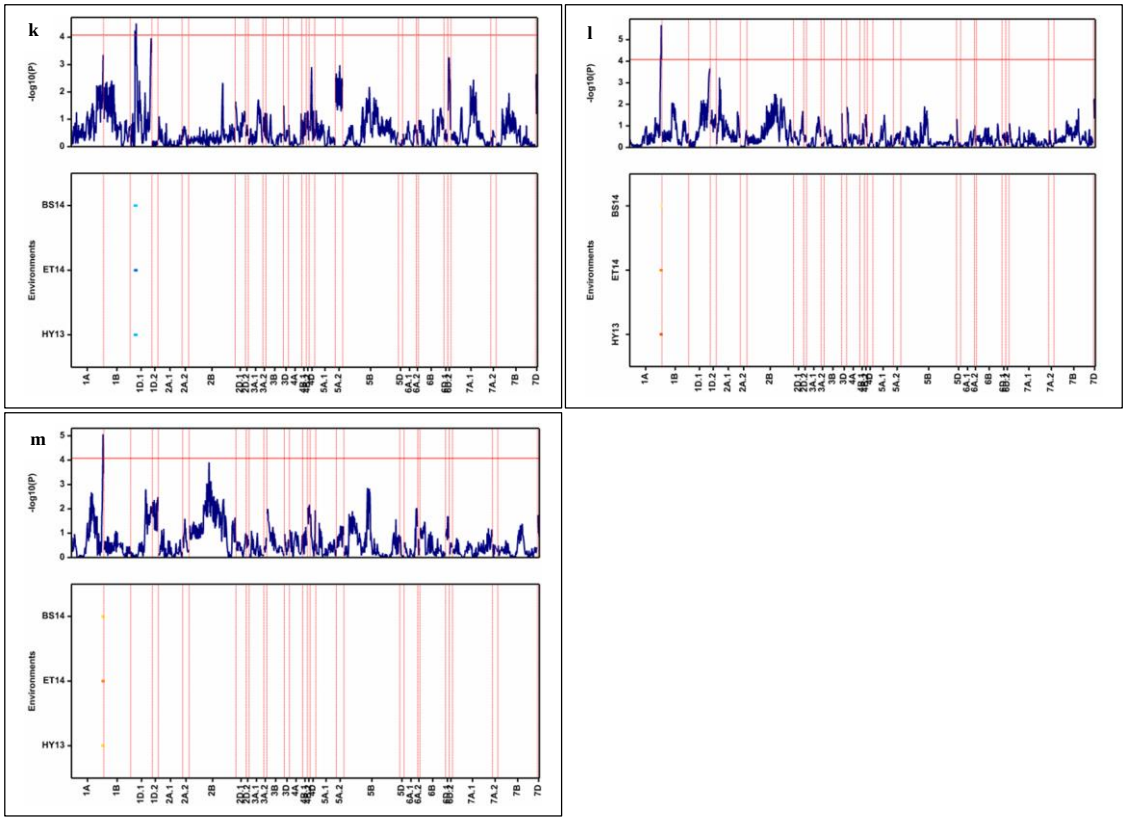

Figure 10 Continued

QTL for kernel characteristics and flour protein content

The kernel HDI QTL was detected on chromosome 2B and 2D.1 both in individual environment (Table 13) and multi-environment analysis (Table 14). The genomic regions of this QTL were consistent in both cases. In the single trait multi-environment model, an additional QTL was detected on chromosome 1A although this QTL showed significant effect only in BS14 suggesting significant effect of the environment on the expression of this QTL (Table 14). We observed significant QEI as indicated by a switch in the source of high value allele (HVA) from one environment to the next (Figure 10).

Table 13 End-use quality QTL detected in Individual environment

Env	QTL name‡	Peak SNP‡	Peak pos.	CI_LL	CI_UL	-log10(P)	R^2	A	Traits†
Bushland14	*Qmli.tamu.1A*	M11264	379.8	370.5	382.0	6.2	14.3	-19.0	MLI
	Qmpi.tamu.1A	M11264	379.8	369.7	382.0	6.2	13.3	-18.0	MPI
	Qmtxw.tamu.1A	M7628	380.4	365.4	382.0	4.8	9.8	-1.7	MTXW
	Qmlt.tamu.1A	M12147	382.0	367.3	382.0	5.7	10.0	-0.4	MLT
	Qmls.tamu.1D.1	M23920	0.3	0.0	5.0	11.2	25.9	-4.0	MLS
	Qmpt.tamu.1D.1	M80856	50.3	46.7	53.9	13.7	32.7	0.8	MPT
	Qmtxv.tamu.1D.1	C3P234	233.9	219.7	248.0	3.0	10.2	-1.7	MTXV
	Qmpi.tamu.1D.1	M65713	247.5	232.9	248.2	4.9	10.0	-16.0	MPI
	Qmtxw.tamu.1D.1	M65713	247.5	237.7	248.2	6.3	13.6	-2.0	MTXW
	Qhdi.tamu.2B	M4514	410.0	401.7	418.3	8.0	15.7	2.0	HDI
	Qwab.tamu.3B	C12P47	47.3	35.4	59.2	4.4	11.7	-0.4	WAB
	Qfpc.tamu.3B	C12P55	54.6	41.6	67.6	4.5	10.9	-0.3	FPC
	Qskw.tamu.7B	M40231	281.4	266.5	296.3	4.4	9.9	-0.7	SKW
Etter14	*Qmri.tamu.1A*	C1P360	359.9	346.4	373.4	4.8	10.6	-14.0	MRI
	Qmlv.tamu.1A	M12354	376.4	365.2	382.0	5.1	12.2	-1.0	MLV
	Qmrv.tamu.1A	M61102	376.6	361.2	382.0	4.1	9.6	-1.1	MRV
	Qmtxv.tamu.1A	M61102	376.6	361.7	382.0	4.6	9.8	-1.2	MTXV
	Qmli.tamu.1A	M12147	382.0	372.5	382.0	6.0	14.0	-19.0	MLI
	Qmlt.tamu.1A	M12147	382.0	365.6	382.0	5.0	9.2	-0.4	MLT
	Qmpi.tamu.1A	M12147	382.0	371.7	382.0	7.3	13.2	-18.0	MPI
	Qmpt.tamu.1A	M12147	382.0	365.6	382.0	5.0	9.2	-0.4	MPT
	Qmtxw.tamu.1A	M12147	382.0	361.3	382.0	4.0	7.9	-1.5	MTXW
	Qmpw.tamu.2A.1	M46662	33.5	16.9	50.1	4.1	9.1	1.5	MPW
	Qkd.tamu.2B	M8143	404.3	389.5	419.1	5.1	9.9	-0.03	KD
	Qhdi.tamu.2B	M3178	406.1	399.9	412.3	10.0	20.0	2.3	HDI
	Qkd.tamu.6A.1	M13129	128.5	120.5	136.5	7.7	16.1	0.03	KD
Hays 13	*Qmrt.tamu.1A*	M11301	355.5	339.2	371.8	4.1	9.2	-0.3	MRT
	Qmpw.tamu.1A	M65288	379.0	365.1	382.0	4.5	10.4	-2.0	MPW
	Qmtxw.tamu.1A	M65288	379.0	365.4	382.0	5.4	10.5	-2.1	MTXW
	Qmrs.tamu.1D.1	M76969	39.9	25.7	54.1	4.5	10.2	0.3	MRS
	Qkd.tamu.2B	M21618	403.8	391.5	416.1	5.2	11.4	-0.03	KD
	Qhdi.tamu.2D.1	C8P51	51.3	44.8	57.8	7.2	19.2	2.4	HDI

Pos., position; CI, confidence interval; LL, lower limit; UL, upper limit; R^2, proportion of variation explained by the QTL; A, additive effect
†FPC, flour protein content; HDI, hardness index; SKW, single kernel weight; MLI, midline left integral; MLT, midline left time; MPI, midline peak integral; MPT, midline peak time; MTXV, midline time_X value; MTXW, midline time_X width; WAB, water absorption; MLS, midline left slope; KD, kernel diameter; MRI, midline right integral; MRV, midline right value; MPW, midline peak width; MRS, midline right slope; MRT, midline right time.
‡SNP markers on the array are abbreviated using letter M and their respective index number whereas pseudo-markers are abbreviated using the linkage group and their position on the linkage group e.g C12P55 is a pseudo-marker on linkage group 12 (chromosome 3B) at position 55 cM.
Negative additive effect indicate high value allele (HVA) from TAM 111, positive values corresponds to HVA from CO960293-2

Table 14 Single trait multi-environment QTL for end-use quality

QTL name	Peak SNP‡	Peak Pos.	CI_LL	CI_UL	-log10(P)	Min. R^2	Max. R^2	Min. A‡‡	Max. A‡‡	Trait†	QEI
Qhdi.tamu.1A	M43982	292.7	282.7	302.7	5.7	13.4	13.4	1.8	1.8	HDI	yes
Qmri.tamu.1A	M6999	357.4	346.7	368.1	5.3	3.9	12.7	10.3	15.8	MRI	yes
Qmrt.tamu.1A	M6999	357.4	330.3	382.0	4.9	4.1	6.7	0.2	0.2	MRT	no
Qmrv.tamu.1A	M61102	376.6	361.2	382.0	5.1	3.7	9.6	0.8	1.1	MRV	yes
Qmtxv.tamu.1A	M65288	379.0	366.5	382.0	6.6	3.1	11.3	1.3	1.3	MTXV	no
Qmpw.tamu.1A	M65373	379.7	364.4	382.0	5.7	3.4	9.7	1.1	2	MPW	yes
Qmtxw.tamu.1A	M65373	379.7	364.2	382.0	6.0	6.3	9.6	1.6	1.6	MTXW	no
Qmli.tamu.1A	M7628	380.4	371.8	382.0	6.2	8.1	15.1	14.8	19.5	MLI	yes
Qmpi.tamu.1A	M7628	380.4	367.2	382.0	9.1	10.1	10.8	16.5	16.5	MPI	no
Qmlt.tamu.1A	M12147	382.0	368.8	382.0	5.5	6.8	10.8	0.4	0.4	MLT	no
Qmpt.tamu.1A	M12147	382.0	368.8	382.0	5.5	6.8	10.8	0.4	0.4	MPT	no
Qmlt.tamu.1B	C2P178	178.1	161.3	194.9	4.2	9.0	9.0	0.4	0.4	MLT	yes
Qmpt.tamu.1B	C2P178	178.1	161.3	194.9	4.2	9.0	9.0	0.4	0.4	MPT	yes
Qmrt.tamu.1D.1	M9742	0.7	0.0	6.0	14.1	22.3	23.1	0.6	0.6	MRT	yes
Qmpi.tamu.1D.1	M26941	12.7	8.4	17.0	21.9	26.5	28.2	26.6	26.6	MPI	no
Qmrw.tamu.1D	M7763	65.8	45.2	86.5	4.5	4.8	7.9	1.0	1.4	MRW	yes
Qmtxv.tamu.1D.1	C3P234	233.9	221.5	246.2	3.4	3.4	11.4	0.7	1.7	MTXV	yes
Qmtxw.tamu.1D.1	M65713	247.5	233.1	248.2	6.2	6.6	10.1	1.7	1.7	MTXW	no
Qkd.tamu.2B	M8143	404.3	393.1	415.5	12.5	2.8	12.2	0.01	0.03	KD	yes
Qskw.tamu.2B	M8143	404.3	386.6	422.0	10.6	8.1	8.7	0.6	0.7	SKW	yes
Qhdi.tamu.2B	M3178	406.1	400.8	411.4	19.1	7.8	23.2	1.5	2.5	HDI	yes
Qhdi.tamu.2D	C8P51	51.3	42.5	60.1	5.3	14.9	14.9	2.1	2.1	HDI	yes
Qkd.tamu.2D	M22544	73.9	37.1	110.7	3.6	2.0	5.7	0.01	0.02	KD	yes
Qfpc.tamu.3B	C12P55	54.6	42.5	66.7	4.2	4.2	11.5	0.1	0.3	FPC	yes
Qfpc.tamu.5B	M35477	82.0	70.3	93.7	5.0	4.5	11.8	0.1	0.3	FPC	yes
Qkd.tamu.6A	M13129	128.5	120.1	136.9	8.0	10.6	15.5	0.03	0.03	KD	yes
Qskw.tamu.6A	M13129	128.5	120.6	136.4	8.3	9.0	16.3	0.6	1.0	SKW	yes

Pos., position; CI, confidence interval; LL, lower limit; UL, upper limit; R^2, proportion of variation explained by the QTL; A, additive effect
†MLI, midline left integral; MLT, midline left time; MPI, midline peak integral; MPT, midline peak time; MPW, midline peak width; MRV, midline right value; MRW, midline right width; MRI, midline right integral; MRT, midline right time; FPC, flour protein content;
HDI, hardness index; KD, kernel diameter; SKW, kernel width; MTXV, midline time_X value; MTXW, midline time_X width
‡‡Additive effect are given as absolute values without regard to source of HVA. Figure 11 has details of the source of HVA.
‡SNP markers on the array are abbreviated using letter M and their respective index number whereas pseudo-markers are abbreviated using the linkage group and their position on the linkage group e.g C2P178 refers to a pseudo-marker on linkage group 2 (chromosome 1A) at position 55 cM.

In BS14 and ET14 the HVA was from the maternal parent whereas in HY13 the HVA was from the paternal parent (Figure 10). The magnitude of the additive effect ranged from 1.5 to 2.5 (Table 14). The QTL on 2D.1 had significant additive effect of 2.1 in HY13 (Table 14). In single trait multi-environment QTL analysis, kernel diameter (KD) was linked to three QTL on chromosome 2B, 2D.1 and 6A.1 with all the three QTL showing significant QEI (Table 14, Figure 10). The additive effect for the KD QTL on 2B ranged from 0.02 to 0.03 mm and was significant in all the environments (Table 14, Figure 11). In single environment QTL mapping, this QTL was detected only in ET14 and BS14 (Table 13).

In a multi-environment model, the KD QTL on 2D.1 and 6A.1 had significant additive effect in two environments and their corresponding additive effect ranged from 0.01 to 0.02 mm and 0.01 to 0.03 mm, respectively (Table 14). In single-environment QTL mapping, no significant QTL was detected on 2D.1 whereas the QTL on 6A.1 was only detected in ET14 (Table 13). QTL for flour protein content (FPC) was mapped on chromosome 3B and 5B (Table 14) and the additive effect for both QTL ranged from 0.1 to 0.3% (Table 14, Figure 11). The QTL on 3B had HVA from the paternal parent whereas the QTL on 5B had HVA from the maternal parent (Figure 10). The QTL for FPC on 3B was also detected in BS14 when data was analyzed using single environment QTL mapping model (Table 13). Co-location was also observed on chromosome 2B for KD, SKW and HDI whereas KD and SKW QTL were co-located on chromosome 6A.1 (Table 14).

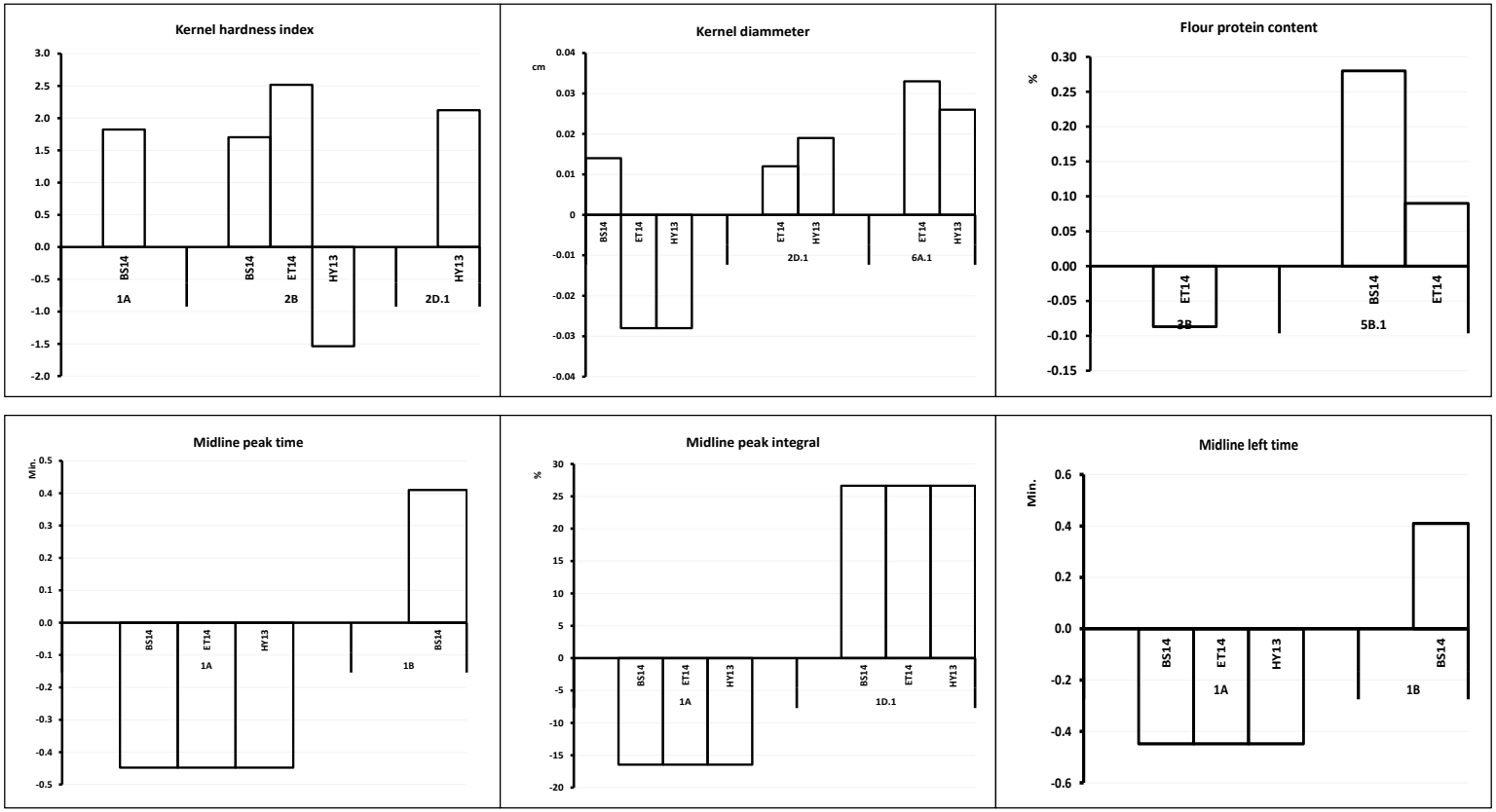

Figure 11. Additive genetic effect for end-use quality QTL detected using single trait multi-environment QTL model. Negative additive effect indicates high value allele (HVA) from TAM 111 whereas positive values indicate HVA from CO960293-2.

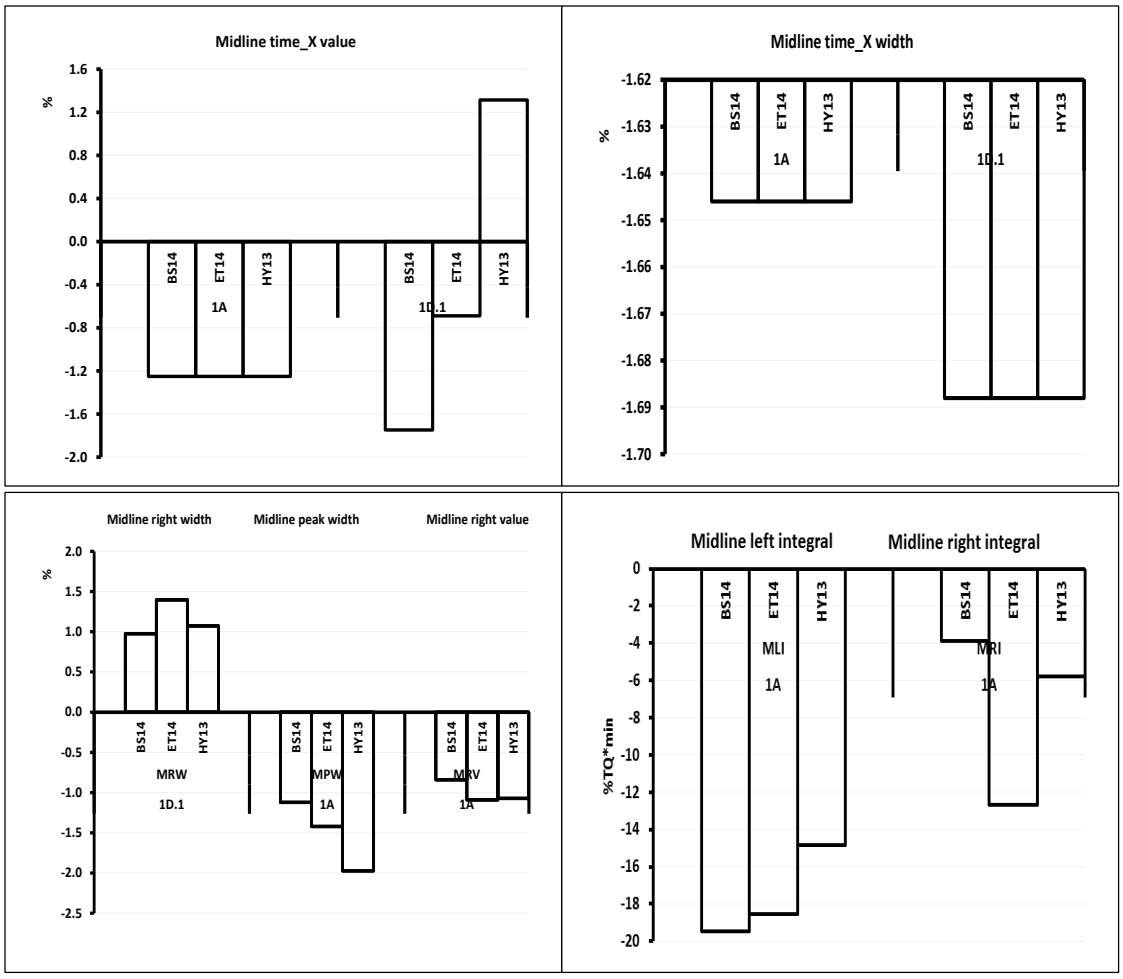

Figure 11. Continued

QTL linked to mixograph parameters

Most QTL for mixograph mixing properties were mapped on chromosome 1A and 1D.1 both in individual environment, multi-environment and multi-trait QTL mapping model (Table 13, 14 and 15). In a multi-environment QTL mapping model, the MLI was mapped on chromosome 1A with an additive effect range of 14.8 to 19.5% min^{-1} (Table 14, Figure 11). The corresponding proportion of phenotypic variation explained by this

QTL ranged from 8.1 to 15.1% (Table 14). In all the environments, the HVA was from the paternal parent, suggesting minimal effect of crossover QEI (Figure 10).

The MLT QTL was mapped on chromosome 1A and 1B in a multi-environment QTL mapping (Table 14). The QTL on 1A was detected in all the three environments and had equal additive effect whereas the QTL on 1B only showed significant additive effect in BS14 (Table 14, Figure 11). The two QTL for MLT showed equal additive effect of 0.4 minutes across environments but the R^2 was variable. For the QTL on 1A, the range in R^2 was 6.8 to 10.8%, whereas the QTL on 1B had an R^2 of 9.0% in BS14 (Table 14). In individual environment QTL analysis, the MLT QTL on 1A was detected in BS14 and ET14 with a corresponding R^2 of 10.0% and 9.2% respectively (Table 13). Data averaged across environments showed MLT QTL on 1A with a corresponding R^2 of 7.7% (Table 15). Similar to MLT, the midline peak time (MPT) under single trait multi-environment QTL analysis was mapped on chromosome 1A and 1B with both QTL showing an additive effect of 0.4 minutes (Table 14). The QTL on 1A was detected in all the environments while the QTL on 1B was detected only in BS14 (Figure 10). The QTL on 1A had HVA from the paternal parent whereas the QTL on 1B showed HVA from the maternal parent (Figure 11). In the individual environment model, QTL for MPT were detected on chromosome 1A in ET14 and 1D.1 in BS14. The QTL on 1A was in the same position as the QTL detected in multi-environment model. In addition, the QTL on chromosome 1A was also detected based on the data averaged across environments (Table 15). The results for MPT and MLT agrees with the results from correlation analysis where the two traits were highly correlated (Table 12).

Table 15 QTL for end-use quality based on data averaged across environments

QTL name	Peak SNP	Peak pos.	CI_LL	CI_UL	-log10(P)	R^2	A	Trait†
Qmrt.tamu.1A	M78618	343.8	305.4	382.0	2.6	5.6	-0.3	MRT
Qmtxv.tamu.1A	C1P378	377.8	366.2	382.0	4.9	11.9	-1.3	MTXV
Qmpw.tamu.1A	M65288	379.0	368.2	382.0	5.8	12.6	-1.4	MPW
Qmrv.tamu.1A	M65373	379.7	366.6	382.0	4.6	10.8	-1.1	MRV
Qmtxw.tamu.1A	M65373	379.7	368.4	382.0	5.9	12.2	-1.7	MTXW
Qmli.tamu.1A	M7628	380.4	371.0	382.0	6.1	14.2	-17.3	MLI
Qmpi.tamu.1A	M7628	380.4	369.3	382.0	7.3	12.4	-15.7	MPI
Qmri.tamu.1A	M7628	380.4	371.1	382.0	5.9	14.2	-17.3	MRI
Qmlt.tamu.1A	M12147	382.0	360.8	382.0	5.2	7.7	-0.4	MLT
Qmpt.tamu.1A	M12147	382.0	360.8	382.0	5.2	7.7	-0.4	MPT
Qmls.tamu.1D.1	C3P2	2.1	0.0	5.8	13.0	32.4	-2.8	MLS
Qmrw.tamu.1D.1	M22056	245.8	233.8	248.2	5.3	11.6	-1.4	MRW
Qmtxw.tamu.1D	M65713	247.5	237.3	248.2	6.3	13.2	-1.8	MTXW
Qmpw.tamu.1D.1	M3277	248.2	232.1	248.2	4.5	9.3	-1.2	MPW

Pos., position; CI, confidence interval; LL, lower limit; UL, upper limit; R^2, proportion of variation explained by the QTL; A, additive effect
†MLI, midline left integral; MLS, midline left slope; MLT, midline left time, MPI, midline peak integral; MPT, midline peak time, MPW, midline peak width; MRI, midline right integral; MRT, midline right time; MRV, midline right value; MRW, midline right width; MTXV, midline time_X value; MTXW, midline time_X width.
‡All SNP markers on the array are abbreviated using letter M and their respective index number whereas pseudo-markers are abbreviated using the linkage group and their position on the linkage group e.g C3P2 refers to a pseudo-marker on linkage group 3 (chromosome 1D.1) at position 2.0 cM.
Negative additive effect indicates high value allele (HVA) from TAM 111, positive values corresponds to HVA from CO960293-2.

The QTL linked to MPI were detected on chromosome 1A and 1D.1. The magnitude of additive effect for both QTL was consistent in all the environments suggesting that these are constitutive QTL (Table 14, Figure 11). The magnitude of additive effect was 16.5 and 26.6% min^{-1} for the QTL on 1A and 1D.1, respectively (Table 14, Figure 11). The range in R^2 for the QTL on 1A was 10.1 to 10.8% whereas the range for the QTL on 1D.1 was 26.5 to 28.2% (Table 14). The QTL on 1A had HVA from the

paternal parent whereas a maternal allele was observed for the QTL on chromosome 1D.1 (Figure 11). The QTL on 1A was also detected in single environment QTL analysis in BS14 and ET14, whereas the QTL on 1D was detected only in BS14 (Table 13). The MPI QTL for the data averaged across environments was detected on chromosome 1A and in the same position as individual and multi-environment QTL analyses (Table 15).

In a multi-environment QTL analysis, one QTL with significant additive genetic effect was detected for MPW on chromosome 1A (Table 14, Figure 10). The magnitude of additive effect ranged from 1.1 to 2.0% with a corresponding R^2 range of 3.4 to 9.7% (Table 14) and in all the environments, the HVA was from the paternal parent (Figure 12). This QTL was also detected in HY13 in a single environment QTL analysis with an additive effect and R^2 of -2.0% and 10.4% respectively (Table 13). Data averaged across environments revealed the MPW QTL on 1A with an additive effect of -1.4% and an R^2 of 12.6% (Table 15). An additional QTL for MPW was detected on 1D.1 for the data averaged across environments. The additive effect and R^2 for this QTL were -1.2% and 9.3% respectively (Table 15).

The MRV QTL was mapped on chromosome 1A both in multi-environment QTL analysis and for the data averaged across environment (Table 14 and 15, Figure 10). The corresponding magnitude of the additive effect ranged from 0.8 to 1.1% and the R^2 ranged from 3.7 to 9.6% (Table 14, Figure 11). For the data averaged across environments, the R^2 and the additive effect were -1.1% and 10.8%, respectively (Table 15). The QTL for MRW was detected on chromosome 1D.1 with a corresponding additive effect and R^2 range of 1.0 to 1.4 and 4.8 to 7.9% respectively (Table 14, Figure 10). The HVA for MRW

was from the maternal parent (Figure 11). The MRI QTL was detected on chromosome 1A with an additive effect range of 10.3 to 15.8% min^{-1} and an R^2 range of 3.9 to 12.7% (Table 14, Figure 11). In all the environments, the HVA was from the paternal parent (Figure 11). Both MRW and MRI QTL were also detected based on the data averaged across environments (Table 15). In individual environment QTL analysis, MRI QTL was detected only in ET14 whereas MRW was not detected in any environment.

In multi-environment QTL model, two QTL for MRT were detected on chromosome 1A and 1D.1 with a corresponding additive effect of 0.2 and 0.6 min, respectively (Table 14, Figure 11). The R^2 range for the QTL on 1A ranged from 4.1 to 6.7% whereas on 1D.1 the range was 22.3 to 23.1% (Table 14). The QTL on 1A had HVA from the paternal parent whereas the QTL 1D.1 had HVA from the maternal parent (Figure 10). The QTL on 1A was detected in HY13 when data was analyzed using single environment QTL model (Table 13). The QTL linked to midline time_X value (MTXV) were mapped on chromosome 1A and 1D.1 (Table 14, Figure 10). In all the environments, the magnitude of the additive effect for the MTXV was 1.3% for the QTL on 1A, whereas the magnitude on 1D.1 ranged from 0.7 to 1.7% (Table 14, Figure 11). The QTL on 1A explained 3.1 to 11.3% of the phenotypic variation whereas the QTL on 1D.1 accounted for 3.4 to 11.4% of the phenotypic variation (Table 14). In all the environments, the QTL on 1A had HVA from the paternal parent whereas the QTL on 1D.1 showed a switch to the maternal parent for the QTL mapped in HY13 indicating a significant cross-over QEI (Figure 10). In a single environment QTL analysis, the MTXV QTL on 1A was detected in ET14 whereas the QTL on 1D.1 was detected in BS14 (Table 13). When data was

averaged across environment only the MTXV QTL on 1A was detected (Table 15). Midline time_X width (MTXW) revealed significant effect QTL on chromosome 1A and 1D.1 with an additive effect of 1.6% and 1.7%, respectively (Table 14, Figure 11). The two QTL were detected in all the environments and the variation in R^2 ranged from 6.3 to 9.6% for the QTL on 1A and 6.6 to 10.1% for the QTL on 1D.1 (Table 14). The HVA for the QTL was from the paternal parent and both QTL showed environment non-specific additive effect (Figure 11). The MTXW QTL on chromosome 1A was also detected in a single environment model in both BS14 and ET14 (Table 13) and when data was averaged across environments (Table 15).

Co-location was observed among QTL linked to different traits (Table 14). The QTL for MLT and MPT were co-located on chromosome 1B whereas MTXV and MTXW were co-located on 1D.1 (Table 13). Furthermore, the QTL for MRI and MRT were co-located on chromosome 1A and on the same chromosome but a different locus, co-location was observed for MRV, MTXV, MPW, MTW, MTXW, MLI, MPI, MTV, MLT, and MPT (Table 14). The MLI, MLT, MPI, MPT, MRV, MTXV, and MTXW were co-located on 1A (Table 14). On the same chromosome but in a different position, MRI and MRT were also co-located (Table 14). Based on data averaged across environments, co-location of MPW and MRW was detected on chromosome 1D.1 (Table 15). The co-location of traits suggests presence of QTL in linkage disequilibrium or QTL with pleotropic effects and further supports the correlation observed in this study.

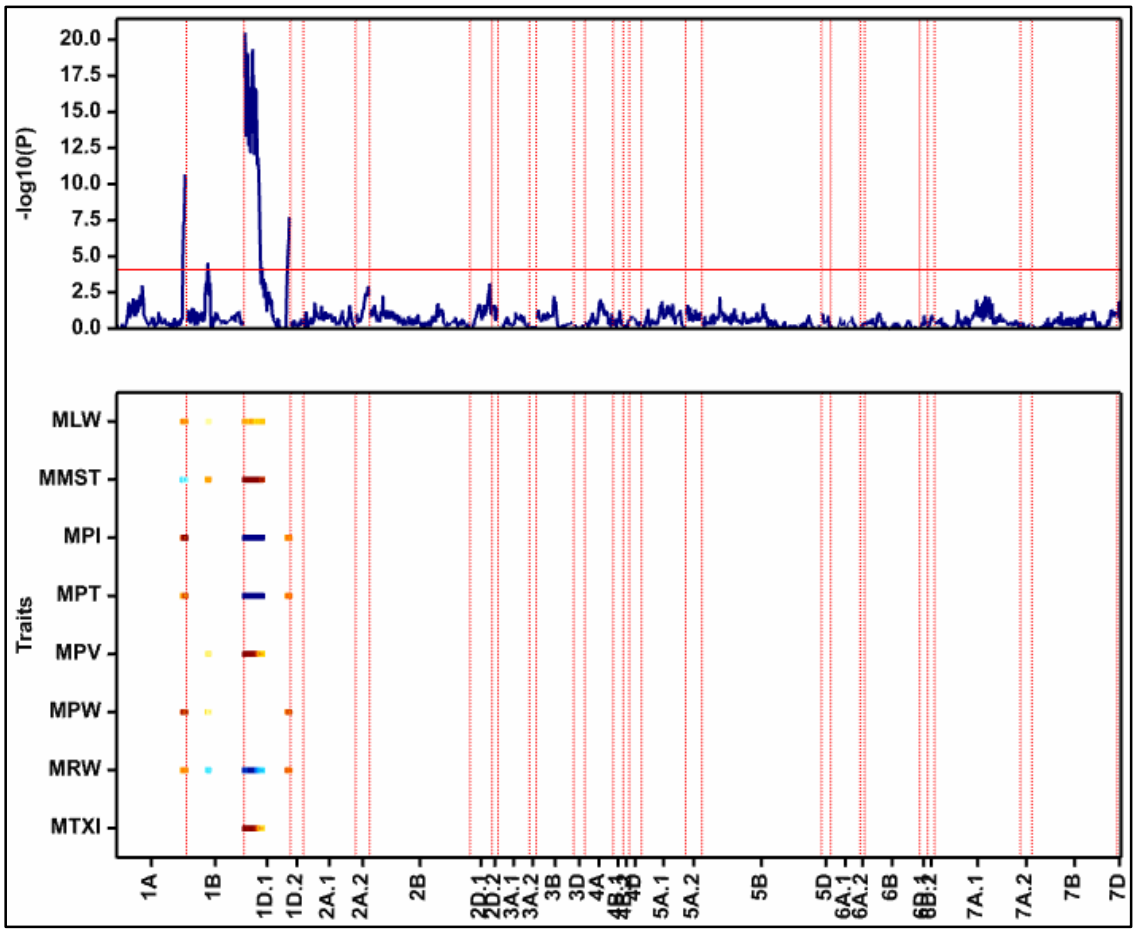

Figure 12. Genome-wide scan for end-use quality QTL detected based on multi-trait QTL model.

The upper graph is QTL profile plot with the y-axis = threshold for declaring significance of QTL. The red line represents the threshold corrected for the number of independent tests using Li and Ji (2005). The lower profile is the genome-wide heat map of significant QTL across traits. The y-axis is the traits and the x-axis represents the chromosomes. The light blue to blue color indicates the favorable allele originates from CO960293-2 and the red color indicates the favorable allele originates from TAM 111. MLW, midline left width; MMST, midline mixing stability or tolerance; MPI, midline peal integral; MPT, midline peak time; MPV, midline peak value; MPW, midline peak width; MRW, midline right width; MTXI, midline time_X integral.

Multi-trait QTL for end-use quality

Multi-trait QTL analysis revealed three QTL on chromosomes 1A, 1B and 1D linked to multiple traits. The QTL detected on chromosome 1A was linked to MLW, MMST, MPI, MPT, MPW, and MRW (Table 16, Figure 12), further supporting the co-location observed in the single trait multi-environment QTL analysis model. On chromosome 1A, all co-located traits detected in single trait multi-environment QTL mapping were also co-located. The absolute magnitude of the additive genetic effects for QTL on 1A ranged from 0.14 for MMST to 0.35 for MPW and the R^2 ranged from 1.9 to 12.5%. The QTL co-located on chromosome 1B were for MMST, MPV, MPW and MRW with an absolute additive range of 0.17 to 0.28 and an R^2 range of 3.0 to 7.8% (Table 16, Figure 12). A significant multi-trait QTL on chromosome 1D explained 7.3 to 37.7% of the phenotypic variation and revealed co-location for MLW, MMST, MPI, MPT, MPV, MRW and MTXI (Table 16, Figure 12). A second QTL located 248 cM away revealed co-location for MPI, MPT, MPW, and MRW although the R^2 was comparatively low and ranged from 4.9 to 8.9%.

The switch in color from blue-red or vice-versa across traits in the QTL heat map indicates presence of significant crossover QTL-by-trait interaction (QTI) (Figure 12). In addition, the variation in color intensity for the same color e.g. from light red to red across traits indicates presence of non-crossover QTI (Boer et al., 2007; Malosetti et al., 2013). Thus, both the QTL mapped on 1A, 1B and 1D had significant QTI (Figure 12), whereas all the QTL except the one at the distal side of chromosome 1D.1 at 247.5 cM revealed crossover QTI (Table 16, Figure 12). The results of multi-trait analysis are also supported

by Pearson correlation coefficient, which showed that among the co-located traits, each trait showed significant correlation with at least another trait (Table 12)

Table 16 Multi-trait QTL for end-use quality based on the data averaged across environments.

QTL name	A‡	Pos.	CI_LL	CI_UL	R^2	Peak SNP	Trait†
Qmlw.tamu.1A	-0.28	379.7	368.8	382.0	7.7	M65373	MLW
Qmmst.tamu.1A	0.14	379.7	368.8	382.0	1.9	M65373	MMST
Qmpi.tamu.1A	-0.34	379.7	368.8	382.0	11.8	M65373	MPI
Qmpt.tamu.1A	-0.27	379.7	368.8	382.0	7.3	M65373	MPT
Qmpw.tamu.1A	-0.35	379.7	368.8	382.0	12.5	M65373	MPW
Qmrw.tamu.1A	-0.26	379.7	368.8	382.0	6.8	M65373	MRW
Qmmst.tamu.1B	-0.28	114.1	93.0	135.2	7.8	M80255	MMST
Qmpv.tamu.1B	-0.19	114.1	93.0	135.2	3.4	M80255	MPV
Qmpw.tamu.1B	-0.19	114.1	93.0	135.2	3.6	M80255	MPW
Qmrw.tamu.1B	0.17	114.1	93.0	135.2	3.0	M80255	MRW
Qmlw.tamu.1D.1	-0.27	0.7	0.0	3.8	7.3	M9742	MLW
Qmmst.tamu.1D.1	-0.55	0.7	0.0	3.8	30.0	M9742	MMST
Qmpi.tamu.1D.1	0.58	0.7	0.0	3.8	34.1	M9742	MPI
Qmpt.tamu.1D.1	0.61	0.7	0.0	3.8	37.7	M9742	MPT
Qmpv.tamu.1D.1	-0.39	0.7	0.0	3.8	15.5	M9742	MPV
Qmrw.tamu.1D.1	0.31	0.7	0.0	3.8	9.7	M9742	MRW
Qmtxi.tamu.1D.1	-0.41	0.7	0.0	3.8	17.1	M9742	MTXI
Qmpi.tamu.1D.2	-0.22	247.5	230.4	248.2	4.9	M65713	MPI
Qmpt.tamu.1D.2	-0.24	247.5	230.4	248.2	5.7	M65713	MPT
Qmpw.tamu.1D.2	-0.30	247.5	230.4	248.2	8.9	M65713	MPW
Qmrw.tamu.1D.2	-0.26	247.5	230.4	248.2	6.5	M65713	MRW

A, additive effect with negative value indicating the high value allele (HVA) is from the paternal parent and positive values indicate HVA from the maternal parent; CI, confidence interval; LL, lower limit, UL, upper limit

‡ Negative additive effect indicate high value allele (HVA) from TAM 111, positive values correspond to HVA from CO960293-2

†MLW, midline left width; MMST, midline mixing stability or tolerance; MPI, midline peak integral; MPT, midline peak time; MPV, midline peak value; MPW, midline peak width; MRW, midline right width; MTXI, midline time_X integral

Pairwise additive-by-additive epistatic interactions

Significant additive-by-additive epistatic interactions were detected for KD, FPC, WAB, MPV, MRI, MTXW, and MTXI. They explained 7.0 to 9.0% of the genotypic variation observed for these traits (Table 17). Among the significant main effect markers used in epistatic interaction analysis, 13 SNP *viz.* M11264, M12147, M13129, M21618, M3178, M4514, M46662, M61102, M65288, M65373, M7628, M78618, and M8143 showed significant results. SNP M46662 was involved in all epistatic interactions for MTXW and among SNP that showed interaction with M46662, M65288 and M65373 were associated with significant QTL in the main effect QTL analysis (Table 13 and 5, respectively). SNP M46662 was also involved in epistatic interaction for MRI. Significant epistatic interactions were observed for WAB although we did not detect any main effect QTL for this trait.

Table 17 Additive-by-additive epistatic interaction among significant loci

Locus1	Locus2	Chr.†	Position††	Trait‡	$Prob_{int}$	Part R^2	$Geno_{AA}$	$Geno_{AB}$	$Geno_{BA}$	$Geno_{BB}$
M11264	M12147	1A/1A	379.8/382.0	KD	0.0004	0.08	2.55	2.60	2.80	2.54
M12147	M61102	1A/1A	382.0/376.6	KD	0.0005	0.08	2.55	2.68	2.57	2.54
M13129	M4514	6A.1/2B	128.5/410.0	FPC	0.0004	0.09	12.90	13.03	13.15	12.75
M21618	M78618	2B/1A	403.8/343.8	FPC	0.0008	0.07	13.09	12.89	12.73	13.05
M3178	M78618	2B/1A	406.1/343.8	FPC	0.0010	0.06	13.11	12.98	12.69	13.04
M78618	M8143	1A/2B	343.8/404.3	FPC	0.0005	0.08	13.11	12.72	12.89	13.05
M13129	M3178	6A.1/2B	128.5/406.1	WAB	0.0007	0.08	60.89	61.14	61.12	60.60
M13129	M4514	6A.1/2B	128.5/410.0	WAB	0.0004	0.08	60.88	61.19	61.08	60.60
M21618	M4514	2B/2B	403.8/410.0	MPV	0.0008	0.08	54.81	48.97	47.60	54.92
M11264	M46662	1A/2A.1	379.8/33.5	MRI	0.0009	0.07	219.74	233.80	276.91	240.01
M46662	M65373	2A.1/1A	33.5/379.7	MRI	0.0005	0.07	220.32	275.78	233.80	237.07
M11264	M46662	1A/2A.1	379.8/33.5	MTXW	0.0005	0.07	9.39	10.83	15.73	11.58
M46662	M65288	2A.1/1A	33.5/379.0	MTXW	0.0002	0.08	9.42	15.75	11.05	11.41
M46662	M65373	2A.1/1A	33.5/379.7	MTXW	0.0003	0.07	9.42	15.61	10.83	11.40
M46662	M7628	2A.1/1A	33.5/380.4	MTXW	0.0005	0.07	9.51	15.74	10.60	11.63
M21618	M4514	2B/2B	403.8/410.0	MTXI	0.0005	0.08	344.03	295.90	299.78	347.05

$Prob_{int}$, probability for interaction; Part R^2, partial R^2; $Geno_{AA}$, genotypic mean for class AA; $Geno_{AB}$, genotypic mean for class AB; $Geno_{BA}$, genotypic mean for class BA; $Geno_{BB}$, genotypic mean for class BB

†The numerator and the denominator are the chromosomal location of Loci1 and Loci2, respectively

†† The numerator and the denominator refers to the positon of the marker in centiMorgans, respectively

KD, kernel diameter; FPC, flour protein content; WAB, water absorption; MPV, midline peak value; MRI, midline right integral; MTXW, midline time_X width; MTXI, midline time_X integral

DISCUSSION

End-use quality analysis is an indispensable component in any wheat-breeding program. All end-use parameters except MTXS showed highly significant genotypic differences with moderate-high heritability for most traits. The high heritability estimates (> 0.6) for MLT, MLS, MLI, MPT, MPI, MRT, MRI, MTXW, HDI, and SKW indicate that significant shift in the mean performance of these traits can be achieved through selection. The Pearson correlation coefficients varied across environments although some traits showed consistency in both individual environments and in the data averaged across environments. The correlation involving FPC and mixograph parameters was consistently positive and significant ($P < 0.05$) for MLW, MLV, MPV, MTXI, MTXV although the magnitude ranged from low to moderate. Positive and significant correlation coefficients were also observed between FPC and MLS, MRV, and MMST in at least two environments and in the data averaged across environments. Similar observation was made for the correlation between MLT and MPT but the direction of the correlation was negative. The results of the correlation in the present study suggest that FPC might not be a good predictor of the mixing properties of the dough. However, the FPC showed consistently positive, high and significant ($P < 0.01$) correlation with WAB suggesting that reliable prediction of WAB can be based on FPC. Similarly, the low correlation between HDI and mixograph mixing properties indicate that kernel physical characteristics are not good predictors of the dough rheology. The negative correlation between FPC and MPT is consistent with results reported by Patil et al. (2009) where a negative correlation was observed. The underlying putative genetic cause of positive

correlations can be attributed to presence of coupling phase linkage or positive pleiotropic effect, whereas negative correlations suggest presence of repulsion phase linkage or negative pleiotropic effects.

Transgression towards both maternal and paternal parents were observed for MLV, MLI, MRW, MTXI, MMST, KD, SKW, FW, FPC, and WAB. The MLS, MRV, and MPI showed transgressive segregation towards the paternal parent, whereas the MLT, MPT, MPV, MPI, MRT, MRS, MRI, MTXV, and MTXS showed transgressive segregation towards the maternal parent. Several potential reasons have been outlined for the underlying genetic basis of transgressive segregation. Epistasis, over-dominance, mutation, reduced developmental stability, chromosome number variation, unraveling of deleterious alleles, and allelic complementarity have all been poised to cause transgressive segregation (Rieseberg et al., 1999). In the present study, the latter seems plausible cause of transgressive segregation because the cross was derived from fixed lines which could explains complementarity between fixed sets of alleles in the parental genotypes. Nonetheless, we cannot rule out the other causes of transgressive segregation.

The QTL mapping was conducted within the framework of a LMM both for multi-trait and single trait multi-environment analysis (Boer et al., 2007; Malosetti et al., 2013). A major QTL for HDI, explaining up to 23.2% of the phenotypic variation, was detected on chromosome 2B with an additive genetic effect range of 1.5 to 2.5. Additional QTL for HDI was mapped on chromosome 1A ($A = 1.8$; $R^2 = 13.4\%$) and 2D ($A = 2.1$; $R^2 = 14.9\%$) although only in a single environment. Similar to the present study, Tsilo et al. (2011) reported a significant QTL for HDI on chromosome 1A in spring wheat RIL fingerprinted

with DArT markers. In their study, they detected additional QTL for HDI on chromosome 2A, 5A, 5B and 5D. In a QTL study using a linear mixed model, Arbelbide and Bernardo (2006) reported QTL for HDI on chromosome 1A and 5D, whereas Crepieux et al. (2005) detected significant QTL for kernel hardness and dough strength on chromosome 1D and 5D. It is known that the *Ha* locus located at the distal end of chromosome 5DS modulates grain hardness in wheat with the wild type linked to soft endosperm phenotype whereas mutant types results in hard endosperm phenotype (Sourdille et al., 1996; Turnbull and Rahman, 2002). In addition, the puroindoline (puroindoline-a and puroindoline-b) and the grain softness protein (GSP-1) genes have been reported to be tightly linked to the *Ha* locus and different point mutation have been reported to cause different degrees of kernel hardness in wheat. It is also known that factors other than the *Ha* and puroindoline control grain textural characteristics in wheat (Giroux and Morris, 1998; Turnbull and Rahman, 2002) and this is underscored in the present study and results from other authors where QTL other than *Ha* were reported. The variation due to factors other than *Ha* locus was the primary focus of kernel hardness in the present studies hence the use of hard × hard wheat RIL population.

The FPC QTL was detected on chromosome 3B (R^2 = 4.2 to 11.5%) and 5B (R^2 = 4.5 to 11.8%) based on a single trait multi-environment QTL analysis. Both QTL had an additive range of 0.1 to 0.3%. The paternal allele increased FPC on 3B whereas maternal allele increased FPC for the QTL on 5B. A number of QTL linked to protein content have been reported in previous studies. Sun et al. (2008) mapped QTL for protein content on 3B with additional QTL detected on chromosome 1A, 2A, 2D, 5A, 6A and 6D. McCartney

et al. (2006) detected QTL for protein content on chromosome 1B, 2B, 4D, 6A, and 6B whereas Huang et al. (2006) reported FPC QTL on chromosome 2D and 4D. Prashant et al. (2015) reported presence of a significant QTL for grain protein content on chromosome 5A whereas Patil et al. (2009) reported a significant QTL for grain protein content on chromosome 7B. These results underscore the polygenic inheritance of protein content in wheat.

The duration to maximum dough consistency as indicated by MPT revealed significant differences among the parents as well among the genotypes. The maternal and paternal parents had MPT values of 5.9 and 2.8 minutes, respectively. The MPT range for RIL was 2.0 to 7.7 minutes. MPT values correspond to maximum mixing resistance and are contingent upon the amount and composition of the protein content. Non-homeologous QTL for MPT were detected on chromosome 1A and 1B, both with significant additive genetic effects. The QTL on chromosome 1A was consistent across all the environments with favorable allele from TAM 111. In a study by Huang et al. (2006), a major QTL for mixing development time explaining 55.9% of the variation was detected on chromosome 1D although it is difficult to determine whether this QTL is homeologous to the QTL in the present study. Significant correlation between MPT and dough strength has been reported with high values associated with a strong dough and vice-versa (Miwako et al., 2015; Zhang et al., 2009). The protein content in a wheat kernel is mainly composed of glutens which comprises glutenins and gliadins subunits (Lindsay and Skerritt, 1999). The subunits of glutenins are categorized as high molecular weight glutenins sub-unit (HMW-GS) encoded by the loci at *Glu-A1*, *Glu-B1* and *Glu-D1* and low molecule weight glutenins

subunit encoded by *Glu-A3*, *Glu-B*3 and *Glu-D3* (Liu et al., 2014; Payne, 1987). The gliadins are encoded by the *Gli* loci which also exhibit allelic diversity. The allelic variability at these loci impacts the protein functionality and defines the end-use quality of wheat. In the present study, the differences in parental MPT suggest presence of allelic variability for protein composition even though the protein content of the parental did not show significant phenotypic differences in quantity.

Energy at various time points as indicated by integral values was consistently mapped on chromosome 1A. In a multi-environment QTL model, the QTL for MLI (R^2=8.1 to 15.1%; A = 14.8 to 19.5% TQ × min) and MPI (R^2 = 10.1 to 10.8%; A = 16.5% TQ × min) were mapped at same position on chromosome 1A whereas the QTL linked to MRI (R^2 = 3.9 to 12.7%; A = 10.3 to 15.8% TQ × min) was mapped 23 cM away from this position. The HVA for the energy QTL on chromosome 1A was from the maternal parent. A major QTL for MPI (R^2 = 26.5 to 28.2%; A = 26.6% TQ × min) was detected on chromosome 1D.1 with the HVA from the maternal parent. The QTL for MPI did not show significant QEI whereas the QTL for MLI and MRI revealed significant QEI. Crepieux et al. (2005) reported significant QTL for dough strength on homeologous region of chromosome 1A, 1B and 1D near the high molecular weight glutenin loci. Huang et al. (2006) mapped large effect energy to peak QTL, equivalent to MPI, on chromosome 1D, which agrees with the present study although in their study they detected additional QTL on chromosome 1B and 3B. In contrast to the present study, Patil et al. (2009) mapped QTL for peak energy on the short arm of chromosome 1B and on chromosome 7A. Although there is no direct match of QTL position for studies using different population

and markers, genomic regions on chromosome 1 seem to be important for dough strength. Integral values reflect the amount work input required to achieve certain levels of dough consistency. Thus, this parameter is important particularly from the perspective of bakers because it is directly related to the economics of production. Less energy without compromising the dough rheology will be preferred by bakers since this will minimize the cost of production and maximize the profit.

QTL for curve widths were mapped on chromosome 1A and 1D. The QTL for MPW (R^2 = 3.4 to 7.9%; A = 1.1 to 2.0%) and MTXW (R^2 = 6.3 to 9.6%; A = 1.6%) were co-located on chromosome 1A. An additional QTL for MTXW (R^2 = 6.6 to 10.1%; A = 1.7%) was detected on chromosome 1D.1. A QTL for MRW (R^2 = 4.8 to 7.9%; A = 1.0 to 1.4%) was mapped on 1D.1 but at a different position from that of MTXW. Both QTL for MTXW did not show significant QEI suggesting that they are constitutive. In addition, the MTXW QTL on chromosome 1A was detected in all the individual environments which further support environment non-specificity for this QTL. The curve width is correlated with the dough tolerance to over mixing with high values corresponding to high tolerance and vice-versa (Miles et al., 2013). On the other hand, the curve heights on the mixogram indicated by MLV, MRV, MPV and MTXV are correlated with dough consistency. The QTL for MRV (R^2 = 3.7 to 9.6%; A = 0.8 to 1.1%) was mapped on chromosome 1A whereas the QTL for MTXV were detected on chromosome 1A (R^2 = 6.3 to 9.6%; A = 1.6%) and 1D.1 (R^2 = 6.6 to 10.1%; A = 1.7%). Both QTL for MTXV did not show significant QEI whereas the QTL for MRV revealed significant QEI.

The ascending and descending slopes are critical parameter in the interpretation of the mixograph as they indicate mixing tolerance or stability (MMST). The QTL linked to mixing tolerance was detected only in a multi-trait model on chromosome 1D.1, consistent with previous studies although the QTL position could be different (Huang et al., 2006; Sun et al., 2008). The magnitude of the R^2 and the effect size were relatively low.

In a single trait multi-environment mapping, co-location of QTL on chromosome 1A was observed for MRI and MRT at 357.4 cM; MPW, MTW, and MTXW at 379.7 cM; MLI and MPI at 380.4 cM; MLT and MPT at 382.0 cM. KD and SKW were co-located on chromosome 2B at 404.3 cM and 6A.1 at 128.5 cM. The MLT and MPT were co-located on chromosome 1B at 178.1 cM. The co-location suggests presence of pleiotropy or that the QTL linked to these traits exist in linkage disequilibrium. The multi-trait QTL analysis revealed co-location of QTL on chromosome 1A, 1B and 1D. The QTL for traits co-located on 1A include MLW, MMST, MPI, MPT, MPW, and MRW whereas QTL co-located on 1B include MMST, MPV, MPW, and MRW. The R^2 for the QTL on 1A ranged from 1.9 to 12.5% whereas the QTL on 1B had an R^2 ranging from 3.0 to 7.8%. Two multi-trait QTL were detected on chromosome 1D.1. At the proximal side, a major QTL revealed co-location for MLW, MMST, MPI, MPT, MPV, MRW, and MTXI and had an R^2 range of 7.3 to 37.7%. The second QTL on 1D located at the distal side revealed co-location for MPI, MPT, MPW, and MRW and had an R^2 range of 4.9 to 8.9%. All the multi-trait QTL except the QTL at the distal side of chromosome 1D.1 showed significant cross-over QTI although most traits had HVA from the paternal parent. Thus, a set of traits with common HVA can be targeted for simultaneous improvement. The co-location

of traits further augment the findings observed in a single trait multi-environment QTL mapping and suggests that simultaneous improvement of these traits through MAS is achievable. The BLAST search of peak SNP detected in the present study revealed that a marker at position 379.8 cM (M11264) is linked to gliadin/avenin-like seed protein mRNA (Table A7) and therefore this could be a candidate marker useful for MAS in wheat. Other markers were linked with different mRNA for predicted proteins.

Significant additive-by-additive epistatic interactions were important for KD, FPC, WAB, MPV, MRI, MTXW, and MTXI. In all cases, the amount of variation explained by epistatic interaction after accounting for main effects was < 10% and ranged from 6.0 to 9.0%. This is relatively substantial amount of variation worthy considering in a wheat breeding program since this can obscure response to selection. Among the peak SNP, 12 of them were involved in epistatic interactions and the most highly epistatic loci was M46662. The SNP M11264 linked to gliadin mRNA was involved in epistatic interactions for KD, MRI, and MTXW.

Compared to our previous work, the genomic region linked to HDI, KD and SKW on chromosome 2B were also linked to grain yield, days to heading, plant height, thousand kernel weight, and spikes metre^{-2}, based on the previous analysis done on this population (chapter II). In the present work, genomic regions on chromosome 1A and 1D seem to be important for end-use quality in wheat. The SNP associated with this QTL could be targeted in MAS for end-use quality and for future wheat breeding work.

CHAPTER V

SUMMARY AND CONCLUSION

This dissertation focused on three different aspects of wheat breeding covering abiotic and biotic stresses, and end-use quality characteristics in wheat. We used a dense genetic map constructed using 90K SNP array and RIL derived from an elite-by-elite winter wheat cross.

In chapter II, we have provided QTL analysis results using both single trait multi-environment and multi-trait analysis framework for grain yield, yield components and agronomic traits. A genome-wide scan revealed significant GY QTL on chromosome 2B, 5A.1 and 5B. The QTL detected on chromosome 2B and 5A.1 showed significant crossover QEI while the one on 5B and others mapped on chromosome 2B showed non-crossover QEI. A major QTL for GY was detected on chromosome 2B with a –log (P) value of 17.3 (Table 4). The maximum proportion of phenotypic variance accounted for by the GY QTL was 46.7% for the first QTL on chromosome 2B and 27.2% for the second QTL on chromosome 2B. The QTL on 5A.1 and 5B had a maximum R^2 of 5.0% and 11.8% of the phenotypic variance, respectively. DTH to heading QTL were detected on chromosome 2B and 2D.1 with no significant QEI observed suggesting that they are environment non-specific. PH QTL were detected on chromosome 1D.1, 2B, 2D.1, 5B and 6B with the QTL on 1D.1, 2B, and 2D.1 revealing significant QEI. Yield components QTL were detected on multiple chromosomes with some QTL showing co-location with GY and agronomic traits. In a multi-environment QTL analysis model, QTL for GY, DTH, PH, TW, TKW, and SPM were co-located on chromosome 2B whereas DTH and PH were

co-located on chromosome 2D.1. The highest additive effect for GY was observed on chromosome 2B where a maximum value of 0.46 t ha^{-1} was observed with HVA originating from the paternal parent. The first GY QTL on chromosome 2B had a maximum additive effect of 0.38 t ha^{-1} with HVA originating from the maternal parent (CO960293-2). The third QTL on 2B and the QTL mapped on chromosome 5A.1 and 5B showed an oscillation in QTL additive effect ranging from 0.06 to 0.27 t ha^{-1}. The HVA for the QTL on 5B was consistent across all the environments indicating a negligible role of QEI on the additive effect for this QTL. The additive effect for agronomic traits and yield components were also variable depending on the environment with exception of few QTL that showed environment non-specificity.

CAPE analysis revealed that GY and biomass were enhanced by QTL on 2B, 5A and 5B The inclusion of GEI terms in QTL analysis provided useful information on underlying genetic basis of quantitative traits measured in the present study. This information together with results from combined analysis of pleiotropy and epistasis provides a platform to build QTL models encompassing enhancement effects for the trait of interest. Results from the present study showed that interactions as well as epistasis played an important role in defining genetic architecture of quantitative traits. This information has a potential application in MAS to improve GY as well as other traits of interest.

In chapter III, the wheat 90K Infinium iSelect SNP array was used in a mapping study for WSMV resistance. Using disease severity data from the growth chamber, we mapped *Wsm2* on the short arm of chromosome 3B. The present results corroborate

previous genetic maps for *Wsm2* gene. The previous study recommended a single SSR marker linked to *Wsm2* but the marker does not work in some genetic backgrounds. In the present study, we zoomed into the genomic region on the short arm of chromosome 3B and detected several SNP within 2.0 cM flanking the target gene. Nine SNP were detected within the 2.0 cM region, and, therefore, we have expanded the marker degrees of freedom for breeders to choose from such that if one SNP does not work in a certain genetic background there is an alternative option of SNP to be tested. Sequences of SNPs flanking *Wsm2* could be used in candidate gene identification and understanding plant defense mechanisms in future genetic studies.

The fourth chapter focused on end-use quality traits analysis in wheat, an essential component of wheat breeding and genetics. The phenotypic data for kernel textural characteristics and the dough mixing properties were used for end-use quality analysis. These properties showed moderate to high heritability and revealed highly significant genetic difference. The QTL for end-use quality traits were detected on chromosome 1A, 1B, 1D, 3B and 5B. Among these chromosomes, 1A and 1D play an important role in modulating end-use quality. The importance of chromosome 1A and 1D was supported by co-location of multiple traits based on both multi-trait QTL mapping model and single trait multi-environment QTL mapping model. The flour protein content was linked to QTL on chromosome 3B and 5B whereas the QTL for kernel harness were detected on 1A, 2B and 2D. Both QEI and QTI interaction were important for end-use quality traits. Thus, it is important to evaluate the kernel textural traits and dough mixing properties based on samples from multiple environments. In addition, epistatic interaction were important for

flour protein content, water absorption, midline peak value, midline right integral, midline time_X width and midline right integral, midline time_X integral. Overall, however, the epistatic interaction accounted for less than 10% of phenotypic variance for each trait above. A BLAST search on NCBI revealed that SNP M11264 on chromosome 1A was linked to the gliadin/avenin-like seed protein mRNA. This SNP was linked to multiple QTL for different parameters in this study, and, therefore, it is a potential marker to be pursued for MAS and future genetic studies related to wheat quality. Other SNP were linked to predicted proteins based on a search on NCBI database. Validation of SNP linked to grain yield, yield components, end-use quality and *Wsm2* gene will be important for future genetic studies. Conversion of these SNP from a multiplex platform to uniplex KASP-based platform, will be a vital step towards validation in diverse genetic backgrounds and for further MAS. Thus, this dissertation has provided crucial genetic information for wheat breeding programs that can be used as a platform for yield improvement in this important crop.

LITERATURE CITED

AACC International. 2010. Approved Methods of Analysis, 11th Ed. American Association of Cereal Chemists (AACC) International, St. Paul, MN, USA.

Akhunov, E., C. Nicolet and J. Dvorak. 2009. Single nucleotide polymorphism genotyping in polyploid wheat with the Illumina GoldenGate assay.123. Theor. Appl. Genet. 119: 507-517. doi:10.1007/s00122-009-1059-5.

Arbelbide, M. and R. Bernardo. 2006. Mixed-model QTL mapping for kernel hardness and dough strength in bread wheat. Theor. Appl. Genet. 112: 885-890. doi:10.1007/s00122-005-0190-1.

Avni, R., M. Nave, T. Eilam, H. Sela, C. Alekperov, Z. Peleg, et al. 2014. Ultra-dense genetic map of durum wheat x wild emmer wheat developed using the 90K iSelect SNP genotyping assay. Mol. Breeding 34: 1549-1562.

Bednarek, J., A. Boulaflous, C. Girousse, C. Ravel, C. Tassy, P. Barret, et al. 2012. Down-regulation of the *TaGW2* gene by RNA interference results in decreased grain size and weight in wheat. J. Exp. Bot. 63: 5945-5955.

Bernardo, R. 2013. Genomewide markers as cofactors for precision mapping of quantitative trait loci. Theor. Appl. Genet. 126: 999-1009. doi:10.1007/s00122-012-2032-2.

Boer, M.P., D. Wright, L. Feng, D.W. Podlich, M. Cooper and F.A. Van Eeuwijk. 2007. Mixed-model quantitative trait loci (QTL) analysis for multiple-environment trial data using environmental covariables for QTL-by-environment interactions, with an example in maize. Genetics 177: 1801-1813.

Bonneau, J., J. Taylor, B. Parent, D. Bennett, M. Reynolds, C. Feuillet, et al. 2013. Multi-environment analysis and improved mapping of a yield-related QTL on chromosome 3B of wheat. Theor. Appl. Genet. 126: 747-761. doi:10.1007/s00122-012-2015-3.

Bordes, J., G. Branlard, F.X. Oury, G. Charmet and F. Balfourier. 2008. Review: agronomic characteristics, grain quality and flour rheology of 372 bread wheats in

a worldwide core collection. J. Cereal Sci. 48: 569-579. doi:10.1016/j.jcs.2008.05.005.

Byamukama, E., S.N. Wegulo, S. Tatineni, G.L. Hein, R.A. Graybosch, P.S. Baenziger, et al. 2013. Quantification of yield loss caused by triticum mosaic virus and wheat streak mosaic virus in winter wheat under field conditions. Plant Dis. 98: 127-133. doi:10.1094/PDIS-04-13-0419-RE.

Carlborg, O. and C.S. Haley. 2004. Epistasis: too often neglected in complex trait studies? Nat. Rev. Genet. 5: 618-625.

Carr, J.P., M.G. Lewsey and P. Palukaitis. 2010. Signaling in induced resistance. In: P. C. John and L. Gad, editors, Adv. Virus Res. Academic Press. p. 57-121.

Carter, G.W., M. Hays, A. Sherman and T. Galitski. 2012. Use of pleiotropy to model genetic interactions in a population. Plos Genetics 8: e1003010. doi:10.1371/journal.pgen.1003010.

Cavanagh, C., S. Chao, S. Wang, B. Huang, S. Stephen, S. Kiani, et al. 2013. Genome-wide comparative diversity uncovers multiple targets of selection for improvement in hexaploid wheat landraces and cultivars. Proc. Nat. Acad. Sci. 110: 8057-8062.

Choulet, F., A. Alberti, S. Theil, N. Glover, V. Barbe, J. Daron, et al. 2014. Structural and functional partitioning of bread wheat chromosome 3B. Science 345. doi:10.1126/science.1249721.

Collard, B.C.Y., C.M. Vera Cruz, K.L. McNally, P.S. Virk and D.J. Mackill. 2008. Rice molecular breeding laboratories in the genomics era: current status and future considerations. Int. J. Plant Genomics 2008. Article ID 524847: 25 pages. doi:10.1155/2008/524847.

Crepieux, S., C. Lebreton, P. Flament and G. Charmet. 2005. Application of a new IBD-based QTL mapping method to common wheat breeding population: analysis of kernel hardness and dough strength. Theor. Appl. Genet. 111: 1409-1419. doi:10.1007/s00122-005-0073-5.

Dixon, J., H.-J. Braun, P. Kosina and J. Crouch. 2009. Wheat facts and futures 2009, Mexico, D.F.: CIMMYT.

Eathington, S.R., T.M. Crosbie, M.D. Edwards, R.S. Reiter and J.K. Bull. 2007. Molecular markers in a commercial breeding program. Crop Sci. 47: 154-163. doi:10.2135/cropsci2007.04.0015IPBS.

Echeverry-Solarte, M., A. Kumar, S. Kianian, S. Simsek, M. Alamri, E. Mantovani, et al. 2015. New QTL alleles for quality-related traits in spring wheat revealed by RIL population derived from supernumerary × non-supernumerary spikelet genotypes. Theor. Appl. Genet. 128: 893-912. doi:10.1007/s00122-015-2478-0.

El-Feki, W.M., P.F. Byrne, S.D. Reid, N.L.V. Lapitan and S.D. Haley. 2013. Quantitative trait locus mapping for end-use quality traits in hard winter wheat under contrasting soil moisture levels. Crop Sci. 53: 1953-1967. doi:10.2135/cropsci2012.12.0674.

Fahim, M., P. Larkin, S. Haber, S. Shorter, P. Lonergan and G. Rosewarne. 2012a. Effectiveness of three potential sources of resistance in wheat against wheat streak mosaic virus under field conditions. Australas. Plant Pathol. 41: 301-309. doi:10.1007/s13313-012-0125-7.

Fahim, M., A. Mechanicos, L. Ayala-Navarrete, S. Haber and P.J. Larkin. 2012b. Resistance to wheat streak mosaic virus- a survey of resources and development of molecular markers. Plant Pathol. 61: 425-440. doi:10.1111/j.1365-3059.2011.02542.x.

Falconer, D.S. and T.F.C. Mackay. 1996. Introduction to quantitative genetics. 4th ed. Longman, Essex, England

Fehr, W.R., E.L. Fehr and H.J. Jessen. 1987. Principles of cultivar development.New York : Macmillan ; London : Collier Macmillan, c1987.

Gao, J.-G. and A. Nassuth. 1992. Cytological changes induced by wheat streak mosaic virus in cereal leaf tissues. Canadian J. Bot. 70: 19-25. doi:10.1139/b92-003.

Gao, J.-G. and A. Nassuth. 1994. Wheat streak mosaic virus-induced cytoplasmic expansion and membrane proliferation. J. Phytopathol 142: 79-87. doi:10.1111/1439-0434.ep14317414.

Giroux, M.J. and C.F. Morris. 1998. Wheat grain hardness results from highly conserved mutations in the friabilin components puroindoline a and b. Proceedings of the National Academy of Sciences 95: 6262-6266.

Graybosch, R.A., C.J. Peterson, P.S. Baenziger, D.D. Baltensperger, L.A. Nelson, Y. Jin, et al. 2009. Registration of 'Mace' hard red winter wheat. J. Plant Reg. 3: 51-56. doi:10.3198/jpr2008.06.0345crc.

Gregorio, A., L. Marco, V. Mateo, P. Ángela, R. Francisco, B. Juan, et al. 2015. META-R (Multi Environment Trial Analysis with R for Windows) Version 4.1, http://hdl.handle.net/11529/10201 .International Maize and Wheat Improvement Center, V10.

Haley, S.D., J.J. Johnson, F.B. Peairs, J.A. Stromberger, E.E. Heaton, S.A. Seifert, et al. 2011. Registration of 'Snowmass' wheat. J. Plant Reg. 5: 87-90. doi:10.3198/jpr2010.03.0175crc.

Haley, S.D., T.J. Martin, J.S. Quick, D.L. Seifers, J.A. Stromberger, S.R. Clayshulte, et al. 2002. Registration of CO960293-2 wheat germplasm resistant to wheat streak mosaic virus and Russian wheat aphid. Crop Sci. 42: 1381-1382. doi:10.2135/cropsci2002.1381.

Hanson, W.D. and H.F. Robinson. 1963. Statistical genetics and plant breeding, a symposium and workshop. Washington. National Academy of Sciences-National Research Council, 1963.

Harvey, T.L., D.L. Seifers, T.J. Martin and J.P. Michaud. 2005. Effect of resistance to wheat streak mosaic virus on transmission efficiency of wheat curl mites. J. Agric. Urban Entomol. 22: 1-6.

Hawkesford, M.J., J.-L. Araus, R. Park, D. Calderini, D. Miralles, T. Shen, et al. 2013. Prospects of doubling global wheat yields. Food and Energy Security 2: 34-48. doi:10.1002/fes3.15.

Hedden, P. 2003. The genes of the green revolution. Trends Genet. 19: 5-9.

Holland, J.B. 1998. Epistacy: a SAS program for detecting two-locus epistatic interactions using genetic marker information. J. Heredity 89: 374-375. doi:10.1093/jhered/89.4.374.

Huang, X.Q., S. Cloutier, L. Lycar, N. Radovanovic, D.G. Humphreys, J.S. Noll, et al. 2006. Molecular detection of QTLs for agronomic and quality traits in a doubled haploid population derived from two Canadian wheats (*Triticum aestivum* L.). Theor. Appl. Genet. 113: 753-766. doi:10.1007/s00122-006-0346-7 .

Jannink, J.L. 2007. Identifying quantitative trait locus by genetic background interactions in association studies. Genetics 176: 553-561. doi:10.1534/genetics.106.062992

Jansen, R.C. and P. Stam. 1994. High resolution of quantitative traits into multiple loci via interval mapping. Genetics 136: 1447-1455.

Jondiko, T. 2014. Prediction of tortilla quality using multivariate modeling of kernel, flour, and dough properties. Ph.D. Dissertation, Texas A&M University, College Station, TX.

Kay, L. 2014. Texas A&M AgriLife program to release two new wheat varieties. Texas A&M AgriLife Research. https://soilcrop.tamu.edu/newsletters_bulletins/aggie_agenda/January%202015.pdf (accessed 21 Feb. 2016).

Kerfal, S., P. Giraldo, M. Rodríguez-Quijano, F. Vázquez, K. Adams, O.M. Lukow, et al. 2010. Mapping quantitative trait loci (QTLs) associated with dough quality in a soft × hard bread wheat progeny. J. Cereal Sci. 52: 46-52 doi:10.1016/j.jcs.2010.03.001.

Lazar, M.D., W.D. Worrall, G.L. Peterson, A.K. Fritz, D. Marshall, L.R. Nelson, et al. 2004. Registration of 'TAM 111' wheat. Crop Sci. 44: 355-356. doi:doi:10.2135/cropsci2004.3550.

Lindsay, M.P. and J.H. Skerritt. 1999. Review: the glutenin macropolymer of wheat flour doughs. structure–function perspectives. Trends in Food Science and Technology 10: 247-253. doi:10.1016/S0924-2244(00)00004-2.

Liu, S., S.O. Assanga, S. Dhakal, X. Gu, C.-T. Tan, Y. Yang, et al. 2016. Validation of chromosomal locations of 90K array single nucleotide polymorphisms in US wheat. Crop Sci. 56: 364-373. doi:10.2135/cropsci2015.03.0194.

Liu, S., C. Griffey, M. Hall, A. McKendry, J. Chen, W. Brooks, et al. 2013. Molecular characterization of field resistance to Fusarium head blight in two US soft red winter wheat cultivars. Theor. Appl. Genet. 126: 2485-2498. doi:10.1007/s00122-013-2149-y.

Liu, S., J.C. Rudd, B. Guihua, S.D. Haley, A.M.H. Ibrahim, X. Qingwu, et al. 2014. Molecular markers linked to important genes in hard winter wheat. Crop Sci. 54: 1304-1321. doi:10.2135/cropsci2013.08.0564.

Lopes, M.S., S. Dreisigacker, R.J. Peña, S. Sukumaran and M.P. Reynolds. 2015. Genetic characterization of the wheat association mapping initiative (WAMI) panel for dissection of complex traits in spring wheat. Theor. Appl. Genet. 128: 453–464. doi:10.1007/s00122-014-2444-2.

Lopes, M.S., M.P. Reynolds, C.L. McIntyre, K.L. Mathews, M.R.J. Kamali, M. Mossad, et al. 2013. QTL for yield and associated traits in the Seri/Babax population grown across several environments in Mexico, in the West Asia, North Africa, and South Asia regions. Theor. Appl. Genet. 126: 971-984. doi:10.1007/s00122-013-2099-4.

Lu, H., R. Kottke, R. Devkota, P.S. Amand, A. Bernardo, G. Bai, et al. 2012. Consensus mapping and identification of markers for marker-assisted selection of *Wsm2* in wheat. Crop Sci. 52: 720-728. doi:10.2135/cropsci2011.07.0363.

Lu, H., J. Price, R. Devkota, C. Rush and J. Rudd. 2011. A dominant gene for resistance to wheat streak mosaic virus in winter wheat line CO960293-2. Crop Sci. 51: 5-12. doi:10.2135/cropsci2010.01.0038.

Lucas, W.J. 2006. Plant viral movement proteins: agents for cell-to-cell trafficking of viral genomes. Virol. 344: 169-184. doi:10.1016/j.virol.2005.09.026.

Mackay, T.F.C., E.A. Stone and J.F. Ayroles. 2009. The genetics of quantitative traits: challenges and prospects. Nat. Rev. Genet. 10: 565-577. doi:10.1038/nrg2612.

Malosetti, M., J.-M. Ribaut and F.A. van Eeuwijk. 2013. The statistical analysis of multi-environment data: modeling genotype-by-environment interaction and its genetic basis. Frontiers in Physiol. 4: 1-17. doi:10.3389/fphys.2013.00044.

Martin, T.J., G. Zhang, A.K. Fritz, R. Miller and M.-S. Chen. 2014. Registration of 'Clara CL' Wheat. J. Plant Reg. 8: 38-42. doi:10.3198/jpr2013.07.0040crc.

Martinant, J.P., L. Saulnier, G. Branlard, Y. Popineau, Y. Nicolas and A. Bouguennec. 1998. Relationships between mixograph parameters and indices of wheat grain quality. J. Cereal Sci. 27: 179-189.

McCartney, C.A., D.J. Somers, O. Lukow, N. Ames, J. Noll, S. Cloutier, et al. 2006. QTL analysis of quality traits in the spring wheat cross RL4452 x 'AC Domain'. Plant Breeding 125: 565-575. doi:10.1111/j.1439-0523.2006.01256.x.

McIntyre, C.L., K.L. Mathews, A. Rattey, S.C. Chapman, J. Drenth, M. Ghaderi, et al. 2010. Molecular detection of genomic regions associated with grain yield and yield-related components in an elite bread wheat cross evaluated under irrigated and rainfed conditions. Theor. Appl. Genet.: 527-541. doi:10.1007/s00122-009-1173-4.

Miles, C.W., A. Van Biljon, W.M. Otto and M.T. Labuschagne. 2013. Grain and milling characteristics and their relationship with selected mixogram parameters in hard red bread wheat. J. Cereal Sci. 57: 56-60. doi:10.1016/j.jcs.2012.09.011.

Miwako, I., M.-F. Wakako, T.M. Ikeda, N. Zenta, N. Koichi and T. Tadashi. 2015. Dough properties and bread-making quality-related characteristics of Yumechikara near-isogenic wheat lines carrying different Glu-B3 alleles. Breeding Sci. 65: 241-248. doi:10.1270/jsbbs.65.241.

Mohtasham, M., S. Peyman, K. Rahmatollah and S. Mohammad Kazem. 2012. Relationships between grain yield and yield components in bread wheat under different water availability (dryland and supplemental irrigation conditions). Notulae Botanicae Horti Agrobotanici Cluj-Napoca 40: 195-200.

Morris, C.F. and S.P. Rose. 1996. Wheat. In: R. J. Henry and P. S. Kettlewell, editors, Cereal grain quality. Chapman and Hall, London. p. 479.

Navia, D., R. de Mendonça, A. Skoracka, W. Szydło, D. Knihinicki, G. Hein, et al. 2013. Wheat curl mite, *Aceria tosichella*, and transmitted viruses: an expanding pest complex affecting cereal crops. Exp. Appl. Acarol. 59: 95-143. doi:10.1007/s10493-012-9633-y.

Olivares-Villegas, J.J., M.P. Reynolds and G.K. McDonald. 2007. Drought-adaptive attributes in the Seri/Babax hexaploid wheat population. Functional plant biology 34: 189-203.

Pastina, M.M., M. Malosetti, R. Gazaffi, M. Mollinari, G.R.A. Margarido, K.M. Oliveira, et al. 2012. Mixed model QTL analysis for sugarcane multiple-harvest-location trial data. Theor. Appl. Genet. 124: 835-849.

Patil, R.M., M.D. Oak, S.A. Tamhankar and V.S. Rao. 2009. Molecular mapping of QTLs for gluten strength as measured by sedimentation volume and mixograph in durum wheat (*Triticum turgidum* L. ssp *durum*). J. Cereal Sci. 49: 378-386. doi:10.1016/j.jcs.2009.01.001.

Payne, P.I. 1987. Genetics of wheat storage proteins and the effect of allelic variation on bread-making quality. Ann. Rev. Plant Physiol. 38: 141-153. doi:10.1146/annurev.pp.38.060187.001041.

Pinto, R.S., M.P. Reynolds, K.L. Mathews, C.L. McIntyre, J.-J. Olivares-Villegas and S.C. Chapman. 2010. Heat and drought adaptive QTL in a wheat population designed to minimize confounding agronomic effects. Theor. Appl. Genet. 121: 1001-1021. doi:10.1007/s00122-010-1351-4.

Postel, S. 2012. Texas Water District Acts to slow depletion of Ogallala aquifer. National Geographic's freshwater initiative. http://voices.nationalgeographic.com/2012/02/07/texas-water-district-acts-to-slow-depletion-of-the-ogallala-aquifer/ (accessed 21 Feb. 2016).

Prashant, R., E. Mani, R. Rai, R.K. Gupta, R. Tiwari, B. Dholakia, et al. 2015. Genotype × environment interactions and QTL clusters underlying dough rheology traits in *Triticum aestivum* L. J. Cereal Sci. 64: 82-91. doi:10.1016/j.jcs.2015.05.002.

Price, J.A., A.R. Simmons, A. Rashed, F. Workneh and C.M. Rush. 2013. Winter wheat cultivars with temperature-sensitive resistance to wheat streak mosaic virus do not recover from early-season infections. Plant Dis. 98: 525-531. doi:10.1094/PDIS-04-13-0455-RE.

Price, J.A., F. Workneh, S.R. Evett, D.C. Jones, J. Arthur and C.M. Rush. 2010. Effects of wheat streak mosaic virus on root development and water-use efficiency of hard red winter wheat. Plant Dis. 94: 766-770. doi:10.1094/PDIS-94-6-0766.

R Core Team. 2015. R: A language and environment for statistical computing. R Foundation for Statistical Computing, Vienna, Austria. https://www.R-project.org/

Ray, D.K., N.D. Mueller, P.C. West and J.A. Foley. 2013. Yield trends are insufficient to double global crop production by 2050. PLoS One 8: 1-8. doi:10.1371/journal.pone.0066428.

Reddy, S.K., L. Shuyu, J.C. Rudd, X. Qingwu, P. Payton, S.A. Finlayson, et al. 2014. Physiology and transcriptomics of water-deficit stress responses in wheat cultivars TAM 111 and TAM 112. J. Plant Physiol. 171: 1289-1298. doi:10.1016/j.jplph.2014.05.005.

Ribaut, J.M., M. Banziger, J. Betran, C. Jiang, G.O. Edmeades, K. Dreher, et al. 2002. Use of molecular markers in plant breeding: drought tolerance improvement in tropical maize.In M.S. Kang (ed.) Quantitative genetics, genomics, and plant breeding.CABI Publishing: Wallingford, UK.

Rieseberg, L.H., M.A. Archer and R.K. Wayne. 1999. Transgressive segregation, adaptation and speciation. Heredity 83: 363-372. doi:10.1046/j.1365-2540.1999.00617.x.

Rudd, J.C., R.N. Devkota, J.A. Baker, G.L. Peterson, M.D. Lazar, B. Bean, et al. 2014. ‘TAM 112’ Wheat, resistant to Greenbug and Wheat Curl Mite and adapted to the dryland production system in the Southern High Plains. J. Plant Reg. 8: 291-297. doi:10.3198/jpr2014.03.0016crc.

SAS Institute Inc. 2015. SAS/STAT 14.1 user's guide. Cary, NC: SAS Institute Inc.

Schlotterer, C. 2004. The evolution of molecular markers-just a matter of fashion? Nat. Rev. Genet. 5: 63-69.

Seifers, D.L., S. Haber, T.J. Martin and Z. Guorong. 2013a. New sources of temperature-sensitive resistance to wheat streak mosaic virus in wheat. Plant Dis. 97: 1051-1056. doi:10.1094/PDIS-11-12-1029-RE.

Seifers, D.L., T.J. Martin and S. Haber. 2013b. Temperature-sensitive resistance to wheat streak mosaic virus in CO960333 and KS06HW79 wheat. Plant Dis. 97: 983-987. doi:10.1094/PDIS-10-12-0971-RE.

Seifers, D.L., T.J. Martin, T.L. Harvey and S. Haber. 2007. Temperature-sensitive wheat streak mosaic virus resistance identified in KS03HW12 wheat. Plant Dis. 91: 1029-1033. doi:10.1094/PDIS-91-8-1029.

Seifers, D.L., T.J. Martin, T.L. Harvey, S. Haber and S.D. Haley. 2006. Temperature sensitivity and efficacy of wheat streak mosaic virus resistance derived from CO960293 wheat. Plant Dis. 90: 623-628. doi:10.1094/PD-90-0623.

Semagn, K., R. Babu, S. Hearne and M. Olsen. 2014. Single nucleotide polymorphism genotyping using Kompetitive Allele Specific PCR (KASP): overview of the technology and its application in crop improvement. Mol. Breeding 33: 1-14. doi:10.1007/s11032-013-9917-x.

Sharp, G.L., J.M. Martin, S.P. Lanning, N.K. Blake, C.W. Brey, E. Sivamani, et al. 2002. Field evaluation of transgenic and classical sources of wheat streak mosaic virus resistance. Crop Sci. 42: 105-110. doi:10.2135/cropsci2002.1050.

Simmonds, J., P. Scott, M. Leverington-Waite, A. Turner, J. Brinton, V. Korzun, et al. 2014. Identification and independent validation of a stable yield and thousand grain weight QTL on chromosome 6A of hexaploid wheat (*Triticum aestivum* L.). BMC Plant Biol 14: 191.

Smith, A.B., B.R. Cullis and R. Thompson. 2005. Analysis of crop cultivar breeding and evaluation trials: an overview of current mixed model approaches. J. Agr. Sci. 143: 449-462.

Sourdille, P., S. Baud and P. Leroy. 1996. Detection of linkage between RFLP markers and genes affecting anthocyanin pigmentation in maize (*Zea mays* L.). Euphytica 91: 21-30. doi:10.1007/BF00035272.

Sukumaran, S., S. Dreisigacker, M. Lopes, P. Chavez and M. Reynolds. 2015. Genome-wide association study for grain yield and related traits in an elite spring wheat population grown in temperate irrigated environments. Theor. Appl. Genet. 128: 453-464.

Sun, H., J. Lü, Y. Fan, Y. Zhao, F. Kong, R. Li, et al. 2008. Quantitative trait loci (QTLs) for quality traits related to protein and starch in wheat. Progress in Natural Science 18: 825-831. doi:10.1016/j.pnsc.2007.12.013.

Tatineni, S., D.H. Van Winkle and R. French. 2011. The N-terminal region of wheat streak mosaic virus coat protein is a host- and strain-specific long-distance transport factor. J. Virol 85: 1718-1731. doi:10.1128/jvi.02044-10.

Tilman, D., K.G. Cassman, P.A. Matson, R. Naylor and S. Polasky. 2002. Agricultural sustainability and intensive production practices. Nature 418: 671-677.

Triebe, B., Y. Mukai, H.S. Dhaliwal, T.J. Martin and B.S. Gill. 1991. Identification of alien chromatin specifying resistance to wheat streak mosaic and greenbug in wheat germplasm by C-banding and in situ hybridization. Theor. Appl. Genet. 81: 381-389. doi:10.1007/BF00228680.

Tsilo, T.J., S. Simsek, J.-B. Ohm, G.A. Hareland, S. Chao and J.A. Anderson. 2011. Quantitative trait loci influencing endosperm texture, dough-mixing strength, and bread-making properties of the hard red spring wheat breeding lines. Genome 54: 460-470. doi:10.1139/G11-012.

Turnbull, K.M. and S. Rahman. 2002. Endosperm texture in wheat. J. Cereal Sci. 36: 327-337. doi:10.1006/jcrs.2002.0468.

Tyler, A.L., W. Lu, J.J. Hendrick, V.M. Philip and G.W. Carter. 2013. CAPE: an R package for combined analysis of pleiotropy and epistasis. Plos Comput. Biol. 9: e1003270. doi:10.1371/journal.pcbi.1003270.

Tyler, A.L., T.C. McGarr, B.J. Beyer, W.N. Frankel and G.W. Carter. 2014. A genetic interaction network model of a complex neurological disease. Genes, Brain, and Behavior 13: 831-840. doi:10.1111/gbb.12178.

Van Eeuwijk, F.A., M.C.A.M. Bink, K. Chenu and S.C. Chapman. 2010. Detection and use of QTL for complex traits in multiple environments. Current opinion in plant biology 13: 193-205. doi:10.1016/j.pbi.2010.01.001.

Van Ooijen, J.W. 2006. 2006. JoinMap ® 4, Software for the calculation of genetic linkage maps in experimental populations. Kyazma B.V., Wageningen, Netherlands. .

Velandia, M., R.M. Rejesus, D.C. Jones, J.A. Price, F. Workneh and C.M. Rush. 2010. Economic impact of wheat streak mosaic virus in the Texas High Plains. Crop Prot. 29: 699-703. doi:10.1016/j.cropro.2010.02.005.

VSN International. 2015. GenStat for Windows 18th Edition. VSN International, Hemel Hempstead, UK. www.GenStat.co.uk.

Waigmann, E., S. Ueki, K. Trutnyeva and V. Citovsky. 2004. The ins and outs of nondestructive cell-to-cell and systemic movement of plant viruses. Crit. Rev. Plant Sci. 23: 195-250.

Walker, A.E. and C.E. Walker. 2004. Documentation and user's instructions for mixsmart for windows. Computerized data acquisition and analysis for the mixograph.

Walsh, B. 2001. Quantitative Genetics. Encyclopedia of Life Sciences. John Wiley & Sons, Ltd., doi: 10.1038/npg.els.0001785.

Wang, S., D. Wong, K. Forrest, A. Allen, S. Chao, B.E. Huang, et al. 2014. Characterization of polyploid wheat genomic diversity using a high-density 90 000 single nucleotide polymorphism array. Plant Biotechnol. J. 12: 787-796. doi:10.1111/pbi.12183.

Wilkinson, P.A., M.O. Winfried, G.L.A. Barker, A.M. Allen, A. Burridge, J.A. Coghill, et al. 2012. CerealsDB 2.0: an integrated resource for plant breeders and scientists. BMC Bioinformatics 13: 19-24. doi:10.1186/1471-2105-13-19.

Workneh, F., D.C. Jones and C.M. Rush. 2009. Quantifying wheat yield across the field as a function of wheat streak mosaic intensity: a state space approach. Phytopathol. 99: 432-440. doi:10.1094/PHYTO-99-4-0432.

Yang, Z., Z. Bai, X. Li, P. Wang, Q. Wu, L. Yang, et al. 2012. SNP identification and allelic-specific PCR markers development for *TaGW2*, a gene linked to wheat kernel weight. Theor. Appl. Genet. 125: 1057-1068.

Zanke, C.D., J. Ling, J. Plieske, S. Kollers, E. Ebmeyer, V. Korzun, et al. 2015. Analysis of main effect QTL for thousand grain weight in European winter wheat (Triticum aestivum L.) by genome-wide association mapping. Frontiers in Plant Science 6: 644. doi:10.3389/fpls.2015.00644.

Zeng, Z. 1994. Precision mapping of quantitative trait loci. Genetics 136: 1457-1468.

Zhang, G., T.J. Martin, A.K. Fritz, R. Miller, M.-S. Chen, R.L. Bowden, et al. 2015. Registration of 'Oakley CL' Wheat. J. Plant Reg. 9: 190-195. doi:10.3198/jpr2014.04.0023crc.

Zhang, G., D.L. Seifers and T.J. Martin. 2014. Inheritance of wheat streak mosaic virus resistance in KS03HW12. Austin J. Plant Biol. 1: 4.

Zhang, Y., Y. Wu, Y. Xiao, J. Yan, Y. Zhang, Y. Zhang, et al. 2009. QTL mapping for milling, gluten quality, and flour pasting properties in a recombinant inbred line population derived from a Chinese soft x hard wheat cross. Crop and Pasture Sci. 60: 587-597. doi:10.1071/CP08392

APPENDIX A

Table A1

Genetic correlation in individual environments. DTH, days to heading; FD, freeze damage; BW, biomass weight; TKW, thousand kernel weight; MSHW, mean single head weight; KPS, kernel spike^{-1}; SPM, spike^{-1}; TW, test weight; GY, grain yield; HI, harvest index; PH, plant height; GM, grains metre-1; TS, number of tillers; GLA, green leaf area; GFL, greenness of the flag leaf. Bold values are significant at P < 0.01, underlined values are significant at P < 0.05

a) Etter 2013 (ET13)

Traits	DTH	FD	BW	TKW	MSHW	KPS	SPM	TW	GY	HI
FD	-0.08									
BW	**0.24**	**-0.63**								
TKW	0.05	**0.52**	**-0.99**							
MSHW	-0.13	**0.41**	**-0.98**	**0.50**						
KPS	**-0.20**	0.10	**-0.24**	**-0.18**	**0.76**					
SPM	-0.07	**-0.61**	**0.99**	**-0.73**	**-0.82**	**-0.38**				
TW	**-0.35**	**0.24**	-0.10	**0.30**	0.14	-0.05	-0.10			
GY	**-0.30**	**-0.38**	**0.89**	**-0.61**	**-0.21**	**0.22**	**0.72**	0.03		
HI	**-0.53**	**0.56**	**-0.95**	**0.44**	**0.54**	**0.29**	**-0.58**	**0.68**	**-0.24**	
GM	**-0.48**	**-0.23**	**0.30**	**-0.84**	**-0.27**	**0.35**	**0.52**	**0.43**	**0.66**	**0.23**

b) Hays 2013 (HY13)

	PH	DTH	BW	TKW	MSHW	KPS	SPM	TW	GY	HI	GM
DTH	**0.20**										
BW	**0.71**	-0.04									
TKW	**0.36**	**-0.41**	**0.53**								
MSHW	**0.40**	-0.17	**0.70**	**0.43**							
KPS	0.02	**0.27**	0.06	**-0.54**	**0.51**						
SPM	-0.09	-0.17	**0.20**	**-0.26**	**-0.63**	**-0.36**					
TW	0.03	**-0.55**	**0.20**	**0.48**	-0.07	**-0.54**	**0.30**				
GY	**0.35**	**-0.37**	**0.99**	**0.18**	**0.41**	**0.19**	**0.44**	**0.24**			
HI	-0.01	**-0.81**	**0.18**	**0.52**	**0.37**	**-0.21**	0.17	**0.67**	**0.59**		
GM	-0.16	**-0.43**	-0.06	**-0.38**	0.15	**0.42**	**0.67**	**0.26**	**0.94**	**0.54**	
TS	**-0.40**	-0.01	**-0.30**	**-0.29**	-0.84	**-0.53**	**0.76**	**0.25**	-0.10	**-0.19**	0.04

c) Bushland 2014 (BS14)

	PH	DTH	BW	TKW	MSHW	KPS	SPM	TW	GY	HI	GM	TS	GLA
DTH	-0.09												
BW	0.08	**0.70**											
TKW	**0.22**	**0.42**	0.06										
MSHW	**0.18**	0.00	**-0.25**	**0.50**									
KPS	-0.01	**-0.38**	**-0.32**	**-0.35**	**0.63**								
SPM	**-0.19**	0.11	**0.72**	**-0.33**	**-0.53**	**-0.28**							
TW	**-0.17**	**0.43**	**0.49**	**0.23**	0.07	-0.14	0.17						
GY	-0.09	0.14	**0.56**	0.02	**0.20**	**0.21**	**0.71**	**0.21**					
HI	**-0.31**	-0.11	**-0.38**	**-0.32**	**0.37**	**0.69**	**0.47**	**-0.18**	**0.80**				
GM	**-0.28**	**-0.20**	0.06	**-0.87**	**-0.25**	**0.50**	**0.71**	-0.12	**0.56**	**0.65**			
TS	**-0.52**	**-0.28**	**0.21**	**-0.62**	**-0.99**	**-0.57**	**0.80**	**0.29**	0.04	**-0.60**	**0.24**		
GLA	**-0.23**	**0.90**	**0.67**	**0.35**	-0.07	**-0.38**	**0.19**	**0.49**	0.15*	**-0.24**	**-0.20**	0.12	
GFL	**-0.44**	**0.96**	**0.41**	**0.44**	-0.08	**-0.49**	0.14	**0.55**	0.07	**-0.52**	**-0.49**	0.09	**0.96**

Table A1 Continued

d) Chillicothe 14 (CH14)

	PH	BW	TKW	MSHW	KPS	SPM2	TW	GY	HI	GM	TS	GLA
BW	**0.56**											
TKW	**0.72**	**0.17**										
MSHW	**0.69**	0.09	**0.56**									
KPS	0.00	-0.14	**-0.42**	**0.52**								
SPM	-0.13	**0.99**	0.12	-0.08	**-0.26**							
TW	**0.34**	**0.61**	**0.33**	0.14	**-0.18**	0.15						
GY	**0.34**	**0.86**	**0.49**	**0.62**	0.14	**0.73**	**0.26**					
HI	-0.10	**-0.73**	**0.46**	**0.43**	0.00	**0.35**	-0.02	**0.55**				
GM	**-0.94**	**-0.56**	**-0.99**	**-0.67**	**0.46**	**0.62**	**-0.19**	0.01	**-0.39**			
TS	**-0.49**	0.14	**-0.53**	**-0.99**	**-0.63**	**0.76**	0.17	-0.08	**-0.48**	**0.35**		
GLA	**-0.24**	-0.13	**-0.43**	**-0.39**	0.02	**-0.28**	0.11	**-0.49**	**-0.63**	0.11	**0.19**	
GFL	**-0.40**	**-0.31**	**-0.50**	**-0.52**	-0.05	**-0.32**	0.04	**-0.62**	**-0.51**	**0.20**	0.16	**0.81**

e) Etter 2014 (ET14)

	PH	TKW	MSHW	KPS	SPM2	TW	GY
TKW	**0.18**						
MSHW	-0.01	**0.66**					
KPS	**-0.18**	**-0.26**	**0.56**				
SPM	0.03	**-0.29**	**-0.82**	**-0.71**			
TW	-0.17	**0.29**	0.05	**-0.26**	0.03		
GY	0.04	**0.39**	-0.12	**-0.53**	**0.65**	0.13	
TS	-0.14	**-0.40**	**-0.99**	**-0.99**	**0.99**	**0.36**	**-0.40**

Table A2

Genetic correlation for end-use quality in individual environments. MLT, midline left time; MLV, midline left value; MLS, midline left slope; MLW, midline left width; MLI, midline left integral; MPT, midline peak time; MPV, midline peak value; MPW, midline peak width; MPI, midline peak integral; MRT, midline right time; MRV, midline right value; MRS, midline right slope; MRW, midline right width; MRI, midline right integral; MTXV, midline time_X value; MTXS, midline time_X slope; MTXW, midline time_X width; MTXI, midline time_X integral; MMST, midline mixing stability or tolerance. Bold values are significant at $P < 0.01$, underlined values are significant at $P < 0.05$

a) Upper diagonal is Etter, 2014 (ET14) and the lower diagonal is Bushland 2014 (BS 14)

	MLT	MLV	MLS	MLW	MLI	MPT	MPV	MPW	MPI	MRT	MRV	MRS	MRW	MRI	MTXV	MTXS	MTXW	MTXI	MMST
MLT		0.00	**-0.72**	**-0.22**	**0.98**	**0.99**	**-0.48**	0.05	**0.96**	**0.84**	-0.10	**0.47**	**0.36**	**0.79**	**0.51**	0.01	**0.82**	**-0.54**	**-0.72**
MLV	0.09		**-0.26**	**0.57**	0.16	0.00	**0.73**	**0.41**	**0.23**	0.12	**0.77**	0.03	**0.43**	**0.39**	**0.68**	**-0.21**	0.06	**0.76**	**-0.22**
MLS	**-0.67**	-0.13		0.17	**-0.75**	**-0.72**	**0.39**	0.06	**-0.75**	**-0.70**	0.07	**-0.54**	**-0.4**	**-0.70**	**-0.43**	0.07	**-0.52**	**0.22**	**0.97**
MLW	**-0.18**	**0.52**	0.10		-0.13	**-0.22**	**0.66**	**0.58**	-0.08	-0.15	**0.65**	0.01	**0.37**	0.05	**0.43**	-0.10	0.00	**0.63**	**0.13**
MLI	**0.93**	**0.31**	**-0.71**	0.00		**0.98**	**-0.36**	0.12	**1.00**	**0.85**	0.02	**0.48**	**0.43**	**0.86**	**0.61**	-0.04	**0.83**	**-0.37**	**-0.75**
MPT	**0.99**	0.09	**-0.67**	**-0.18**	**0.93**		**-0.48**	0.05	**0.96**	**0.84**	-0.10	**0.47**	**0.36**	**0.79**	**0.51**	0.01	**0.82**	**-0.54**	**-0.72**
MPV	**-0.32**	**0.77**	**0.48**	**0.54**	-0.15	**-0.32**		**0.52**	**-0.29**	**-0.37**	**0.84**	**-0.34**	0.17	-0.10	**0.40**	**-0.16**	**-0.27**	**0.90**	**0.42**
MPW	-0.08	0.14	0.05	**0.62**	0.06	-0.08	0.17		0.16	0.03	**0.71**	**0.19**	**0.66**	**0.20**	**0.64**	0.02	**0.38**	**0.48**	-0.01
MPI	**0.90**	**0.43**	**-0.67**	0.08	**0.99**	**0.9**	-0.02	0.08		**0.84**	0.09	**0.47**	**0.46**	**0.88**	**0.66**	-0.05	**0.82**	**-0.31**	**-0.74**
MRT	**0.64**	**0.29**	**-0.47**	-0.12	**0.59**	**0.64**	-0.02	**-0.20**	**0.60**		-0.15	**0.55**	**0.40**	**0.94**	**0.53**	-0.10	**0.65**	**-0.37**	**-0.73**
MRV	0.04	**0.68**	-0.04	**0.63**	**0.23**	0.04	**0.56**	**0.55**	**0.32**	-0.06		-0.08	**0.50**	0.13	**0.70**	-0.11	0.11	**0.79**	0.08
MRS	**0.42**	-0.09	**-0.50**	-0.16	**0.42**	**0.42**	**-0.35**	-0.04	**0.38**	**0.53**	-0.13		**0.56**	**0.50**	**0.40**	0.01	**0.51**	-0.16	**-0.74**
MRW	**0.29**	0.13	**-0.49**	**0.29**	**0.41**	**0.29**	-0.16	**0.49**	**0.40**	**0.19**	**0.46**	**0.53**		**0.50**	**0.75**	-0.02	**0.54**	**0.28**	**-0.49**
MRI	**0.53**	**0.63**	**-0.34**	0.16	**0.6**	**0.53**	**0.37**	-0.05	**0.65**	**0.86**	**0.31**	**0.33**	**0.19**		**0.71**	-0.15	**0.68**	-0.09	**-0.71**
MTXV	**0.57**	**0.70**	**-0.36**	**0.45**	**0.74**	**0.57**	**0.41**	**0.39**	**0.80**	**0.42**	**0.68**	**0.22**	**0.47**	**0.62**		-0.10	**0.62**	**0.38**	**-0.47**
MTXS	0.10	-0.07	-0.07	-0.13	0.07	0.10	-0.12	0.02	0.06	0.04	-0.09	0.07	0.01	0.01	-0.04		0.02	-0.16	0.05
MTXW	**0.77**	0.09	**-0.43**	0.09	**0.78**	**0.77**	-0.13	**0.25**	**0.77**	**0.41**	0.16	**0.34**	**0.40**	**0.42**	**0.63**	0.07		**-0.29**	**-0.58**
MTXI	**-0.47**	**0.76**	**0.26**	**0.65**	**-0.18**	**-0.47**	**0.83**	**0.36**	-0.07	**-0.18**	**0.70**	**-0.25**	0.14	**0.23**	**0.38**	-0.15	**-0.24**		**0.23**
MMST	**-0.67**	-0.10	**0.99**	0.12	**-0.72**	**-0.67**	**0.49**	0.05	**-0.67**	**-0.52**	-0.01	**-0.63**	**-0.54**	**-0.37**	**-0.36**	-0.08	**-0.44**	**0.28**	

Table A2 Continued

b) Hays, 2013 (HY13)

	MLV	MLS	MLW	MLI	MPT	MPV	MPW	MPI	MRT	MRV	MRS	MRW	MRI	MTXV	MTXS	MTXW	MTXI	MMST
MLT	**-0.50**	**-0.64**	**-0.42**	**0.85**	**1.00**	**-0.58**	-0.11	**0.76**	**0.46**	-0.08	**0.17**	0.06	**0.33**	**-0.24**	-0.01	**0.63**	**-0.73**	**-0.62**
MLV		**0.25**	**0.59**	-0.04	**-0.50**	**0.97**	**0.39**	0.13	0.02	**0.53**	**-0.29**	**0.13**	**0.37**	**0.92**	-0.10	0.04	**0.92**	**0.29**
MLS			**0.31**	**-0.67**	**-0.64**	**0.43**	**0.18**	**-0.61**	**-0.48**	0.04	**-0.32**	**-0.14**	**-0.44**	0.15	-0.07	**-0.36**	**0.36**	**0.97**
MLW				-0.10	**-0.42**	**0.63**	**0.77**	0.01	-0.17	**0.27**	0.08	**0.46**	-0.02	**0.61**	-0.05	0.12	**0.63**	**0.26**
MLI					**0.85**	-0.16	0.17	**0.99**	**0.51**	0.14	**0.17**	**0.22**	**0.53**	**0.22**	-0.03	**0.79**	**-0.28**	**-0.64**
MPT						**-0.58**	-0.11	**0.76**	**0.46**	-0.08	**0.17**	0.06	**0.33**	**-0.24**	-0.01	**0.63**	**-0.73**	**-0.62**
MPV							**0.43**	0.01	-0.06	**0.51**	**-0.34**	0.10	**0.27**	**0.90**	-0.10	-0.01	**0.92**	**0.46**
MPW								**0.24**	-0.07	**0.26**	**0.20**	**0.59**	0.05	**0.52**	0.08	**0.49**	**0.40**	0.11
MPI									**0.50**	**0.23**	0.12	**0.24**	**0.58**	**0.37**	-0.05	**0.79**	-0.12	**-0.58**
MRT										-0.16	**0.13**	-0.09	**0.77**	0.11	-0.11	**0.23**	**-0.19**	**-0.47**
MRV											**-0.40**	**0.43**	**0.46**	**0.51**	0.00	**0.25**	**0.52**	0.13
MRS												**0.4**	**-0.19**	-0.12	0.04	0.08	**-0.23**	**-0.53**
MRW													0.12	**0.28**	0.03	**0.29**	**0.2**	**-0.22**
MRI														**0.40**	-0.09	**0.34**	**0.18**	**-0.34**
MTXV															**-0.16**	**0.29**	**0.77**	**0.17**
MTXS																0.02	-0.04	-0.08
MTXW																	**-0.14**	**-0.35**
MTXI																		**0.38**

Table A3
Best linear unbiased predictors for data averaged across all the environments

Genotype	GY	DTH	TW	PH	HI	GM	BW	SPM	KPS	MSHW	TKW	TS	GLA	GFL
	tha^{-1}	d	Ib/bu	cm	#	#	g	#	#	g	g	#	%	%
CT2	3.4	141.5	57.4	53.8	0.3	3697.0	118.4	370.6	27.3	0.7	26.3	100.9	3.8	26.3
CT3	3.7	140.3	60.2	62.3	0.3	3365.3	107.9	334.8	27.4	0.8	27.9	88.6	17.5	31.3
CT4	3.7	142.0	59.2	66.9	0.3	3235.3	113.3	332.0	27.0	0.8	29.3	88.3	20.5	47.5
CT5	3.3	141.1	57.6	63.0	0.3	3504.3	109.9	323.6	27.3	0.8	27.4	94.8	8.8	40.0
CT7	3.5	143.4	58.2	64.4	0.2	2825.9	106.9	377.7	23.7	0.7	27.6	95.0	18.8	52.5
CT8	3.8	142.6	57.8	64.4	0.2	3108.7	111.6	421.6	23.0	0.6	27.4	96.5	12.5	52.5
CT9	3.9	139.3	56.8	62.6	0.3	3926.6	112.9	378.7	29.7	0.8	25.5	92.5	1.5	22.5
CT10	3.7	143.6	58.1	61.4	0.3	3306.8	108.6	332.5	30.8	0.8	26.4	77.6	37.5	56.3
CT11	3.7	140.4	58.7	66.3	0.3	3860.0	111.1	360.2	28.8	0.8	25.3	96.4	5.5	30.0
CT12	3.9	141.0	57.6	63.8	0.3	3912.2	108.8	427.0	26.2	0.6	23.6	109.6	21.3	60.0
CT13	3.7	141.9	58.6	61.2	0.3	3448.9	114.4	445.4	24.1	0.6	24.4	117.9	6.3	25.0
CT15	3.9	141.8	57.7	68.4	0.3	3837.6	134.0	356.2	27.9	0.8	28.4	94.8	7.5	36.3
CT16	3.8	141.6	60.4	62.5	0.3	3699.2	111.0	421.0	26.0	0.6	24.7	96.6	27.5	68.8
CT17	3.5	141.8	58.3	60.0	0.2	3823.5	121.4	372.8	31.4	0.7	23.2	95.4	37.5	78.8
CT18	3.7	140.9	59.6	58.8	0.3	3915.8	113.0	412.3	27.6	0.6	23.2	106.4	31.3	66.3
CT19	3.5	139.9	61.4	58.4	0.3	3716.7	109.1	372.7	27.2	0.7	25.0	98.0	3.8	27.5
CT20	3.9	141.0	57.9	68.4	0.3	3288.6	112.7	363.7	26.3	0.7	27.0	93.9	14.8	47.5
CT21	3.6	141.4	59.6	66.4	0.3	3404.3	109.3	390.8	24.8	0.7	27.9	100.8	19.5	55.0
CT22	4.0	142.1	57.3	61.8	0.3	3833.6	108.4	425.8	25.7	0.7	25.1	100.8	12.5	43.8
CT23	3.8	142.3	56.7	60.8	0.2	3904.4	116.6	416.0	29.2	0.7	24.0	97.1	23.8	60.0
CT24	4.0	139.9	59.2	64.8	0.3	3635.1	117.2	407.2	30.5	0.7	25.4	103.1	NA	NA
CT26	3.4	141.6	58.8	60.8	0.3	3354.9	104.0	321.6	30.3	0.9	28.0	80.5	23.8	70.0
CT27	3.8	141.8	58.8	63.6	0.3	4160.5	119.3	380.9	29.4	0.8	25.1	100.3	16.3	45.0
CT28	4.4	142.1	59.3	66.3	0.3	3721.2	113.0	470.5	24.4	0.7	26.8	98.4	5.8	32.5
CT29	3.6	143.1	57.1	63.2	0.2	3337.4	117.5	411.8	24.3	0.7	26.3	103.5	23.8	68.8
CT30	3.1	141.5	59.3	55.9	0.3	3609.0	116.7	362.3	26.2	0.7	25.5	102.5	6.5	27.5
CT31	3.6	142.4	55.3	64.6	0.2	3332.2	105.9	395.4	26.1	0.6	24.3	97.1	29.3	65.0
CT32	3.4	144.3	58.8	66.7	0.3	3257.0	116.0	330.1	28.1	0.8	28.6	87.3	36.3	75.0
CT33	3.6	142.8	58.5	64.2	0.3	3143.8	112.1	331.9	26.3	0.8	29.0	79.9	12.5	40.0
CT34	3.9	143.3	55.2	61.6	0.2	3267.6	110.4	441.5	26.9	0.6	24.4	104.3	42.5	75.0
CT35	3.9	141.4	59.0	65.5	0.3	3258.7	109.4	348.9	25.1	0.8	29.5	91.4	17.0	38.8
CT36	3.4	143.6	56.6	63.3	0.2	3261.3	122.6	363.0	29.9	0.7	25.0	98.3	36.3	71.3
CT37	3.9	141.5	60.5	62.4	0.3	3498.1	108.8	433.0	25.2	0.7	25.3	108.4	6.3	33.8
CT38	3.3	141.8	57.8	65.4	0.3	3154.8	101.7	381.7	25.5	0.6	24.6	96.5	6.8	31.3
CT39	3.8	140.9	58.1	61.3	0.3	3788.2	113.8	454.3	26.1	0.7	25.0	105.6	22.5	63.8
CT40	4.0	141.8	59.7	66.1	0.3	3998.9	115.6	440.2	24.8	0.6	25.0	103.4	12.8	47.5
CT42	3.8	141.9	60.5	60.9	0.3	3784.9	106.9	374.2	30.8	0.8	24.1	98.5	18.8	41.3
CT43	3.6	141.9	57.8	61.6	0.2	3387.0	109.6	394.2	27.8	0.7	24.4	98.8	17.5	51.3
CT44	3.3	141.5	59.6	66.3	0.2	2764.4	93.6	364.0	23.9	0.7	28.0	88.9	8.8	31.3
CT45	4.0	141.9	59.0	60.9	0.3	4087.8	112.2	546.5	23.1	0.6	23.4	128.8	21.8	56.3
CT46	3.8	141.6	58.0	65.4	0.3	3542.7	106.8	369.3	29.0	0.8	27.1	80.6	3.8	26.3
CT47	3.7	141.1	59.7	64.6	0.3	3779.1	110.4	444.4	25.1	0.6	25.3	99.1	11.3	37.5
CT48	3.3	140.9	59.9	66.1	0.2	2502.0	107.2	361.1	22.9	0.7	27.8	92.5	20.0	51.3
CT49	3.2	144.4	58.6	62.6	0.2	3392.7	113.2	375.5	26.3	0.6	25.1	103.0	38.8	75.0
CT50	3.4	143.5	57.5	64.8	0.2	3121.4	102.6	317.4	29.1	0.8	26.3	86.8	20.5	66.3
CT51	3.6	141.0	56.5	61.6	0.3	3665.1	109.1	337.0	31.4	0.8	25.5	85.8	22.5	57.5
CT52	3.4	141.0	59.6	61.2	0.3	3409.0	107.1	325.5	31.5	0.8	27.0	81.6	15.0	40.0
CT53	4.2	142.3	59.4	62.9	0.2	4217.1	130.7	434.6	28.2	0.7	26.3	108.6	33.8	72.5
CT54	3.4	144.9	58.5	61.4	0.3	3622.3	110.3	378.5	28.8	0.7	23.0	90.9	26.3	66.3
CT55	3.7	144.0	57.0	65.4	0.2	3284.5	114.3	399.1	25.9	0.7	25.4	108.4	46.3	77.5
CT56	2.9	142.3	58.4	64.6	0.3	3248.0	103.1	299.2	25.4	0.7	28.0	85.3	20.0	40.0
CT57	3.6	141.9	58.7	63.7	0.3	3710.0	118.9	366.9	25.8	0.7	27.7	98.6	20.8	50.0
CT58	3.4	140.1	59.2	66.0	0.3	3313.9	101.8	374.8	27.3	0.7	25.9	89.9	12.5	46.3

Table A3 Continued

Genotype	GY	DTH	TW	PH	HI	GM	BW	SPM	KPS	MSHW	TKW	TS	GLA	GFL
	tha^{-1}	d	Ib/bu	cm	#	#	g	#	#	g	g	#	%	%
CT2	3.4	141.5	57.4	53.8	0.3	3697.0	118.4	370.6	27.3	0.7	26.3	100.9	3.8	26.3
CT3	3.7	140.3	60.2	62.3	0.3	3365.3	107.9	334.8	27.4	0.8	27.9	88.6	17.5	31.3
CT4	3.7	142.0	59.2	66.9	0.3	3235.3	113.3	332.0	27.0	0.8	29.3	88.3	20.5	47.5
CT5	3.3	141.1	57.6	63.0	0.3	3504.3	109.9	323.6	27.3	0.8	27.4	94.8	8.8	40.0
CT7	3.5	143.4	58.2	64.4	0.2	2825.9	106.9	377.7	23.7	0.7	27.6	95.0	18.8	52.5
CT8	3.8	142.6	57.8	64.4	0.2	3108.7	111.6	421.6	23.0	0.6	27.4	96.5	12.5	52.5
CT9	3.9	139.3	56.8	62.6	0.3	3926.6	112.9	378.7	29.7	0.8	25.5	92.5	1.5	22.5
CT10	3.7	143.6	58.1	61.4	0.3	3306.8	108.6	332.5	30.8	0.8	26.4	77.6	37.5	56.3
CT11	3.7	140.4	58.7	66.3	0.3	3860.0	111.1	360.2	28.8	0.8	25.3	96.4	5.5	30.0
CT12	3.9	141.0	57.6	63.8	0.3	3912.2	108.8	427.0	26.2	0.6	23.6	109.6	21.3	60.0
CT13	3.7	141.9	58.6	61.2	0.3	3448.9	114.4	445.4	24.1	0.6	24.4	117.9	6.3	25.0
CT15	3.9	141.8	57.7	68.4	0.3	3837.6	134.0	356.2	27.9	0.8	28.4	94.8	7.5	36.3
CT16	3.8	141.6	60.4	62.5	0.3	3699.2	111.0	421.0	26.0	0.6	24.7	96.6	27.5	68.8
CT17	3.5	141.8	58.3	60.0	0.2	3823.5	121.4	372.8	31.4	0.7	23.2	95.4	37.5	78.8
CT18	3.7	140.9	59.6	58.8	0.3	3915.8	113.0	412.3	27.6	0.6	23.2	106.4	31.3	66.3
CT19	3.5	139.9	61.4	58.4	0.3	3716.7	109.1	372.7	27.2	0.7	25.0	98.0	3.8	27.5
CT20	3.9	141.0	57.9	68.4	0.3	3288.6	112.7	363.7	26.3	0.7	27.0	93.9	14.8	47.5
CT21	3.6	141.4	59.6	66.4	0.3	3404.3	109.3	390.8	24.8	0.7	27.9	100.8	19.5	55.0
CT22	4.0	142.1	57.3	61.8	0.3	3833.6	108.4	425.8	25.7	0.7	25.1	100.8	12.5	43.8
CT23	3.8	142.3	56.7	60.8	0.2	3904.4	116.6	416.0	29.2	0.7	24.0	97.1	23.8	60.0
CT24	4.0	139.9	59.2	64.8	0.3	3635.1	117.2	407.2	30.5	0.7	25.4	103.1	NA	NA
CT26	3.4	141.6	58.8	60.8	0.3	3354.9	104.0	321.6	30.3	0.9	28.0	80.5	23.8	70.0
CT27	3.8	141.8	58.8	63.6	0.3	4160.5	119.3	380.9	29.4	0.8	25.1	100.3	16.3	45.0
CT28	4.4	142.1	59.3	66.3	0.3	3721.2	113.0	470.5	24.4	0.7	26.8	98.4	5.8	32.5
CT29	3.6	143.1	57.1	63.2	0.2	3337.4	117.5	411.8	24.3	0.7	26.3	103.5	23.8	68.8
CT30	3.1	141.5	59.3	55.9	0.3	3609.0	116.7	362.3	26.2	0.7	25.5	102.5	6.5	27.5
CT31	3.6	142.4	55.3	64.6	0.2	3332.2	105.9	395.4	26.1	0.6	24.3	97.1	29.3	65.0
CT32	3.4	144.3	58.8	66.7	0.3	3257.0	116.0	330.1	28.1	0.8	28.6	87.3	36.3	75.0
CT33	3.6	142.8	58.5	64.2	0.3	3143.8	112.1	331.9	26.3	0.8	29.0	79.9	12.5	40.0
CT34	3.9	143.3	55.2	61.6	0.2	3267.6	110.4	441.5	26.9	0.6	24.4	104.3	42.5	75.0
CT35	3.9	141.4	59.0	65.5	0.3	3258.7	109.4	348.9	25.1	0.8	29.5	91.4	17.0	38.8
CT36	3.4	143.6	56.6	63.3	0.2	3261.3	122.6	363.0	29.9	0.7	25.0	98.3	36.3	71.3
CT37	3.9	141.5	60.5	62.4	0.3	3498.1	108.8	433.0	25.2	0.7	25.3	108.4	6.3	33.8
CT38	3.3	141.8	57.8	65.4	0.3	3154.8	101.7	381.7	25.5	0.6	24.6	96.5	6.8	31.3
CT39	3.8	140.9	58.1	61.3	0.3	3788.2	113.8	454.3	26.1	0.7	25.0	105.6	22.5	63.8
CT40	4.0	141.8	59.7	66.1	0.3	3998.9	115.6	440.2	24.8	0.6	25.0	103.4	12.8	47.5
CT42	3.8	141.9	60.5	60.9	0.3	3784.9	106.9	374.2	30.8	0.8	24.1	98.5	18.8	41.3
CT43	3.6	141.9	57.8	61.6	0.2	3387.0	109.6	394.2	27.8	0.7	24.4	98.8	17.5	51.3
CT44	3.3	141.5	59.6	66.3	0.2	2764.4	93.6	364.0	23.9	0.7	28.0	88.9	8.8	31.3
CT45	4.0	141.9	59.0	60.9	0.3	4087.8	112.2	546.5	23.1	0.6	23.4	128.8	21.8	56.3
CT46	3.8	141.6	58.0	65.4	0.3	3542.7	106.8	369.3	29.0	0.8	27.1	80.6	3.8	26.3
CT47	3.7	141.1	59.7	64.6	0.3	3779.1	110.4	444.4	25.1	0.6	25.3	99.1	11.3	37.5
CT48	3.3	140.9	59.9	66.1	0.2	2502.0	107.2	361.1	22.9	0.7	27.8	92.5	20.0	51.3
CT49	3.2	144.4	58.6	62.6	0.2	3392.7	113.2	375.5	26.3	0.6	25.1	103.0	38.8	75.0
CT50	3.4	143.5	57.5	64.8	0.2	3121.4	102.6	317.4	29.1	0.8	26.3	86.8	20.5	66.3
CT51	3.6	141.0	56.5	61.6	0.3	3665.1	109.1	337.0	31.4	0.8	25.5	85.8	22.5	57.5
CT52	3.4	141.0	59.6	61.2	0.3	3409.0	107.1	325.5	31.5	0.8	27.0	81.6	15.0	40.0
CT53	4.2	142.3	59.4	62.9	0.2	4217.1	130.7	434.6	28.2	0.7	26.3	108.6	33.8	72.5
CT54	3.4	144.9	58.5	61.4	0.3	3622.3	110.3	378.5	28.8	0.7	23.0	90.9	26.3	66.3
CT55	3.7	144.0	57.0	65.4	0.2	3284.5	114.3	399.1	25.9	0.7	25.4	108.4	46.3	77.5
CT56	2.9	142.3	58.4	64.6	0.3	3248.0	103.1	299.2	25.4	0.7	28.0	85.3	20.0	40.0
CT57	3.6	141.9	58.7	63.7	0.3	3710.0	118.9	366.9	25.8	0.7	27.7	98.6	20.8	50.0
CT58	3.4	140.1	59.2	66.0	0.3	3313.9	101.8	374.8	27.3	0.7	25.9	89.9	12.5	46.3

Table A3 Continued

Genotype	GY	DTH	TW	PH	HI	GM	BW	SPM	KPS	MSHW	TKW	TS	GLA	GFL
	tha^{-1}	d	Ib/bu	cm	#	#	g	#	#	g	g	#	%	%
CT59	3.8	140.3	59.1	61.9	0.3	3645.6	101.7	303.3	33.4	0.8	25.0	80.9	6.8	27.5
CT60	3.9	141.6	60.0	65.9	0.3	3344.8	104.3	409.1	25.7	0.7	27.1	97.1	16.3	51.3
CT61	3.7	141.0	57.4	62.6	0.3	3201.8	109.0	351.9	26.5	0.7	28.0	84.4	5.0	26.3
CT62	3.9	142.9	58.1	58.5	0.3	3389.6	109.5	392.3	26.9	0.7	25.6	92.6	40.0	53.8
CT63	3.6	144.6	56.7	68.5	0.2	3483.8	113.5	369.6	29.3	0.7	24.1	94.0	43.8	66.3
CT64	3.9	141.5	58.4	60.7	0.3	3666.3	108.8	419.8	26.2	0.7	26.5	97.6	10.5	22.5
CT65	3.5	144.1	57.9	69.2	0.2	3535.7	117.7	412.5	26.7	0.7	25.2	97.8	38.8	68.8
CT66	3.9	141.0	60.5	62.0	0.3	4175.1	119.6	392.9	28.5	0.7	24.6	109.0	17.5	51.3
CT67	3.4	143.0	57.9	61.5	0.3	3351.7	112.5	333.7	29.3	0.8	26.7	93.6	28.0	46.3
CT68	3.9	141.5	58.7	64.4	0.3	3400.2	114.8	366.7	26.3	0.7	28.7	97.0	10.0	47.5
CT69	3.9	141.6	60.5	72.7	0.3	3562.8	121.1	347.4	28.1	0.8	28.4	88.4	13.8	45.0
CT70	3.7	141.1	60.5	68.8	0.3	3829.3	110.3	423.6	27.5	0.7	26.1	101.3	10.0	32.5
CT71	4.0	141.0	59.2	70.1	0.3	3219.2	112.5	377.0	27.3	0.8	29.2	84.5	6.3	36.3
CT73	3.6	141.8	60.5	61.5	0.3	3518.5	105.2	372.2	27.8	0.7	25.4	94.5	15.0	58.8
CT75	3.3	141.3	60.6	62.8	0.3	4058.9	121.6	380.4	27.6	0.7	25.9	106.6	9.5	30.0
CT76	3.4	140.5	60.3	61.9	0.3	3854.9	113.2	460.6	25.0	0.6	23.7	106.8	13.0	58.8
CT77	3.4	143.8	57.9	63.4	0.2	2900.1	109.9	307.8	30.2	0.8	25.2	83.8	36.3	71.3
CT78	3.6	141.1	59.1	61.2	0.4	3865.8	112.8	368.7	28.1	0.8	29.5	92.1	15.5	48.8
CT79	3.6	141.5	57.9	66.5	0.3	3547.9	111.2	360.3	28.6	0.8	26.7	96.9	20.0	63.8
CT80	3.6	142.0	59.2	61.2	0.3	3320.4	103.6	378.9	26.9	0.7	25.9	92.4	13.8	47.5
CT81	3.9	143.0	57.1	67.5	0.2	3444.8	118.2	340.7	27.4	0.7	27.2	91.5	20.0	56.3
CT82	3.6	139.9	60.9	62.0	0.3	4327.7	123.2	393.4	30.5	0.8	25.1	95.4	18.8	46.3
CT83	3.2	142.1	55.5	60.9	0.3	3926.3	112.7	365.1	30.7	0.7	22.4	101.0	8.8	57.5
CT84	3.5	143.6	59.9	63.9	0.2	2851.7	113.1	377.8	25.4	0.7	27.7	91.6	33.8	63.8
CT85	3.7	143.1	59.7	65.2	0.3	3160.1	111.8	364.5	26.4	0.7	27.5	103.9	20.5	52.5
CT86	3.8	142.0	57.8	66.6	0.3	3865.4	121.8	344.9	27.6	0.8	28.4	86.9	12.5	50.0
CT87	3.6	143.9	57.0	65.8	0.3	3167.1	105.0	357.5	27.0	0.7	26.3	86.1	42.5	67.5
CT88	3.9	144.6	59.7	69.6	0.3	3909.1	117.8	387.1	30.2	0.8	24.5	91.0	45.0	71.3
CT89	3.3	141.3	59.6	60.0	0.3	3561.9	101.0	310.1	30.8	0.8	25.2	87.1	26.8	61.3
CT90	3.0	145.1	57.8	61.5	0.2	3592.3	115.5	419.6	26.0	0.5	20.9	116.3	63.8	82.5
CT91	3.2	141.1	56.2	60.9	0.3	3432.8	102.5	347.4	31.5	0.7	23.4	89.1	12.5	41.3
CT92	3.6	142.1	58.8	60.6	0.3	3742.5	106.5	389.5	27.2	0.7	24.1	98.8	7.5	45.0
CT93	3.6	141.1	60.3	64.2	0.3	3822.9	117.5	388.9	25.7	0.7	25.9	102.3	20.0	57.5
CT94	4.0	142.0	58.7	63.1	0.3	4049.0	109.4	381.6	29.0	0.7	24.9	96.5	4.3	26.3
CT95	4.2	140.6	60.0	60.6	0.3	4118.7	117.5	451.0	27.2	0.7	24.6	103.6	8.8	33.8
CT96	3.4	142.6	58.7	59.7	0.3	3623.0	112.3	377.6	27.3	0.7	24.7	97.9	20.0	60.0
CT97	4.0	141.6	58.6	66.0	0.3	3856.3	120.9	414.9	26.4	0.7	27.1	102.1	21.3	60.0
CT98	3.9	141.1	61.4	65.5	0.3	3084.5	114.9	368.1	23.8	0.8	30.9	104.1	7.5	27.5
CT99	3.4	141.0	57.1	61.4	0.3	3288.7	105.6	381.3	26.9	0.7	25.9	91.8	6.3	37.5
CT100	3.7	140.5	58.6	64.8	0.3	3682.4	110.8	379.2	27.1	0.7	27.1	94.1	25.0	51.3
CT101	3.4	141.3	59.3	59.4	0.3	3919.7	116.1	386.1	25.3	0.6	25.2	109.3	11.3	36.3
CT102	4.0	139.5	58.7	57.4	0.3	3779.1	107.8	392.8	28.6	0.7	25.9	90.4	7.3	27.5
CT103	3.9	141.9	57.3	64.3	0.3	4184.7	117.4	394.0	30.7	0.7	23.9	94.9	4.3	21.3
CT104	3.6	141.6	58.5	57.9	0.2	3938.3	116.8	395.2	28.9	0.7	24.0	99.6	26.8	61.3
CT105	3.6	144.4	57.5	62.6	0.2	3319.3	105.0	355.8	28.8	0.6	22.4	92.5	46.3	62.5
CT106	3.3	140.5	59.8	59.1	0.2	3187.7	98.2	263.8	34.4	0.8	23.6	82.6	23.8	53.8
CT107	3.6	142.5	57.0	65.5	0.2	3352.8	116.3	371.9	26.7	0.7	26.0	99.4	33.8	67.5
CT108	3.7	142.5	56.6	65.6	0.3	4129.9	112.3	402.8	27.2	0.7	25.0	97.1	16.8	55.0
CT109	3.7	142.8	57.7	62.2	0.3	3452.2	113.4	319.2	29.5	0.8	27.2	87.3	30.5	51.3
CT110	3.1	145.6	57.7	66.4	0.2	3053.2	113.6	346.7	25.9	0.6	24.9	102.0	50.0	70.0
CT111	4.2	141.5	58.2	63.6	0.3	4297.5	119.5	354.2	32.7	0.8	25.1	94.4	3.8	27.5
CT112	2.6	142.6	58.8	60.3	0.3	3437.6	98.7	316.2	25.3	0.7	25.6	98.0	21.3	48.8
CT113	3.7	140.9	57.9	55.4	0.3	4096.1	107.5	416.7	26.6	0.6	23.7	113.3	10.0	55.0

Table A3 Continued

Genotype	GY	DTH	TW	PH	HI	GM	BW	SPM	KPS	MSHW	TKW	TS	GLA	GFL
	tha^{-1}	d	lb/bu	cm	#	#	g	#	#	g	g	#	%	%
CT114	3.4	141.5	57.2	60.3	0.2	4046.5	116.4	369.5	29.5	0.6	21.5	98.5	14.3	37.5
CT115	3.7	141.6	58.4	62.8	0.3	3391.6	116.3	334.8	27.2	0.8	29.1	94.8	12.3	45.0
CT116	3.9	141.1	58.4	59.6	0.3	3458.1	104.3	378.4	25.3	0.7	26.4	95.4	6.3	35.0
CT117	3.6	141.4	57.4	58.7	0.3	4390.6	110.1	395.9	29.3	0.7	23.4	106.0	1.8	18.8
CT118	3.6	141.9	56.8	64.6	0.3	3605.4	114.7	385.6	28.0	0.7	25.8	88.6	14.3	57.5
CT119	3.6	140.6	56.8	61.6	0.3	3985.6	113.1	388.2	26.5	0.6	24.0	101.9	3.0	25.0
CT120	3.7	143.6	57.3	62.1	0.2	3287.8	111.3	393.3	27.1	0.7	24.0	93.9	35.0	72.5
CT121	4.1	144.0	58.8	65.7	0.3	3342.0	111.7	386.7	25.5	0.7	27.8	84.4	13.8	51.3
CT122	3.4	141.6	58.3	64.0	0.3	3201.5	106.3	372.9	28.2	0.7	25.9	92.4	8.8	30.0
CT124	3.5	140.9	59.8	62.1	0.3	3712.6	120.2	344.8	26.9	0.7	26.8	95.9	17.5	37.5
CT125	3.4	143.0	60.2	65.0	0.3	3378.2	114.6	325.8	27.0	0.7	27.2	91.6	30.0	71.3
CT126	3.8	141.9	56.0	64.7	0.2	3377.0	112.9	324.3	29.9	0.8	26.0	87.3	13.0	57.5
CT127	3.4	142.6	56.9	67.9	0.3	3193.9	105.7	351.4	28.1	0.7	25.4	92.5	20.5	55.0
CT128	3.8	140.9	57.6	64.4	0.3	3520.8	111.3	408.9	28.5	0.7	24.3	96.9	11.8	40.0
CT129	3.5	140.8	60.6	68.3	0.3	2650.6	110.2	277.4	25.8	0.9	34.7	72.1	20.0	48.8
CT130	3.6	141.9	58.4	72.0	0.3	3481.5	111.9	346.7	29.7	0.8	26.5	85.8	12.5	47.5
CT131	3.6	140.8	59.7	69.7	0.3	3262.1	118.3	288.0	29.8	0.9	31.4	82.8	9.0	27.5
CT132	3.1	143.1	58.9	59.2	0.2	3410.9	104.1	372.5	26.9	0.6	23.6	92.4	36.3	56.3
CT133	3.4	143.5	57.5	63.6	0.3	3275.7	112.8	367.6	24.9	0.7	28.2	95.0	19.3	60.0
CT134	4.2	141.0	59.5	64.0	0.3	3843.5	109.0	398.9	27.3	0.7	24.6	104.5	17.5	55.0
CT135	3.9	141.8	59.8	61.6	0.3	4305.6	126.1	406.0	30.8	0.8	24.9	96.5	30.0	72.5
CT136	3.1	143.5	57.8	70.5	0.2	3012.2	106.6	352.2	27.7	0.7	25.5	101.1	33.8	75.0
CT137	3.8	141.0	58.7	63.3	0.3	3593.5	109.2	383.4	28.1	0.7	25.5	94.3	9.3	45.0
CT138	3.4	144.3	56.9	66.9	0.3	4093.6	115.2	412.2	29.9	0.7	22.2	104.8	36.3	72.5
CT139	4.0	140.8	58.2	61.2	0.3	3855.5	108.0	417.7	27.7	0.7	24.3	101.1	6.3	22.5
CT140	4.2	141.9	57.4	59.9	0.3	3684.2	105.8	387.3	29.0	0.7	23.8	95.0	12.5	43.8
CT141	3.7	141.0	58.8	57.1	0.3	3640.6	114.9	400.0	27.2	0.7	24.7	105.8	5.0	36.3
CT142	3.3	141.5	56.9	57.4	0.2	3559.5	116.7	404.9	25.9	0.6	23.6	113.0	12.5	48.8
CT143	4.0	141.3	55.3	63.2	0.3	3567.5	104.8	314.0	32.1	0.8	25.8	75.4	3.8	28.8
CT145	3.9	141.8	57.5	63.4	0.3	3937.0	112.2	402.8	29.0	0.7	22.9	102.3	24.3	57.5
CT146	3.2	140.5	58.5	58.1	0.3	2921.5	93.5	291.8	30.9	0.8	25.4	82.1	7.5	42.5
CT147	3.2	144.1	59.3	64.3	0.3	3659.4	121.1	378.8	27.3	0.7	26.0	110.3	38.8	65.0
CT148	3.7	143.9	58.9	71.2	0.2	3225.1	111.2	393.9	27.0	0.6	23.5	95.5	28.0	73.8
CT149	3.8	140.0	55.0	59.2	0.3	3400.4	105.1	326.1	31.0	0.8	25.7	75.5	6.3	27.5
CT150	4.0	144.1	58.2	65.8	0.3	4146.4	117.7	346.8	31.7	0.8	24.5	93.6	34.3	63.8
CT151	3.8	143.1	59.7	65.2	0.3	3627.8	122.4	336.5	28.6	0.8	26.4	93.0	25.5	62.5
CT152	4.0	140.4	57.8	63.6	0.3	4224.6	118.8	366.6	31.0	0.8	25.4	91.6	6.8	28.8
CT153	3.5	140.4	57.4	67.3	0.3	3072.4	98.6	276.2	32.3	0.9	28.4	72.4	6.3	27.5
CT154	3.1	142.8	57.4	56.4	0.3	3286.6	100.8	312.5	30.7	0.8	24.5	83.8	30.5	55.0
CT155	3.0	140.4	58.9	58.9	0.3	3455.1	108.6	404.1	25.5	0.6	23.4	110.4	6.3	47.5
CT156	3.9	141.1	60.9	67.3	0.3	3745.8	116.2	332.9	31.2	0.8	27.0	76.6	NA	NA
CT157	3.8	141.4	59.5	63.6	0.3	3864.5	122.1	400.8	24.7	0.7	28.1	103.9	31.3	60.0
CT158	3.4	141.0	58.9	60.1	0.3	3760.8	113.6	363.7	27.1	0.7	25.0	115.6	25.5	66.3
CT159	3.5	141.3	59.7	64.3	0.3	3993.5	109.1	394.1	25.2	0.6	25.2	100.9	12.5	33.8
CT161	3.4	140.6	58.8	63.2	0.2	2817.4	103.8	305.4	27.6	0.8	27.8	90.0	17.5	43.8
CT162	3.7	144.5	57.5	62.3	0.3	4246.3	125.1	431.4	28.3	0.7	24.1	112.5	61.3	80.0
CT163	3.6	142.4	58.3	58.8	0.3	3521.8	101.4	381.7	28.7	0.6	22.9	93.0	23.8	65.0
CT164	3.6	142.3	58.3	63.6	0.3	4172.9	113.0	406.1	29.4	0.7	21.9	104.6	15.0	66.3
CT166	3.9	139.1	60.1	62.3	0.3	4258.7	123.9	404.2	26.5	0.7	27.4	104.1	NA	NA
CT173	3.5	144.4	58.7	68.0	0.3	3047.9	111.0	361.9	25.6	0.7	27.0	104.1	46.3	80.0
CT174	3.4	144.8	58.4	61.5	0.2	3744.0	112.2	414.7	31.6	0.6	20.0	94.8	55.0	75.0
CT181	3.4	142.5	60.2	57.8	0.3	3643.0	107.5	365.9	28.9	0.7	24.4	87.4	16.3	60.0
CT183	3.9	141.6	59.8	67.2	0.3	3601.5	108.0	400.6	27.0	0.7	25.2	96.1	15.0	48.8

Table A3 Continued

Genotype	GY	DTH	TW	PH	HI	GM	BW	SPM	KPS	MSHW	TKW	TS	GLA	GFL
	tha^{-1}	d	lb/bu	cm	#	#	g	#	#	g	g	#	%	%
CT184	3.4	140.9	58.8	66.0	0.3	3533.8	110.5	395.7	26.7	0.7	25.8	101.8	5.5	32.5
CT185	3.6	140.1	60.0	62.7	0.3	3978.0	104.1	341.8	29.5	0.8	25.3	95.3	5.0	17.5
CT189	3.5	142.3	60.0	62.6	0.3	3653.2	112.0	392.2	24.5	0.6	25.4	108.4	25.0	65.0
CT190	4.2	141.5	57.7	66.1	0.3	3969.4	118.5	452.7	25.5	0.7	25.8	110.1	3.8	28.8
CT191	3.8	142.6	59.4	63.1	0.3	4430.5	120.6	416.8	29.6	0.6	21.1	112.0	36.3	75.0
CT192	3.6	143.0	59.6	65.7	0.3	3755.8	117.9	403.4	25.8	0.7	25.5	102.1	43.8	72.5
CT193	3.9	142.1	58.4	64.2	0.2	4020.3	118.3	449.9	27.5	0.7	23.6	105.4	5.8	25.0
CT194	3.9	144.0	57.7	61.7	0.2	3214.4	117.4	390.9	25.7	0.7	27.0	88.8	26.3	68.8
CT196	3.8	141.8	57.8	64.2	0.3	3772.7	112.4	351.2	28.7	0.8	26.8	90.0	14.3	50.0
CT197	3.2	141.4	58.5	60.9	0.2	2870.3	103.0	355.6	24.8	0.6	24.9	104.3	17.3	62.5
CT198	3.7	142.8	57.8	61.8	0.3	3635.0	107.2	337.1	30.1	0.8	24.8	88.6	2.5	18.8
CT199	4.2	141.5	58.7	67.2	0.3	3876.7	119.8	382.3	29.3	0.8	26.9	98.1	8.0	41.3
CT200	3.7	142.5	57.8	69.0	0.3	3344.3	112.3	331.5	29.1	0.8	26.5	84.5	25.5	55.0
CT201	3.8	142.9	57.5	69.0	0.3	3428.4	109.1	370.1	28.8	0.8	26.6	83.8	28.8	52.5
CT202	3.8	140.5	59.6	62.9	0.3	3858.4	108.8	383.8	30.0	0.7	23.6	94.8	10.5	35.0
CT203	3.6	141.9	57.2	64.9	0.3	3509.4	112.2	343.3	29.5	0.8	26.5	88.1	13.8	41.3
CT204	3.3	142.9	57.0	69.8	0.2	3076.4	107.2	329.5	26.8	0.7	26.9	91.6	28.8	63.8
CT205	3.8	143.4	59.9	59.4	0.3	4160.5	111.6	424.4	29.3	0.7	22.7	97.9	18.0	51.3
CT207	3.3	141.5	58.7	67.5	0.3	3400.3	109.1	307.1	30.9	0.8	26.8	87.5	12.5	55.0
CT208	3.5	140.3	58.0	58.1	0.3	3501.9	103.8	330.6	29.1	0.8	26.4	86.8	5.0	27.5
CT209	3.7	141.9	58.8	61.7	0.2	3461.6	110.8	384.1	27.2	0.7	25.7	101.1	27.5	60.0
CT210	3.0	141.8	59.0	63.4	0.2	3787.2	122.0	352.7	25.6	0.7	26.1	107.8	22.0	41.3
CT211	3.6	144.3	57.1	60.6	0.2	3285.3	106.4	369.8	28.2	0.7	22.9	87.1	35.0	62.5
CT212	3.8	141.5	56.3	57.5	0.2	3970.2	110.0	428.5	28.1	0.6	22.7	112.3	3.8	16.3
CT213	3.4	142.0	58.8	64.7	0.2	3214.6	111.7	327.3	26.8	0.7	27.4	83.6	10.5	40.0
CT214	3.3	143.1	56.2	68.1	0.3	3642.7	110.4	311.0	30.3	0.8	24.7	90.5	23.8	61.3
CT215	3.7	142.0	58.9	57.8	0.3	4377.8	126.3	348.6	30.7	0.8	24.7	102.6	12.5	45.0
CT216	4.2	142.8	57.0	65.6	0.3	3802.6	113.0	343.1	31.2	0.9	27.1	84.5	12.0	42.5
CT219	3.6	140.4	60.3	62.8	0.2	3533.2	116.6	408.0	26.2	0.7	25.9	111.8	7.5	30.0
CT220	3.8	143.0	59.1	62.8	0.3	3674.2	118.5	354.3	29.6	0.8	26.8	95.4	18.8	60.0
CT221	3.9	142.9	59.6	67.2	0.3	4187.2	121.1	463.9	27.5	0.6	22.1	117.6	28.3	64.5
CT222	3.7	140.8	58.1	53.1	0.3	3862.4	107.7	377.9	30.9	0.7	23.6	96.9	12.0	38.8
CT223	3.7	142.6	57.9	63.9	0.2	3657.2	108.5	366.4	29.2	0.7	24.2	95.4	42.5	66.3
CT224	2.5	142.1	57.8	62.2	0.2	2984.9	106.0	281.3	22.8	0.6	27.2	90.5	14.5	33.8
CT225	3.4	143.6	58.9	67.7	0.2	3487.1	117.7	369.4	27.0	0.7	25.6	101.6	36.3	75.0
CT226	3.9	143.6	58.1	60.1	0.3	3909.6	121.5	404.0	25.6	0.6	24.6	108.4	31.3	72.5
CT227	3.6	141.5	57.6	60.5	0.3	3978.1	107.7	377.3	31.5	0.7	22.6	87.8	2.5	22.5
CT228	3.8	143.8	58.7	65.0	0.3	2927.3	96.3	408.3	24.8	0.7	26.0	92.9	36.3	78.8
CT229	3.6	142.3	58.2	60.6	0.3	3500.0	112.8	372.1	28.4	0.7	25.5	95.8	45.0	77.5
CT230	3.8	141.5	58.2	59.3	0.3	4061.0	106.8	344.3	34.6	0.8	21.5	88.6	23.0	57.5
CT231	3.4	144.6	57.0	69.2	0.2	3343.7	127.8	368.4	26.9	0.7	24.9	98.9	38.8	72.5
CT232	3.0	145.4	56.8	62.8	0.2	2973.6	105.0	355.2	28.3	0.7	24.1	94.3	43.8	71.3
CT233	3.6	141.4	58.0	62.4	0.2	3613.0	119.1	408.8	26.5	0.7	25.5	97.6	26.8	62.5
CT234	3.7	141.4	58.8	62.6	0.2	3526.9	119.5	422.3	24.6	0.7	26.6	104.9	27.5	66.3
CT235	3.5	140.6	57.5	64.6	0.3	3887.1	107.9	395.8	27.4	0.7	24.6	96.8	3.8	23.8
CT236	4.1	141.5	56.5	64.0	0.3	3210.5	98.5	419.8	26.3	0.7	25.6	86.8	5.5	38.8
CT237	3.3	142.0	59.1	55.6	0.3	4076.6	109.9	425.6	26.9	0.6	22.2	117.5	17.0	66.3
CT238	3.7	142.6	58.5	61.8	0.3	3370.8	113.5	402.2	26.2	0.7	25.6	95.5	25.5	67.5
CT239	3.6	142.8	55.9	62.4	0.3	3498.3	111.5	367.8	30.7	0.7	24.1	95.8	31.3	65.0
CT240	3.3	141.9	56.1	62.9	0.3	3589.6	106.0	382.9	28.1	0.7	23.7	94.3	26.3	46.3
CT241	3.4	144.3	57.1	64.3	0.2	3657.8	125.2	401.9	26.0	0.7	25.4	105.3	30.0	71.3
CT242	3.5	142.1	59.3	67.5	0.3	3272.7	100.9	356.0	26.2	0.7	25.6	92.6	6.3	33.8
CT243	3.7	141.3	59.1	62.9	0.3	3834.5	109.3	373.1	28.7	0.8	26.0	95.8	13.8	43.8

Table A3 Continued

Genotype	GY	DTH	TW	PH	HI	GM	BW	SPM	KPS	MSHW	TKW	TS	GLA	GFL
	tha^{-1}	d	lb/bu	cm	#	#	g	#	#	g	g	#	%	%
CT244	3.8	141.3	60.6	63.0	0.3	3774.1	112.5	357.8	29.7	0.8	27.1	91.5	8.8	36.3
CT245	3.8	142.6	58.5	64.5	0.3	3378.7	106.6	348.1	29.0	0.8	26.5	83.9	11.8	53.8
CT246	3.6	141.8	56.1	63.6	0.3	4047.0	115.2	434.0	27.8	0.7	23.9	96.4	38.8	76.3
CT247	3.6	141.9	59.2	61.5	0.3	3851.5	114.8	416.7	29.4	0.7	23.9	102.9	21.8	53.8
CT248	3.1	141.5	60.1	57.8	0.3	4261.2	121.7	359.4	30.0	0.7	24.0	109.1	17.5	51.3
BYRD	4.3	137.5	58.8	65.3	0.2	3998.5	130.3	437.5	28.9	0.7	23.8	105.0	3.8	22.5
CO960293	3.7	141.4	59.4	58.9	0.3	3629.6	123.1	473.7	22.2	0.6	26.5	121.9	22.5	65.0
Karl92	3.4	139.5	58.6	65.5	0.3	3493.5	115.8	368.0	23.7	0.6	26.2	101.4	1.5	16.3
SNOWMASS	3.9	142.0	57.9	68.6	0.2	3578.6	124.8	378.9	29.0	0.7	26.3	90.5	20.0	28.8
TAM111	3.6	141.1	60.0	65.2	0.3	4038.6	126.3	334.4	33.6	0.9	26.8	91.1	3.8	27.5
TAM112	3.7	139.1	59.3	62.7	0.3	3397.6	110.7	395.3	27.8	0.8	27.0	96.3	0.3	21.3

Table A4
Average disease severity scores for RIL evaluated for resistance to wheat streak mosaic virus

Genotype	21 DPI	28 DPI	Genotype	21 DPI	28 DPI	Genotype	21 DPI	28 DPI
CT2	2.8	3.1	CT52	3.0	3.2	CT99	1.0	1.0
CT3	3.0	3.3	CT53	1.0	1.0	CT100	1.0	1.0
CT4	3.0	3.3	CT54	3.0	3.8	CT101	2.9	3.2
CT5	2.9	2.9	CT55	3.0	3.3	CT102	2.9	3.0
CT7	2.9	3.1	CT56	1.0	1.0	CT103	2.3	2.9
CT8	2.8	3.4	CT57	1.0	1.1	CT104	1.0	1.1
CT9	1.0	1.0	CT58	1.0	1.0	CT105	2.9	3.4
CT10	1.0	1.0	CT59	3.0	3.4	CT106	2.8	3.3
CT11	1.0	1.0	CT60	2.6	3.0	CT107	1.0	1.0
CT12	1.0	1.1	CT61	1.0	1.0	CT108	1.0	1.1
CT13	3.0	3.2	CT62	1.0	1.1	CT109	3.0	3.3
CT15	3.4	3.4	CT63	2.4	2.3	CT110	3.0	3.4
CT16	3.0	3.0	CT64	3.2	3.7	CT111	1.0	1.0
CT17	1.0	1.0	CT65	1.0	1.1	CT112	1.0	1.2
CT18	1.0	1.0	CT66	1.0	1.1	CT113	1.0	1.0
CT19	2.6	3.0	CT67	2.8	3.3	CT114	1.0	1.0
CT20	2.7	3.3	CT68	1.0	1.0	CT115	2.9	3.6
CT21	1.0	1.0	CT69	1.0	1.0	CT116	2.9	3.0
CT22	1.0	1.0	CT70	1.0	1.0	CT117	1.1	1.2
CT23	1.0	1.1	CT71	2.1	2.3	CT118	1.0	1.1
CT26	2.8	3.3	CT73	3.1	3.7	CT119	1.0	1.0
CT27	2.5	2.7	CT75	3.2	3.5	CT120	3.0	3.9
CT28	2.9	3.0	CT76	1.0	1.0	CT121	1.0	1.0
CT29	2.6	2.9	CT77	3.1	3.6	CT122	1.0	1.1
CT30	3.0	3.1	CT78	1.0	1.0	CT124	1.0	1.0
CT31	1.0	1.0	CT79	3.1	3.7	CT125	1.0	1.0
CT32	3.5	3.9	CT80	1.0	1.0	CT126	1.0	1.0
CT33	3.0	3.8	CT81	1.0	1.0	CT127	1.0	1.0
CT34	1.0	1.0	CT82	2.0	3.3	CT128	1.0	1.0
CT35	3.2	3.4	CT83	2.3	3.1	CT129	1.0	1.0
CT36	1.0	1.1	CT84	2.9	3.6	CT130	1.0	1.1
CT37	1.0	1.1	CT85	2.9	3.3	CT131	3.0	3.6
CT38	1.0	1.0	CT86	1.0	1.0	CT132	1.0	1.0
CT39	3.1	3.2	CT87	3.0	3.7	CT133	1.0	1.1
CT40	1.0	1.1	CT88	1.0	1.0	CT134	3.0	3.4
CT42	2.9	3.2	CT89	2.9	3.3	CT135	1.0	1.0
CT43	2.1	2.3	CT90	2.4	2.8	CT136	2.8	3.6
CT44	3.3	3.6	CT91	1.0	1.0	CT137	1.0	1.0
CT45	1.0	1.0	CT92	1.0	1.0	CT138	1.7	2.0
CT46	1.0	1.0	CT93	1.0	1.0	CT139	3.0	3.4
CT47	1.0	1.2	CT94	3.0	3.3	CT140	2.9	3.6
CT48	2.3	2.5	CT95	1.0	1.0	CT141	1.0	1.0
CT49	3.0	3.2	CT96	3.0	3.4	CT142	1.0	1.0
CT50	2.5	2.9	CT97	3.0	3.0	CT143	1.0	1.1
CT51	3.0	3.0	CT98	3.0	3.3	CT145	2.9	3.5

Table A4 Continued

Genotype	21 DPI	28 DPI	Genotype	21 DPI	28 DPI
CT146	2.9	3.3	CT213	1.0	1.0
CT147	1.0	1.0	CT214	1.0	1.0
CT148	2.9	3.4	CT215	1.0	1.0
CT149	1.0	1.0	CT216	3.0	3.6
CT150	1.0	1.0	CT219	3.0	3.1
CT151	3.0	3.6	CT220	1.0	1.0
CT152	1.5	1.5	CT221	2.8	3.3
CT153	1.0	1.0	CT222	1.0	1.0
CT154	3.0	3.5	CT223	3.0	3.4
CT155	2.5	2.9	CT224	1.4	1.6
CT157	1.6	1.9	CT225	1.0	1.0
CT158	2.9	3.2	CT226	3.0	3.3
CT159	1.0	1.2	CT227	1.0	1.0
CT161	2.8	3.2	CT228	1.0	1.0
CT162	1.0	1.0	CT229	1.0	1.0
CT163	2.9	3.4	CT230	2.6	2.9
CT164	2.9	3.3	CT231	1.0	1.1
CT173	1.0	1.0	CT232	1.1	1.2
CT174	1.0	1.0	CT233	1.0	1.0
CT181	1.0	1.0	CT234	1.0	1.0
CT183	2.1	2.4	CT235	1.0	1.0
CT184	3.0	3.6	CT236	2.8	3.2
CT185	3.0	3.3	CT237	3.0	3.2
CT189	2.9	3.5	CT238	1.0	1.0
CT190	1.0	1.0	CT239	3.0	3.3
CT191	1.5	3.3	CT240	2.8	3.5
CT192	1.0	1.0	CT241	1.0	1.0
CT193	3.0	3.5	CT242	1.0	1.0
CT194	1.0	1.0	CT243	2.7	3.2
CT196	2.2	2.5	CT244	1.4	1.8
CT197	1.0	1.0	CT245	1.0	1.0
CT198	3.0	3.5	CT246	2.9	3.3
CT199	1.0	1.0	CT247	3.0	3.3
CT200	2.9	3.4	CT248	1.0	1.0
CT201	1.6	1.8	CO960293	1.0	1.2
CT202	1.2	1.3	TAM111	2.8	3.2
CT203	3.0	3.6	Karl92	3.1	3.6
CT204	1.0	1.1	RonL	1.0	1.0
CT205	1.3	1.3	Snowmass	1.7	1.8
CT207	3.0	3.4	T81	3.2	3.5
CT208	1.0	1.0	TAM112	2.5	2.8
CT209	1.0	1.1			
CT210	3.0	3.3			
CT211	2.9	3.2			
CT212	2.7	2.9			

Table A5
Best linear unbiased predictors for mixograph parameters

Gen	MLT	MLV	MLS	MLW	MLI	MPT	MPV	MPW	MPI	MRT	MRV	MRS	MRW	MRI	MTXW	MTXI	MMST
	min	%	%min^{-1}	%	%TQxmin	min	%	%	% TQxmin	min	%	%min^{-1}	%	% TQxmin	%	% TQxmin	%
CT2	6.6	48.6	2.4	28.1	245.0	7.6	51.9	34.7	295.2	5.7	51.9	-2.8	16.0	244.5	31.0	317.5	41.2
CT3	5.0	52.2	5.0	31.8	173.5	6.0	54.2	26.4	227.1	6.9	53.1	-2.2	15.9	300.9	15.1	339.7	34.7
CT4	3.5	52.7	7.4	34.8	126.9	4.5	56.9	26.6	182.3	5.7	51.3	-2.5	16.5	258.2	13.3	362.0	42.8
CT5	4.7	45.6	5.6	28.8	155.6	5.7	50.7	30.0	204.2	6.6	53.4	-1.9	22.8	290.0	16.9	327.1	40.4
CT7	3.5	52.5	8.0	28.9	115.5	4.5	55.3	19.4	169.9	6.1	49.4	-3.0	13.6	259.4	10.5	346.1	31.2
CT8	3.3	48.5	5.6	30.3	109.8	4.3	51.9	18.8	160.3	5.9	48.3	-2.0	13.4	243.5	9.7	337.5	31.2
CT9	1.9	48.9	14.2	34.1	57.2	2.9	56.2	23.1	111.0	4.5	50.3	-5.1	11.7	199.2	8.4	354.0	29.5
CT10	4.1	51.8	6.8	35.1	145.6	5.1	54.7	25.7	199.3	5.9	52.3	-2.5	18.6	270.9	15.3	349.7	30.3
CT11	1.6	45.5	21.4	30.5	46.0	2.6	57.9	22.9	99.7	4.3	48.1	-5.7	7.7	189.6	5.5	350.8	41.0
CT12	1.5	45.9	23.6	29.9	41.9	2.5	58.0	20.3	95.9	4.2	49.1	-4.6	8.6	185.4	5.9	354.0	58.9
CT13	1.6	46.1	21.3	29.7	46.0	2.6	56.8	21.4	99.3	4.3	48.8	-3.4	8.9	187.6	6.5	353.2	52.9
CT15	3.3	48.3	7.5	30.9	107.2	4.3	53.3	22.8	158.5	5.3	47.5	-3.8	11.5	223.8	10.5	334.0	27.5
CT16	6.0	45.2	4.4	36.1	200.2	7.0	48.0	30.6	247.2	7.7	52.6	-1.5	23.1	339.5	24.4	301.6	30.8
CT17	1.9	50.1	15.8	35.4	57.7	2.9	58.9	19.7	113.5	4.6	49.4	-3.8	9.1	203.6	6.8	356.6	35.7
CT18	5.6	45.8	4.1	27.3	179.8	6.6	47.5	20.6	226.7	7.9	49.9	-1.1	18.3	326.2	16.8	298.4	24.2
CT19	6.1	42.7	3.9	25.8	186.7	7.1	45.3	24.4	231.1	8.2	55.9	0.6	27.5	363.2	18.1	277.8	28.6
CT20	4.9	44.7	3.6	21.7	147.4	5.9	47.6	19.8	193.7	6.8	47.7	-2.1	14.3	272.5	13.5	295.9	28.2
CT21	6.6	39.6	1.2	26.2	194.6	7.6	41.3	20.9	235.0	5.7	51.9	-2.8	16.0	244.5	20.3	250.4	24.2
CT22	5.2	41.2	4.4	23.7	155.5	6.2	44.5	22.6	198.4	7.1	47.0	1.6	18.2	277.1	13.3	285.1	15.3
CT23	5.2	44.0	3.3	24.7	158.1	6.2	45.8	21.1	203.1	7.2	45.2	-0.9	15.2	277.9	16.2	287.2	24.3
CT26	5.5	45.8	5.5	28.0	165.2	6.5	48.2	28.7	212.5	7.6	51.2	-1.2	19.5	312.9	18.9	295.5	30.2
CT27	2.4	48.4	10.9	32.9	72.9	3.4	55.6	26.9	125.8	5.0	49.0	-4.6	10.7	213.0	7.5	343.6	37.5
CT28	5.4	39.5	3.3	22.2	148.0	6.4	41.2	17.2	188.6	7.5	45.9	-0.6	16.3	288.3	13.2	268.1	28.0
CT29	6.1	38.1	4.2	22.2	169.1	7.1	41.4	21.3	209.0	7.5	46.8	-2.7	17.7	264.1	15.2	254.6	24.7
CT30	5.7	56.6	6.4	42.7	209.0	6.7	61.2	33.0	268.2	8.0	55.9	-1.3	18.4	356.2	23.4	346.3	35.2
CT31	2.2	50.8	14.0	31.4	67.5	3.2	57.9	20.5	122.9	4.9	49.5	-3.3	9.2	214.4	6.4	353.7	48.8
CT32	4.6	50.1	5.3	43.0	151.3	5.6	53.6	29.2	203.5	6.5	51.6	-1.9	18.9	271.4	16.4	326.3	46.8
CT33	4.1	54.7	4.1	33.1	150.5	5.1	56.9	22.0	206.5	6.3	53.3	-2.0	19.5	290.8	13.7	359.8	35.4
CT34	5.4	44.8	4.7	27.4	159.5	6.4	47.7	22.3	206.0	7.6	47.4	-0.9	17.3	289.2	16.5	281.6	26.3
CT35	2.4	54.9	18.5	34.8	70.9	3.4	61.8	24.6	130.7	5.1	54.7	-3.8	12.8	230.1	6.2	378.1	53.2
CT36	3.6	52.9	6.4	33.8	112.0	4.6	57.2	25.1	167.4	6.3	52.9	-2.4	16.8	261.3	14.4	349.5	40.0
CT37	4.5	50.8	4.6	29.5	141.7	5.5	52.7	21.4	193.6	6.5	49.5	-1.6	16.4	266.3	13.4	317.3	35.0
CT38	3.7	46.6	8.1	24.8	104.1	4.7	52.1	19.9	154.0	5.6	45.4	-2.9	10.2	209.1	8.9	306.7	32.4
CT39	2.8	46.4	11.5	30.5	75.4	3.8	53.2	19.9	126.2	5.5	48.8	-2.7	12.9	211.8	7.2	324.4	36.5
CT40	3.2	47.4	10.4	25.0	87.9	4.2	52.7	18.6	138.7	5.9	48.2	-3.0	13.1	223.8	8.0	320.6	36.2
CT42	6.2	40.0	4.4	22.5	169.0	7.2	41.7	16.6	210.1	8.4	46.7	-1.5	13.2	312.1	12.8	249.5	22.8
CT43	2.2	48.7	12.9	27.5	65.4	3.2	56.1	19.8	119.0	4.9	47.3	-3.8	7.5	206.2	5.5	339.0	41.6

Table A5 Continued

Gen	MLT	MLV	MLS	MLW	MLI	MPT	MPV	MPW	MPI	MRT	MRV	MRS	MRW	MRI	MTXW	MTXI	MMST
	min	%	%min^{-1}	%	% TQxmin	min	%	%	% TQxmin	min	%	%min^{-1}	%	% TQxmin	%	% TQxmin	%
CT44	3.7	50.4	6.7	31.2	121.3	4.7	53.8	22.5	174.0	5.5	50.2	-2.0	16.5	218.9	12.1	336.8	42.5
CT45	6.4	39.9	1.3	22.7	176.5	7.4	41.4	18.9	217.2	5.7	51.9	-2.8	16.0	244.5	15.6	244.1	20.0
CT46	2.7	44.3	10.1	28.1	70.5	3.7	50.3	20.6	118.7	5.4	46.5	-3.1	13.7	200.5	9.7	313.2	34.6
CT47	6.1	42.9	4.5	24.2	178.2	7.1	45.1	18.9	222.5	5.7	51.9	-2.8	16.0	244.5	13.5	267.7	26.5
CT48	2.1	48.6	19.1	30.0	55.8	3.1	59.4	22.1	111.5	4.7	51.7	-4.3	10.3	205.8	6.8	360.6	52.9
CT49	5.1	47.3	9.6	33.8	152.8	6.1	52.4	26.8	203.5	7.0	52.3	-1.5	18.0	283.6	17.8	307.6	28.8
CT50	4.8	47.6	10.2	29.8	144.3	5.8	53.6	28.4	195.5	6.6	54.5	-2.7	16.4	279.2	16.2	317.4	32.6
CT51	4.3	49.6	6.1	24.0	130.3	5.3	51.8	17.9	181.4	6.3	49.0	-3.6	11.1	256.4	9.1	314.1	27.1
CT52	3.1	46.9	10.6	21.2	88.6	4.1	51.7	16.4	138.8	5.8	45.1	-4.1	7.6	219.0	6.3	311.0	34.6
CT53	3.4	43.5	8.4	24.8	93.9	4.4	50.2	22.7	141.4	6.0	47.2	-1.4	14.7	221.2	10.4	314.3	30.4
CT54	4.1	46.2	8.5	25.9	122.2	5.1	51.6	18.3	171.7	6.0	47.9	-3.8	9.8	236.1	9.6	309.6	27.7
CT55	4.2	46.5	8.1	24.0	124.1	5.2	51.5	18.6	173.7	6.1	46.7	-2.2	14.9	231.4	8.5	306.9	27.9
CT56	4.2	55.1	8.9	33.3	135.9	5.2	61.9	31.5	195.1	6.4	57.7	-1.8	25.7	273.7	12.8	355.3	40.8
CT57	4.4	47.6	9.4	29.3	130.2	5.4	52.4	27.5	180.9	6.0	52.7	-2.7	17.3	249.3	15.6	315.3	36.7
CT58	5.9	49.0	3.0	28.2	189.3	6.9	50.6	25.1	239.1	7.6	53.7	-2.2	21.1	320.8	20.4	297.4	25.7
CT59	6.7	45.0	4.3	28.7	211.6	7.7	48.5	28.6	258.5	5.7	51.9	-2.8	16.0	244.5	28.1	274.9	25.9
CT60	5.9	37.9	5.7	24.9	156.7	6.9	41.8	24.2	197.0	8.2	50.5	0.7	22.9	322.0	17.7	246.4	22.5
CT61	4.1	46.8	5.0	23.1	124.6	5.1	49.8	17.9	173.4	6.0	47.1	-1.5	14.3	235.2	9.1	307.0	27.6
CT62	4.5	49.6	4.8	30.7	147.5	5.5	52.1	22.6	198.7	6.3	50.7	-2.3	16.3	264.4	15.4	323.5	34.5
CT63	2.0	45.8	13.4	28.8	54.7	3.0	53.0	20.4	105.2	4.7	47.0	-3.6	11.8	187.7	7.7	331.7	43.7
CT64	4.3	46.3	5.0	32.7	124.6	5.3	50.4	22.7	173.4	6.1	48.6	-2.3	16.8	236.0	12.5	304.6	38.3
CT65	5.1	47.2	5.1	25.6	153.0	6.1	49.9	17.9	201.9	7.2	48.1	-0.8	15.0	275.3	12.4	297.4	26.0
CT66	6.7	33.3	2.9	19.8	169.1	7.7	36.0	18.4	204.1	5.7	51.9	-2.8	16.0	244.5	17.8	213.0	12.6
CT67	2.5	46.9	10.6	26.6	69.9	3.5	52.6	18.4	120.5	5.2	47.3	-3.2	12.2	203.8	6.9	328.0	43.5
CT68	4.0	46.0	7.8	25.7	117.5	5.0	50.1	20.0	166.2	5.8	47.1	-2.2	15.2	227.8	10.7	305.0	33.2
CT69	3.2	50.2	11.5	34.6	95.6	4.2	57.6	20.2	150.8	6.2	48.9	-3.2	9.2	250.2	7.5	340.2	29.0
CT70	3.2	56.7	13.9	35.0	97.1	4.2	64.5	20.1	159.0	6.1	50.9	-4.5	8.6	266.5	6.8	364.9	33.7
CT71	4.6	48.8	7.8	31.5	140.2	5.6	55.0	25.7	192.7	6.3	60.7	-3.2	19.5	287.5	16.0	329.7	22.5
CT73	5.7	47.0	2.5	24.7	168.7	6.7	48.4	19.1	216.6	7.6	48.5	-1.7	12.6	292.2	14.2	285.1	30.7
CT75	1.6	44.7	27.6	28.5	40.5	2.6	61.6	20.6	95.9	4.3	45.9	-5.5	7.0	185.6	5.6	340.1	51.5
CT76	3.0	55.6	14.6	41.0	97.1	4.0	62.4	25.4	157.3	5.6	54.7	-4.6	13.0	255.9	10.0	375.5	44.4
CT77	4.3	57.4	6.2	36.9	168.7	5.3	61.2	28.3	228.4	6.0	56.5	-2.2	20.8	279.2	13.0	380.4	35.2
CT78	2.4	49.3	4.7	35.5	83.2	3.4	54.3	22.5	135.5	4.9	51.0	-3.1	13.2	207.5	6.6	356.7	25.6
CT79	2.7	51.5	7.6	31.2	96.4	3.7	55.0	25.2	150.3	5.1	52.3	-2.9	17.3	221.1	8.8	362.9	37.2
CT80	6.1	42.3	2.4	22.5	192.9	7.1	43.5	17.0	235.9	7.8	51.4	-2.3	15.9	324.8	14.9	282.4	18.5
CT81	5.4	43.8	4.3	27.5	169.3	6.4	46.4	23.9	214.7	7.0	50.7	0.8	22.2	279.3	17.9	297.4	24.1
CT82	4.0	47.7	6.8	31.6	130.5	5.0	51.6	28.5	180.6	4.9	54.3	-1.7	19.3	221.0	15.4	335.2	25.0

Table A5 Continued

Gen	MLT	MLV	MLS	MLW	MLI	MPT	MPV	MPW	MPI	MRT	MRV	MRS	MRW	MRI	MTXW	MTXI	MMST
	min	%	%min^{-1}	%	% TQxmin	min	%	%	% TQxmin	min	%	%min^{-1}	%	% TQxmin	%	% TQxmin	%
CT83	3.7	51.0	6.1	33.2	128.5	4.7	53.3	21.6	181.1	5.2	51.5	-2.8	17.6	222.0	9.9	346.6	40.0
CT84	3.8	50.1	5.8	42.8	131.0	4.8	54.5	32.2	183.6	5.4	56.5	-0.7	26.6	233.2	15.7	357.0	41.0
CT85	4.2	51.1	5.4	41.6	142.6	5.2	54.8	28.3	195.9	5.1	56.5	-1.9	21.1	231.2	17.3	349.4	43.0
CT86	2.7	55.2	10.5	31.5	94.8	3.7	59.0	26.8	152.6	5.0	54.8	-4.2	15.1	226.9	8.1	379.3	38.7
CT87	4.8	52.1	9.3	34.0	152.4	5.8	56.1	25.7	207.3	6.1	54.5	0.0	21.2	251.8	17.1	323.3	32.4
CT88	4.0	50.8	4.4	33.4	134.6	5.0	53.8	20.3	187.3	5.1	52.1	-2.9	21.8	227.1	10.1	338.7	38.7
CT89	4.4	52.5	6.0	34.5	148.5	5.4	55.0	25.2	202.7	5.6	55.7	-4.1	16.1	247.8	13.4	339.3	43.6
CT90	1.9	47.2	15.7	32.0	58.1	2.9	55.4	21.7	110.7	4.2	49.3	-5.9	10.1	179.5	6.7	350.1	46.5
CT91	3.2	46.3	7.0	24.0	99.8	4.2	50.1	20.3	148.5	4.0	49.6	-4.4	11.2	172.3	7.2	323.5	36.6
CT92	4.6	43.9	5.9	25.2	140.0	5.6	47.6	22.3	186.1	5.8	48.4	-1.8	16.1	231.3	12.3	299.1	27.9
CT93	2.6	50.9	8.1	29.1	85.0	3.6	54.9	21.6	138.3	5.3	49.3	-3.0	13.4	224.3	8.4	351.3	37.0
CT94	1.9	51.9	15.0	38.5	64.7	2.9	57.7	23.6	120.7	4.5	51.5	-4.9	11.2	211.0	8.3	374.1	34.2
CT95	3.9	47.5	6.5	25.3	120.4	4.9	51.4	22.0	170.3	5.3	49.5	-2.9	13.6	223.6	9.9	317.8	35.8
CT96	2.6	51.6	15.2	32.3	80.9	3.6	58.0	24.7	136.9	5.3	53.1	-3.9	11.7	228.7	8.5	362.6	46.8
CT97	2.9	54.4	9.5	33.7	103.3	3.9	58.7	26.9	160.6	5.6	54.7	-3.8	18.0	253.2	11.4	376.3	44.8
CT98	5.4	49.6	2.8	30.4	186.4	6.4	53.6	24.2	238.1	7.5	53.0	-2.3	18.3	318.5	17.7	324.4	26.2
CT99	3.2	48.3	8.0	33.0	101.0	4.2	52.7	22.9	152.1	5.0	49.2	-2.4	16.6	213.6	11.3	332.8	31.8
CT100	3.5	47.7	7.2	24.8	108.4	4.5	51.7	18.3	158.6	5.2	48.1	-4.4	8.9	212.7	6.7	321.1	39.0
CT101	2.1	48.1	14.1	30.2	66.6	3.1	54.8	23.3	119.3	4.5	51.0	-4.7	10.3	188.7	5.9	351.4	54.0
CT102	4.2	48.3	4.8	26.3	136.8	5.2	51.2	20.4	187.0	5.2	51.7	-3.4	16.1	212.7	9.2	325.0	36.3
CT103	3.6	49.1	6.7	31.3	124.6	4.6	53.6	27.5	176.6	4.4	55.8	-0.7	24.7	195.9	14.7	353.6	32.6
CT104	6.0	41.8	4.0	27.3	187.8	7.0	44.3	27.5	230.9	8.4	56.3	-0.5	22.4	369.2	21.8	271.8	30.6
CT105	2.8	55.8	10.6	37.8	98.9	3.8	61.2	25.4	158.0	5.1	56.0	-4.5	14.0	235.9	7.7	382.9	49.1
CT106	2.7	51.2	10.4	28.9	86.3	3.7	56.1	21.2	140.8	5.0	51.2	-3.7	12.7	210.4	6.3	353.3	36.0
CT107	3.4	52.3	4.8	34.5	124.5	4.4	54.4	24.1	178.2	4.9	54.2	-2.2	19.2	221.8	11.9	358.9	35.0
CT108	1.5	43.2	19.2	24.8	41.3	2.5	54.0	20.2	91.6	3.9	47.9	-5.6	8.8	158.6	5.1	337.4	50.5
CT109	5.3	49.4	5.1	31.9	182.2	6.3	52.3	27.7	233.4	6.9	54.6	-0.1	26.1	289.4	19.0	326.8	37.5
CT110	4.3	53.5	5.3	33.3	150.3	5.3	56.2	23.6	205.6	5.9	55.6	-2.3	15.5	260.7	9.1	347.7	41.4
CT111	4.3	44.4	4.1	29.4	129.1	5.3	47.4	26.5	175.4	5.5	54.9	-1.0	20.8	238.8	14.2	316.4	30.3
CT112	4.1	49.9	3.7	26.2	142.3	5.1	51.9	19.5	193.4	5.4	50.8	-2.3	17.7	234.5	10.3	337.0	45.6
CT113	5.2	48.2	3.2	35.7	176.6	6.2	50.0	26.0	225.7	7.1	53.3	-0.3	21.3	296.1	16.8	318.0	25.3
CT114	4.8	49.1	6.4	34.5	166.2	5.8	54.1	33.3	218.2	6.1	54.1	-1.1	27.9	261.7	23.9	334.7	33.3
CT115	4.1	54.7	6.1	34.5	147.3	5.1	56.9	25.0	203.4	5.4	54.7	-3.2	25.3	247.6	11.8	353.4	40.0
CT116	5.7	41.7	3.2	22.1	175.0	6.7	44.2	19.9	218.1	7.4	48.7	-0.1	18.4	288.0	15.7	285.7	25.6
CT117	4.7	46.7	3.4	30.2	151.0	5.7	49.5	22.8	199.4	5.9	52.7	-0.7	22.0	251.7	15.0	320.8	33.8
CT118	2.9	51.1	7.1	29.3	95.6	3.9	54.1	20.3	148.7	5.2	51.4	-2.6	12.6	216.7	7.1	355.7	43.1
CT119	5.8	38.6	3.2	19.6	151.4	6.8	40.6	15.9	191.1	6.0	55.0	-4.4	19.8	285.6	10.0	254.7	21.8

Table A5 Continued

Gen	MLT	MLV	MLS	MLW	MLI	MPT	MPV	MPW	MPI	MRT	MRV	MRS	MRW	MRI	MTXW	MTXI	MMST
	min	%	%min^{-1}	%	% TQxmin	min	%	%	% TQxmin	min	%	%min^{-1}	%	% TQxmin	%	% TQxmin	%
CT120	3.8	50.6	5.3	31.0	124.3	4.8	53.5	21.1	176.7	5.6	52.0	-3.2	19.0	231.7	8.0	336.1	36.5
CT121	2.3	50.1	8.9	27.4	74.2	3.3	53.9	21.1	126.9	4.6	49.9	-4.1	12.1	194.9	5.4	350.8	48.6
CT122	2.8	58.2	7.6	38.4	120.9	3.8	61.9	31.7	181.4	5.2	59.5	-2.7	22.7	265.7	16.2	419.0	46.7
CT124	3.4	58.0	4.3	34.9	136.1	4.4	60.3	24.0	195.6	5.7	56.5	-4.3	16.5	275.9	7.5	394.6	55.2
CT125	2.7	53.5	11.3	38.3	97.3	3.7	60.8	27.6	155.6	5.4	55.8	-4.5	15.7	252.3	7.8	388.1	36.9
CT126	2.5	54.1	9.8	31.6	87.6	3.5	58.5	23.0	144.7	4.8	53.6	-4.0	13.3	221.2	7.4	375.9	42.0
CT127	3.9	55.6	1.6	29.5	162.1	4.9	56.8	22.3	218.3	6.2	54.9	-1.8	18.4	293.3	14.9	385.5	35.3
CT128	3.2	67.0	3.9	27.2	154.9	4.2	69.3	19.8	223.3	5.5	66.6	-5.2	16.5	324.2	17.9	466.4	26.5
CT129	2.9	54.9	9.0	31.5	99.6	3.9	59.4	26.3	157.5	5.3	57.0	-3.1	16.4	235.3	9.4	379.3	42.7
CT130	3.2	56.3	7.7	39.0	117.0	4.2	60.4	30.1	176.1	5.5	57.2	-3.6	17.3	256.2	9.9	385.7	43.7
CT131	2.3	52.9	11.9	36.8	76.8	3.3	58.0	28.2	133.3	4.6	55.5	-2.4	18.0	208.6	11.8	383.0	45.2
CT132	3.1	49.2	5.4	28.9	111.2	4.1	51.8	23.8	161.9	5.1	49.9	-2.3	15.5	212.7	9.7	347.7	38.4
CT133	1.2	43.0	19.2	32.0	34.8	2.2	54.2	21.6	85.2	3.2	49.4	-4.9	10.3	137.3	5.3	348.0	62.1
CT134	3.3	52.0	7.9	29.4	111.3	4.3	55.5	22.5	165.6	5.6	51.4	-2.5	16.9	238.7	10.9	355.5	38.5
CT135	3.5	46.0	3.6	23.2	109.9	4.5	52.5	20.8	160.0	5.8	49.0	-3.0	13.0	229.2	9.3	332.7	46.7
CT136	1.5	46.1	18.1	28.1	44.6	2.5	56.5	18.9	97.5	3.9	48.5	-4.6	12.0	167.2	6.2	347.7	53.4
CT137	4.5	54.2	4.4	33.9	165.1	5.5	56.8	25.5	220.8	6.8	52.1	-2.5	18.1	296.7	15.1	355.0	42.3
CT138	2.1	51.0	12.0	31.5	71.7	3.1	56.8	23.6	126.6	4.4	51.9	-3.3	12.8	200.9	8.2	371.4	36.1
CT139	2.3	46.6	9.0	25.2	70.0	3.3	51.4	19.7	119.7	4.6	46.9	-2.6	14.6	187.8	8.6	336.6	41.3
CT140	2.9	49.2	7.9	27.1	92.8	3.9	53.0	21.3	144.6	5.3	48.7	-1.8	13.4	214.9	10.9	339.9	37.9
CT141	5.4	56.6	5.4	35.5	199.8	6.4	59.7	26.7	258.4	7.3	54.5	-2.9	16.8	317.1	17.6	352.9	37.7
CT142	3.7	56.1	10.6	40.1	130.6	4.7	61.7	28.6	190.4	6.0	54.9	-3.7	21.0	270.3	11.5	372.0	48.4
CT143	2.8	53.2	4.9	33.8	99.1	3.8	56.3	26.6	154.4	5.1	52.0	-2.8	15.3	230.1	10.3	370.0	40.8
CT145	5.7	51.5	9.2	28.8	198.4	6.7	54.8	23.5	252.1	8.1	53.5	0.5	16.3	325.5	17.4	325.8	30.9
CT146	4.0	49.0	10.3	31.0	122.9	5.0	54.0	26.6	175.2	6.3	51.0	-2.8	16.4	246.1	11.4	329.2	39.1
CT147	4.1	50.0	7.6	28.3	142.3	5.1	53.9	20.0	194.8	6.0	50.3	-3.0	14.8	252.7	11.7	338.8	28.2
CT148	3.6	55.6	5.5	32.9	134.2	4.6	58.3	22.8	191.6	5.9	53.5	-3.2	14.4	269.2	11.2	378.1	34.1
CT149	2.9	48.7	9.5	38.4	97.3	3.9	55.4	27.0	150.5	5.2	53.5	-2.2	17.0	226.6	11.9	364.0	50.4
CT150	5.3	50.3	2.3	24.2	192.0	6.3	51.1	20.3	242.9	7.4	49.5	-0.5	13.8	309.2	16.3	329.6	27.9
CT151	3.2	56.1	9.1	30.0	113.0	4.2	60.3	23.2	171.9	5.5	54.4	-2.6	14.6	250.2	9.0	378.3	39.3
CT152	4.0	49.8	4.5	26.7	134.7	5.0	51.8	17.0	185.8	6.3	47.0	-3.2	10.9	252.6	9.2	327.5	31.1
CT153	3.5	49.5	2.8	23.4	120.2	4.5	51.2	17.0	170.6	5.8	47.3	-1.8	13.8	239.0	11.0	337.3	31.3
CT154	3.1	56.2	6.0	40.1	129.0	4.1	59.0	25.6	187.0	5.4	53.0	-2.6	15.6	266.2	13.0	395.8	43.7
CT155	6.7	48.1	6.4	30.3	231.5	7.7	51.2	28.5	281.6	5.7	51.9	-2.8	16.0	244.5	27.9	299.4	18.9
CT157	2.7	54.7	10.7	33.2	104.2	3.7	62.5	26.6	163.8	5.1	56.4	-3.0	17.0	247.4	10.4	401.0	52.6
CT158	2.5	55.0	9.6	36.3	84.3	3.5	59.1	23.7	142.2	4.8	52.9	-3.1	13.4	218.9	7.9	372.5	65.6
CT159	4.9	52.2	6.9	31.9	182.2	5.9	55.2	26.8	236.5	5.0	58.1	-2.1	23.2	232.0	17.7	355.2	35.9

Table A5 Continued

Gen	MLT	MLV	MLS	MLW	MLI	MPT	MPV	MPW	MPI	MRT	MRV	MRS	MRW	MRI	MTXW	MTXI	MMST
	min	%	%min^{-1}	%	% TQxmin	min	%	%	% TQxmin	min	%	%min^{-1}	%	% TQxmin	%	% TQxmin	%
CT161	3.6	58.9	5.0	33.0	143.4	4.6	61.2	23.7	203.7	6.1	53.9	-2.6	16.9	286.8	11.6	390.1	38.4
CT162	5.5	54.0	3.4	33.2	203.7	6.5	55.9	27.2	258.8	7.6	55.0	-2.0	24.2	317.1	19.8	342.1	29.7
CT163	2.9	50.3	17.9	35.4	102.3	3.9	60.1	25.7	159.1	5.3	51.4	-2.8	15.7	233.0	11.7	359.4	56.2
CT164	3.7	51.0	7.1	32.9	137.7	4.7	54.3	21.1	191.0	5.5	49.5	5.1	15.5	245.9	11.6	355.8	37.5
CT173	3.4	55.2	8.2	44.4	123.7	4.4	59.4	26.9	181.6	5.7	55.5	-2.0	20.1	259.4	14.0	380.1	40.9
CT174	4.2	52.7	6.4	36.7	155.0	5.2	56.1	28.1	210.0	6.6	52.0	-2.6	20.1	284.4	16.0	356.6	36.8
CT181	3.5	53.0	9.4	38.9	121.9	4.5	58.7	25.1	178.4	5.9	52.4	-3.9	12.8	255.3	8.8	360.3	48.3
CT183	3.4	55.4	6.9	40.6	134.6	4.4	59.7	29.3	192.6	5.8	54.5	-2.4	22.7	269.0	9.9	383.3	44.4
CT184	4.1	53.2	6.1	31.0	138.6	5.1	56.2	22.4	193.8	6.5	51.3	-2.9	15.3	267.6	10.4	344.9	37.1
CT185	2.7	57.4	9.4	42.4	107.6	3.7	61.0	30.2	167.6	5.0	56.3	-3.6	17.9	247.6	12.4	403.4	42.1
CT189	1.5	54.8	19.6	42.1	52.2	2.5	64.3	26.4	113.5	3.9	56.9	-5.0	14.4	196.0	9.3	406.9	47.1
CT190	2.7	51.2	8.0	38.5	98.0	3.7	56.6	22.0	152.6	5.0	50.7	-3.3	12.9	226.0	7.5	363.9	49.5
CT191	2.2	56.7	11.6	37.4	84.1	3.2	61.9	27.3	144.4	4.5	55.1	-3.8	16.3	224.7	9.2	400.2	58.5
CT192	6.3	52.6	4.3	32.8	241.3	7.3	54.9	29.2	295.3	8.5	53.9	0.3	20.4	366.2	26.6	331.9	35.1
CT193	6.0	48.6	2.5	25.6	214.6	7.0	50.4	21.4	264.2	7.6	47.1	-1.7	14.3	289.2	16.9	317.2	24.9
CT194	5.2	47.9	4.2	30.9	179.4	6.2	51.8	28.6	229.5	7.6	50.7	-0.5	19.6	299.7	19.2	322.7	30.2
CT196	3.2	52.8	7.0	27.5	120.3	4.2	56.0	21.7	175.2	5.6	51.1	-2.4	14.7	248.5	8.6	365.1	31.5
CT197	4.7	57.4	9.2	47.6	189.4	5.7	61.9	37.9	249.5	6.4	58.2	-2.5	23.6	315.0	25.5	386.1	35.2
CT198	4.4	53.1	6.9	30.4	158.3	5.4	56.0	24.1	213.4	6.7	52.4	-2.6	17.5	287.5	13.1	350.7	38.6
CT199	4.1	49.2	4.3	27.9	137.9	5.1	51.8	19.9	188.7	6.4	47.9	-2.2	14.6	255.7	12.7	328.2	31.8
CT200	3.5	50.6	8.0	26.7	121.0	4.5	55.0	20.1	174.4	5.8	49.4	-2.6	12.9	246.2	10.6	348.4	35.6
CT201	3.6	50.5	8.4	35.0	121.1	4.6	54.4	25.2	174.3	5.9	51.4	-2.5	16.9	246.2	12.3	347.4	36.3
CT202	4.3	40.0	6.4	21.6	116.4	5.3	44.6	22.2	159.1	5.9	45.3	-1.4	14.3	209.8	13.2	282.8	22.8
CT203	4.7	53.2	3.6	36.2	181.5	5.7	55.4	23.7	236.0	6.8	53.3	-0.9	18.2	314.5	16.4	359.9	36.1
CT204	5.0	52.6	5.5	32.6	182.0	6.0	56.0	26.6	236.7	7.1	54.3	-2.1	20.7	318.9	16.3	346.4	40.2
CT205	3.7	55.6	9.6	35.3	133.1	4.7	60.6	25.4	191.9	6.0	55.0	-2.9	15.8	270.6	9.5	374.5	37.4
CT207	1.9	53.9	11.0	34.6	66.9	2.9	59.9	24.0	124.7	4.2	53.5	-3.7	12.8	201.1	8.4	385.2	51.8
CT208	5.3	53.7	2.6	24.0	206.0	6.3	55.3	25.9	260.7	6.9	54.6	-3.0	16.2	314.6	18.5	352.5	37.6
CT209	3.7	54.6	5.7	38.6	136.4	4.7	57.3	21.3	193.0	6.0	51.4	-2.9	13.1	267.9	9.3	365.8	57.3
CT210	4.2	53.9	8.4	34.0	149.5	5.2	59.3	23.9	206.7	6.1	53.9	-3.5	14.4	276.0	11.6	358.0	43.8
CT211	1.8	52.3	21.2	38.4	56.3	2.8	62.7	25.3	115.8	4.1	54.5	-4.1	16.4	196.8	9.6	389.2	61.0
CT212	3.5	54.9	5.5	34.8	141.3	4.5	58.2	19.7	198.2	5.8	53.4	-2.6	17.3	276.8	12.9	384.3	48.4
CT213	3.1	54.1	8.3	32.1	107.9	4.1	59.7	21.6	165.3	5.4	52.5	-3.5	14.2	245.1	9.4	371.3	42.5
CT214	2.8	52.0	11.4	32.9	99.4	3.8	58.4	24.0	155.7	5.2	53.5	-2.8	15.8	233.9	10.0	376.0	31.2
CT215	5.7	51.0	5.0	37.8	212.8	6.7	54.3	29.2	265.8	8.1	50.4	-0.9	20.1	334.4	25.7	336.7	35.5
CT216	2.5	54.8	10.0	41.8	90.6	3.5	59.8	28.2	148.7	4.9	54.1	-3.2	17.8	225.5	9.0	383.1	44.3
CT219	4.3	56.5	8.1	34.9	166.6	5.3	59.9	27.0	225.3	6.6	55.4	-2.6	16.1	304.6	14.2	375.6	44.0

Table A5 Continued

Gen	MLT	MLV	MLS	MLW	MLI	MPT	MPV	MPW	MPI	MRT	MRV	MRS	MRW	MRI	MTXW	MTXI	MMST
	min	%	%min^{-1}	%	% TQxmin	min	%	%	% TQxmin	min	%	%min^{-1}	%	% TQxmin	%	% TQxmin	%
CT220	3.9	57.8	8.6	35.6	146.3	4.9	61.4	28.9	206.5	6.3	56.9	-2.6	19.5	287.8	13.0	381.6	45.0
CT221	1.6	43.9	21.8	25.3	46.0	2.6	56.2	19.7	97.8	4.0	47.3	-3.2	13.0	169.5	8.2	343.3	50.8
CT222	2.7	52.8	10.5	31.8	92.9	3.7	57.2	24.6	148.7	5.1	52.8	-2.7	16.4	224.5	12.6	370.5	44.2
CT223	2.1	52.4	12.9	34.7	73.9	3.1	58.9	24.8	130.6	4.5	52.2	-3.3	15.7	206.3	7.3	373.7	46.1
CT224	2.4	52.1	12.4	29.1	82.0	3.4	59.5	20.8	138.8	4.7	51.4	-5.0	9.7	214.2	6.5	367.2	51.9
CT225	1.6	48.8	18.8	32.8	48.3	2.6	58.5	18.6	103.7	4.0	49.8	-4.0	10.8	178.8	5.9	359.7	55.3
CT226	1.2	44.9	22.8	29.5	35.9	2.2	59.6	23.6	90.0	3.6	49.2	-4.2	9.4	163.1	4.4	358.2	65.9
CT227	3.2	49.5	7.0	32.7	115.2	4.2	53.8	27.1	167.4	5.2	52.3	-2.0	20.1	220.6	10.8	361.3	31.7
CT228	1.0	48.0	21.5	31.3	37.0	2.0	59.0	29.7	92.5	3.0	53.2	-7.1	10.1	149.1	4.5	376.0	65.0
CT229	1.4	50.2	21.7	40.8	45.5	2.4	59.9	25.5	102.4	3.4	53.5	-7.2	10.1	159.6	6.3	375.9	70.8
CT230	1.5	46.8	18.8	38.8	49.7	2.5	55.9	22.0	102.7	3.5	51.1	-4.8	11.4	156.5	6.4	360.2	55.6
CT231	1.3	49.3	16.7	32.7	47.6	2.3	57.8	28.8	102.6	3.3	53.4	-5.6	12.8	158.6	5.8	376.6	55.4
CT232	1.4	47.0	14.7	31.7	49.8	2.4	54.5	26.4	101.8	3.4	50.6	-4.5	10.3	154.6	6.0	362.8	56.9
CT233	4.0	48.6	6.8	31.2	140.2	5.0	51.6	27.4	190.9	6.0	48.6	-3.1	13.5	241.1	13.5	331.3	41.1
CT234	3.7	50.1	10.2	41.2	129.2	4.7	56.2	30.0	183.3	5.7	53.8	-3.0	18.6	238.5	14.5	356.7	42.2
CT235	1.9	54.4	15.6	50.1	73.3	2.9	62.1	30.7	132.8	3.9	58.1	-5.1	16.2	193.4	8.7	400.7	66.1
CT236	1.6	50.5	14.6	39.6	52.4	2.6	57.9	31.0	107.8	3.8	53.5	-2.6	19.6	171.3	8.3	377.5	60.0
CT237	2.1	53.0	11.9	42.0	77.2	3.1	58.8	25.8	134.1	4.1	54.8	-4.4	15.2	191.2	7.5	386.0	50.1
CT238	2.5	51.7	9.3	38.6	92.6	3.5	57.6	36.6	148.2	4.5	56.0	-2.1	22.8	205.1	10.8	388.0	41.9
CT239	2.6	54.3	9.0	40.6	100.0	3.6	57.9	30.3	157.0	4.6	56.2	-2.6	21.0	214.3	11.5	392.9	46.0
CT240	3.4	50.9	6.4	37.7	122.1	4.4	54.2	27.6	175.1	5.4	52.7	-1.8	18.0	228.7	11.3	357.1	46.8
CT241	1.7	50.9	14.2	32.5	58.7	2.7	56.4	25.0	113.3	3.7	52.9	-4.6	12.7	168.4	6.2	373.1	52.4
CT242	1.7	51.1	13.3	35.0	59.7	2.7	58.2	23.9	115.5	3.7	52.9	-6.5	9.4	171.6	6.3	372.8	55.8
CT243	4.7	54.2	2.3	37.8	185.0	5.7	56.2	30.0	240.3	6.7	54.5	-1.3	21.2	295.6	16.1	368.2	39.4
CT244	2.6	49.4	9.7	38.2	90.2	3.6	55.3	32.3	143.2	4.6	53.3	-2.5	17.5	197.7	7.4	362.6	45.1
CT245	2.3	48.4	13.5	38.7	83.1	3.3	56.9	27.3	137.0	4.3	53.4	-4.4	15.4	192.4	8.3	368.4	48.3
CT246	2.8	48.8	7.6	28.2	103.3	3.8	53.5	26.3	155.1	4.8	51.7	-3.6	14.7	208.0	7.5	357.1	43.9
CT247	3.8	48.8	7.1	34.6	133.5	4.8	52.7	26.7	184.8	5.8	51.0	-3.1	16.1	236.8	11.9	346.1	36.6
CT248	4.6	49.5	5.0	31.9	164.1	5.6	52.1	26.8	215.3	6.1	53.3	-2.0	21.5	258.7	13.7	339.4	30.4
CO96029	4.9	47.9	3.8	30.6	173.4	5.9	50.3	23.6	222.9	6.4	49.9	-2.1	18.2	256.3	12.2	325.6	34.0
KARL92	3.2	55.3	12.8	33.9	116.6	4.2	62.4	26.9	176.7	5.5	56.3	-3.5	16.3	259.0	9.0	388.2	42.4
TAM111	1.8	51.6	13.3	41.8	65.4	2.8	59.4	30.6	122.2	4.2	54.0	-3.3	16.2	199.0	9.6	385.9	47.6
TAM112	3.9	52.7	4.5	34.6	142.1	4.9	54.7	24.2	196.0	6.6	52.0	-2.2	16.9	285.4	15.2	356.4	31.4

Table A6
Best linear unbiased predictors for kernel characteristics, protein content and water absorption

Gen	HDI	KD	KW	FPC	WAB	Gen	HDI	KD	KW	FPC	WAB
	#	mm	mg	%	%		#	mm	mg	%	%
CT2	66.7	2.5	28.6	12.4	60.9	CT52	66.6	2.6	29.8	12.5	60.9
CT3	70.9	2.6	30.7	12.7	60.5	CT53	67.3	2.5	28.2	12.1	60.1
CT4	75.4	2.7	32.9	13.1	61.1	CT54	65.7	2.4	25.4	12.8	61.8
CT5	64.3	2.6	30.2	12.9	60.9	CT55	63.8	2.5	28.8	12.4	61.0
CT7	71.0	2.6	31.5	12.8	60.8	CT56	72.8	2.6	30.2	13.1	62.1
CT8	66.6	2.6	30.5	12.1	59.2	CT57	67.6	2.7	32.1	12.8	61.5
CT9	63.3	2.5	28.3	12.2	59.5	CT58	70.8	2.6	29.3	12.5	61.1
CT10	68.0	2.6	30.8	13.0	60.8	CT59	69.5	2.5	26.9	12.9	61.9
CT11	64.7	2.5	28.3	13.1	61.0	CT60	70.8	2.6	30.3	12.5	61.1
CT12	68.2	2.5	26.5	12.9	60.8	CT61	64.3	2.6	29.8	12.2	60.7
CT13	72.4	2.6	28.7	13.5	61.5	CT62	72.3	2.5	29.1	12.3	60.9
CT15	59.8	2.5	30.7	12.1	59.4	CT63	69.1	2.6	28.1	13.1	61.8
CT16	73.6	2.5	29.0	12.5	60.3	CT64	67.4	2.6	28.8	12.7	61.5
CT17	73.4	2.5	26.6	13.1	61.0	CT65	66.1	2.5	29.4	13.1	61.7
CT18	71.7	2.5	27.3	12.9	61.0	CT66	75.7	2.6	28.1	12.3	60.1
CT19	70.8	2.5	26.4	13.5	62.1	CT67	72.8	2.6	30.9	13.3	62.2
CT20	68.9	2.7	31.3	12.5	62.6	CT68	63.4	2.6	32.0	13.0	62.1
CT21	75.3	2.6	30.9	12.5	60.4	CT69	69.9	2.6	30.6	12.8	61.1
CT22	72.8	2.6	28.5	12.5	60.5	CT70	69.0	2.5	27.7	12.3	60.3
CT23	68.2	2.5	27.0	12.5	60.1	CT71	71.8	2.6	30.2	12.6	60.7
CT26	66.5	2.6	32.0	12.2	59.7	CT73	73.1	2.5	29.1	12.5	61.0
CT27	64.4	2.5	27.8	12.3	59.7	CT75	60.8	2.6	29.8	12.9	61.6
CT28	69.2	2.5	28.1	13.0	61.4	CT76	66.7	2.5	27.1	12.8	61.1
CT29	62.7	2.5	28.3	13.0	61.0	CT77	70.9	2.5	29.1	13.4	61.7
CT30	64.2	2.6	29.6	12.9	60.9	CT78	64.7	2.7	32.8	12.0	59.8
CT31	62.3	2.5	28.4	13.3	61.7	CT79	71.7	2.6	28.9	13.1	61.0
CT32	69.9	2.7	33.5	12.0	59.5	CT80	72.9	2.6	28.1	12.8	60.8
CT33	70.3	2.7	31.6	13.3	61.6	CT81	70.2	2.6	30.9	12.4	60.2
CT34	67.5	2.5	29.2	12.9	60.8	CT82	69.5	2.5	27.0	13.1	61.3
CT35	71.0	2.6	31.6	13.0	60.9	CT83	65.5	2.4	24.7	12.9	60.6
CT36	71.4	2.6	28.7	14.1	62.4	CT84	72.7	2.6	32.3	12.9	60.6
CT37	68.9	2.5	28.7	13.0	61.0	CT85	70.0	2.6	30.7	13.4	61.7
CT38	63.1	2.5	28.3	12.7	60.6	CT86	60.5	2.7	31.7	12.8	60.7
CT39	71.9	2.5	28.0	12.2	60.1	CT87	73.1	2.5	27.2	12.8	60.6
CT40	71.5	2.5	27.2	13.0	61.1	CT88	75.0	2.5	27.9	12.5	60.3
CT42	68.6	2.5	27.7	12.6	60.5	CT89	74.1	2.5	27.5	13.2	61.5
CT43	63.8	2.5	27.8	12.9	61.0	CT90	66.1	2.4	25.2	13.4	61.4
CT44	68.1	2.6	30.3	13.2	61.5	CT91	64.7	2.5	26.8	12.8	60.7
CT45	71.5	2.5	27.4	12.3	60.0	CT92	72.1	2.6	27.9	12.9	61.2
CT46	59.5	2.6	29.4	12.4	60.1	CT93	74.2	2.6	29.5	12.9	61.4
CT47	69.5	2.5	27.3	12.2	59.8	CT94	68.4	2.5	28.2	12.5	60.4
CT48	69.5	2.6	32.8	13.5	61.8	CT95	63.2	2.5	26.7	12.2	60.0
CT49	74.6	2.5	28.0	13.7	62.1	CT96	72.5	2.5	27.6	13.2	61.0
CT50	57.9	2.5	30.9	12.9	61.0	CT97	63.1	2.5	29.4	12.4	60.6
CT51	68.1	2.6	28.5	12.5	61.2	CT98	68.9	2.8	34.9	13.1	61.4

Table A6 Continued

Gen	HDI	KD	KW	FPC	WAB	Gen	HDI	KD	KW	FPC	WAB
	#	mm	mg	%	%		#	mm	mg	%	%
CT99	61.5	2.5	28.7	12.6	60.7	CT146	65.2	2.5	28.4	12.6	60.2
CT100	70.3	2.6	28.4	12.7	60.9	CT147	72.5	2.6	30.0	12.7	59.7
CT101	70.0	2.5	28.5	13.0	61.2	CT148	65.0	2.5	28.6	13.2	60.6
CT102	67.5	2.5	28.0	12.0	59.6	CT149	62.0	2.6	29.7	12.7	60.0
CT103	63.1	2.5	27.2	12.7	60.6	CT150	73.4	2.5	27.1	12.8	60.3
CT104	66.8	2.5	28.6	12.5	60.4	CT151	73.8	2.6	28.7	13.6	61.3
CT105	69.1	2.4	26.4	12.7	60.7	CT152	60.0	2.5	28.5	12.7	60.1
CT106	72.0	2.5	25.6	13.2	61.6	CT153	62.1	2.6	32.0	13.2	61.1
CT107	71.3	2.6	28.8	13.6	62.2	CT154	67.4	2.6	27.7	13.4	61.1
CT108	71.7	2.6	27.8	13.7	62.3	CT155	68.1	2.5	27.0	12.9	60.3
CT109	74.9	2.6	30.6	13.5	61.9	CT157	67.0	2.6	31.6	13.0	60.5
CT110	69.2	2.5	28.8	13.6	61.8	CT158	74.8	2.6	28.6	13.8	61.7
CT111	67.7	2.6	28.1	13.3	61.5	CT159	70.6	2.5	29.0	13.2	61.3
CT112	75.6	2.5	27.9	13.1	61.3	CT161	69.6	2.7	32.1	14.6	62.9
CT113	67.4	2.4	26.1	12.6	59.9	CT162	68.5	2.5	27.3	12.8	60.4
CT114	71.8	2.5	26.0	12.7	60.4	CT163	66.4	2.5	26.9	13.8	61.7
CT115	65.0	2.6	32.8	13.0	61.0	CT164	66.9	2.5	25.6	13.0	60.7
CT116	66.2	2.6	29.7	11.7	59.4	CT173	74.9	2.6	30.0	13.5	61.1
CT117	67.1	2.5	25.6	12.8	60.9	CT174	70.6	2.4	24.1	13.2	60.5
CT118	71.4	2.5	28.5	13.0	61.1	CT181	72.9	2.5	28.3	13.5	62.1
CT119	60.8	2.5	28.3	12.1	59.8	CT183	71.0	2.6	29.3	12.8	60.4
CT120	69.7	2.5	27.7	13.1	61.2	CT184	64.6	2.6	27.9	12.9	60.3
CT121	75.9	2.6	30.7	12.6	60.4	CT185	64.6	2.5	28.0	13.2	60.8
CT122	66.4	2.6	29.1	12.4	60.2	CT189	71.2	2.6	29.7	13.3	60.7
CT124	78.1	2.6	29.7	13.0	60.7	CT190	67.2	2.6	28.7	12.6	59.9
CT125	70.1	2.6	29.9	13.0	60.7	CT191	70.3	2.4	24.6	13.5	61.5
CT126	69.0	2.5	26.9	12.8	60.2	CT192	68.5	2.6	30.5	13.4	61.2
CT127	66.6	2.6	29.6	13.0	60.9	CT193	64.8	2.5	27.0	13.0	60.7
CT128	69.8	2.4	26.8	13.0	60.9	CT194	67.5	2.5	29.5	13.8	61.9
CT129	71.6	2.8	37.8	13.7	62.2	CT196	70.0	2.6	28.9	13.5	61.5
CT130	70.1	2.6	28.2	13.9	62.5	CT197	64.3	2.5	28.4	14.0	62.0
CT131	72.0	2.7	32.2	13.6	62.0	CT198	64.2	2.5	28.4	13.8	62.1
CT132	68.7	2.5	28.4	12.8	60.7	CT199	67.2	2.6	29.6	12.6	59.9
CT133	65.0	2.6	31.2	13.1	61.0	CT200	71.9	2.6	30.1	13.6	61.5
CT134	77.4	2.5	27.0	12.8	60.5	CT201	76.4	2.6	30.2	13.4	61.3
CT135	77.8	2.5	27.7	12.2	59.6	CT202	71.9	2.4	25.7	13.3	61.2
CT136	71.7	2.6	29.2	12.6	60.2	CT203	68.7	2.5	29.2	13.3	61.2
CT137	67.9	2.5	28.7	12.8	60.6	CT204	66.2	2.6	30.6	13.6	61.4
CT138	71.4	2.4	24.0	12.5	59.9	CT205	66.6	2.5	26.3	13.4	61.4
CT139	61.2	2.5	27.3	12.6	60.1	CT207	72.9	2.6	30.2	12.9	60.8
CT140	74.9	2.5	25.9	12.7	60.2	CT208	73.8	2.6	28.7	13.0	60.6
CT141	69.9	2.6	28.2	13.2	60.8	CT209	69.9	2.5	28.5	13.1	61.5
CT142	74.5	2.5	27.4	12.9	60.6	CT210	75.0	2.6	29.2	12.9	60.5
CT143	62.2	2.5	29.4	12.9	60.3	CT211	64.6	2.5	27.3	13.8	61.6
CT145	75.7	2.4	26.1	13.1	61.0	CT212	65.3	2.4	25.7	12.5	60.1

Table A6 Continued

Genotype	HDI	KD	KW	FPC	WAB
	#	mm	mg	%	%
CT213	65.7	2.6	30.3	13.6	62.2
CT214	68.6	2.5	27.1	13.4	61.4
CT215	69.6	2.6	28.6	13.3	61.3
CT216	63.6	2.6	30.5	12.7	60.3
CT219	71.4	2.6	29.2	13.6	61.6
CT220	71.5	2.6	30.4	13.7	61.9
CT221	66.5	2.5	25.9	12.8	60.3
CT222	68.5	2.4	25.2	13.4	61.3
CT223	65.5	2.5	28.5	13.4	61.2
CT224	65.0	2.6	30.1	13.6	61.8
CT225	70.4	2.6	28.6	13.9	62.1
CT226	63.4	2.5	27.9	13.6	62.0
CT227	65.6	2.5	25.0	13.5	61.9
CT228	68.0	2.6	28.5	14.0	62.4
CT229	68.9	2.6	28.8	13.8	61.9
CT230	72.2	2.4	24.2	13.1	60.8
CT231	65.0	2.5	28.6	12.8	60.5
CT232	65.4	2.5	27.1	13.4	61.3
CT233	65.3	2.6	30.4	13.5	61.5
CT234	64.0	2.6	31.3	12.8	60.7
CT235	61.6	2.6	28.7	13.5	61.8
CT236	69.9	2.6	29.4	12.7	60.6
CT237	70.4	2.5	25.7	13.5	61.2
CT238	62.0	2.5	29.7	12.8	60.2
CT239	73.2	2.5	27.1	13.2	60.8
CT240	72.6	2.5	26.2	13.3	61.0
CT241	63.6	2.5	29.3	14.0	62.0
CT242	67.1	2.5	28.3	13.7	61.9
CT243	67.6	2.6	28.4	13.2	61.1
CT244	68.4	2.6	28.9	13.1	60.6
CT245	69.7	2.6	28.9	13.5	61.3
CT246	61.1	2.5	27.4	12.7	60.2
CT247	67.3	2.6	27.4	13.2	61.0
CT248	75.0	2.5	27.6	13.8	61.9
CO960293	78.3	2.6	29.5	13.3	61.2
KARL92	55.0	2.5	28.5	14.1	62.8
TAM111	61.1	2.6	29.8	13.1	60.9
TAM112	68.6	2.5	29.0	13.1	61.1

Table A7
Basic Local Alignment Search Tool (BLAST) results for peak markers linked to end-use quality

SNP	Chr	Accession	Description
M3277	1D	AK332171	*Triticum aestivum* cDNA, clone: WT003_F03, cultivar: Chinese Spring
M4514	2B	AK371307	*Hordeum vulgare* subsp. *vulgare* mRNA for predicted protein, complete cds, clone: NIASHv2130E04
M6058	1D	AK331500	*Triticum aestivum* cDNA, clone: WT007_K13, cultivar: Chinese Spring
M8143	2B	AK374637	*Hordeum vulgare* subsp. *vulgare* mRNA for predicted protein, complete cds, clone: NIASHv3071F23
M11264	1A	GU211167	*Triticum aestivum* clone 07e6 gliadin/avenin-like seed protein mRNA, partial cds
M12147	1A	AK334998	*Triticum aestivum* cDNA, clone: WT011_L23, cultivar: Chinese Spring
M13129	6A	DQ139268	*Triticum aestivum* geranylgeranyl hydrogenase mRNA, complete cds
M17816	1D	XM_003559945	*Brachypodium distachyon* histone deacetylase 5-like (LOC100826085), mRNA
M21618	2B	AK360096	*Hordeum vulgare* subsp. vulgare mRNA for predicted protein, complete cds, clone: NIASHv1110D14
M22056	1D	AY579884	*Hordeum vulgare* AML6 mRNA, complete cds
M22544	2D	AK334006	*Triticum aestivum* cDNA, clone: WT008_J12, cultivar: Chinese Spring
M23920	1D	AK355870	*Hordeum vulgare* subsp. *vulgare* mRNA for predicted protein, complete cds, clone: NIASHv1027E14
M40231	7B	AK362110	*Hordeum vulgare* subsp. *vulgare* mRNA for predicted protein, complete cds, clone: NIASHv2002H24
M43982	1A	AK363416	*Hordeum vulgare* subsp. *vulgare* mRNA for predicted protein, complete cds, clone: NIASHv2015E12
M46662	2A	AK333737	*Triticum aestivum* cDNA, clone: WT008_M23, cultivar: Chinese Spring
M65288	1A	AK336136	*Triticum aestivum* cDNA, clone: SET3_F03, cultivar: Chinese Spring
M77496	1D	AK333050	*Triticum aestivum* cDNA, clone: WT005_I08, cultivar: Chinese Spring
M80856	1D	HG670306	*Triticum aestivum* chromosome 3B, genomic scaffold, cultivar Chinese Spring

Table A8
Genetic map derived from CO960293-2/TAM 111 RIL fingerprinted using 90K SNP array is included as a separate file